

This electronic thesis or dissertation has been downloaded from the King's Research Portal at <https://kclpure.kcl.ac.uk/portal/>



Cardiovascular Magnetic Resonance Guided Revascularisation

Morton, Geraint

Awarding institution:
King's College London

The copyright of this thesis rests with the author and no quotation from it or information derived from it may be published without proper acknowledgement.

END USER LICENCE AGREEMENT



Unless another licence is stated on the immediately following page this work is licensed

under a Creative Commons Attribution-NonCommercial-NoDerivatives 4.0 International

licence. <https://creativecommons.org/licenses/by-nc-nd/4.0/>

You are free to copy, distribute and transmit the work

Under the following conditions:

- Attribution: You must attribute the work in the manner specified by the author (but not in any way that suggests that they endorse you or your use of the work).
- Non Commercial: You may not use this work for commercial purposes.
- No Derivative Works - You may not alter, transform, or build upon this work.

Any of these conditions can be waived if you receive permission from the author. Your fair dealings and other rights are in no way affected by the above.

Take down policy

If you believe that this document breaches copyright please contact librarypure@kcl.ac.uk providing details, and we will remove access to the work immediately and investigate your claim.

This electronic theses or dissertation has been downloaded from the King's Research Portal at <https://kclpure.kcl.ac.uk/portal/>



Title: Cardiovascular Magnetic Resonance Guided Revascularisation

Author: Geraint Morton

The copyright of this thesis rests with the author and no quotation from it or information derived from it may be published without proper acknowledgement.

END USER LICENSE AGREEMENT



This work is licensed under a Creative Commons Attribution-NonCommercial-NoDerivs 3.0 Unported License. <http://creativecommons.org/licenses/by-nc-nd/3.0/>

You are free to:

- Share: to copy, distribute and transmit the work

Under the following conditions:

- Attribution: You must attribute the work in the manner specified by the author (but not in any way that suggests that they endorse you or your use of the work).
- Non Commercial: You may not use this work for commercial purposes.
- No Derivative Works - You may not alter, transform, or build upon this work.

Any of these conditions can be waived if you receive permission from the author. Your fair dealings and other rights are in no way affected by the above.

Take down policy

If you believe that this document breaches copyright please contact librarypure@kcl.ac.uk providing details, and we will remove access to the work immediately and investigate your claim.

CARDIOVASCULAR MAGNETIC RESONANCE
GUIDED REVASCULARISATION

Geraint Morton

King's College London

United Kingdom

Submitted for the

Degree of Doctor of Philosophy

May 2012

ABSTRACT

Introduction

Coronary revascularisation is a key component of the management of patients with coronary artery disease (CAD). The importance of combining functional with anatomic information to select appropriate patients is increasingly recognised. Established Cardiovascular Magnetic Resonance (CMR) techniques already provide much of the relevant functional information and the absence of ionising radiation makes CMR ideal for serial examinations. However, new CMR techniques continue to emerge, and require appropriate clinical evaluation.

Methods

This thesis comprises a series of clinical studies developing and evaluating techniques for guiding revascularisation:

- i. Comparison of a high-resolution *k-t* accelerated perfusion sequence with a standard sequence.
- ii. Validation of CMR quantification of absolute myocardial perfusion using the high-resolution sequence against PET.
- iii. Investigation of the relationship between an angiographic score (BCIS-1 Jeopardy score) and CMR estimations of CAD burden.
- iv. Determination of the inter-study reproducibility of perfusion imaging and strain analysis with CMR feature tracking (CMR-FT).
- v. Evaluation of a novel scar imaging technique using a dual-inversion recovery (dual-IR) pre-pulse for the first time in patients.

- vi. The feasibility of combined CMR and coronary intervention in a hybrid laboratory.

Results

The main findings for each component were:

- i. Perfusion imaging with the k - t accelerated sequence resulted in significantly improved image quality, signal and contrast to noise ratios and a reduction in dark rim artefacts compared to the standard sequence.
- ii. There was good correlation between quantitative myocardial perfusion reserve (MPR) derived from CMR and PET. CMR and PET-derived MPR were both comparable and accurate for the detection of CAD. However, absolute perfusion values from both modalities were only weakly correlated.
- iii. The correlation between the BCIS-1 Jeopardy score and CMR ischaemic burden was good and the score predicted a prognostically important ischaemic threshold of 12% with high specificity.
- iv. The inter-study reproducibility of quantitative myocardial perfusion and CMR-FT was reasonable and better for global rather than regional measures. There was no detectable variation in perfusion or strain during the day.
- v. The dual-IR sequence improved scar imaging compared to the IR technique.
- vi. Combined CMR and interventional coronary procedures were successful and well tolerated.

Conclusions

Quantitative analysis of perfusion is an exciting prospect with considerable potential and has demonstrated clinically utility, however, its application remains challenging. Novel scar and strain imaging techniques have also shown promising results. Further method refinement and appropriate clinical studies should allow the full potential of these tools for guiding revascularisation to be realised.

TABLE OF CONTENTS

CARDIOVASCULAR MAGNETIC RESONANCE GUIDED REVASCULARISATION	1
ABSTRACT	2
INTRODUCTION	2
METHODS	2
RESULTS	3
CONCLUSIONS	4
TABLE OF CONTENTS	5
ACKNOWLEDGEMENTS	10
STATEMENT OF ROLES AND RESPONSIBILITIES	11
PUBLICATIONS	12
PAPERS	12
SUBMITTED PAPERS	13
ABSTRACTS	14
LIST OF FIGURES	16
LIST OF TABLES	18
LIST OF ABBREVIATIONS	19
1 GENERAL INTRODUCTION	20
ISCHAEMIA	22
VIABILITY	27
NON-INVASIVE FUNCTIONAL ASSESSMENT	30
NON INVASIVE ISCHAEMIA DETECTION	30
CMR ISCHAEMIA TESTING BY WALL MOTION ASSESSMENT	31
NON-INVASIVE ASSESSMENT OF MYOCARDIAL PERFUSION	33
NON-INVASIVE MYOCARDIAL PERFUSION IMAGING	39
CMR ASSESSMENT OF VIABILITY	55
ADDITIONAL VALUE FROM CMR IMAGING	59
CLINICAL APPLICATIONS	60
SUMMARY AND OBJECTIVES	61
2 GENERAL METHODS	63
STUDY PARTICIPANTS	63
EXCLUSION CRITERIA	63
CMR PROTOCOL	64
PERFUSION IMAGING	66
FIRST-PASS PERFUSION IMAGING CONTRAST AGENT DELIVERY-THE DUAL BOLUS TECHNIQUE	67
SCAR IMAGING	70
INVASIVE CATHETER LABORATORY INVESTIGATIONS	70

3A: PERFUSION IMAGING. OPTIMISATION OF THE CMR PERFUSION SEQUENCE-SEQUENCE SELECTION	72
ABSTRACT	72
OBJECTIVES	72
BACKGROUND	72
METHODS	72
RESULTS	73
CONCLUSIONS	73
BACKGROUND	75
METHODS	77
STUDY POPULATION	78
DATA ACQUISITION	78
DATA ANALYSIS	80
STATISTICAL ANALYSIS	83
RESULTS	84
HUMAN STUDIES	84
IMAGE QUALITY	86
IMAGE ARTEFACTS	90
DIAGNOSIS OF CAD	91
PHANTOM DATA	93
DISCUSSION	94
IMAGE QUALITY	96
SNR AND CNR	97
ARTEFACTS	98
LIMITATIONS	101
CONCLUSIONS	102
 3B PERFUSION IMAGING. OPTIMISATION OF THE CMR PERFUSION SEQUENCE-CONTRAST AGENT DOSE SELECTION	 103
ABSTRACT	103
OBJECTIVES	103
BACKGROUND	103
METHODS	103
RESULTS	104
CONCLUSIONS	104
BACKGROUND	105
METHODS	105
PHANTOM STUDIES	105
PATIENT STUDIES	106
DATA ANALYSIS	106
RESULTS	106
PHANTOM STUDIES	106
PATIENT STUDIES	107
DISCUSSION	110
LIMITATIONS	113
CONCLUSIONS	113
 4 PERFUSION IMAGING. VALIDATION OF FULLY QUANTITATIVE CMR PERFUSION AGAINST POSITRON EMISSION TOMOGRAPHY IN PATIENTS WITH CORONARY ARTERY DISEASE	 114
ABSTRACT	114
OBJECTIVES	114

BACKGROUND	114
METHODS	114
RESULTS	115
CONCLUSIONS	115
BACKGROUND	116
METHODS	117
PATIENT POPULATION AND STUDY DESIGN	117
DATA ACQUISITION	117
DATA ANALYSIS	119
STATISTICAL ANALYSIS	121
RESULTS	122
STUDY POPULATION	122
MYOCARDIAL PERFUSION	124
MYOCARDIAL PERFUSION-AGREEMENT BETWEEN CMR AND PET	127
DIAGNOSIS OF CAD	131
DISCUSSION	136
METHODOLOGICAL CONSIDERATIONS	138
PHYSIOLOGICAL CONSIDERATIONS	140
CLINICAL IMPLICATIONS	140
LIMITATIONS	142
CONCLUSIONS	143
 5 PERFUSION IMAGING. COMPARISON OF CMR ISCHAEMIC BURDEN AND THE ANGIOGRAPHIC EXTENT OF CORONARY ARTERY DISEASE.	 144
ABSTRACT	144
OBJECTIVES	144
BACKGROUND	144
METHODS	144
RESULTS	145
CONCLUSIONS	145
BACKGROUND	146
METHODS	147
PATIENT POPULATION AND STUDY DESIGN	147
DATA ACQUISITION	148
DATA ANALYSIS	149
STATISTICAL ANALYSIS	149
RESULTS	150
CMR	152
CORONARY ANGIOGRAPHY	153
CORRELATION BETWEEN BCIS-JS AND MYOCARDIAL ISCHAEMIC BURDEN	155
DISCUSSION	157
BCIS-JS	158
CLINICAL IMPLICATIONS	159
LIMITATIONS	163
CONCLUSIONS	164
 6 PERFUSION IMAGING. INTER-STUDY REPRODUCIBILITY OF QUANTITATIVE CMR MYOCARDIAL PERFUSION IMAGING.	 165
ABSTRACT	165
OBJECTIVES	165
BACKGROUND	165
METHODS	165
RESULTS	166

CONCLUSIONS	166
INTRODUCTION	167
METHODS	168
POPULATION	168
DATA ACQUISITION	168
DATA ANALYSIS	170
RESULTS	171
PERFUSION IMAGING	172
LEFT VENTRICULAR VOLUMES AND FUNCTION	178
DISCUSSION	179
THE VALUE OF INTER-STUDY REPRODUCIBILITY	179
INTER-STUDY REPRODUCIBILITY OF QUANTITATIVE PERFUSION IMAGING	180
DIURNAL VARIATION	185
LIMITATIONS	186
CONCLUSIONS	186
 <u>7 MYOCARDIAL VIABILITY AND ISCHAEMIA. EVALUATION OF THE INTER-STUDY REPRODUCIBILITY OF CMR FEATURE TRACKING</u>	 188
ABSTRACT	188
OBJECTIVES	188
BACKGROUND	188
METHODS	188
RESULTS	189
CONCLUSIONS	189
BACKGROUND	191
METHODS	192
POPULATION	192
DATA ACQUISITION	192
DATA ANALYSIS	193
RESULTS	195
PARTICIPANT DETAILS	195
FEATURE TRACKING	195
LV VOLUMES AND FUNCTION	200
DISCUSSION	202
CMR FEATURE TRACKING	202
INTER-STUDY REPRODUCIBILITY	203
PHYSIOLOGICAL VARIATION	206
COMPARISON WITH SPECKLE TRACKING	206
LIMITATIONS	208
CONCLUSIONS	208
 <u>8 MYOCARDIAL VIABILITY. EVALUATION OF A NOVEL DUAL INVERSION RECOVERY SEQUENCE FOR IMPROVED VISUALIZATION OF MYOCARDIAL INFARCTION</u>	 209
ABSTRACT	209
OBJECTIVES	209
INTRODUCTION	209
METHODS	209
RESULTS	210
CONCLUSION	210
INTRODUCTION	211
METHODS	215
DATA ACQUISITION	215

DATA ANALYSIS	216
RESULTS	217
EXPERT OBSERVER QUANTITATIVE AND QUALITATIVE ANALYSIS	222
SNR AND CNR	225
DISCUSSION	226
LIMITATIONS	228
CONCLUSION	229
<u>9 MYOCARDIAL PERFUSION AND VIABILITY. FEASIBILITY OF COMBINED CMR IMAGING AND PCI IN A HYBRID LABORATORY</u>	<u>230</u>
ABSTRACT	230
OBJECTIVES	230
BACKGROUND	230
METHODS	230
RESULTS	231
CONCLUSIONS	231
BACKGROUND	232
METHODS	233
XMR LABORATORY	233
SAFETY	234
PATIENT RECRUITMENT	235
DATA ACQUISITION	235
RESULTS	237
DISCUSSION	243
INTERVENTIONAL CARDIOVASCULAR MAGNETIC RESONANCE	243
XMR LABORATORY APPLICATIONS	244
LIMITATIONS	247
CONCLUSION	247
<u>10 DISCUSSION AND CONCLUSIONS</u>	<u>248</u>
DISCUSSION	248
QUANTIFICATION OF PERFUSION WITH CMR	248
NOVEL CMR METHODS FOR GUIDING REVASCULARISATION	254
FUTURE PERSPECTIVES	255
CONCLUSIONS	257
<u>REFERENCES</u>	<u>258</u>
<u>APPENDIX A STUDY PROTOCOLS, PATIENT INFORMATION SHEETS AND CONSENT FORMS</u>	<u>295</u>
<u>APPENDIX B: BCIS-1 JEOPARDY SCORE</u>	<u>312</u>

ACKNOWLEDGEMENTS

Completion of this work has only been possible because of the contributions of many people. I am indebted to Professor Eike Nagel, my primary supervisor, for the opportunities that he has given me, his unwavering support, assistance and encouragement and for teaching me the techniques of CMR. I am also indebted to Dr Divaka Perera, my clinical supervisor, for his consistent support, enthusiasm, guidance and assistance with patient enrolment. Both have been important academic mentors to me.

I am extremely grateful to the patients and volunteers for their altruistic participation in my studies.

I would like to thank all members of our research group who have all given up precious time to teach, analyze data, and provide practical help and support. I owe a particular gratitude to Amedeo Chiribiri, Masaki Ishida, Andreas Schuster, Shazia Hussain and Roy Jogya, for their help and also their friendship.

I undertook a number of specific collaborations during the course of this thesis, and I would like to thank the following for their help, Mr. Stephen Sinclair, Mr. John Totman, Ms. Lorna Smith and Ms. Annette Leinan Dahl (KCL radiographers), Professor Tobias Schaeffter, Ms. Sarah Peel (Imaging Sciences Physicists), Professor Michael O'Doherty, Dr Sally Barrington, Ms. Stacey Baker (KCL PET center), Dr Sven Plein (KCL), Dr Kalpa De Silva (GSTT) and Siobhan Crichton (KCL statistician).

I am grateful to my family who provide me with a strong support network and my parents for their enduring wisdom and guidance. I am grateful to Lyn and Margery, my parents in law, for also providing emergency statistical and childcare support on numerous occasions. Finally, I am particularly indebted to my wife, Beth, for her unconditional support, counsel and encouragement throughout all of my work and to my children Abi, Tom and Catrin for putting up with my long days away at work and providing me with a welcome distraction when at home. Though last in my acknowledgments, they are always foremost in my thoughts. Thank you.

STATEMENT OF ROLES AND RESPONSIBILITIES

For all of the studies described I produced original study paperwork or amended existing study protocols, obtained ethics committee and research and development department approval and performed the routine study administration. Some sample study paperwork is included in Appendix A. I was responsible for study design, subject recruitment, all CMR and PET imaging and data collation, analysis, interpretation and reporting. These tasks were conducted under the supervision and guidance of my supervisors. All of the work presented here is my own original work. The work presented in chapter 8 “Evaluation of a Novel Dual Inversion Recovery Sequence for Improved Visualization of Myocardial Infarction” was performed in conjunction with Sarah Peel, a physicist in the department.

PUBLICATIONS

Papers

Morton G, Schuster A, Perera D, Nagel E. Cardiac Magnetic Resonance Imaging to Guide Complex Revascularisation in Stable Coronary Artery Disease. *European Heart Journal*. 2010;31(18):2209-15.

Morton G, Ishida M, Schuster A, Hussain S, Schaeffter T, Chiribiri A, Nagel E. Cardiovascular Magnetic Resonance Perfusion Imaging: Comparison of an Advanced, High-Resolution and a Standard Sequence. *Journal of Cardiovascular Magnetic Resonance*. 2012;14(1):34.

Morton G, Chiribiri A, Ishida M, Hussain S, Schuster A, Indermuehle A, Perera D, Knuuti J, Baker S, Hedström E, Marsden P, O'Doherty M, Barrington S, Nagel E. Quantification of Absolute Myocardial Perfusion in Patients with Coronary Artery Disease: Comparison Between Cardiovascular Magnetic Resonance and Positron Emission Tomography. *Journal of the American College of Cardiology*. 2012. 60:1546–55.

Morton G, De Silva K, Ishida I, Chiribiri A, Indermuehle A, Schuster A, Redwood S, Nagel E, Perera. Validation of the BCIS-1 Myocardial Jeopardy Score Using Cardiac Magnetic Resonance Perfusion Imaging. *Clinical Physiology and Functional Imaging* 2012; doi: 10.1111/j.1475-097X.2012.01167.

Morton G, Jogiya R, Schuster A, Chiribiri A, Nagel E. Quantitative Cardiovascular Magnetic Resonance Perfusion Imaging: Inter-study Reproducibility. *European Heart Journal-Cardiovascular Imaging*. 2012. doi: 10.1093/ehjci/jes103.

Morton G, Schuster A, Jogiya R, Kutty S, Beerbaum P, Nagel E. Inter-study Reproducibility of Cardiovascular Magnetic Resonance Myocardial Feature Tracking. *Journal of Cardiovascular Magnetic Resonance*. 2012; 14(1):43.

Peel S, **Morton G**, Chiribiri A, Schuster A, Nagel E, Botnar R. A dual-IR MRI sequence for reduced blood signal in LGE images of myocardial scar. *Radiology* 2012; doi:10.1148/radiol.12112004.

Submitted papers

Morton G, Hussain S, De Silva K, Dahl A, Redwood S, Razavi R, Plein S, Perera D, Nagel E. Feasibility of Combined Cardiovascular Magnetic Resonance Imaging and Percutaneous Coronary Intervention in a Hybrid Laboratory.

Abstracts

Morton G, Chiribiri A, Ishida M, Hussain S, Schuster A, Indermuehle A, Perera D, Hedstrom E, Barrington S, Nagel E. Quantification of Absolute Myocardial Perfusion in Patients with Coronary Artery Disease: Comparison between Cardiac Magnetic Resonance and Positron Emission Tomography. *Journal Of the American College Cardiology* 2012; 59; 13 (Suppl A) 908-3 A261 (oral presentation ACC 2012).

Morton G, Jogiya R, Schuster A, Chiribiri A, Nagel E. Quantitative cardiovascular magnetic resonance myocardial perfusion imaging: inter-study reproducibility. *British Cardiac Society* 2012.

Morton G, Hussain S, De Silva K, Dahl A, Redwood S, Razavi R, Plein S, Perera D, Nagel E. Feasibility of combined cardiovascular magnetic resonance imaging and percutaneous coronary intervention in a hybrid laboratory. *British Cardiac Society* 2012.

Morton G, Chiribiri A, Ishida M, Schuster A, Hussain S, Nagel E. The Diagnostic Accuracy Of Quantitative CMR Perfusion Imaging May Not Be The Same For All Coronary Arteries. *Journal of Cardiovascular Magnetic Resonance* 2012; 14(Suppl 1):P8

Morton G, Ishida M, Schuster A, Schaeffter T, Chiribiri A, Nagel E. Advanced Techniques Improve The Performance Of Myocardial Perfusion Imaging. *Journal of Cardiovascular Magnetic Resonance* 2012, 14(Suppl 1):P12

Morton G, De Silva K, Ishida M, Chiribiri A, Indermuhle A, Schuster A, Redwood S, Nagel E, Perera D. Validation of the BCIS-1 Myocardial Jeopardy Score Using Cardiac Magnetic Resonance Imaging. *Heart* 2011;97:A71-A72.

Morton G, Ishida M, Chiribiri A, Schuster A, Baker S, Hussain S, Perera D, O'Doherty M, Barrington S, Nagel E. High-Resolution Cardiac Magnetic Resonance Perfusion Imaging Versus Positron Emission Tomography for the Detection and Localization of Coronary Artery Disease. *Heart* 2011;97:A68.

Morton G, Ishida M, De Silva K, Sicard P, Chiribiri A, Schuster A, Hussain S, Paul, M, Perera D, Nagel E. Correlation Between an Angiographic and a Cardiac Magnetic Resonance Score of Myocardial Jeopardy Using Standard and High-Resolution Perfusion Sequences. *Journal of Cardiovascular Magnetic Resonance*. 2011. 13(Suppl 1):P89.

Morton G, Ishida M, Chiribiri A, Schuster A, Baker S, Hussain S, Perera D, O'Doherty M, Barrington S, Nagel E. Comparison of Cardiac Magnetic Resonance Imaging and Positron Emission Tomography for the Diagnosis and Localization of Coronary Artery Disease. *Journal of Cardiovascular Magnetic Resonance* 2011, 13(Suppl 1):P83.

Peel S, **Morton G**, Nagel E, Botnar R. Non-Selective Double Inversion Recovery Pre-Pulse for Flow-Independent Black Blood Myocardial Viability Imaging: Optimization of T1 Suppression Range. *ISMRM* 2011.

LIST OF FIGURES

<i>Figure 1.1: Relationship between myocardial ischaemic burden and risk of cardiac death.</i>	23
<i>Figure 1.2: Mortality for patients with and without myocardial viability treated by revascularisation or medical therapy.</i>	28
<i>Figure 1.3: The ischaemic cascade.</i>	31
<i>Figure 1.4: The coronary circulation.</i>	34
<i>Figure 1.5: Relationship between scar transmuralty and the likelihood of improved function after revascularization.</i>	57
<i>Figure 1.6: Low-dose dobutamine versus scar imaging for viability assessment.</i>	58
<i>Figure 2.1: Standard CMR protocol</i>	65
<i>Figure 2.2: Dual-bolus set-up</i>	69
<i>Figure 3.1: Image quality and respiratory artefact scores for volunteers and patients with both sequences.</i>	86
<i>Figure 3.2: Signal and contrast to noise ratios for volunteer rest perfusion scans.</i>	88
<i>Figure 3.3: First pass rest perfusion images with segmental signal intensity curves.</i>	89
<i>Figure 3.4: Stress perfusion images from patients with coronary artery disease using both sequences.</i>	92
<i>Figure 3.5: Signal intensity curves from the left myocardial compartment of the perfusion phantom.</i>	107
<i>Figure 3.6: Image quality and respiratory artefact scores with kt-SSFP 0.075 and kt-SSFP 0.1.</i>	109
<i>Figure 4.1: Scatter plots comparing CMR and PET derived MPR</i>	128
<i>Figure 4.2: Agreement between CMR and PET MPR</i>	129
<i>Figure 4.3: Correlation and agreement between CMR and PET derived absolute perfusion values.</i>	130
<i>Figure 4.4: Diagnosis of significant CAD against QCA using quantitative CMR and PET derived MPR.</i>	132
<i>Figure 4.5: Case example.</i>	134

<i>Figure 4.6: ROC curves for the identification of significant CAD in each individual coronary artery using MPR2_{PET} (left) and MPR2_{CMR} (right).</i>	135
<i>Figure 5.1: Mean LV myocardial ischaemia and scar burden according to BCIS-JS</i>	153
<i>Figure 5.2: X-ray coronary angiogram and CMR stress perfusion and scar imaging from one patient.</i>	154
<i>Figure 5.3: Correlation between the BCIS-JS and myocardial ischaemic burden</i>	155
<i>Figure 5.4: ROC curve for BCIS-JS to detect myocardial ischaemic burden $\geq 12\%$.</i>	156
<i>Figure 6.1: Stress perfusion image with territorial segmentation.</i>	173
<i>Figure 6.2: Perfusion imaging inter-study agreement</i>	177
<i>Figure 7.1: Inter-study agreement of CMR-FT segmental strain analysis</i>	199
<i>Figure 8.1: The inversion recovery technique</i>	212
<i>Figure 8.2: Schematic representation of the inversion recovery (IR) (a) and dual inversion recovery (dual-IR) (b) sequences.</i>	214
<i>Figure 8.3: Dual IR and standard IR scar images from a patient with transmural scar in the LAD territory.</i>	219
<i>Figure 8.4: Standard versus dual-IR scar images</i>	220
<i>Figure 8.5: Long axis scar imaging using the IR and dual IR techniques</i>	221
<i>Figure 8.6: Expert observer confidence scores</i>	223
<i>Figure 8.7: Agreement between observers for scar size assessment with IR and dual-IR scar imaging.</i>	224
<i>Figure 9.1: The XMR laboratory</i>	234
<i>Figure 9.2 and 9.3: CMR and X-ray coronary angiogram from patient 10.</i>	240
<i>Figure 9.4: Coronary angiogram and stress perfusion images from patient 9.</i>	241
<i>Figure 9.5: Coronary angiogram and stress perfusion images pre and post PCI.</i>	242

LIST OF TABLES

<i>Table 1.1: Summary of non-invasive myocardial perfusion imaging modalities.</i>	45
<i>Table 3.1: Imaging parameters for the standard (st-GrE) and high-resolution (kt-SSFP) sequences</i>	77
<i>Table 3.2: Sequence selection study participant characteristics</i>	85
<i>Table 3.3: Dark rim artefacts</i>	91
<i>Table 3.4: SNR and CNR values in a perfusion phantom for both sequences at increasing doses of CA</i>	93
<i>Table 3.5: Baseline characteristics of the kt-SSFP 0.075 and 0.1 patients</i>	108
<i>Table 3.6: Dark rim artefacts at kt-SSFP 0.075 and kt-SSFP 0.1.</i>	110
<i>Table 4.1: Baseline characteristics of the 41 study participants.</i>	123
<i>Table 4.2: Summary (mean\pmSD) of the haemodynamic data for all 38 participants during the imaging studies.</i>	124
<i>Table 4.3: Quantitative perfusion values in patients with and without significant CAD.</i>	126
<i>Table 4.4: Area under the ROC curves (ROC AUC), optimal MPR2 cut-off and sensitivity and specificity for detection of significant CAD in each coronary territory.</i>	136
<i>Table 5.1: Characteristics of the patients included in the analysis</i>	151
<i>Table 5.2: Haemodynamics during CMR perfusion imaging.</i>	152
<i>Table 6.1: Myocardial perfusion and haemodynamics for the subjects during each of the three scans.</i>	174
<i>Table 6.2: Inter-study reproducibility of perfusion imaging (Scan A vs. B).</i>	175
<i>Table 6.3: Inter-study reproducibility between Scans A and C.</i>	176
<i>Table 6.4: Mean values, intra-subject differences and inter-study reproducibility for LV volumes and function.</i>	178
<i>Table 7.1: Strain values for the combined study population.</i>	196
<i>Table 7.2: The inter-study reproducibility of CMR-FT strain</i>	198
<i>Table 7.3: Mean LV volumes and function for the entire study population.</i>	201
<i>Table 7.4: Inter-study reproducibility of LV volumes and function.</i>	201
<i>Table 8.1: Characteristics of the 12 patients included in the analysis</i>	218
<i>Table 9.1: Patient characteristics and summary of XMR cases.</i>	238

LIST OF ABBREVIATIONS

AIF	Arterial input function
AUC	Area under the curve
CA	Contrast agent
CABG	Coronary artery bypass grafting
CAD	Coronary artery disease
CI	Confidence interval
CFR	Coronary flow reserve
CMR	Cardiovascular magnetic resonance
CNR	Contrast to noise ratio
CT	Computed tomography
DRA	Dark rim artefact
DSE	Dobutamine stress echocardiography
EF	Ejection fraction
FFR	Fractional flow reserve
LAD	Left anterior descending artery
LGE	Late gadolinium enhancement
LV	Left ventricle
LVEF	Left ventricular ejection fraction
MCE	Myocardial contrast echocardiography
MPR	Myocardial perfusion reserve
MRI	Magnetic resonance imaging
PET	Positron emission tomography
PCI	Percutaneous coronary intervention
RCA	Right coronary artery
RF	Radiofrequency
ROC	Receiver operating characteristic
SD	Standard deviation
SI	Signal intensity
SNR	Signal to noise ratio
SPECT	Single-photon emission computed tomography
SSFP	Steady state free precession

1 GENERAL INTRODUCTION

Despite many advances in prevention, detection and treatment coronary artery disease (CAD) remains a major public health problem. CAD is the leading cause of death worldwide and the World Health Organization estimates it caused 7.25 million or 12.8% of all deaths in 2008¹. In the United Kingdom alone more than 2 million people have CAD and in 2009 there were 82,000 deaths from CAD².

Coronary revascularisation has a central role in the management of patients with stable CAD, however, despite extensive published literature, appropriate selection of patients and lesions for revascularisation in stable CAD continues to be an area of controversy. Patients with complex CAD including multivessel disease, complex anatomy and with associated left ventricular (LV) impairment are at higher risk of procedural complications but also potentially benefit the most from revascularisation. Information regarding risks and benefits is therefore of critical importance for appropriate patient selection.

The literature on coronary revascularisation is dominated by anatomical classification of CAD with decisions regarding revascularisation made solely on the basis of coronary angiographic appearances. Such an anatomy-driven approach fails to assess coronary blood flow, myocardial perfusion and viability, which are central to the pathophysiology of CAD. Coronary artery blood flow is reduced when the luminal diameter of a coronary artery narrows below a threshold and as a result a reduction in coronary artery diameter of $\geq 50\%$ - 70% is considered to be flow limiting. However this relationship between flow

and luminal narrowing was determined in animal models using discrete, non-atherosclerotic narrowings of the coronary arteries³ and does not translate well into human clinical practice. Anatomic assessment of the severity of a coronary artery stenosis has been repeatedly shown to correlate poorly with the haemodynamic effects^{4, 5}. A number of factors contribute to the discrepancy between anatomic and physiologic assessment such as the diffuse nature of CAD, the presence of collateral vessels and calcification, dynamic changes in vasomotor tone, and difficulties identifying a truly normal vessel segment as a reference diameter. In addition, the anatomy-only approach fails to take into account the viability of the myocardium subtended by the diseased artery.

These considerations are widely accepted and the importance of functional assessment prior to revascularisation is reflected in guidelines for percutaneous coronary intervention (PCI) in stable CAD⁶. Despite this, many major contemporary trials continue to treat CAD as a purely anatomical disease. An example is the relatively recent SYNTAX trial⁷, which compared PCI and coronary artery bypass grafting (CABG) for the treatment of left main stem and/or three vessel CAD. Patients randomised to both PCI and CABG underwent protocol-mandated complete anatomic revascularisation, i.e. all lesions of $\geq 50\%$ in vessels of $\geq 1.5\text{mm}$ were treated without prior physiologic assessment.

There may, of course, be some value in classifying patients according to their anatomy. For example CABG has been shown to confer a prognostic benefit in patients with left main stem disease or reduced LV function and two or three vessel disease involving the proximal left anterior descending (LAD) artery⁸.

However, consideration of anatomy alone, and ignoring the physiology when selecting patients and lesions for revascularisation over simplifies a complex disease and trials adopting this approach risk underestimating the benefits of revascularisation. (This particular evidence also pre-dates modern medical and surgical therapy and is therefore of questionable current relevance).

Ischaemia

The presence of myocardial ischaemia in stable CAD is associated with an adverse prognosis whether detected by exercise testing⁹, single photon emission computed tomography (SPECT)¹⁰, stress echocardiography¹¹, or cardiovascular magnetic resonance (CMR)¹². However the evidence that myocardial revascularisation improves prognosis in these patients is limited.

Hachamovitch et al¹³ assessed survival in 10,627 patients who had undergone clinical SPECT studies in a single US centre. Patients with no or mild baseline ischaemia had an improved prognosis with medical therapy compared to revascularisation whilst conversely those with moderate to severe ischaemia had an improved prognosis with revascularisation. An ischaemic threshold of 10-12.5% of myocardium differentiated patients who benefited from revascularisation from those who did not (figure 1.1). Even though these data are from a very large cohort and the conclusions are interesting there are inherent limitations to the study as it was a non-randomised, retrospective observational study, which used a propensity score to adjust for non-randomisation.

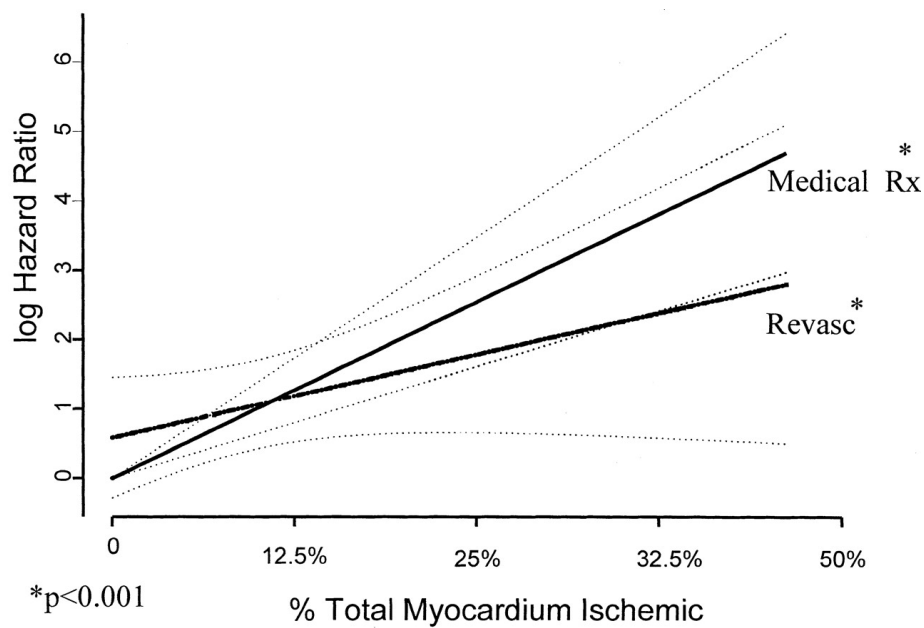


Figure 1.1: Relationship between myocardial ischaemic burden and risk of cardiac death.

Hazard ratio for cardiac death in patients treated with revascularisation (Revasc) versus medical therapy (Medical Rx). A threshold of 10-12% ischaemia burden defines those who appear to derive a prognostic benefit from revascularisation; from ¹³.

In the Asymptomatic Cardiac Ischemia Pilot (ACIP) study patients with asymptomatic ischaemia randomised to revascularisation (PCI or CABG) had significantly lower rates of death or myocardial infarction than those randomised to medical therapy¹⁴. There were, however, relatively few events (31 in total) and the medical therapy used reflected practice at the time rather than current routine aggressive therapy. In the SWISSI II trial patients post myocardial infarction with demonstrable silent ischaemia had a significantly

reduced rate of major adverse cardiac events with PCI than with medical therapy¹⁵.

The landmark randomised controlled COURAGE trial¹⁶ on the other hand concluded that there is no prognostic benefit from PCI in addition to optimal medical therapy as an initial treatment for stable CAD. This was despite the fact that the majority of participants had objective evidence of ischaemia at baseline-including 54% of patients with reversible defects on nuclear imaging. These data generated considerable controversy and led many to re-evaluate entirely the role of PCI in stable CAD. It seems paradoxical that there was no incremental benefit from PCI given that the presence of demonstrable ischaemia confers a worse prognosis. There are a number of possible explanations for this. It could be that the procedural risks of PCI outweigh the benefits from ischaemia reduction. This however seems unlikely given that exclusion of peri-procedural myocardial infarction from the COURAGE data does not alter the findings. It may be that the techniques for revascularization were not optimal for reducing ischaemia. Some have certainly criticized the relatively low overall rate (94%), and number of stents used, the low rate of drug eluting stent use (3%) and the relatively low procedural success rate (89%). However, the most important contributory factor is likely to be that the study design favored inclusion of lower risk patients with a lower burden of pre treatment myocardial ischaemia. As an example, patients with an exercise test positive in the first stage were excluded.

In apparent contradiction to the main study the nuclear sub study of the same trial suggested that PCI might confer a prognostic benefit especially in patients with moderate to severe baseline ischaemia¹⁷. However, the sub study was underpowered and this finding did not reach statistical significance. Since the study design included lower risk patients 40% had <5% ischaemia on baseline nuclear perfusion testing and only a third of patients in the PCI arm had a significant reduction of ischaemia following PCI. This suggests that revascularization may confer a prognostic benefit in patients with a significant ischaemic burden and improved patient selection may allow this benefit to be realised.

Recognition of the importance of ischaemia is reflected in patients undergoing PCI with a change of emphasis away from complete anatomic revascularisation towards targeted revascularisation i.e. treating only the lesions causing ischaemia. Complete revascularisation and incomplete revascularisation are purely anatomic terms. By also assessing the physiology it is possible to achieve complete resolution of ischaemia without performing complete anatomic revascularisation. In patients undergoing PCI there is evidence from subgroup analyses¹⁸ and registry data¹⁹ that complete anatomic revascularisation is superior to incomplete anatomic revascularisation. The most compelling data however supports intervention targeted only at flow limiting lesions even when this results in incomplete anatomic revascularisation. The DEFER study²⁰ demonstrated that in single vessel disease it is safe to defer treatment of angiographically moderate stenoses that do not cause ischaemia as determined by fractional flow reserve (FFR). The more recent FAME study demonstrated

the utility of extending this approach to a multivessel setting²¹. This large multicentre, randomised, controlled trial demonstrated that ischaemia-guided PCI confers a prognostic benefit (reduced rate of death, nonfatal MI and repeat revascularization) over PCI guided by angiographic appearances alone.

The follow-up FAME II study²² is likely to add further support to ischaemia-driven revascularisation with PCI. This study randomised 1219 patients with stable CAD to FFR-guided PCI plus optimal medical therapy or optimal medical therapy alone. The results have yet to be formally published however the data safety monitoring board recently recommended cessation of recruitment after an interim analysis demonstrated a significant reduction in the need for hospital readmission and urgent revascularization in the FFR-guided arm.

Conversely, in the case of CABG, there is a large volume of evidence demonstrating a symptomatic and prognostic benefit with complete over incomplete revascularisation and thus complete revascularisation is widely considered the gold standard²³. Unlike with PCI these data are largely non-randomised and retrospective. However improved prognosis with complete revascularisation has been consistently reported and it is plausible that technical differences between the two techniques may explain why complete revascularisation is the method of choice in CABG and targeted revascularisation in PCI. In the case of PCI the risk of complications is proportional to the number of lesions treated whereas the number of grafts seems to add little to the overall risk of CABG.

Viability

LV dysfunction is an important determinant of prognosis²⁴. When considering revascularisation in stable patients with LV impairment it is important to also consider viability as there is evidence that revascularisation of patients with significant viable myocardium is associated with improved LV function and survival.

Demonstration that the function of viable myocardium improves after restoration of coronary blood flow comes from pooled data from 105 trials using nuclear techniques or stress echocardiography²⁵. This meta-analysis demonstrated a combined mean sensitivity of 84% and specificity of 69% for the prediction of regional functional recovery. An improvement in global left ventricular ejection fraction (LVEF) was detected in 28 studies. In patients with viable myocardium LVEF improved on average from 37% to 45% whilst patients without viability showed no improvement in LVEF (36% before and after revascularization).

A 2002 meta-analysis that pooled the data of 3088 patients from 24 viability studies²⁶ demonstrated improved survival with revascularisation in patients with viable myocardium. Viability was determined using nuclear perfusion techniques, positron emission tomography (PET) or dobutamine stress echocardiography (DSE) and patients followed-up for approximately 2 years. Analysis of the combined results demonstrated a strong association between myocardial viability identified by non-invasive testing and improved survival after revascularisation. Revascularisation in patients with viable myocardium

was associated with a 79.6% reduction in mortality from 16% with medical therapy to 3.2%. Conversely, in the absence of viability, there was no significant difference between the risk of death with revascularisation (7.7%) or medical therapy (6.2%) (figure 1.2).

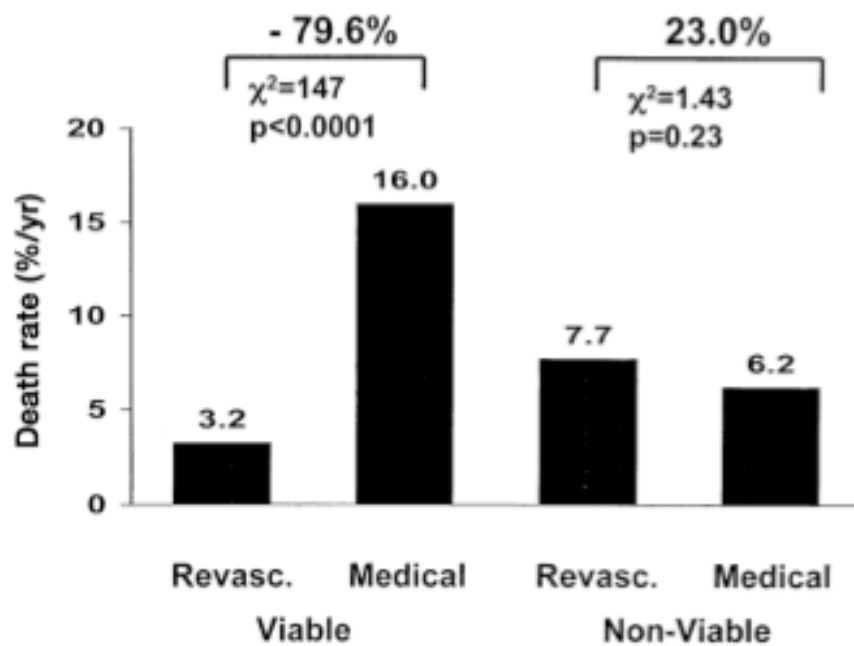


Figure 1.2: Mortality for patients with and without myocardial viability treated by revascularisation or medical therapy.

There is 79.6% reduction in mortality for patients with viability treated by revascularisation. In patients without myocardial viability, there is no significant difference in mortality between patients treated with revascularisation and those treated with medical therapy; from²⁶.

In contrast, a sub study of the recent STICH trial²⁷, has questioned the role of viability testing prior to revascularisation. This prospective study of 601

patients used SPECT or DSE to identify viability. Patients were randomly assigned to intensive medical therapy and CABG or intensive medical therapy alone. 37% of patients with viable myocardium and 51% of patients without died during follow-up. After adjustment for differences in baseline variables and risk factors, there was no significant association between viability and mortality. Furthermore patients with viable myocardium who were assigned to CABG plus medical therapy did not have improved survival compared to those assigned to medical therapy alone. However, it is important to understand the limitations of this study, which may well have affected the findings. Firstly, patients were not assigned to a treatment group based on the result of the imaging test. Secondly, viability imaging was not mandated as part of the main study protocol and was only performed at the discretion of the investigators. It is not clear which factors influenced the decision to perform viability imaging. Thirdly, the combination of two different modalities to determine viability resulted in different, and somewhat arbitrary, criteria being used to define viability. Viability was defined as the presence of 11 or more viable segments based on relative tracer activity with SPECT, or five or more segments with abnormal resting systolic function but manifesting contractile reserve during dobutamine administration with DSE. Fourthly, 81% of patients were defined as having viability and only 19% were defined as non-viable. Fifthly, the imaging findings were not related to the coronary anatomy. Finally, there were important differences between the two treatment groups as patients in the medical therapy arm of the trial had a significantly higher rate of aspirin and statin use at baseline compared to patients who underwent CABG.

There is therefore conflicting evidence about the role of viability imaging to guide revascularisation. To date there are still no prospective randomised trials on the prognostic value of viability imaging.

Non-invasive functional assessment

On the basis of all of the above evidence most clinicians accept that combining anatomical information with a functional assessment pre revascularisation in patients with complex CAD is important. A number of non-invasive imaging modalities are available each with its own inherent advantages and disadvantages. Clinicians frequently decide which method is most appropriate according to the clinical situation and to local expertise and the availability of different modalities.

Non invasive ischaemia detection

When myocardial oxygen demand exceeds supply a sequence of haemodynamic and cardiac electrophysiologic changes occur that culminate in angina. This sequence of events is termed the ischaemic cascade²⁸ (figure 1.3). Detection of one of the steps of this cascade forms the basis of all non-invasive ischaemia detection. Investigations targeting earlier steps in the cascade in theory should be more sensitive than techniques targeting later steps in the cascade. This notion is supported by a study using echocardiography in dogs²⁹. In this study myocardial contrast echocardiography (MCE) detected both lower grade stenoses and abnormalities of perfusion at lower doses of dobutamine than wall motion assessment. Furthermore, MCE identified a larger volume of abnormal

myocardium than wall motion assessment. These findings particularly applied in cases of single vessel stenosis compared to multivessel stenosis

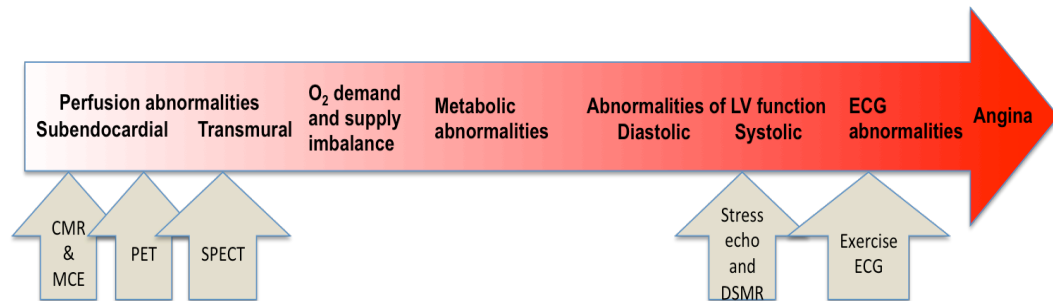


Figure 1.3: The ischaemic cascade.

Diagnostic investigations target different steps on the pathway as marked.

Targeting earlier steps may result in increased test sensitivity.

Exercise-ECG testing detects ECG changes and angina. Stress echocardiography and CMR detect wall motion abnormalities. Perfusion imaging is considered in more detail below.

CMR ischaemia testing by wall motion assessment

Ischaemia detection by wall motion assessment requires the use of pharmacologic or exercise stress. Pharmacologic stress involves administration of a standard dobutamine/atropine protocol to achieve a target heart rate. The occurrence of new wall motion abnormalities during increasing doses of dobutamine is considered diagnostic of ischaemia. Nagel et al³⁰ were the first to validate dobutamine CMR for the detection of CAD. Dobutamine CMR

performed better than stress echocardiography in the identification of CAD using at least 50% stenosis on coronary angiography as the gold standard. CMR sensitivity and specificity in this study of 208 patients were 88.7% and 85.7% respectively. Many validation studies have been performed and reported similar results since. However as the studies are relatively small the confidence intervals are often wide. Nandalur et al³¹ pooled the data from 14 studies and 724 patients and confirmed good sensitivity (83%; 95% CI 79-88%) and specificity (86%; 95% CI 81-91%) of stress induced wall motion abnormalities against X-ray coronary angiography for the detection of CAD. It is noteworthy that there was a high prevalence of CAD (70.5%) in the 735 participants included in the 13 studies combined.

High dose dobutamine-atropine stress CMR is safe in addition to being effective. In a series of 1000 patients³² adverse events included one case (0.1%) of sustained and four cases (0.4%) of non-sustained ventricular tachycardia, 16 cases (1.6%) of atrial fibrillation, and two cases (0.2%) of transient second degree AV block.

Exercise stress CMR is also technically possible using a specific MRI-compatible cycle ergometer. Recent work suggests that it may be possible to overcome some of the technical limitations, such as motion and difficulties in breath holding by using real time exercise stress CMR images³³. However at present exercise stress is not in routine clinical use despite good preliminary clinical results³⁴.

Non-invasive assessment of myocardial perfusion

A number of different modalities have been developed for imaging myocardial perfusion. In order to understand these imaging techniques some knowledge of the myocardial blood supply is required.

Coronary physiology

Under resting conditions myocardial oxygen extraction from the blood is very high-around two thirds of the available oxygen. Myocardial perfusion is therefore tightly controlled by autoregulation and in normal hearts perfusion can increase up to 3 or 4 fold within seconds in response to an increase in demand.

The coronary circulation is divided into three functional compartments (figure 1.4). The proximal compartment, represented by the epicardial arteries, has a capacitance function. The mid compartment consists of pre-arterioles and the distal compartment is made up of arterioles. The function of the pre-arterioles is to maintain a constant pressure at the origin of the arterioles. Proximal pre-arterioles respond to shear stress and higher flows result in flow-mediated dilatation. Distal pre-arterioles are more pressure-responsive and dilate in response to increased intravascular pressure under myogenic control. The arterioles and endothelium have an important role in the regulation of myocardial perfusion. They have a high resting tone and dilate in response to the release of metabolites by the myocardium as a result of an increase in

oxygen consumption³⁵. Blood flow through the coronary system is regulated almost entirely by this vascular response to local demand.

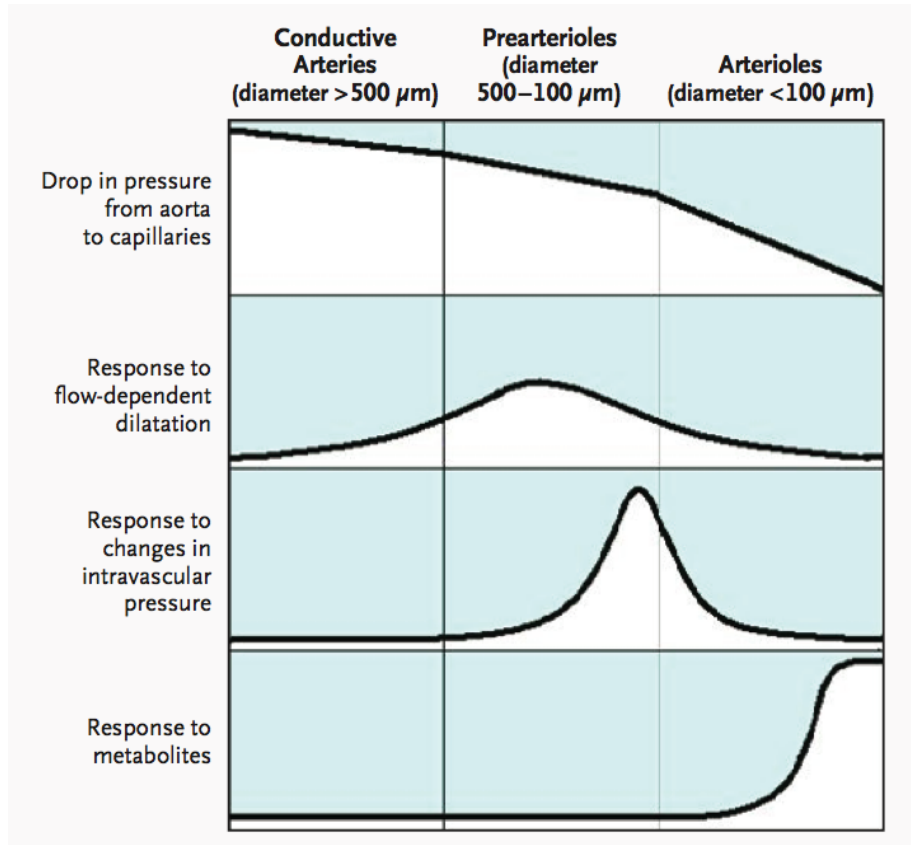


Figure 1.4: The coronary circulation.

The three functional compartments of the coronary circulation are shown together with an illustration of the associated pressure changes and their responsiveness to shear stress, pressure and metabolites. From ³⁶.

At rest, myocardial perfusion is in the region of 0.5-1.0 millilitres/minute/gram (ml/min/g), which is equivalent to approximately 5% of the total cardiac output. In the presence of obstructive CAD rest perfusion is maintained by autoregulation until the mean diameter stenosis reaches approximately 85%³.

Hyperaemic perfusion however begins to reduce in the presence of stenoses of approximately 40%³. Myocardial perfusion imaging must therefore be performed during hyperaemia to detect flow-limiting CAD. Coronary vessel wall structure³⁷ and their epi to endocardial direction coupled with high left ventricular systolic pressures³⁸ result in the endocardium being more vulnerable to ischaemia than the epicardium. High-resolution imaging techniques, which can differentiate the endo and epicardial layers, may therefore be more sensitive than lower resolution techniques.

Stress perfusion imaging

The most physiological and therefore best stressor to achieve coronary hyperaemia is exercise. However this is frequently impossible or difficult due to limitations related to the imaging technique or the patient. Imaging frequently requires the patient to be still or within a scanner limiting their ability to exercise. In addition patient motivation or comorbidity may prevent them from achieving hyperaemia through exercise. As a result pharmacologic agents are frequently used to achieve hyperaemia. Vasodilators (adenosine, dipyridamole) are the preferred agents however catecholamines (dobutamine) can also be useful. Adenosine is used most frequently and induces hyperaemia by A_{2A} receptor mediated vasodilation of the smooth muscle cells of coronary vessels. Dipyridamole indirectly activates the same pathway by inhibiting the cellular uptake of adenosine and, consequently, increasing its interstitial concentrations. The excess adenosine nonselectively activates all adenosine receptor subtypes, including the A_{2A} receptors, resulting in vasodilation.

Unfortunately adenosine is not a selective A_{2A} receptor agonist and stimulation of A₁, A_{2B}, and A₃ receptors frequently results in adverse effects. These are usually self-limiting and include flushing, chest pain, dyspnoea, dizziness, and nausea. However despite being medically trivial these symptoms can be distressing to the patient. Rarely, more serious adverse events, including bronchospasm (mediated by the A₁, A_{2B}, and A₃ receptors), atrioventricular block (A₁ receptor), and peripheral vasodilation (A_{2B} receptor) resulting in hypotension can occur. Adenosine is thus contraindicated in subjects with asthma, advanced atrioventricular block or severe hypotension.

Most published studies have used adenosine or dipyridamole however newer, more selective A_{2A} agonists such as regadenoson appear to provide equivalent diagnostic information with an improved adverse effect profile³⁹.

Qualitative versus quantitative assessment of perfusion

Broadly, myocardial perfusion can be assessed qualitatively or quantitatively. Qualitative assessment relies on the presence of a normally perfused area of myocardium. Abnormal areas can then identified as they have relatively less perfusion in comparison. The main advantage of this approach is that it is simpler to implement and does not require complex image post-processing allowing rapid interpretation and reporting of studies.

However, in general, quantification of images results in more precise and user-

independent results⁴⁰. Absolute quantification of myocardial perfusion involves calculating myocardial perfusion in ml/min/g and is therefore not dependent on the presence of a normally perfused region of myocardium. Full quantification has proven benefits and also potential advantages over non-quantitative methods⁴¹. The benefits of quantitative perfusion have been largely confirmed by PET studies. The PET-derived ratio of the absolute stress to rest perfusion values, known as the coronary flow reserve (CFR) or myocardial perfusion reserve (MPR), decreases in proportion to the coronary artery luminal diameter stenosis. CFR and MPR can thus be used for the diagnosis of CAD^{42 43}. Recent studies using ¹³N-ammonia PET have also demonstrated that an abnormal MPR is an independent predictor of an adverse prognosis^{44, 45}. Furthermore, quantitative data also provides unique information about the coronary microcirculation which is not available from non-quantitative methods³⁶.

In addition to these proven benefits, more precise, user-independent, quantitative measurements of myocardial perfusion should allow more robust assessment of perfusion in cases where visual assessment is difficult such as multivessel disease, severe left ventricular impairment and after CABG. Moreover, it may eventually allow the definition of thresholds of perfusion associated with myocardial ischaemia⁴⁶ and viability both of which are known to be important for selecting patients for revascularization procedures.

However, in order to be clinically useful, techniques for non-invasive quantification of myocardial perfusion must fulfil a number of criteria. Firstly

they must be validated against gold-standard techniques to ensure accuracy of the results. Secondly they must be reproducible-intra and inter-observer and inter-study reproducibility must be within acceptable limits. Thirdly imaging and post-processing methods must be widely available. Fourthly methods must be quick and automated insofar as possible. Overly time-consuming methods will not be used or cost-efficient. Finally they must be acceptable to the patient.

The following section considers the different modalities available for non-invasive assessment of myocardial perfusion. Each modality is outlined including: a description of the method, advantages, diagnostic and prognostic performance and finally their limitations. This comparison between the various methods is summarised in table 1.1 on page 45.

For the detection of CAD all of the imaging methods are reported to be very accurate with high sensitivity and specificity. However although these data are presented together caution is required when comparing methods. The accuracy of any test will vary depending on the prevalence of the condition under consideration and on other factors specific to the population being tested. Studies tend to include a high proportion of patients with CAD, which will often improve the accuracy of the imaging technique but may not reflect its performance in other cohorts of patients.

Non-invasive myocardial perfusion imaging

Nuclear perfusion techniques

Nuclear perfusion techniques involve the administration of a radioisotope, which emits gamma photons by radioactive decay. Uptake of the radioisotope by the heart is related to myocardial perfusion. Detection of the radioisotopes by a gamma camera thus allows assessment of myocardial perfusion.

Single Photon Emission Tomography (SPECT)

Description and Advantages

Cardiac SPECT uses radiotracers, which emit single photons, particularly thallium-201, and technetium-99m, which are extracted from the circulation as a function of blood flow. Comparison of stress and rest imaging allows the identification of regions of reduced perfusion compared to remote normal regions. Stress imaging can be performed during exercise, pharmacological stress or a combination of both. Modern gamma cameras have resulted in faster imaging and studies can now be completed within minutes. SPECT is widely available, well established and effective. It has a robust evidence base and most evidence today supporting the concept of ischaemia imaging as an essential part of the workup of these patients comes from SPECT imaging.

Diagnostic and Prognostic Performance

There are a large number of studies evaluating the diagnostic performance of SPECT imaging. These studies have reported high sensitivity and moderate to

high specificity for the detection of CAD. The reported sensitivity and specificity of exercise SPECT when compared with invasive angiography range between 85–90% and 70–75%, respectively⁴⁷. Furthermore, there is a very extensive literature demonstrating that SPECT imaging provides prognostic information. In one meta-analysis of 39,173 patients with a mean follow-up of 2.3 years a normal scan was shown to predict a good outcome (0.6% annual rate of non-fatal myocardial infarction or cardiac death). Conversely an abnormal scan predicts a significantly higher risk of myocardial infarction or death (5.9% annual event rate over 3 years in the same meta-analysis)¹⁰.

Limitations

Nuclear techniques involve the use of ionising radiation which is particularly important in younger patients or when repeated examinations are required. Spatial resolution of SPECT is also sub-optimal-in the region of 10x10mm. This has been proven to be clinically relevant as it is less accurate for the detection of subendocardial myocardial infarction than CMR⁴⁸. Lower spatial resolution also limits the detection of transmural differences in perfusion, which translates to a lower sensitivity for moderate stenoses compared to CMR⁴⁹.

Positron Emission Tomography (PET)

Description and Advantages

PET uses positron-emitting radiotracers with physical properties identical to naturally occurring elements and emission-computed tomography to produce images of myocardial perfusion (and also metabolism). Radiotracers emit

positrons from their nuclei; these positrons collide with electrons and the ensuing annihilation reaction results in the emission of two photons travelling in opposite directions. The PET scanner detects photons and only registers events when paired photons are detected by opposing detectors (temporal coincidence). This temporal coincidence results in improved accuracy compared to SPECT. Myocardial perfusion is evaluated using ^{13}N -ammonia, ^{15}O -water or $^{82}\text{Rubidium}$.

Advantages of PET imaging include the ability to fully quantify myocardial perfusion, superior resolution to SPECT and a lower radiation dose than SPECT (see table 1.1).

Diagnostic and Prognostic Performance

PET has been shown to be more accurate than SPECT for the diagnosis of CAD⁵⁰ against coronary angiography with a meta analysis including 1442 patients demonstrating 92% sensitivity and 85% specificity. Furthermore, the prognostic value of PET myocardial perfusion imaging has also been demonstrated in several studies with abnormal scans associated with an increase in adverse cardiac events and mortality^{51 52 53}. One study of 685 patients followed up for a mean of 3.4 years demonstrated that the prognostic utility is similar to SPECT. A normal PET study was associated with 0.9% annual cardiac mortality and a 4.3% rate in those with abnormal scans⁵².

Limitations

Disadvantages of PET include the use of ionizing radiation and inferior spatial resolution compared to CMR. The main limitation of PET-imaging however is the requirement for an on-site cyclotron to produce many of the radiotracers with resulting high costs and limited availability.

Myocardial contrast echocardiography (MCE)

Echocardiographic evaluation of ischaemia usually involves the identification of wall motion abnormalities, which occur during pharmacological or exercise stress. However perfusion can also be evaluated using MCE.

Description and Advantages

Echocardiography contrast agents contain microbubbles. Contrast agent is infused intravenously until a steady state is reached within the circulation. The bubbles within the imaging field are then destroyed by high-energy ultrasound.

Microbubbles remain within the intravascular space and the rate of microbubble replenishment reflects myocardial perfusion. This method can be used with pharmacological stress to detect regions of hypoperfusion.

Evaluation of this microbubble replenishment can be qualitative or quantitative.

The rate of replenishment can be used to calculate blood velocity and subsequently absolute perfusion. MCE is a non-ionising, relatively low-cost technique with high spatio-temporal resolution.

Diagnostic and Prognostic Performance

MCE also been reported to be accurate for the detection of CAD with a sensitivity of 82% and specificity of 80% in a combined analysis including 1088 patients⁵⁴. Furthermore, there is evidence from a retrospective study that MCE can also provide prognostic information with abnormal perfusion associated with a higher rate of death and non-fatal myocardial infarction in 788 patients followed up for 1.7 years⁵⁵.

Limitations

MCE can be limited by poor acoustic windows and endocardial definition.

Despite the evidence behind MCE uptake of this technique has been limited due to difficulties performing the examinations compared to wall motion assessment and a lack of suitable expertise.

Computed Tomography

Description and Advantages

Computed tomography (CT) is a rapidly emerging cardiovascular imaging modality and can assess left ventricular function⁵⁶, and potentially perfusion and viability⁵⁷. CT perfusion imaging is similar to CMR in that the first pass of a contrast agent into the myocardium is imaged. During hyperaemia perfusion of contrast into the myocardium subtended by vessels with flow-limiting CAD does not increase as much as perfusion of contrast into myocardium supplied by normal vessels resulting in perfusion defects. In contrast to CMR perfusion imaging, which is dynamic, CT perfusion usually involves acquisition of a single

image of the first pass of contrast agent in order to limit the dose of radiation.

There are however small studies demonstrating the feasibility⁵⁸ and validity⁵⁹ of continuous imaging of the first pass and subsequent quantitative evaluation of perfusion.

Advantages of CT perfusion imaging include rapid data acquisition at very high spatial resolution. Another potential advantage is the possibility of a single comprehensive cardiac examination incorporating anatomy (coronary angiography and scar) and function (LV function and perfusion).

Table 1.1: Summary of non-invasive myocardial perfusion imaging modalities.

<i>Modality</i>	<i>SPECT</i>	<i>PET</i>	<i>MCE</i>	<i>CT</i>	<i>CMR</i>
Ionizing radiation	+++ 13-25mSv ⁶²	++ 2.5-18mSv* ⁶²	-	+++ 11-21mSv ^{57, 63}	-
Spatial resolution (in plane)	+ ~10x10mm	++ ~5x5mm	++++ ~0.1x0.1mm	++++ ~0.5x0.5mm	+++ ~3x3mm
Availability	++++	++	+	+	+++
Cost***	~£300	~£2500	~£200 ⁶⁴	?	~£500
CAD detection					
n	4480	1442	1088		1516
Prevalence	76%	77%	69%		57%
Sensitivity	0.87 (0.86–0.88)	0.92 (0.90–0.94)	0.82 (0.76–0.88)		0.91 (0.88–0.94)
Specificity	0.73 (0.70–0.76) ⁶³	0.85 (0.79–0.90) ⁵⁰	0.80 (0.73–0.87) ⁵⁴		0.81 (0.77–0.85) ³¹
Prognostic value					
n	++++ >39000	+++ >2400	+		++ 513 (prospective)
Follow-up (yrs.)	2.3	3.4	788 (retrospective) 1.7		2.3
Fully-quantitative	+	+++	++	+	++

*dependent on tracer used and whether CT also done. ***approximate cost of the examination in UK

Diagnostic and Prognostic Performance

Small single-centre studies have recently demonstrated that CT perfusion is accurate compared to SPECT⁶⁰, CMR⁶¹ and coronary angiography⁵⁷.

Limitations

CT perfusion techniques are not currently well established and its main strength at present is coronary artery imaging. The major disadvantage of CT is its significant radiation exposure particularly if coronary angiography, function, perfusion and viability are all studied or when repeated examinations are required. The quality of CT data is also compromised by tachycardia, which can cause problems when pharmacologic stress is used. Furthermore the risk of contrast nephropathy with iodinated contrast agents limits its use in patients with renal dysfunction.

CMR perfusion imaging

Description and Advantages

Magnetic resonance describes a property of elements with an uneven number of protons and neutrons to rotate or “spin” around their axis. In a strong magnetic field these spins align parallel or anti-parallel to the external magnetic field. A small excess of spins align parallel to the field producing a detectable net magnetisation vector. For clinical magnetic resonance imaging hydrogen nuclei are imaged due to the abundance of these nuclei in human tissue.

Radiofrequency waves are transmitted into the heart (RF pulse) and cause a brief excitation and subsequent relaxation of the hydrogen nuclei. Excitation of

the hydrogen nuclei results in two important changes to the net magnetisation vector. Firstly it tips in the longitudinal direction out of alignment with the external magnetic field. Secondly the RF pulse causes the spins to rotate together or in phase in the transverse direction. Following this excitation the net magnetisation vector returns to baseline, which is termed relaxation. This relaxation is exponential and the rate of relaxation is defined by two parameters known as T1 and T2. T1 describes the time it takes for 63% of the longitudinal magnetisation to recover after a 90-degree displacement. T2 describes the transverse relaxation as the spins de-phase. Relaxation is associated with energy release, which can be detected by receiver coils, which act like antennae. This can then be converted to images by Fourier transformation. T1 and T2 values vary according to the tissue composition and this can be exploited to produce an intrinsic contrast between different tissues.

CMR first pass perfusion imaging was first introduced in 1990. A bolus of contrast agent is injected into a peripheral vein and a series of images are acquired during the first pass of the contrast agent into the myocardium. High temporal resolution is required in order to image multiple regions of the heart repeatedly during transit of the contrast agent. Perfusion imaging is based on the same principles as described above. Modern perfusion imaging uses single-shot fast gradient echo based sequences. A non-selective 90-degree (saturation) RF pulse starts the sequence as this is independent of heart rate and magnetization history and also results in a heavily T1-weighted image. This is important as the contrast agent contains chelated gadolinium, which shortens myocardial T1 and therefore allows differentiation of tissues based on their

gadolinium content during subsequent imaging. This process is repeated for each slice of myocardium imaged every 1-2 heartbeats. During hyperaemia perfusion of contrast into the myocardium subtended by vessels with flow-limiting CAD does not increase as much as perfusion of contrast into myocardium supplied by normal vessels. These regions contain less gadolinium and therefore less signal after the saturation pulse and are dark compared to the normally perfused regions, which are bright. In the clinical setting this is usually interpreted qualitatively as a defect in the contrast perfusion into the myocardial wall visible with stress but not at rest. However quantitative evaluation is also possible as discussed below.

Advantages of CMR include freedom from ionising radiation, high quality images and most importantly, the generation of a complete workup incorporating LV volumes and function, myocardial viability and scar, as well as ischaemia within a single study lasting approximately one hour.

Diagnostic and Prognostic Performance

There are a number of single-centre studies and a few multi-centre trials comparing CMR to established methods of detecting myocardial ischaemia. In a meta-analysis³¹, perfusion CMR was assessed using data from 24 studies and 1516 patients resulting in a sensitivity of 91% (95% CI 88 to 94%) and a specificity of 81% (95% CI 77 to 85%) against X-ray coronary angiography.

MR-IMPACT was the first multi-centre perfusion CMR trial comparing CMR and

SPECT for the detection of myocardial ischaemia⁶⁵. Perfusion CMR was determined to be non-inferior to SPECT for the detection of CAD with $\geq 50\%$ stenosis on quantitative X-ray coronary angiography as the reference standard. This was however a dose-finding study and only 42 patients formed the CMR cohort on which this analysis was based.

The larger and more recent CE-MARC study⁶⁶ extended these findings and found CMR to be superior to SPECT for the diagnosis of CAD. 628 patients with suspected angina underwent SPECT, CMR and X-ray coronary angiography. The CMR protocol included coronary angiography, functional, and scar imaging in addition to perfusion imaging. The sensitivity and negative predictive value of CMR were significantly better than SPECT imaging. Furthermore area under the receiver operating characteristic (ROC) curve was significantly higher for stress perfusion CMR compared to SPECT.

One of the difficulties in validating all non-invasive methods for the detection of myocardial ischaemia is the absence of a clear gold standard for comparison. The studies discussed above use coronary angiography as the gold standard with the limitations discussed previously in this article. For a more direct comparison of invasive versus non-invasive physiological measurements, CMR has been validated against FFR. These studies have also revealed overall good agreement between the two methods with CMR perfusion sensitivities ranging from 88%-92.9% and specificities from 56.7%-94%⁶⁷⁻⁶⁹.

Jahnke et al¹² demonstrated that CMR perfusion imaging can also provide prognostic data. In a study of 513 patients an abnormal perfusion imaging was associated with a significantly higher incidence of cardiac death or non-fatal myocardial infarction over a median 2.3-year follow-up period.

Limitations

CMR perfusion imaging has a number of limitations at present. The main disadvantages are that imaging is contraindicated in patients with certain implants e.g. pacemakers, limited availability and rarely reduction of imaging quality due to patient claustrophobia, poor gating or patient motion. Other limitations are specific to perfusion imaging. Most CMR images (for example cines and scar imaging) are reconstructed from a number of cardiac cycles using ECG gating. This is not possible with perfusion imaging as it is necessary to image the first passage of the contrast through the myocardium. As a consequence of the increased temporal resolution required to do this spatial resolution is reduced and imaging is more prone to artefacts. Dark rim artefacts (DRA) are the most problematic type of artefacts for perfusion imaging and are discussed in more detail in chapter 3.

Quantification of myocardial perfusion with CMR

Quantification of perfusion with CMR can be sub-divided into semi and fully quantitative analysis.

Semi-quantitative analysis

Initial progress towards quantification with CMR involved the use of semi-quantitative methods. These techniques make use of the changes in signal intensity within a region of interest over time-the time intensity curve. The myocardial time intensity curve is compared at stress and rest to calculate an index of perfusion reserve. The upslope of this curve is usually used for this calculation but the initial area under the curve and the amplitude have also been used. These methods have been validated in animal models^{70, 71} and can improve the diagnostic accuracy over visual analysis alone in humans⁷². Whilst these methods are widely accepted and available they are not routinely used outside clinical studies, probably as the post-processing required is not felt to add sufficient value to visual assessment-alone.

Fully quantitative analysis

Full quantification also involves interrogation of signal intensity curves. Calculating absolute perfusion from these curves requires the use of complex mathematical models that fit the kinetics of the gadolinium contrast medium. Two main models for quantification of absolute myocardial perfusion have been described namely the linear time-invariant model, including Fermi constrained deconvolution, and the compartment model.

Both models make a number of assumptions that must be upheld in order to accurately calculate perfusion and sufficient myocardial contrast to noise ratio and reasonable linearity of signal intensity in the blood and myocardium are

crucial with both methods for accurate quantification.

This causes a problem, as at lower doses of contrast agent there is a linear relationship between contrast agent concentration and signal intensity.

However at higher doses of contrast agent, which are required for visual analysis and high myocardial CNR, T1-saturation effects occur with loss of this linearity⁷³. Signal attenuation is particularly a problem in the LV cavity where the signal intensity-time curve usually represents the arterial input function (AIF). Potential solutions to this problem are the use of:

1. a low dose of contrast, e.g. 0.025-0.05 mmol/L with a strongly T1-weighted sequence for the whole perfusion study,
2. one low-dose and one high dose injection of contrast agent for each perfusion acquisition-the dual bolus technique,
3. or a hybrid perfusion sequence that obtains a separate image for the AIF on each heartbeat.

Quantification with a low-dose techniques have been demonstrated to be feasible and accurate⁷⁴. However, this approach is limited by a low contrast to noise ratio (CNR) in the myocardium and images which are sub-optimal for visual interpretation⁶⁵.

The dual bolus technique uses a low dose of contrast to calculate the AIF without signal saturation and a subsequent higher dose to preserve myocardial CNR. Christian et al demonstrated in dogs that this allows accurate measurement of absolute epicardial and endocardial perfusion across a wide

range of blood flow rates⁷⁵. In a subsequent comparison of single and dual bolus methods both single-bolus (0.025 mmol/kg) and dual-bolus (0.0025 mmol/kg and 0.10 mmol/kg) perfusion methods correlated closely with perfusion, but with greater signal and contrast in the dual-bolus images⁷⁶. Furthermore, the dual-bolus method provided more accurate measurements when smaller myocardial regions were analyzed which is likely to be as a result of the higher myocardial signal. Another study⁷⁷ demonstrated that the dual-bolus technique (0.005 mmol/kg and 0.05 mmol/kg) was superior to a single-bolus (0.05 mmol/kg) protocol for the assessment of myocardial perfusion reserve (MPR) with the dual bolus associated with a reduced coefficient of variation.

A hybrid perfusion sequence has also been shown to be an alternative method to overcome this problem⁷⁸. However, experience with this method is much more limited.

Validation of CMR quantitative perfusion

Fully quantitative measurement of myocardial perfusion by CMR has been validated in a number of animal and human studies however these studies have used a number of different methods for quantification.

Animal models allow validation of measurements against microspheres, which are a pathological gold standard of regional perfusion. CMR perfusion measurements have been validated against microspheres using model-independent deconvolution and low-dose contrast agent and also Fermi function deconvolution and a dual bolus method^{75, 76}. CMR-derived perfusion

values in these studies correlated very strongly with microsphere measurements.

In human studies validation has been performed in patients with CAD against FFR using high dose contrast agent and Fermi deconvolution⁶⁸ and also against CFR⁷⁹ using a dual bolus of contrast agent and a compartmental analysis method. The former study demonstrated that the MPR from quantitative CMR perfusion imaging detected significant CAD (FFR ≤ 0.75) with high sensitivity (93%) but only modest specificity (57%). The latter demonstrated a strong correlation between MPR and invasive Doppler derived CFR measurements and that MPR < 2 had high sensitivity and specificity (88% and 90% respectively) for predicting CFR < 2 .

Finally three previous studies have validated CMR and PET measures of quantitative perfusion in healthy volunteers as discussed in more detail in chapter 4. Two of these studies used compartmental analysis to obtain quantitative CMR perfusion whilst the third used model independent deconvolution.

Measurements obtained with CMR in all of these human studies both at rest and with adenosine stress are in the same ranges as published values from other methods of measuring myocardial perfusion⁸⁰.

However all of these studies are relatively small and important differences exist between the CMR techniques used including the use of different pulse

sequences, contrast agents and delivery regimens, doses of gadolinium and models for quantification. As a consequence of the complexity of full quantification current techniques require expertise and time-consuming post-processing. We remain some considerable way from achieving methodological consensus and full quantification remains a new and developing application for CMR. This is in contrast to many other areas of CMR practice, that are performed routinely in clinical practice according to standardised international evidence-based guidelines⁸¹.

CMR assessment of viability

CMR is the gold standard for evaluation of LV volumes and function, which are routinely obtained during any CMR examination. CMR viability assessment is achieved using low dose dobutamine (functional response), late gadolinium enhancement (LGE) scar imaging (morphologic assessment of viability), or a combination of both methods. A comparison between PET and low dose dobutamine CMR demonstrated close agreement between the two techniques for the assessment of viability with CMR sensitivity of 88% and specificity of 87% compared to PET⁸². When contractile improvement post revascularisation, rather than PET, is considered to be the gold standard dobutamine CMR maintains a high specificity and sensitivity although the sensitivity may be reduced with more severely impaired baseline LV function⁸³.

LGE scar imaging correlates very closely with post mortem infarct assessment in animals⁸⁴ and also with PET data in humans⁸⁵. When contractile

improvement post revascularisation is taken as the gold standard LGE can predict viability as demonstrated in a seminal paper in 2000⁸⁶. This study demonstrated that transmural extent of LGE and the likelihood of functional recovery following revascularisation are inversely related. The positive and negative predictive values of this technique vary according to the extent of scar that is taken as a cut-off value to define viability. These values also vary depending on whether all segments or only the most dysfunctional are considered. For example, using a cut-off >25% transmural extent of scar and considering all segments, the positive and negative predictive values are 71% and 79%. When only akinetic or dyskinetic segments are considered this increases to 88% and 89%. On the other hand if a 50% cut off value is used and all segments considered, the negative predictive value increases to 92% but the positive predictive value falls to 66%. This is clinically important as patients with scar of intermediate transmural extent (1-50%) have an intermediate chance of recovery of function following revascularisation (figure 1.5) so LGE-alone is not a good discriminator in these patients.

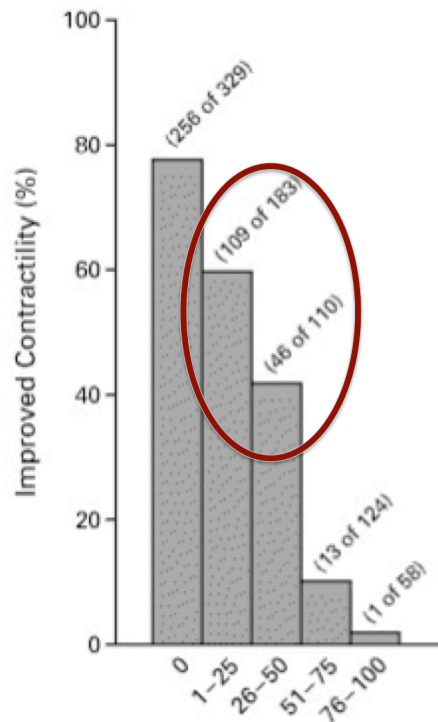


Figure 1.5: Relationship between scar transmural extent and the likelihood of improved function after revascularization.

These data are based on all dysfunctional segments in a study of 50 patients.

The ring draws attention to the fact that an intermediate extent of scar is associated with an intermediate likelihood of recovery. Adapted from⁸⁶.

Wellnhofer et al⁸⁷ compared dobutamine and LGE CMR for the prediction of viability in 29 patients and found dobutamine CMR to be slightly superior in predicting recovery after revascularisation. LGE CMR predicted 73% of hibernating segments correctly compared to 85% correctly predicted by low-dose dobutamine. This difference was particularly relevant for myocardial segments with an intermediate extent (1-74%) of LGE (figure 1.6).

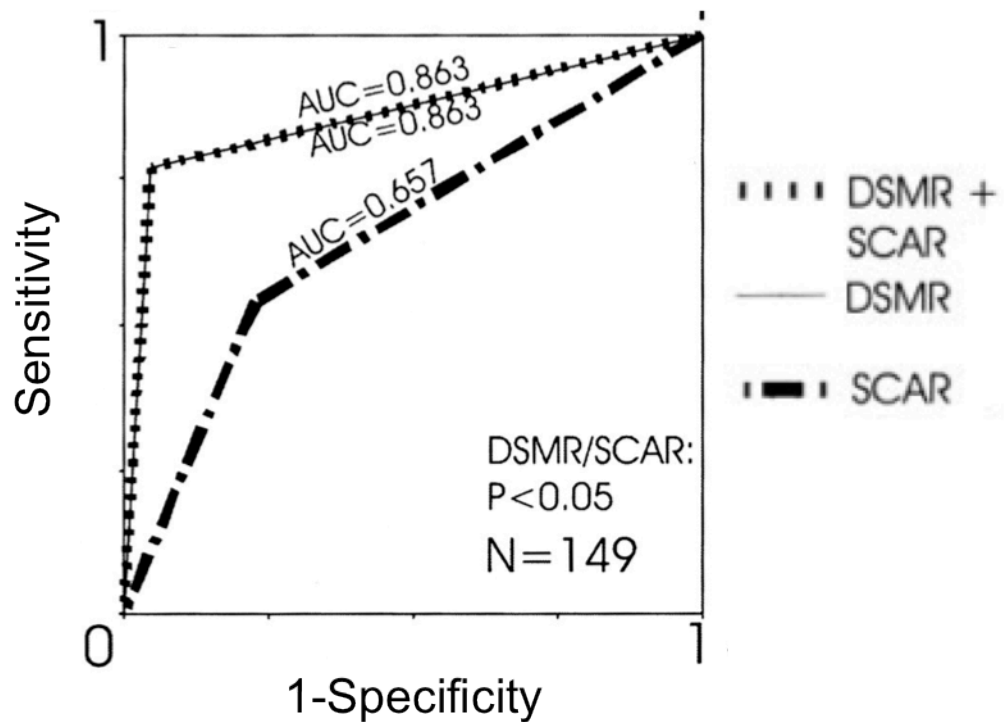


Figure 1.6: Low-dose dobutamine versus scar imaging for viability assessment.

ROC curves demonstrate significantly higher area under the curve for predicting recovery after revascularisation with low dose dobutamine alone or low dose dobutamine and scar compared to using scar alone. These data are based on 149 dysfunctional segments in a study of 29 patients using a cut-off of 25% scar transmural. Adapted from ⁸⁷.

These findings are supported by another study of 48 patients which demonstrated that 42% of segments with 50-75% LGE show contractile reserve during low dose dobutamine stimulation whereas 58% did not⁸⁸.

LGE and low dose dobutamine are both therefore useful with some evidence from small studies to suggest that a combination of both is optimal. However both clearly also have limitations and, as with ischaemia testing, there is no clear gold standard for validation purposes.

Additional value from CMR imaging

CMR examination of patients being worked-up for coronary revascularisation frequently provides the clinician with other valuable data including prognostic information and even alternative diagnoses. High spatial resolution allows for analysis of the distribution of the scar within the myocardial wall and differentiation of ischaemic from dilated cardiomyopathy⁸⁹. Such additional information obtained from CMR is clinically relevant as demonstrated in a registry of 11,040 patients⁹⁰. A CMR examination for suspected coronary artery disease or ischaemia assessment resulted in a new, previously unsuspected diagnosis in 19.6% of patients. Furthermore patient management was influenced in >70% of these patients. Similarly, 23% of patients with suspected CAD but no history or ECG evidence of prior myocardial infarction have a myocardial infarction detected by LGE⁹¹. This has prognostic implications as detection of even a very small scar is associated with a >7-fold increase in major adverse cardiovascular events. Finally, there are also data to suggest that scar detected by CMR is a stronger predictor of adverse clinical outcome than left ventricular ejection fraction and volumes⁹².

CMR coronary angiography is also possible and the technique has evolved over the years^{93, 94}. It may form a useful component of a comprehensive CMR study for CAD⁶⁶. However coronary artery imaging with CMR is still a cumbersome method with a higher failure rate, longer scan times and lower positive predictive than CT.

Clinical applications

CMR provides the clinician with comprehensive and clinically relevant information about patients with CAD who are being considered for revascularisation. The first question that can be answered after the CMR examination is whether revascularisation should be undertaken at all. From the available evidence it is safe and probably preferable to defer revascularisation in the absence of demonstrable ischaemia or LV dysfunction with significant viability regardless of the coronary anatomy.

The second question that can be answered is which vessel should be revascularised. Pre-procedural CMR assessment in complex patients allows targeted PCI and avoids treatment of inappropriate lesions and therefore potentially will reduce complications whilst maximising benefit.

The CMR information will also be useful to a surgeon by determining the likely benefits from CABG and also in guiding the surgical approach for example targeting the best quality conduits and choosing between minimally invasive and open surgery. CMR data will be useful to retrospectively compare outcome

in patients undergoing complete anatomic and complete functional revascularisation, although prospective randomized data on this are unlikely to be forthcoming in the near future.

Finally, in addition to guiding the management strategy information obtained from a CMR examination allows more accurate risk stratification of patients with stable CAD. This is important for all patients with stable CAD, regardless of the treatment strategy, as it provides a platform for meaningful discussions about care with patients and their families.

Summary and objectives

Despite the advances in the treatment of CAD it remains an important disease and many patients continue to experience preventable morbidity and mortality. One of the main management decisions concerns which patients and lesions should be revascularised. Revascularisation carries a risk to patients and so it is important that in deciding whether it is appropriate we obtain as much information as possible. From the available evidence it is clear that information on coronary anatomy alone is often insufficient to make this decision and it is crucial to know also about myocardial ischaemia and viability.

CMR provides a safe, non-invasive and comprehensive assessment, which yields valid, reliable information on pathophysiology in patients with stable CAD.

However, all current imaging modalities, including CMR, have limitations. CMR hardware and software continue to improve, allowing faster, higher-resolution

imaging and the potential for the development of new techniques. One such development is the emerging field of quantification of myocardial perfusion. Absolute quantification has been shown to be feasible and there are some data supporting its validity. However, thus far, it remains challenging and consequently the necessary expertise and availability are limited. Viability assessment may also benefit from the development of new techniques and also more data to define its exact role in patient care.

The objective of this work was to evaluate and validate emerging CMR methods for guiding revascularization in a series of clinical studies with a particular focus on perfusion imaging. Firstly, we compared an advanced high-resolution perfusion sequence with a standard sequence in a phantom, in volunteers and in patients and tested a number of different contrast agent doses. Visual and quantitative analysis of this sequence were subsequently used in validation studies against PET perfusion imaging and invasive coronary angiography. We have also examined the inter-study reproducibility of quantitative perfusion imaging. In addition we have evaluated novel, non-perfusion CMR techniques with potential applications in CAD. CMR feature tracking is a tool that permits quantitative analysis of wall motion and may have utility for functional assessment of both viability and ischaemia. A novel sequence for improved scar imaging has also been compared to the standard inversion recovery sequence. Finally a pilot study explored the feasibility of combined CMR imaging and invasive investigations and PCI in a hybrid laboratory.

2 GENERAL METHODS

Study participants

All study participants involved in this work were recruited into a formal research study approved by the local ethics committee and all gave written informed consent to participate in research. Patient information sheets and consent forms from some of the studies are included in Appendix A. Inclusion criteria and study protocols varied for each study and are detailed in the relevant chapters.

All patients undergoing stress perfusion examination were asked to abstain from caffeine and other adenosine antagonists including smoking for a minimum of 24 hours prior to the scan. Patients who admitted having food or drink containing caffeine or other adenosine antagonists during the 24 hours preceding imaging were rebooked if possible. However, patients who failed to abstain from smoking were included regardless as smokers are unlikely to manage complete abstention.

General exclusion criteria, which applied to all studies, are listed below:

Exclusion criteria

1. General exclusions
 - a. Inability to consent
 - b. Pregnancy/Breast feeding
 - c. Medically unstable

2. Contraindication to MRI

- a. implanted electronic devices, metallic foreign bodies, and others according to manufacturer's recommendations and generally accepted guidelines
- b. known claustrophobia
- c. inability to lie flat

3. Contraindication to gadolinium based contrast agent

- a. Estimated glomerular filtration rate $<30\text{ml/min/1.73m}^2$. This level of renal impairment was chosen as Gadobutrol/Gadovist is a cyclic, non-ionic agent with no reported cases of nephrogenic systemic sclerosis and is therefore classified as a low risk contrast agent.
- b. Known allergy to study drugs/contrast agents.

4. Contraindication to adenosine for protocols including stress perfusion imaging

- a. Known significant bradycardia or high-degree atrio-ventricular block
- b. Asthma

CMR protocol

All studies were performed on a Philips MRI 1.5 Tesla or a 3 Tesla Achieva scanner (Philips Healthcare, Best, The Netherlands) using a 32-channel coil

phased array receiver coil and vectorcardiogram (VCG) gating. CMR assessment of volumes, function, scar and wall-motion were performed using standard techniques and in accordance with internationally recognised guidelines published on behalf of the Society for Cardiovascular Magnetic Resonance⁸¹.

A standard CMR protocol for all studies was defined and is shown in figure 2.1. Any deviations from this protocol are described in the relevant chapters.

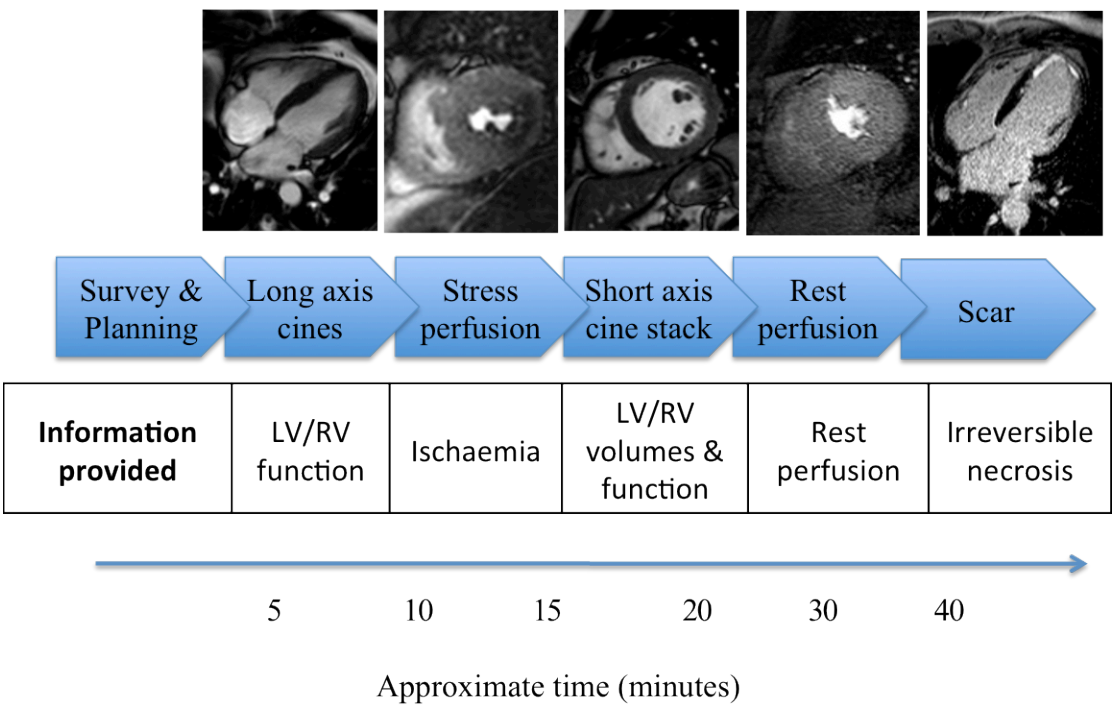


Figure 2.1: Standard CMR protocol.

The standard protocol used for the majority of patient studies. The images acquired with examples are shown with the specific information ascertained from each part summarised at the bottom. Details are provided in the text. For a comprehensive viability assessment low-dose dobutamine can be added to the CMR protocol. However this was not included as part of these studies.

An initial survey and planning allowed the definition of appropriate planes for further imaging.

Functional imaging

Long axis cines in 2, 3 and 4 chamber orientations and short axis cines covering the entire left and right ventricles were acquired using a steady state free precession (SSFP) sequence.

Perfusion imaging

Part of the objectives of this work was to compare and develop perfusion sequences and consequently these sequences are described in more detail in the appropriate chapters.

Prior to entering the scanner room the breath-holding routine was described to participants and the importance of following these commands emphasized.

Perfusion imaging was planned from the systolic phase of the 4 and 2-chamber cines. 3 equally spaced short axis slices at basal, mid and apical left ventricular levels were acquired every heartbeat⁹⁵. This allowed visualization of 16 of the 17 standard myocardial segments⁹⁶ during perfusion imaging. Ten-second test scans without CA using both sequences were performed first and any problems identified were addressed (e.g. artefacts, breath-holding or ECG problems). The imaging geometry and field of view were kept constant for stress and rest perfusion.

For stress imaging 140mcg/kg/minute of adenosine was administered via an intravenous cannula in the left antecubital fossa. Participants' heart rate were monitored continuously throughout the examination by VCG. Blood pressure was monitored non-invasively via a sphygmomanometer on the subjects' right arm prior to commencing adenosine and every 60 seconds during the infusion except during contrast agent (CA) injection. Stress perfusion imaging was commenced 3 minutes into the adenosine infusion and continued for 70 seconds. The adenosine was routinely discontinued at the end of the perfusion sequence. Adenosine was discontinued immediately in the presence of intolerable or severe symptoms (for example significant chest pain, severe respiratory difficulty, at subjects' request), severe (<90 mmHg systolic) or symptomatic hypotension or significant cardiac arrhythmias, e.g. severe bradycardia or high-degree atrio-ventricular block.

Rest perfusion was performed at least 10 minutes after stress perfusion. CA administration during perfusion imaging is described in more detail below.

First-pass perfusion imaging contrast agent delivery-the dual bolus technique

A weight adjusted dose of the gadolinium based CA Gadobutrol (Gadovist, Schering, Germany) was used for all first-pass perfusion imaging.

As discussed in the introduction above, there is a conflict in selecting the optimal dose of CA, with doses producing high myocardial CNR resulting in signal saturation effects, particularly in the LV blood pool where the AIF is determined. We adopted the dual bolus method to overcome this problem.

However since no simple method to deliver a dual-bolus had been described we devised a universal dual-bolus scheme for simple and consistent CA administration and quantification of perfusion⁹⁷.

Important considerations in the design of the dual-bolus method were^{75-77, 98}:

- 1) Both the main-bolus of neat gadolinium contrast agent, and the dilute pre-bolus should be of equal volume and administered at the same flow rate.
- 2) Each bolus should be followed by an equal volume saline flush to maintain a compact contrast agent bolus in the LV chamber.
- 3) The time delay between each bolus of CA can be controlled to minimise temporal overlap, this delay can also be adjusted to heart rate if required.
- 4) The system should be easy to set up.
- 5) The procedure is easy to perform and repeat within a routine clinical or research scan.

The dual bolus set-up involved the use of a saline-filled double-headed power injector connected to a 15cm extension tube to hold the contrast agent. The extension tube was connected to participants via an intravenous cannula placed in the right antecubital fossa. A three-way tap placed between the power-injector and the extension tube allowed the contrast agent to be introduced into the system. This set-up is shown in figure 2.2.



Figure 2.2: Dual-bolus set-up

From left: Both syringes of the power injector (Spectris Solaris® EP, MEDRAD, INC., USA) are filled with normal saline. A length of extendable tubing connects both injector syringes to a 3-way tap. The 3-way tap is connected to a 15cm extension tube, which is then connected to the intravenous cannula. The 3-way tap was positioned outside the bore of the magnet for accessibility. A syringe is connected to the 3-way tap here to demonstrate how both the CA boluses were introduced into the system for perfusion imaging.

Adapted from ⁹⁷.

CA was prepared in advance of all perfusion studies. The dual bolus consisted of equal volumes of dilute and neat CA. The main bolus was a weight-adjusted volume of 1 mol/litre CA. Dilute (10%) CA was prepared by mixing CA with normal saline in a 1:9 ratio. Prior to the commencement of perfusion imaging the power injector was programmed to deliver 2 x 20ml (or 25ml) saline flushes at 4ml/second separated by a 20-second (or 25-second) delay. In the initial studies (chapters 3-5) 20ml and 20-seconds were used respectively. This was increased to 25ml and 25-seconds for all subsequent studies to prevent any overlap in the pre bolus and main bolus SI curves which was observed rarely in the early studies. One of the investigators entered the scan room for perfusion

studies and immediately prior to imaging injected the first bolus via the 3-way tap into the extension tubing. The participant was instructed to breathe gently then imaging was commenced. The power injector was then immediately activated to deliver the first saline flush. This flushed the first bolus into the participants' circulation. During the following pre-programmed delay between power injections the main bolus of contrast agent was injected via the 3-way tap into the extension tubing. At the end of the interval the second saline flush given by the power injector delivered the main CA bolus. During this second flush participants were instructed to take a small breath in and hold their breath for as long as possible to minimise respiratory artefact.

Scar imaging

Scar imaging was commenced 10-15 minutes after a total dose of 0.2mmol/kg of gadolinium and was performed using an inversion recovery turbo gradient echo sequence with the prepulse delay optimized for maximum suppression of myocardial signal. Acquired spatial resolution was 1.6 x 1.8 x 10mm (1.5T) and 1.75 x 1.75 x 8mm (3T) except where stated otherwise.

Invasive catheter laboratory investigations

All invasive studies and interventions were clinically indicated apart from some of the pressure wire data in chapter 9.

X-ray coronary angiography was performed from the right femoral artery according to the standard Judkin's technique. Multiple projections of the

coronary arteries were acquired, after administration of intracoronary isosorbide dinitrate, in at least two orthogonal views, to assess stenosis severity.

PCI was performed using standard techniques, equipment and adjunctive therapy at the discretion of the operator.

3A: PERFUSION IMAGING. Optimisation of the CMR Perfusion

Sequence-Sequence Selection

Abstract

Objectives

Compare image quality, signal to noise ratio (SNR) and contrast to noise ratio (CNR), dark rim and respiratory artefacts using a standard and an advanced, high-resolution perfusion sequence and determine the perfusion sequence to be used for further studies.

Background

Technical advances in CMR perfusion imaging, particularly accelerated data acquisition methods, allow myocardial perfusion imaging with unprecedented spatial resolution. However, it is not clear how implementation of these recent advances affects perfusion image quality, SNR and CNR and the occurrence of important artefacts.

Methods

A standard ultrafast gradient echo perfusion sequence (st-GrE) was compared with an advanced kt-accelerated steady state free precession sequence (kt-SSFP) at 1.5T in a perfusion phantom, healthy volunteers (n=16) and patients (n=32) with known or suspected coronary artery disease. Volunteers were imaged with both sequences at rest and patients underwent stress and rest

perfusion imaging with either st-GrE or kt-SSFP prior to X-ray coronary angiography. Phantom data were used to generate signal intensity curves for SNR and CNR analysis.

A blinded expert scored image quality and respiratory artefact severity and also classified patients for the presence of CAD. The extent, transmural and duration of dark rim artefacts (DRA) as well as SNR and CNR were quantified.

Results

In normal hearts kt-SSFP imaging resulted in significantly improved image quality ($p=0.003$), SNR (21.0 ± 6.7 vs. 18.8 ± 6.6 ; $p=0.009$), CNR (15.4 ± 6.1 vs. 14.0 ± 6.0 ; $p=0.034$) and a reduced extent ($p<0.0001$) and transmural (p=0.0001) of DRA. In patients kt-SSFP imaging resulted in significantly improved image quality ($p=0.012$), and a reduced extent ($p<0.0001$), duration ($p=0.004$) and transmural (p=0.0001) of DRA. Sensitivity and specificity for the detection of CAD against X-ray angiography was comparable with both sequences. There was a non-significant trend towards increased respiratory artefacts with kt-SSFP in both patients and volunteers. Phantom studies demonstrated comparable SNR and CNR for both sequences.

Conclusions

Advanced high resolution CMR perfusion imaging using a kt-accelerated SSFP technique results in significantly improved image quality, SNR and CNR and a reduction in the extent and transmural of DRA compared to a standard

sequence. These findings support the use of advanced perfusion sequences for clinical perfusion imaging and the kt-SSFP sequence for subsequent studies.

Background

Detection of myocardial ischaemia is important, particularly in CAD, for diagnostic purposes, identification of patients with an adverse prognosis¹² and for guiding revascularization^{20, 21} as discussed above. CMR perfusion imaging has become established as a valuable, non-invasive tool for ischaemia detection that is free of ionizing radiation and is at least as reliable other imaging techniques^{31, 65, 66, 99, 100}. However, despite this, the requirement to acquire large amounts of data in a short duration means that perfusion imaging is technically challenging, and still has important limitations. These limitations are most notably that the requirement to maintain high temporal resolution constrains spatial resolution and there is an increased tendency for imaging to be affected by problematic artefacts. Artefacts occur both as a result of the competing constraints of spatial and temporal resolution and of the method of first pass imaging itself. Imaging during the arrival of a concentrated bolus of contrast agent (CA) into the left ventricle contributes to the occurrence of DRA. DRA are a particular concern as they can mimic or hide subendocardial defects resulting in diagnostic errors. These perfusion imaging related demands are in addition to the usual requirements for patient breath holding, and for precise gating with the cardiac cycle, both of which can be more difficult during vasodilator stress. Respiratory artefacts as a result of inadequate breath holding can also compromise study interpretation.

Currently a number of types of sequence, each with different advantages and disadvantages, are used for perfusion imaging. Common sequences include ultrafast gradient echo sequences, single-shot echo planar imaging, hybrid echo

planar imaging and more recently steady-state free precession (SSFP) sequences. Whilst some previous studies have compared perfusion sequences¹⁰¹⁻¹⁰⁵ CMR hardware and software has continued to evolve rapidly and it is not known whether the implementation of more recent advances can address the current limitations associated with perfusion imaging.

Parallel imaging techniques such as sensitivity encoding (SENSE) are now routinely used to accelerate perfusion imaging and this acceleration can be used to improve spatial resolution. However, in practice, this is limited to 2-fold acceleration due to associated artefact and noise penalties¹⁰⁶. Advanced *k-t* acceleration techniques allow higher degrees of acceleration than SENSE and have been proposed more recently as a useful technique to improve the spatial resolution of perfusion imaging even further whilst preserving temporal resolution and cardiac coverage¹⁰⁷.

The objective of this study was to compare a standard perfusion sequence with an advanced, high-resolution method to determine whether there is a measurable difference in performance. We therefore compared a standard turbo field echo (st-GrE) perfusion sequence (ultrafast gradient echo sequence), to an advanced, high-resolution *k-t* BLAST accelerated balanced turbo field echo sequence (kt-SSFP), in normal hearts, in patients with known or suspected CAD and in a perfusion phantom.

Methods

The st-GrE and kt-SSFP perfusion sequences were compared in 16 volunteers, in 32 patients and in a perfusion phantom using the 1.5T MRI scanner. The imaging parameters for both sequences are shown in table 3.1.

Table 3.1: Imaging parameters for the standard (st-GrE) and high-resolution (kt-SSFP) sequences.

<i>Parameter</i>	<i>st-GrE</i>	<i>kt-SSFP</i>
Acquired spatial resolution	2.6 x 2.8 x 10mm	1.7 x 1.9 x 10mm
Echo time (TE)	shortest (range 1.61-1.91ms)	shortest (range 1.29-1.59ms)
Repetition time (TR)	shortest (range 3.6-3.9ms);	shortest (range 2.59-3.18ms)
Flip angle	18°	50°
Prepulse	90°	90°
Prepulse delay*	100ms	100ms
Image acquisition time	140-152ms	80-99ms
Water-fat shift	0.438pixel	0.165pixel
Bandwidth	496Hz	1316 Hz
Acceleration technique	SENSE: factor 2	kt-BLAST factor 5 with 11 training profiles (effective k-t factor 3.8)

*Prepulse delay: time between saturation preparation pulse and centre of k-space acquisition.

Study population

Volunteers

Volunteers referred for a clinically indicated non-perfusion CMR scan with a high pre-test probability of a normal scan were recruited prospectively. General exclusion criteria are detailed in chapter 2.

Patients

32 patients with a history of stable angina, known or suspected CAD, and a clinical indication for a diagnostic X-ray coronary angiography were recruited prospectively. These patients underwent a CMR examination including stress and rest perfusion prior to their angiogram. Exclusion criteria were the same as for volunteers and also an acute coronary syndrome within 6 weeks and contraindication to adenosine.

Data acquisition

Perfusion Imaging

All perfusion imaging was performed using a dual bolus of weight-adjusted gadolinium CA (Gadobutrol/Gadovist) injected at 4ml/s by a power injector as described above.

Human studies

0.1mmol/kg of CA was used for all studies. Perfusion imaging was planned from the systolic phase of the 4 and 2-chamber cines. Three equally spaced short axis slices at basal, mid and apical left ventricular levels were acquired every heartbeat⁹⁵. The imaging geometry and field of view were kept constant for each perfusion sequence. During the perfusion image acquisition the patient was instructed to breath gently until delivery of the main bolus of contrast agent commenced at which point the patient was instructed to take a small breath in and hold their breath for as long as possible.

Volunteers

Volunteers underwent rest perfusion imaging using both st-GrE and kt-SSFP in addition to the clinical scan protocol. The order of the perfusion sequences was alternated to control for the effect of higher baseline myocardial signal following the first administration of contrast agent. There were no deviations from the perfusion sequence parameters listed in table 1.

Patient studies

Patients were allocated sequentially to undergo either st-GrE or kt-SSFP perfusion imaging with the first 16 recruited to the st-GrE group and the second 16 to the kt-SSFP group. Patients underwent stress and rest perfusion, functional and scar imaging. Stress imaging always preceded rest imaging. In order to account for higher heart rates at stress, if required, the voxel size was increased stepwise, to maintain imaging at every heartbeat. This was required

in 3 patients in the st-GrE group (resulting in a spatial resolution of 3.0 x 3.0 in 2 patients and 3.5 x 3.5 in 1 patient). Conversely voxel size did not need to be increased in any patients in the kt-SSFP group.

Phantom studies

Our research group have designed and described a dedicated perfusion phantom which replicates the anatomy of a 60kg person's heart and great vessels and allows reproducible performance and imaging of dynamic first-pass myocardial perfusion¹⁰⁸. Perfusion imaging was performed with this phantom using both sequences with 0.025, 0.05, 0.075 and 0.1mmol/kg equivalent concentrations of CA. Absolute signal intensity (SI) curves were generated from the left myocardial compartment at each CA dose.

X-ray coronary angiography

X-ray coronary angiography was performed according to standard techniques.

Data analysis

Data analysis was performed with the dedicated software CMR42 (Circle, Calgary, Canada) except where specifically stated otherwise.

Human studies

Image quality

Image quality was assessed qualitatively in all participants and graded on a 5-point scale (4=excellent, 3 good, 2 moderate, 1 poor and 0 non diagnostic) by an expert observer blinded to the clinical details and the perfusion sequence used. The observer was blinded to the clinical data, to which sequence was used and to the purpose of the study at the time of analysis. Perfusion images were presented along with the corresponding LGE images. Areas of scar were not analysed since scar may affect perfusion image quality.

Signal-to-noise and contrast-to-noise ratios

SNR and CNR were calculated from the mid ventricular slice in all 16 volunteers. Epi and endocardial borders were manually traced on the first dynamic where the main bolus of CA was visible in the myocardium. The superior right ventricular insertion point was manually defined. This subsequently allowed 6 standard myocardial segments⁹⁶ to be automatically defined in each dynamic of the perfusion scan. This segmentation was manually corrected if required. Time versus SI curves were then generated for each segment. Subsequently, the mean SI and the standard deviation (SD) of the SI in each segment on the frame with peak myocardial enhancement were measured. Baseline segmental mean SI and SD measurements were obtained for both sequences prior to any contrast injection. From these measurements, the segmental baseline and peak SNR of the myocardium were calculated as follows¹⁰³:

$$SNR_{baseline} = Mean SI_{baseline} / SD_{baseline}$$

$$SNR_{peak} = Mean SI_{peak} / SD_{baseline}$$

Then, CNR values were calculated as follows:

$$CNR = SNR_{peak} - SNR_{baseline}$$

Image artefacts

The severity of respiratory artefacts was evaluated by the same blinded expert and graded as follows: 4=nil significant, 3=minor, 2 moderate 1=severe, 0=non-diagnostic due to respiratory artefact. Respiratory artefacts were defined as any artefact due to respiratory motion that impaired visualisation of the myocardium during the first pass of CA.

A second, unblinded expert observer evaluated the extent, transmural and duration of DRA. The extent of DRA was defined as the percentage of segments affected. Transmurality was graded as 1 (1-25%), 2 (26-50%), 3(51-75%) or 4 (76-100%). Duration was recorded as the number of frames (and therefore heartbeats) for which the artefact was present. Perfusion images were analysed in conjunction with LGE images. Perfusion defects, which occurred only in the area of scar, were not classified as DRA.

Diagnosis of CAD

Patient CMR studies and X-ray angiograms were evaluated by independent experts blinded to the results of the other investigation. CMR perfusion and LGE data were analysed in conjunction by an experienced physician (8 years CMR experience) and classified as positive or negative for CAD. The observer was blinded to the clinical data, to which sequence was used and to the purpose of the study at the time of analysis. Angiograms were analysed visually by a consultant cardiologist, blinded to the CMR and clinical data, and classified as positive or negative for the presence of at least one stenosis of $\geq 70\%$ in a coronary artery $\geq 2\text{mm}$ in diameter to allow calculation of a sensitivity and specificity for the detection of CAD.

Phantom studies

Since parallel imaging reconstruction affects the noise across the field of view, noise values were taken from noise maps. For this, reconstruction was modified to replace the under-sampled data with white noise while retaining the training data signals and coil sensitivity information¹⁰⁹. The standard deviation of the real part of the noise signal was determined in identical locations of the reconstructed noise images. SNR and CNR were then calculated using the above formulae for each dose of CA with both sequences.

Statistical analysis

Statistical analysis was performed using IBM SPSS Statistics version 19. Data are expressed as the mean \pm SD. Differences between the two groups of patients

were compared using unpaired t tests or Fisher's exact test for normally distributed or non-parametric data respectively. Image quality and respiratory artefacts scores were compared using the Wilcoxon signed ranks test or the two-sample Kolmogorov-Smirnov test in volunteers and patients respectively. Mean scores for SNR, CNR and DRA were compared using paired t tests for within group and unpaired t-tests for between group comparisons. Significance was determined at <0.05 .

Results

Human studies

Study population

All volunteer studies were completed successfully. The CMR examination was normal in 13 volunteers. Three volunteers were found to have slightly abnormal scans: 2 had mildly impaired left ventricular function whilst 1 had a mildly dilated right ventricle. These were isolated abnormalities in each case.

One patient from the st-GrE group did not complete the protocol due to claustrophobia and was excluded. Participant characteristics are shown in table 3.2. Patients in both the st-GrE and kt-SSFP arms were well matched for age, sex, body mass index and cardiovascular risk factors. There were significantly more patients who had undergone previous percutaneous coronary intervention (PCI) in the kt-SSFP arm and these patients also had a lower systolic blood pressure at rest. However, heart rate, systolic blood pressure during stress and rate pressure product were not different.

Table 3.2: Sequence selection study participant characteristics.

	<i>Volunteers</i>	<i>Patients</i>		
	<i>(n=16)</i>	<i>st-GrE (n=15)</i>	<i>kt-SSFP (n=16)</i>	<i>p value</i>
Age	43±20	64±9	64±11	0.89
Male	8 (50%)	10 (67%)	13 (81%)	0.3
Body Mass Index (kg/m²)	24 ±4	30±5	28±4	0.21
Diabetes	0	6 (40%)	7 (44%)	1
Hypertension	0	12 (80)	9 (56%)	0.25
Smoker	0	2 (13%)	2 (13%)	1
Previous PCI	0	0	4 (25%)	0.02
LVEF	58±7%	58 ±12%	63 ±10%	0.23
RVEF		59±8%	60±8%	0.67
CAD	0	12 (80%)	13 (81%)	1
Scar present	0	5 (33%)	2 (13%)	0.22
Haemodynamics				
HR rest	69±10	64±15	65±11	0.8
stress		85±20	84±15	0.93
SBP rest		148±21	132±17	0.03
stress		142±21	129±23	0.15
RPP rest		8851±2545	8562±1950	0.74
stress		10942±2319	10823±2662	0.91

p values refer to differences between patients in the st-GrE and the kt-SSFP

group. HR: heart rate (beat per minute); SBP: systolic blood pressure (mmHg);

RPP: rate-pressure product (HR x SBP).

Image quality

Qualitative assessment

Image quality was significantly better with kt-SSFP compared to st-GrE in both volunteers ($p=0.003$) and in patients ($p=0.012$) (figure 3.1). Image quality was good or excellent in 19% of volunteers with st-GrE compared to 81% with kt-SSFP. In patients 50% of images were good or excellent with st-GrE whereas the corresponding figure for kt-SSFP was 94%.

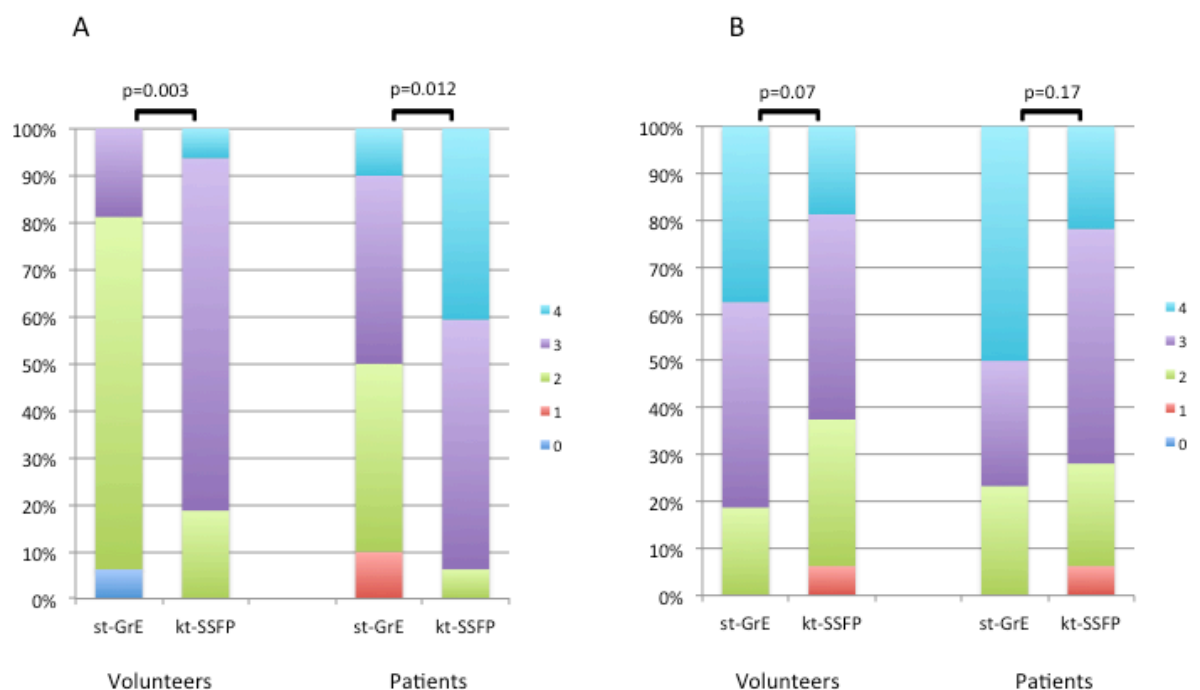


Figure 3.1: Image quality and respiratory artefact scores for volunteers and patients with both sequences.

Scores for image quality (A) and respiratory artefacts (B) in volunteers and patients ranging from 0 to 4 (4=excellent, 3 good, 2 moderate, 1 poor and 0 non diagnostic for image quality; 4=nil significant, 3=minor, 2 moderate 1=severe, 0=non-diagnostic due to respiratory artefact for respiratory artefacts) . Image

quality scores were significantly higher with kt-SSFP and there was a non-significant trend towards fewer respiratory artefacts with st-GrE.

SNR and CNR

SNR and CNR were both significantly higher with the kt-SSFP sequence (figure 3.2). SNR was 18.8 ± 6.6 with st-GrE and 21.0 ± 6.7 with kt-SSFP ($p=0.009$). CNR was 14.0 ± 6.0 with st-GrE and 15.4 ± 6.1 with kt-SSFP ($p=0.034$). Myocardial signal intensity was lower with kt-SSFP compared to st-GrE but noise was reduced proportionately more resulting in increased SNR. Segmental signal intensity curves from a volunteer are shown in figure 3.3.

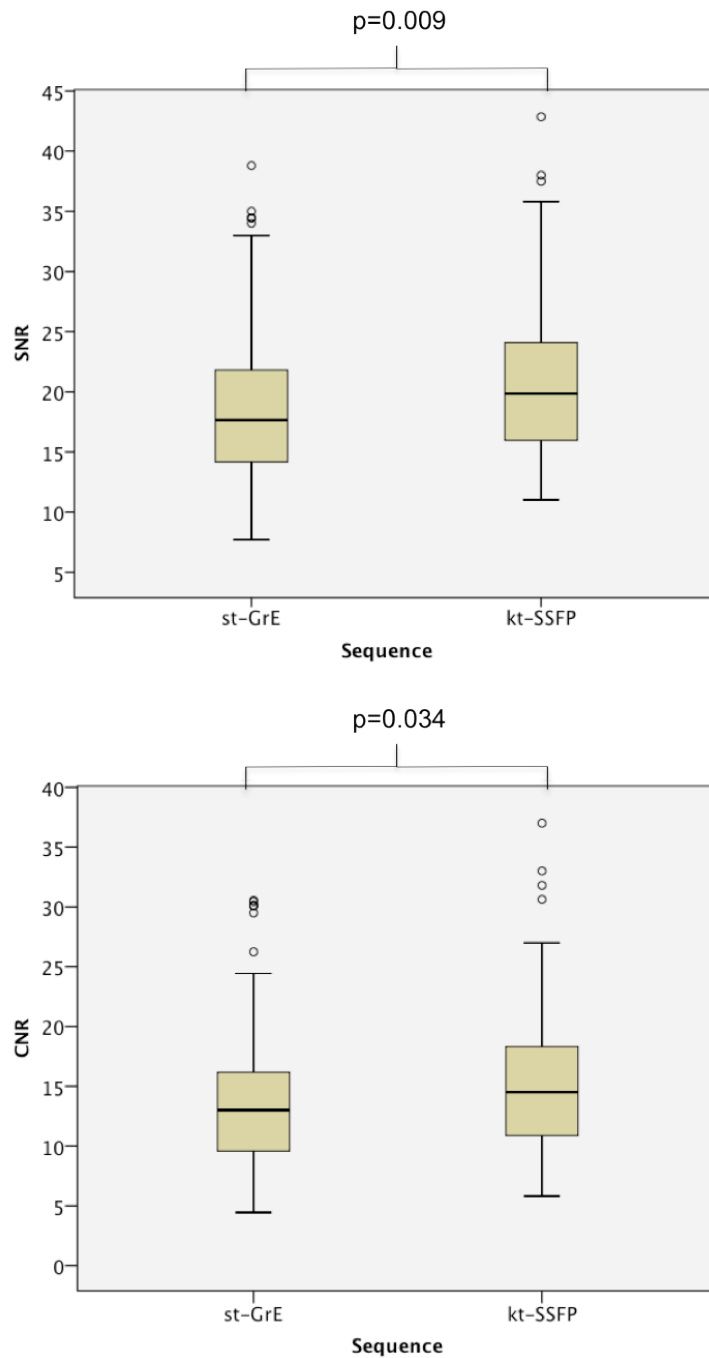


Figure 3.2: Signal and contrast to noise ratios for volunteer rest perfusion scans.

Boxplots showing segmental SNR and CNR values in the volunteers with each sequence. Both SNR and CNR were significantly higher with kt-SSFP.

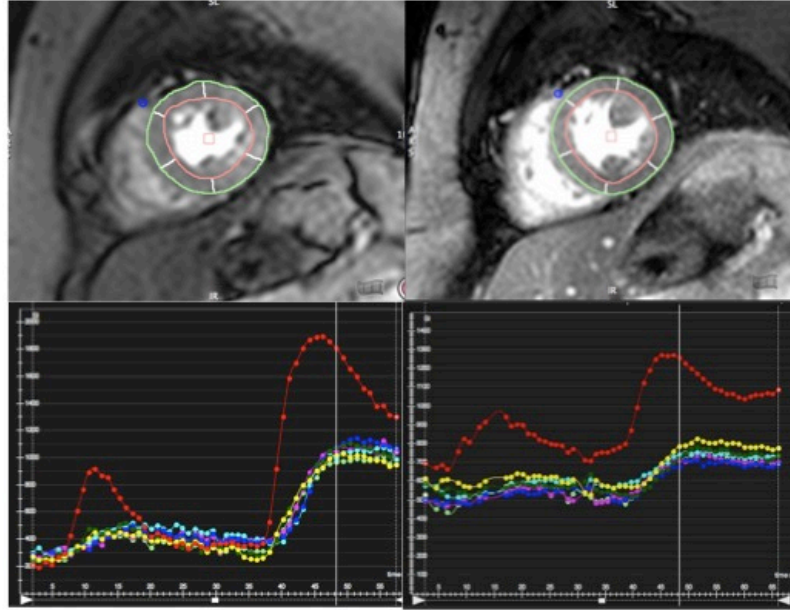


Figure 3.3: First pass rest perfusion images with segmental signal intensity curves.

Segmented mid-ventricular slice during first-pass rest-perfusion with the st-GrE (left) and kt-SSFP sequences (right) with corresponding signal intensity curves. A dual bolus of contrast is used as standard but full-quantification was not performed as part of this study. The red curve is the left ventricular blood pool signal. All other colours represent the signal from each of the six standard segments. Baseline signal is lower with the st-GrE sequence as this sequence was used first in this volunteer.

Image artefacts

Respiratory artefacts

There was a non-significant trend for increased respiratory artefacts with the kt-SSFP sequence in both volunteers ($p=0.07$) and patients ($p=0.17$) (figure 3.1). No studies were non-diagnostic due to respiratory artefact. No st-GrE studies had severe respiratory artefacts in either patients or volunteers whereas with the kt-SSFP sequence severe respiratory artefacts affected both rest and stress scans in one patient and also one volunteer scan. In volunteers 38% of st-GrE scans compared to 19% of kt-SSFP were free of any respiratory artefact. In patients the corresponding figures were 50% and 22% respectively. Respiratory artefacts consisted of ghosting in space and time due to rapid motion caused by respiration.

Dark rim artefacts

The extent, and transmural of DRA was significantly lower with kt-SSFP in both volunteers and patients. The duration of DRA was also significantly less in patients with kt-SSFP although there was no difference with volunteers. These findings are summarised in table 3.3. DRA was apparent in 39% of segments in volunteers and 33% in patients with st-GrE compared to 15% and 12% with kt-SSFP. DRA involved the basal slice most frequently (64-76% of affected segments), followed by the mid ventricular segments (24-33%), and the apical segments least often (0-5%).

Table 3.3: Dark rim artefacts.

DRA	<i>Volunteers</i>			<i>Patients</i>		
	st-GrE	kt-SSFP	p value	st-GrE	kt-SSFP	p value
Extent (%)	39±13	15±12	<0.0001	33±14	12±10	<0.0001
Transmurality	1.83±0.58	1.02±0.06	<0.0001	1.57±0.40	1.07±0.17	<0.0001
Duration	10.6±3.56	9.7±2.51	0.373	10.8±3.7	8.0±2.7	0.004
n	Volunteers			Patients		
	st-GrE	kt-SSFP	p value	st-GrE	kt-SSFP	p value
	16	16		15	16	
DRA						
Extent (%)	39±13	15±12	<0.0001	33±14	12±10	<0.0001
Transmurality	1.83±0.58	1.02±0.06	<0.0001	1.57±0.40	1.07±0.17	<0.0001
Duration	10.6±3.56	9.7±2.51	0.373	10.8±3.7	8.0±2.7	0.004

Extent refers to the percentage of segments affected.

Transmurality was scored as 1=1-25%, 2=26-50%, 3=51-75% and 4=76-100%.

Duration refers to the number of frames for which the defect was visible.

The p values relate to the difference between the scores with st-GrE and kt-SSFP in both patients and volunteers.

Diagnosis of CAD

Sensitivity and specificity for the detection of CAD against X-ray angiography:

st-GrE 82% (48-97%) and 100% (31-100%), kt-SSFP 78% (40-96%) and 80%

(30-99%) respectively. The 95% confidence intervals for sensitivity and specificity are almost identical and therefore there is no significant difference between the sequences. Formal statistical comparison was not performed as the small sample size meant that the study was underpowered to detect such differences. An example of a perfusion defect in one patient from each group is shown in figure 3.4.

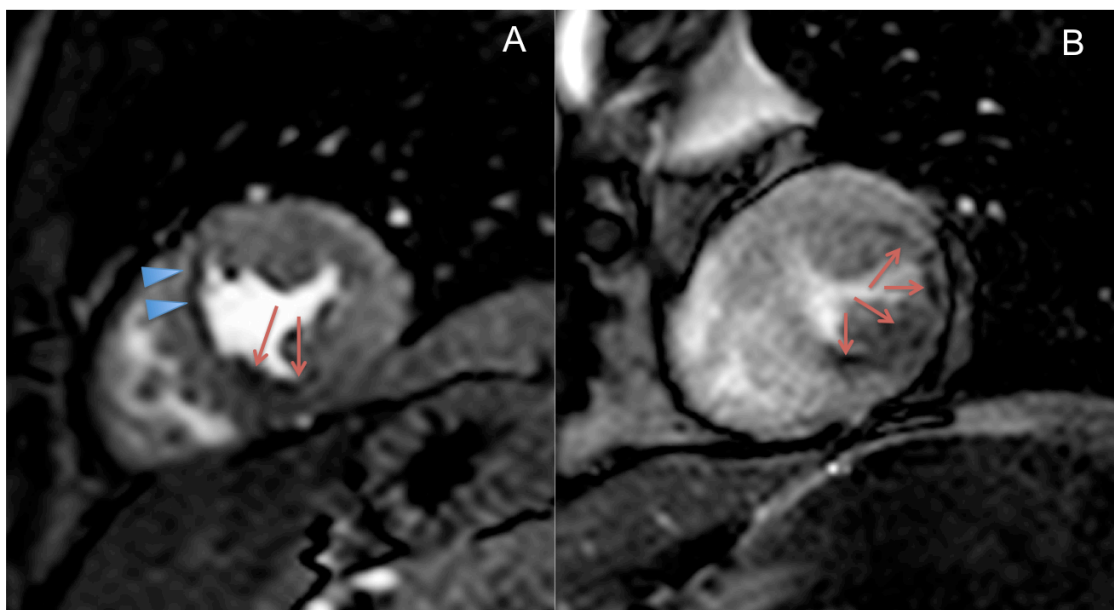


Figure 3.4: Stress perfusion images from patients with coronary artery disease using both sequences.

Still images from the first pass of contrast agent during adenosine stress from two different patients. 4A is a st-GrE image in a patient with angina. There is a perfusion defect in the inferior/inferoseptal wall (arrows). There is also dark rim artefact visible, particularly in the anteroseptal segment (arrowheads). The patient was subsequently found to have an occluded right coronary artery. 4B is from another patient with angina. The lateral wall is thinned whilst the inferior/inferolateral wall is of normal thickness. There is a subendocardial

perfusion defect in both of these regions (arrows). LGE revealed scar in the lateral wall but not the inferior/inferoseptal wall (not shown). This patient had a severe lesion in his proximal right coronary artery and an occluded circumflex artery.

Phantom data

SNR and CNR values for both sequences are shown in table 3.4. Despite the much higher spatial-resolution the kt-SSFP sequence had similar SNR and CNR to the st-GrE sequence across the full range of CA doses. In keeping with the data from humans SI was greater with st-GrE however the noise was also greater resulting in similar SNR and CNR. SI values are higher in the phantom than in humans as the coil is closer to the myocardial compartment.

Table 3.4: SNR and CNR values in a perfusion phantom for both sequences at increasing doses of CA.

<i>CA dose (mmol/kg)</i>	<i>SNR</i>		<i>CNR</i>	
	<i>St-GrE</i>	<i>kt-SSFP</i>	<i>St-GrE</i>	<i>kt-SSFP</i>
0.025	72.3	67.5	41.7	36.4
0.05	91.2	91.0	60.1	59.7
0.075	108.1	103.5	77.5	72.4
0.1	115.2	119.2	83.6	88.0

Discussion

This study demonstrates that newer, advanced imaging techniques can improve the resolution of perfusion imaging and also result in significantly improved image quality, SNR and CNR and significantly reduced DRA in humans.

CMR has emerged relatively recently as a valuable tool for the assessment of cardiac patients. However on-going technical developments have resulted in continuing rapid evolution of CMR and perfusion techniques. It is difficult to predict the effects of sequence alterations on image quality and artefacts or diagnostic accuracy and as such it is necessary to continually evaluate new methods against those that have been previously established through clinical trials and practice. We therefore sought to compare the performance of a state-of-the-art perfusion sequence with an optimised established sequence. We evaluated both sequences in a dedicated perfusion phantom, which enabled evaluation of each perfusion sequence at varying CA concentrations within a consistent set-up, in normal hearts and in patients. This provided a comprehensive and clinically relevant assessment of image quality and artefacts, and also SNR and CNR.

A number of different types of CMR sequence can be used for perfusion imaging and we have only compared two in this study. However, each sequence also has very many parameters, each of which can be adjusted to influence imaging. Consequently, a large number of permutations and combinations exist which cannot all realistically be compared. We therefore opted to comprehensively compare an optimised standard perfusion sequence to a state-of-the-art

sequence. An ultrafast gradient echo sequence was chosen as the standard sequence as it is very commonly used in the clinical setting and has been used in important recent CMR perfusion studies⁶⁶. Our advanced sequence was not simply a modification of this but a sequence that we felt was most likely to produce results of the highest quality using technology that is widely available.

Previous studies have evaluated *k-t* acceleration techniques for improving perfusion imaging. In keeping with our findings a study by Maredia et al in 10 normal volunteers found reduced DRA with a *k-t* SENSE accelerated gradient echo sequence compared to a reference SENSE accelerated sequence¹¹⁰. These authors used *k-t* acceleration to improve spatial resolution, temporal resolution or a combination of both and found that maximizing spatial resolution produced the greatest reduction in DRA.

Another study compared *k-t* SENSE accelerated gradient echo sequences in 14 volunteers and in 37 patients at 1.5 and 3T¹¹¹. In addition a standard lower resolution SENSE accelerated gradient echo sequence was compared to a *k-t* accelerated sequence at 3T. This study also demonstrated improved image quality and reduced DRA with the *k-t* accelerated sequence compared to the standard sequence. In keeping with our study they did not demonstrate improved diagnostic accuracy for CAD with the higher resolution sequence in this relatively small study. Our current study builds on these previous studies as we have demonstrated consistent findings using a *k-t* BLAST accelerated balanced sequence, in both patients and volunteers, at 1.5T. At present 1.5T scanners are used most commonly for clinical perfusion imaging despite the

potential advantages associated with imaging at 3T.

In this study the use of k - t acceleration allowed higher resolution imaging with preservation of three-slice coverage of the heart each heartbeat even at higher heart rates. Higher spatial resolution may improve the detection of sub-endocardial perfusion defects and thus result in improved sensitivity for CAD. To date this has not been confirmed in clinical studies, however, limited early data support the possibility that high-resolution techniques may be more accurate¹¹². Furthermore, in patients with higher heart rates during stress perfusion imaging, the constraints of the sequence may make it necessary to reduce spatial resolution, cardiac coverage or temporal resolution by imaging on alternate heartbeats. This occurred in 3 patients in the st-GrE group and spatial resolution had to be reduced further but higher speed-up with k - t acceleration meant that it did not occur in the kt-SSFP group despite the higher spatial resolution of this sequence. Lower temporal resolution may also compromise diagnostic accuracy and, for example, is known to affect the calculation of a myocardial perfusion reserve index¹¹³.

Image quality

Although image quality was at least moderate in almost all volunteers and patients with both sequences kt-SSFP images were significantly better and most were scored as good or excellent. Perfusion image quality is important, as good quality high-resolution scans are required to accurately delineate regions of ischaemia. This is particularly required for evaluating epi-endocardial

differences in perfusion or, in combination with LGE imaging, for establishing whether there is peri-infarct ischaemia. Such findings can be useful diagnostically and also for patient management, for example when decisions are made regarding revascularisation. This study was too small to demonstrate whether improved image quality results in a difference in diagnostic performance. However, previous work has demonstrated that sensitivity to perfusion defects and inter-observer reproducibility are related to image quality and also to SNR¹¹⁴.

SNR and CNR

The kt-SSFP sequence voxel size was approximately half that of the st-GrE sequence and consequently a reduction in SNR and CNR by a factor of 2 may have been expected. However, both the phantom and human data show that this is not the case. The use of a balanced sequence, which results in higher signal has compensated for the reduction in voxel size. Previous studies^{104, 115} have also found a higher SNR and CNR with a balanced SSFP sequence compared to a GRE perfusion sequence.

Noise can vary greatly across the field of view with the use of parallel imaging¹¹⁶ and thus SNR and CNR measurements can be difficult. In an attempt to overcome this, true noise measurements were obtained from noise maps in the perfusion phantom. The SNR and CNR values from the phantom are much higher than those from human studies due to the close proximity of the coil to the CA when using the phantom. In contrast to the human studies SNR and CNR

were comparable with both sequences reflecting the different methodology used. In the human studies, signal and noise were measured from standard myocardial segments defined on the reconstructed images. These results demonstrated an improved SNR and CNR with the kt-SSFP sequence. Whilst the SNR and CNR values obtained from the reconstructed images are not the same as the true values they remain relevant, as the reconstructed images are the ones used for clinical interpretation. SNR and CNR were not measured in patients given the heterogeneous nature of pathologic perfusion defects. We used the mid-ventricular slice to minimise partial volume effects, which are more likely to occur in the basal and apical slices and also DRA, which occurred more frequently in the basal slice. In addition the use of automatically generated myocardial segments as regions of interest resulted in a standardised, less user-dependent, approach.

Artefacts

DRA is related to juxtaposition of the high signal from blood pool and low signal from myocardium and is often reported as transient. However if the blood pool remains bright, for example if the arrival of the bolus is dispersed, it can be persistent. DRA can therefore be particularly troublesome given that pathological perfusion also results in dark areas of myocardium and can make image interpretation difficult even for experienced observers. Furthermore quantitative analysis of perfusion relies on obtaining accurate myocardial SI curves and can also be severely compromised by the presence of DRA. Inclusion of DRA within regions of interest will result in incorrect perfusion values,

particularly from the sub-endocardium. Myocardial borders can be manually defined to exclude areas of DRA however automated algorithms for myocardial border detection are unlikely to be able to accurately differentiate DRA from true-defects. In turn quantitative assessment of perfusion are unlikely to make the transition from research tool to clinically useful tool without robust and rapid automated methods.

The causes of DRA are incompletely understood but cardiac motion during image acquisition and lower spatial resolution are suspected to contribute¹¹⁷. In this study DRA was significantly reduced with the kt-SSFP sequence. This may be a result of increased spatial resolution reducing truncation artefacts and/or the shorter acquisition time and thus reduced cardiac motion during acquisition. However, it would have been difficult to predict this in advance, as the increased difference in signal between the blood pool and myocardium expected with a balanced SSFP sequence could have resulted in increased DRA.

Respiratory artefacts can also compromise qualitative and quantitative perfusion imaging particularly stress imaging in patients with cardiac pathology, when breath holding in combination with adenosine stimulation can be more challenging. Temporal under-sampling with the kt-SSFP sequence would be expected to exacerbate this problem. Respiratory artefacts were seen as ghosting in space and time and were worst with large respiratory movements. Although correct breath holding resulted in fewest artefacts kt-SSFP associated respiratory artefacts were usually only minor when subjects continued to take shallow breaths and in general were only slightly more severe than those we

encountered during non-*k-t* perfusion imaging. However although there was a trend towards more respiratory artefact with kt-SSFP it was not significant. The phase encoding direction with both sequences in this study was antero-posterior and it may be possible to further reduce respiratory artefacts by using the head-foot direction, although this may itself subsequently increase acquisition times.

In principle ECG mistriggering could result in inconsistencies of data in *xf*-space, which would lead to additional artefacts with the kt-SSFP sequence. However we did not encounter any other significant artefacts, such as ECG mistriggering, with either sequence in this study. Methodical patient preparation and attention to the test scan allows prevention or correction of the majority of such problems prior to the perfusion imaging.

There were more patients with scar in the st-GrE group ($n=5$) compared to the kt-SSFP ($n=2$) group, although this was not statistically significant ($p=0.22$) in this relatively small cohort. Potentially the presence of scar may have affected image quality or DRA assessment, for example, a perfusion defect related to LGE may be erroneously classified as DRA. However in order to minimise such effects perfusion images were always analysed in conjunction with LGE images in keeping with usual clinical practice. This allowed areas of LGE to be excluded from quality and artefact assessments.

Limitations

It may have been preferable to use both sequences in the same patients rather than two different groups. However our patients were well matched overall.

Both sequences were compared in the same conditions in the same volunteers and phantom studies and the quantitative assessments were performed in these groups. Performing perfusion imaging with both sequences in patients also has problems; either stress perfusion has to be repeated on the same day (possibly at the expense of rest perfusion due to CA dose limitations) or patients have to attend on two occasions, when conditions such as myocardial perfusion or patient positioning in the magnet, may not be the same.

The half-life of the CA used is approximately 90 minutes (depending on renal function)¹¹⁸. Therefore in humans, after the first dose of CA, myocardial signal does not reduce to baseline within the timeframe of a single CMR examination (as seen in figure 3.3). To account for this we alternated which perfusion sequence we used first in volunteers. Inadequate coil response non-uniformity correction may also have resulted in variations in signal intensity the field of view in some cases. However since the same segments were compared with both sequences this would not have affected the overall result.

Finally, a relatively small number of patients were included in the study, and the prevalence of CAD was very high (approximately 80%) resulting in wide confidence intervals for the sensitivity and specificity of both sequences for the detection of CAD. Consequently it was not possible to determine whether there is a difference in diagnostic performance between the two sequences. However,

each sequence was comprehensively assessed in a phantom and volunteers in addition to patients. This study therefore provides a platform for larger scale studies to evaluate whether CMR sequences using advanced techniques also improve diagnostic accuracy.

Conclusions

Advanced, high-resolution CMR perfusion imaging using a k - t accelerated SSFP technique results in significantly improved image quality, signal and contrast to noise ratios and a reduction in dark-rim artefacts in humans. These findings support the use of an advanced high-resolution sequence in preference to a standard sequence for clinical myocardial perfusion imaging and for subsequent studies. Further studies exploring whether the use of advanced methods can be translated into superior diagnostic accuracy for coronary disease are desirable.

3B PERFUSION IMAGING. Optimisation of the CMR

Perfusion Sequence-Contrast Agent Dose Selection

Abstract

Objectives

Compare CA doses in a phantom and in patients using the kt-SSFP sequence to determine the dose to be used for further studies.

Background

On the basis of the previous study the kt-SSFP was used in further studies but there remains uncertainty regarding the optimal dose of CA for perfusion imaging.

Methods

The perfusion phantom was used to generate signal intensity curves using 0.025, 0.05, 0.075 and 0.1mmol/kg equivalent doses of CA at 1, 2.5 and 5ml/kg/min. Sixteen sequential patients with angina and suspected CAD referred for clinical perfusion imaging were enrolled. CMR imaging was identical to the first part of the study except that a CA dose of 0.0075 and 0.075mmol/kg was used. Images were analysed for quality and artefacts as previously and compared to the previous results at 0.1mmol/kg.

Results

The relationship between CA dose and SI was linear with CA doses up to approximately 0.06mmol/kg. Signal saturation effects were seen at higher CA doses. There was no difference in image quality or artefacts between patients receiving 0.1 and 0.075mmol/kg of CA.

Conclusions

Based on these findings and previous published dose-finding studies 0.1mmol/kg CA, with a dual bolus injection method, was selected for subsequent perfusion studies at 1.5T.

Background

CMR perfusion imaging has developed rapidly over the past few years. This rapid growth and evolution has resulted in a lack of standardisation of CMR perfusion methodology. This is in contrast to nuclear imaging, which has been established for far longer and is more standardised. CMR perfusion studies and clinical practice is performed using various pulse sequences, CA, CA delivery regimens and field strengths.

A limited number of studies have evaluated different CA doses^{65, 119, 120}, however, results have been conflicting and much of the data relates to early perfusion techniques. Since the optimal dose of CA may well depend on the exact set-up used evaluation of the optimal dose of CA is desirable. The optimal dose also depends on whether the images will be analysed visually or quantitatively as discussed in chapter 1.

Having identified that the kt-SSFP sequence was superior and would be used in subsequent work we compared different CA doses using this sequence in the perfusion phantom and in patients.

Methods

Phantom studies

Perfusion imaging was performed using the kt-SSFP and 0.025, 0.05, 0.075 and 0.1mmol/kg equivalent concentrations of CA at perfusion rates of 1, 2.5 and 5ml/min/kg.

Patient studies

A further 16 sequential patients with angina and known or suspected CAD, who were referred for a clinically indicated CMR perfusion imaging, were recruited. Exclusion criteria were identical to the first part of the study. All imaging methods were identical to the first part of the study except that the dose of CA for perfusion imaging was changed to a dual bolus regimen of 0.0075 and 0.075mmol/kg.

Data analysis

Stress perfusion images were analysed and image quality and artefacts were graded in the same way as previously. Patients receiving 0.075mmol/kg CA (kt-SSFP 0.075) were compared to those who received 0.1mmol/kg (kt-SSFP 0.1) using the same statistical analytical methods as above.

Results

Phantom studies

SI curves with increasing CA doses are shown in Figure 3.5. SI increases progressively with increasing CA dose. At all 3 perfusion rates there is a linear relationship between CA dose and SI up to approximately 0.06mmol/kg. Higher doses are associated with loss of linearity.

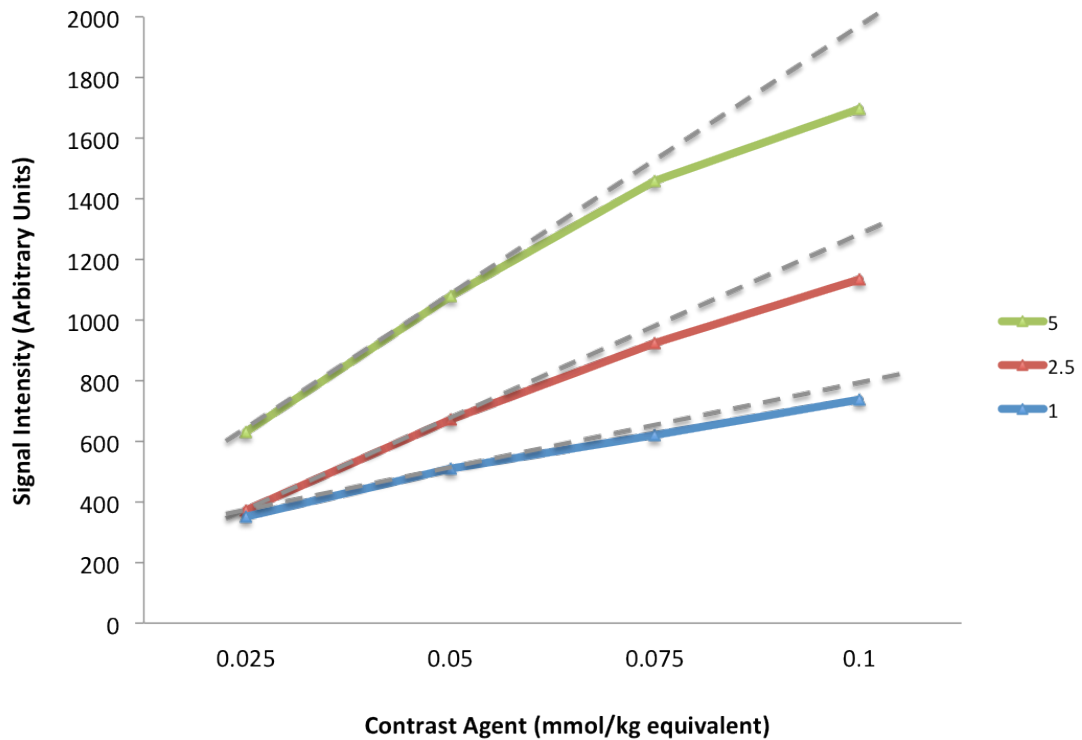


Figure 3.5: Signal intensity curves from the left myocardial compartment of the perfusion phantom.

The broken grey lines are linear reference lines. SI is linearly related to CA dose up to approximately 0.06mmol/kg. Signal saturation effects are evident at higher dose of CA.

Patient studies

One patient in the kt-SSFP 0.075 was later excluded due to uncertainty regarding the dose of CA given. Patient characteristics in the two groups are shown in table 3.5. Patients were well matched with no significant differences in these baseline characteristics.

Table 3.5: Baseline characteristics of the kt-SSFP 0.075 and 0.1 patients.

	<i>kt-SSFP 0.075</i> <i>(n=15)</i>	<i>kt-SSFP 0.1</i> <i>(n=16)</i>	<i>p value</i>
Age	60±10	64±11	0.36
Male	12 (80%)	13 (81%)	1
BMI	28±5	28±4	0.82
DM	2 (13%)	7 (44%)	0.11
Hypertension	7 (47%)	9 (56%)	0.72
Smoker	6 (40%)	2 (13%)	0.11
Previous PCI	2 (13%)	4 (25%)	0.22
LVEF	60±7	63 ±10%	0.33
Haemodynamics			
HR rest	65±11	69±11	0.47
stress	88±17	84±15	0.47
SBP rest	132±17	135±23	0.72
stress	129±23	131±26	0.89
RPP rest	8562±1950	9582±3086	0.34
stress	10823±2662	12298±28700	0.25
CAD	9 (60%)	13 (81%)	0.25
Scar present	6 (40%)	2 (13%)	0.11

Image quality

Image quality was not significantly different at either CA dose (p=1.0). 14/15 (93%) and 16/16 (100%) of the studies were good or excellent in the kt-SSFP 0.075 group and the kt-SSFP 0.1 groups respectively (figure 3.6).

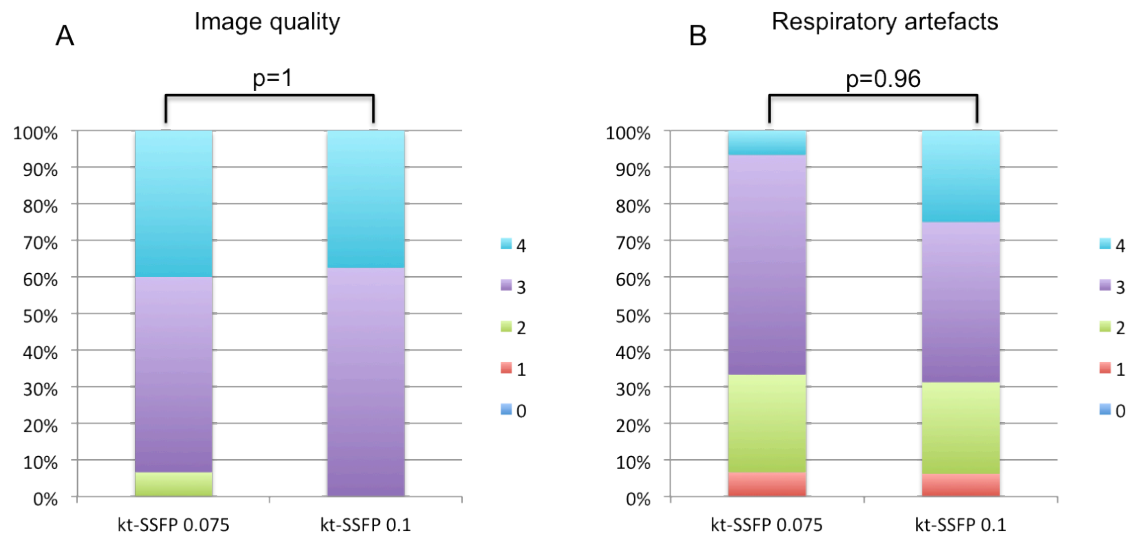


Figure 3.6: Image quality and respiratory artefact scores with kt-SSFP 0.075 and kt-SSFP 0.1.

Scores for image quality (A) and respiratory artefacts (B) in patients ranging from 0 to 4 (4=excellent, 3 good, 2 moderate, 1 poor and 0 non diagnostic for image quality; 4=nil significant, 3=minor, 2 moderate 1=severe, 0=non-diagnostic due to respiratory artefact for respiratory artefacts). There were no significant differences between the CA doses

Image artefacts

Respiratory artefacts

There was no significant difference in respiratory artefacts between the groups (p=0.96, figure 3.6).

Dark rim artefacts

There was no difference in the extent, transmurality or duration of DRA between the groups (table 3.6).

Table 3.6: Dark rim artefacts at kt-SSFP 0.075 and kt-SSFP 0.1.

<i>Dark rim artefact</i>	<i>kt-SSFP 0.075</i> <i>(n=15)</i>	<i>kt-SSFP 0.1</i> <i>(n=16)</i>	<i>p value</i>
Extent (%)	16±16	13±10	0.62
Transmurality	1.14±0.31	1.08±0.19	0.54
Duration (frames)	8.4±3.0	8.0±2.0	0.68

The extent refers to the percentage of segments affected. Transmurality was scored as 1=1-25%, 2=26-50%, 3=51-75% and 4=76-100%. Duration refers to the number of frames (and therefore heartbeats) for which the defect was visible. The differences are not significant.

Discussion

The perfusion phantom data demonstrate that across the full physiological range of myocardial perfusion signal saturation effects were evident in the myocardium with doses of CA above approximately 0.06mmol/kg. In patients with known or suspected CAD there are no important differences in image quality or artefacts between 0.075 or 0.1mmol/kg Gadobutrol/Gadovist CA with the kt-SSFP sequence.

Signal saturation effects are well known to occur at higher doses of CA. The perfusion phantom allowed these effects to be clearly demonstrated with loss of linearity between CA dose and SI occurring at approximately 0.06mmol/kg. Notwithstanding the non-physiological conditions associated with imaging a phantom extrapolation of these results to human subjects suggests that a dual bolus of CA is likely to be required for quantitative analysis regardless of whether 0.075 or 0.1mmol/kg CA is used.

Only limited and somewhat conflicting data are available to guide CA dose selection for perfusion imaging. 3 multi-centre studies have compared area under the ROC curve (AUC) for the detection of CAD against QCA at different doses of CA. Giang et al¹¹⁹ evaluated doses of 0.05, 0.1 and 0.15mmol/kg in 80 patients with known or suspected CAD and found 0.1 and 0.15mmol/kg to be comparable and significantly better than 0.05mmol/kg (AUC 0.91 ± 0.07 ; 0.86 ± 0.08 and 0.53 ± 0.13 respectively). In keeping with this Schwitter et al⁶⁵ evaluated 212 patients in the more recent multicentre MR-IMPACT study and found that 0.1mmol/kg CA performed better than 0.01, 0.025, 0.05 and 0.075mmol/kg (AUC 0.86 ± 0.06 vs. 0.69 ± 0.09 , 0.60 ± 0.14 , 0.64 ± 0.10 and 0.60 ± 0.09 , respectively). In contrast in a third multicentre evaluation of 75 patients Wolff et al¹²⁰ found 0.05mmol/kg to be significantly better than 0.1mmol/g and non-significantly better than 0.15mmol/kg (AUC 0.90 ± 0.04 , 0.72 ± 0.09 , and 0.83 ± 0.09 respectively). All three studies were performed at 1.5T. Giang et al. and Wolff et al. used an echo planar imaging perfusion sequence with Gd-DTPA/Magnevist CA whilst the MR-IMPACT used gradient echo and hybrid echo planar imaging sequences and Gd-DTPA-BMA/Omniscan.

Different CA doses would probably not be expected to result in changes in image quality and should not affect the severity of respiratory artefacts. Conversely, increased LV blood pool signal intensity with higher doses of CA may have resulted in increased DRA, but this was not seen at the doses of CA used here. Although diagnostic confidence in the images was not assessed directly confidence is a result of a combination of image quality and artefacts and sufficient SNR and CNR. Since image quality and artefacts were the same and there was only a small difference in CNR and SNR between the doses diagnostic confidence in the images is also likely to be similar at both doses.

This study was too small to allow evaluation of the diagnostic accuracy of different doses of CA however this is related to image quality and artefacts as discussed above. Furthermore, it is not entirely clear how well the results of previous studies translate to perfusion imaging using a different set-up. However, on balance, a number of factors favoured the use of 0.1mmol/kg CA. Firstly myocardial SNR and CNR in the phantom were higher with 0.1mmol/kg and both doses were associated with signal saturation effects. Secondly the higher SNR and CNR with 0.1mmol/kg did not incur a penalty of increased DRA or reduction in image quality. Thirdly a dual bolus of CA will be required for quantitative analysis regardless of whether 0.075 or 0.1mmol/kg CA is administered. Fourthly combining perfusion imaging with LGE scar imaging improves diagnostic accuracy¹²¹ and our local protocol was to use 0.2mmol/kg CA for LGE imaging. Therefore using 0.1mmol/kg for stress and again for rest perfusion does not increase the CA dose to study participants. Finally the

weight of previously published evidence supports this as two of the three studies; involving the overall majority of patients, found it to be the optimal dose for diagnostic purposes.

Limitations

The same limitations regarding sample size and the use of different CA doses in different patients rather than both doses in all patients which are discussed in the first part of this study are also applicable to this dose-comparison sub study. It would have been ideal to compare a number of different sequences and CA doses in the same patients. However this was not practical given the number of patients that would have required and the perfusion phantom did allow comparison of multiple perfusion rates and CA doses.

Conclusions

Image quality and artefacts were the same in patients imaged with both 0.075 and 0.1mmol/kg of CA using the kt-SSFP sequence. Myocardial signal saturation effects were evident at both 0.075 and 0.1mmol/kg CA. On the basis of these findings and previous dose-finding studies 0.1mmol/kg with a dual bolus regimen was used for subsequent perfusion studies.

4 PERFUSION IMAGING. Validation of Fully Quantitative CMR Perfusion Against Positron Emission Tomography in Patients with Coronary Artery Disease

Abstract

Objectives

Compare fully quantitative CMR and PET myocardial perfusion and myocardial perfusion reserve (MPR) measurements in patients with CAD.

Background

Absolute quantification of myocardial perfusion and MPR using PET have proven diagnostic and prognostic roles in patients with CAD. Quantitative CMR perfusion imaging has been established more recently and has been validated against PET in normal hearts. However, there are no studies comparing fully quantitative CMR against PET perfusion imaging in patients with CAD.

Methods

41 patients with known or suspected CAD prospectively underwent quantitative ^{13}N -ammonia PET and CMR perfusion imaging prior to coronary angiography.

Results

CMR-derived MPR (MPR_{CMR}) correlated well with PET-derived measurements (MPR_{PET}) ($r=0.75$, $p<0.0001$). MPR_{CMR} and MPR_{PET} for the two lowest scoring segments in each coronary territory also correlated strongly ($r=0.79$, $p<0.0001$). Absolute CMR perfusion values correlated significantly but weakly with PET values both at rest ($r=0.32$; $p=0.002$) and during stress ($r=0.37$; $p<0.0001$).

Area under the receiver-operating characteristic curve for MPR_{PET} to detect significant CAD was 0.83 (95% CI 0.73-0.94) and for MPR_{CMR} was 0.83 (0.74-0.92). $MPR_{PET} \leq 1.44$ predicted significant CAD with 82% sensitivity and 87% specificity and $MPR_{CMR} \leq 1.45$ with 82% sensitivity and 81% specificity.

Conclusions

There is good correlation between MPR_{CMR} and MPR_{PET} . For the detection of significant CAD MPR_{PET} and MPR_{CMR} appear comparable and accurate. However, absolute perfusion values from PET and CMR are only weakly correlated therefore although quantitative CMR is clinically useful further refinements are still required.

Background

Non-invasive assessment of myocardial perfusion is clinically important, particularly for the detection and management of patients with CAD. Currently, clinical decision-making is usually based on visual estimates of relative perfusion. However, this approach relies on the presence of a normally perfused region of myocardium. Quantification of perfusion addresses this limitation and PET studies have confirmed that it provides incremental value compared to non-quantitative method¹²².

PET can accurately quantify perfusion and MPR and is currently the non-invasive reference-standard. Fully quantitative methods are accurate for the detection of CAD¹²² and can result in improved diagnostic accuracy compared to relative perfusion analysis¹²³. Recent studies have also demonstrated that an abnormal quantitative MPR is an independent predictor of an adverse prognosis^{44, 45}. Furthermore, quantitative data provides unique information about the coronary microcirculation which is not available from non-quantitative methods³⁶.

CMR has, relatively recently, established itself as an accurate and valuable tool for perfusion imaging³¹. Currently, visual assessment is standard, however absolute quantification of perfusion has also been demonstrated to be feasible and accurate^{74, 75, 124, 125}. Quantitative CMR methods have been validated against microspheres in animals⁷⁵, coronary sinus flow in patients¹²⁵ and PET in healthy volunteers¹²⁶⁻¹²⁸. However, to date, there is a lack of evidence comparing quantitative CMR with PET in patients with CAD. Patient studies are

clinically more relevant given the inherent differences between patients and healthy volunteers. The primary aim of this study was therefore to compare quantitative assessment of myocardial perfusion and MPR using CMR and PET in a cohort of patients with known or suspected CAD.

Methods

Patient population and study design

Patients with a history of stable angina and known or suspected CAD underwent CMR and PET perfusion imaging prior to planned X-ray coronary angiography. Exclusion criteria: acute coronary syndrome <6 weeks, previous CABG, previous ST-elevation infarction, or a contraindication to MRI or adenosine. The UK Administration of Radioactive Substances Advisory Committee licensed radiation exposure.

Data acquisition

CMR imaging

Data were acquired with the 1.5T scanner. Examinations included high-resolution perfusion, functional and scar imaging. Perfusion imaging was performed with the kt-SSFP sequence and consisted of 3 short axis slices acquired every heartbeat covering 16 of the standard myocardial segments⁹⁶ (apex excluded). Stress imaging preceded rest by 14 ± 2 minutes (range 10-19 minutes). A dual bolus (equal volumes of 0.01mmol/kg followed by

0.1mmol/kg after a 20 second pause) of weight adjusted CA was injected as previously described.

PET imaging

This was performed using a GE, Discovery VCT PET-CT scanner (GE Healthcare, Wisconsin, USA) after administration of ^{13}N ammonia, with 47 transaxial slices reconstructed over an axial field of view of 15cm. Acquired resolution 4.8x4.8x4.9mm. CT scout data determined patient position and a low dose CT used for attenuation correction. Acquisition consisted of dynamic scans 0 - 6 mins (12x10seconds, 6x20seconds and 2x60seconds) and then a single static scan frame for 20 minutes. For the rest study a total of 550 MBq of ^{13}N -ammonia was injected intravenously. Approximately 50 minutes later stress imaging was performed following a second CT scan. 140 μg /kg/minute of adenosine was administered intravenously for 6 minutes with a second equivalent dose of ^{13}N -ammonia administered 2 minutes into the infusion. Patients remained on the scanner table throughout the entire study however attenuation correction was repeated for the stress study.

X-ray coronary angiography

This was performed according to the standard Judkin's technique. Multiple projections of the coronary arteries were acquired including at least two orthogonal views to assess stenosis severity.

Data analysis

Visual analysis

Studies were analysed by two independent experts blinded to all other data. PET scans were classified as positive for CAD in the presence of a stress-induced perfusion defect involving ≥ 2 myocardial segments and CMR scans in the presence of a stress-induced perfusion defect, which was transmural or involved ≥ 2 myocardial segments. In the case of disagreement between the observers the images were reviewed together and a consensus reached.

Quantitative analysis

Quantitative analysis was performed by one of the experts. Perfusion was quantified in 16 standard AHA segments. Segments were defined separately for the PET and CMR images using the RV insertion points for reference. Segment 17 was excluded. Myocardial border detection was automated and manually corrected where required. Segments unsuitable for analysis due to artefact or poor image quality were excluded. CMR segments demonstrating LGE and PET data from patients with >10 mm movement between the CT and PET were considered unreliable and also excluded. Coronary territories were excluded if all relevant segments were unsuitable for analysis.

PET: Original dynamic raw PET scans were used to calculate arterial input function and mean segmental perfusion calculated over the linear portion of the curve from 70-210 seconds, using Quick Cardiac (Hermes Medical Solutions, Stockholm, Sweden) in conjunction with software developed at our institution

based on the Patlak method as previously described and validated.¹²⁹

CMR: Mean segmental perfusion values were obtained using dedicated prototype ViewForum software (Philips, Best, The Netherlands). Myocardial border definition results in automated production of pixel-wise signal intensity curves in the myocardium and an AIF from the blood pool of the basal slice. The observer defines the time points of AIF onset and offset and myocardial signal onset. Perfusion is then be calculated in 120 radial segments per slice using the previously validated Fermi deconvolution method⁷⁵. These values are then translated into mean perfusion values for each standard segment.

PET and CMR: Each segment was assigned to the appropriate perfusion territory⁹⁶, with segment 15 assigned to the dominant coronary artery (defined by the observer analysing the angiogram). MPR was defined as stress perfusion divided by rest perfusion and was calculated for each segment and territory. For CAD detection mean MPR of the 2 lowest scoring segments for each perfusion territory (MPR2) was used for further analysis as described previously¹³⁰.

X-ray angiography: All coronary arteries >2 mm in diameter were assessed by an independent cardiologist blinded to all other data. Stenoses <30% and >95% on visual analysis were judged to be non flow-limiting or flow-limiting respectively without further assessment. Quantitative coronary angiography (QCA) was performed for all arteries with a visual stenosis severity of 30-95% using a

dedicated software programme (Medcon UK, Middlesex, UK). Mean diameter stenosis from 2 orthogonal views was recorded and $\geq 70\%$ regarded as significant. Coronary territories subtended by a coronary artery with $\geq 70\%$ stenosis were classified as stenotic territories and all others as remote.

Statistical analysis

IBM SPSS Statistics version 19 and Medcalc were used. Data are presented as mean \pm standard deviation except where stated. Shapiro-Wilk analysis defined when non-parametric tests were required. Agreement and correlations between PET and CMR were determined using Bland Altman plots and Spearman's test of correlation with a two-tailed test of significance respectively. Analyses were performed on a per observation basis. Since 3 perfusion territories were analysed per patient analyses were repeated within each territory to ensure that any strong correlations did not simply reflect high within-subject correlations. Intra and inter-observer reproducibility was determined by a coefficient of variation (CV): standard deviation of the differences divided by the mean. Paired and independent T-tests were used for comparison of paired and unpaired mean data respectively. ROC analysis determined the accuracy of visual analysis, MPR2 and stress perfusion values from PET and CMR for predicting a corresponding coronary artery stenosis of $\geq 70\%$ on QCA. Areas under ROC curves were compared using the Hanley and McNeil method. Optimal cut-offs were determined by the maximum Youden index. Logistic regression models were used to calculate the area under the ROC curve when information from both CMR and PET were combined and this was

compared to the ROC curves when CMR or PET was used alone. Sensitivity and specificity were compared with McNemar's test. Significance was determined at <0.05 .

Results

Study population

Forty-one patients were recruited. Table 4.1 shows baseline characteristics. The study protocol was completed in 38 patients (exclusions: 1 AV block, 1 withdrawal of consent, 1 claustrophobia) and further analysis relates to these patients. Haemodynamics during imaging are shown in table 4.2. Resting heart rate was significantly higher during CMR studies (66 vs. 63 beats per minute respectively). There were no significant differences between rate pressure product, systolic blood pressure or stress heart rate during CMR and PET studies.

Table 4.1: Baseline characteristics of the 41 study participants.

<i>Characteristic</i>	
Age	63±9
Male	32 (78%)
BMI	29±5
LVEF	63±12%
Angina (CCS)	
Class 1	11 (27%)
Class 2	22 (54%)
Class 3	8 (20%)
Diabetes	13 (32%)
Hypertension	30 (73%)
Smoking	
current	5 (12%)
previous	21 (51%)
Family history CAD	19 (46%)
Cerebrovascular disease	4 (10%)
Previous PCI	13 (32%)
Previous myocardial infarct	5 (12%)
Medications	
Aspirin	33 (80%)
Clopidogrel	18 (44%)
Statin	35 (85%)
ACE inhibitor	22 (54%)
Angiotensin receptor blocker	6 (15%)
Betablocker	21 (51%)
Calcium channel blocker	13 (32%)
Nitrate	7 (17%)
Coronary disease ≥70%	
Left anterior descending	7 (17%)
Circumflex	12 (29%)
Right coronary artery	13 (32%)

The interval between PET and CMR scans was 3 ± 6 days; 26(63%) patients underwent both on the same day. The coronary angiogram was 17 ± 19 and 17 ± 21 days after the CMR and PET respectively. Twenty-five patients (61%) had ≥ 1 stenosis of $\geq 70\%$ diameter. Nineteen had single-vessel disease, 5 two-vessel disease and 1 three-vessel disease. The affected coronary artery was dominant in 3 of the 12 patients with circumflex disease and 12 of the 13 patients with right coronary artery disease. Left ventricular ejection fraction (CMR) was $63\pm12\%$.

Table 4.2: Summary (mean \pm SD) of the haemodynamic data for all 38 participants during the imaging studies.

	<i>Rest</i>			<i>Stress</i>		
	<i>PET</i>	<i>CMR</i>	<i>p</i>	<i>PET</i>	<i>CMR</i>	<i>p</i>
HR (bpm)	63 \pm 10	66 \pm 11	0.002	84 \pm 15	86 \pm 15	0.14
SBP (mmHg)	138 \pm 18	137 \pm 17	0.75	128 \pm 21	132 \pm 19	0.164
RPP (HRxSBP)	8734 \pm 336	9122 \pm 329	0.12	10781 \pm 479	11344 \pm 445	0.08

Myocardial perfusion

All perfusion studies were suitable for visual analysis. Quantitative MPR data were available for 89%, 84% and 73% of territories with CMR, PET and both modalities respectively. Results are summarized in table 4.3. In patients with CAD stress perfusion, MPR and MPR2 were significantly lower in stenotic territories compared to remote territories with both PET and CMR. Conversely, rest perfusion was not significantly different.

MPR2_{PET} was 1.36 ± 0.32 and 1.74 ± 0.32 in stenotic and remote territories respectively ($p < 0.0001$). MPR2_{CMR} values were 1.31 ± 0.30 and 1.70 ± 0.42 ($p < 0.0001$). In patients without significant CAD there was a trend towards higher MPR and MPR2 compared to remote territories in patients with CAD but this was not significant. In patients without CAD MPR2_{PET} was 1.92 ± 0.39 and MPR2_{CMR} was 1.93 ± 0.53 ($p = 0.14$ and $p = 0.16$ respectively compared to remote territories in patients with CAD).

Table 4.3: Quantitative perfusion values in patients with and without significant CAD.

	<i>CAD</i>			<i>No CAD</i>	
	<i>Stenotic</i>	<i>Remote</i>	<i>p value*</i>	<i>All territories</i>	<i>p value†</i>
	<i>territory</i>	<i>territory</i>			
	<i>(n=32)</i>	<i>(n=43)</i>		<i>(n=39)</i>	
Stress perfusion					
(ml/minute/g)					
PET	1.24±0.49	1.56±0.66	<0.0001	1.72±0.66	0.49
CMR	1.54±0.34	1.94±0.59	0.001	2.03±0.63	0.68
Rest perfusion					
(ml/minute/g)					
PET	0.77±0.24	0.81±0.25	0.08	0.85±0.26	0.71
CMR	1.03±0.30	1.06±0.33	0.28	0.98±0.29	0.47
MPR					
PET	1.57±0.31	1.87±0.36	<0.0001	2.06±0.44	0.20
CMR	1.55±0.36	1.90±0.48	0.001	2.20±0.56	0.13
MPR2					
PET	1.36±0.32	1.74±0.32	<0.0001	1.92±0.39	0.14
CMR	1.31±0.30	1.70±0.42	<0.0001	1.93±0.53	0.16

A stenotic territory is subtended by a coronary artery with ≥70% diameter stenosis and a remote territory by a coronary artery with <70% stenosis.

Myocardial perfusion-agreement between CMR and PET

There was good correlation between MPR_{CMR} and MPR_{PET} ; $r=0.75$ ($p<0.0001$; figure 4.1A) and between $MPR2_{CMR}$ and $MPR2_{PET}$; $r=0.79$ ($p<0.0001$, figure 4.1B). A Bland Altman plot demonstrates good agreement between MPR_{CMR} and MPR_{PET} (Figure 4.2).

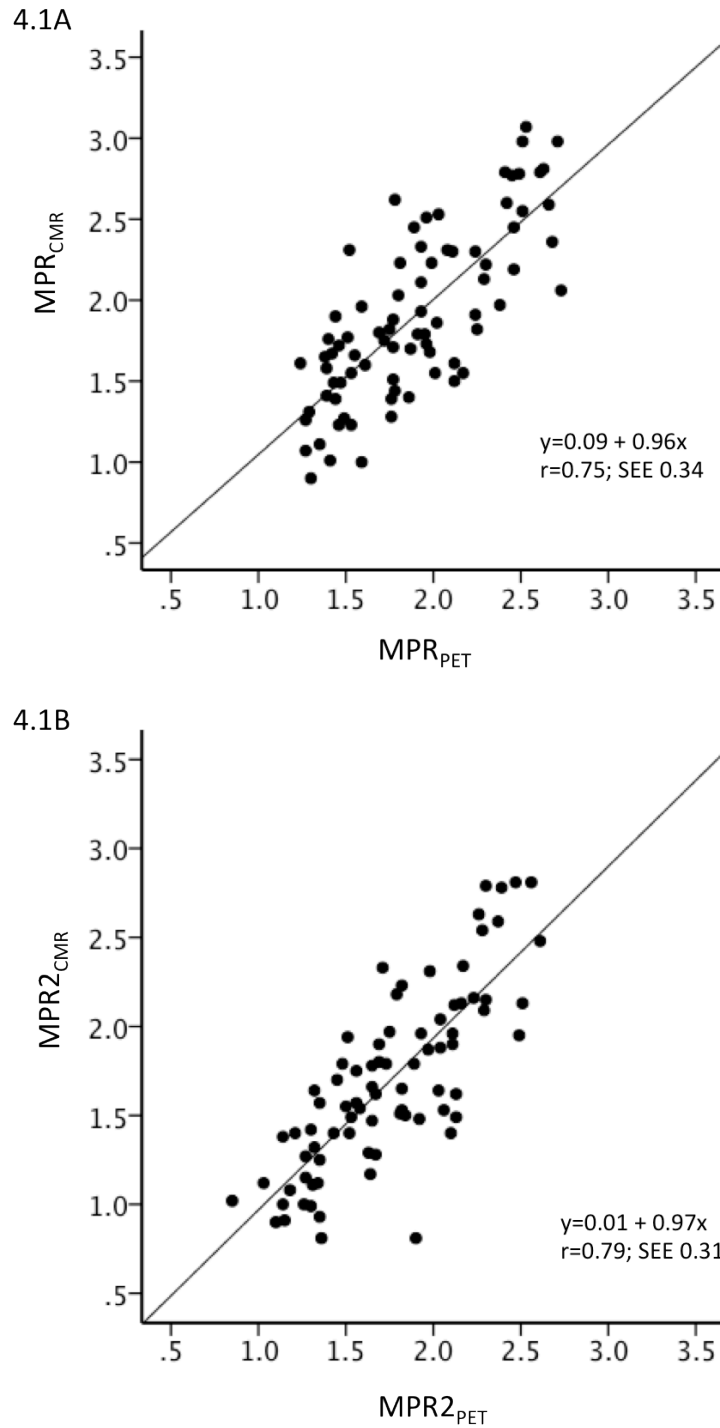


Figure 4.1: Scatter plots comparing CMR and PET derived MPR.

Scatter plots with fit lines comparing myocardial perfusion reserve values from cardiac magnetic resonance (MPR_{CMR}) and positron emission tomography (MPR_{PET}) for the entire myocardial territory (A) and the mean of the lowest two segments in each territory (MPR2) (B).

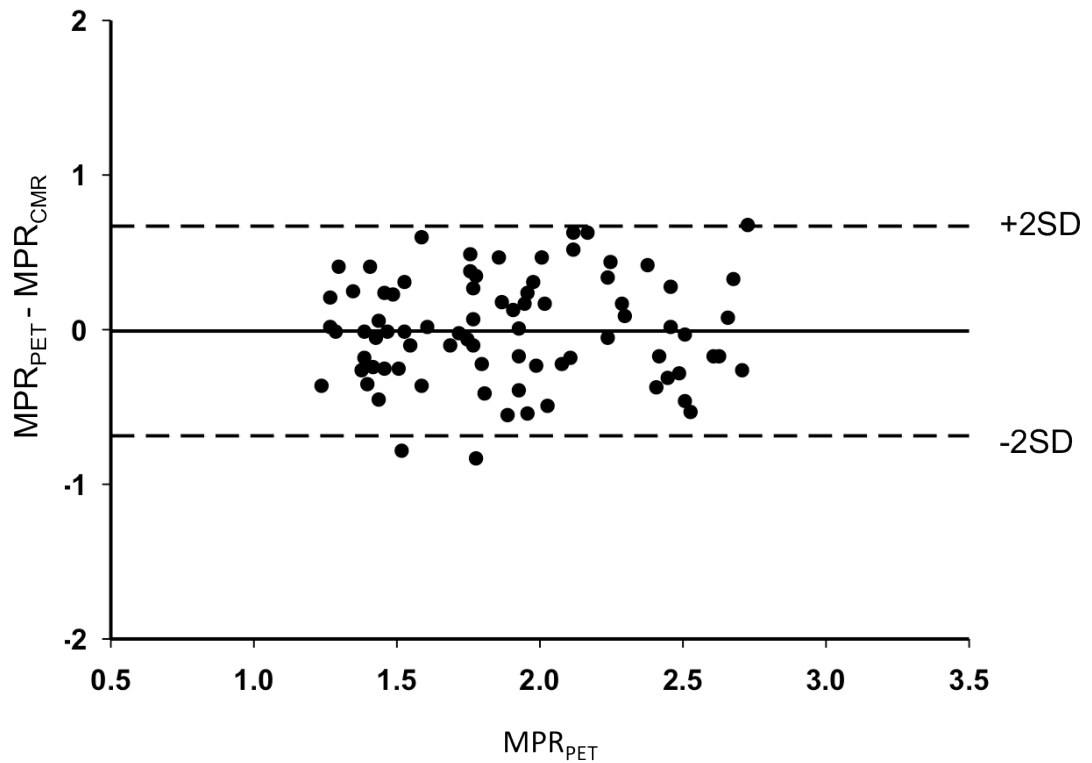


Figure 4.2: Agreement between CMR and PET MPR.

Bland Altman plot showing the agreement between CMR and PET derived absolute MPR measurements.

Absolute CMR perfusion values correlated significantly but weakly with PET values both at rest ($r=0.32$; $p=0.002$) and during stress ($r=0.37$; $p<0.0001$) (figure 3). Results were similar when analyses were repeated within each territory. MPR_{CMR} correlated well with MPR_{PET} in the LAD ($r=0.79$; $p<0.0001$), circumflex ($r=0.64$; $p<0.0001$) and RCA territories ($r=0.77$; $p<0.0001$). Bland Altman limits of agreement for MPR_{CMR} and MPR_{PET} also remained similar in the LAD (-0.71 to 0.58), circumflex (-0.7 to 0.8) and RCA territories (-0.62 to 0.48).

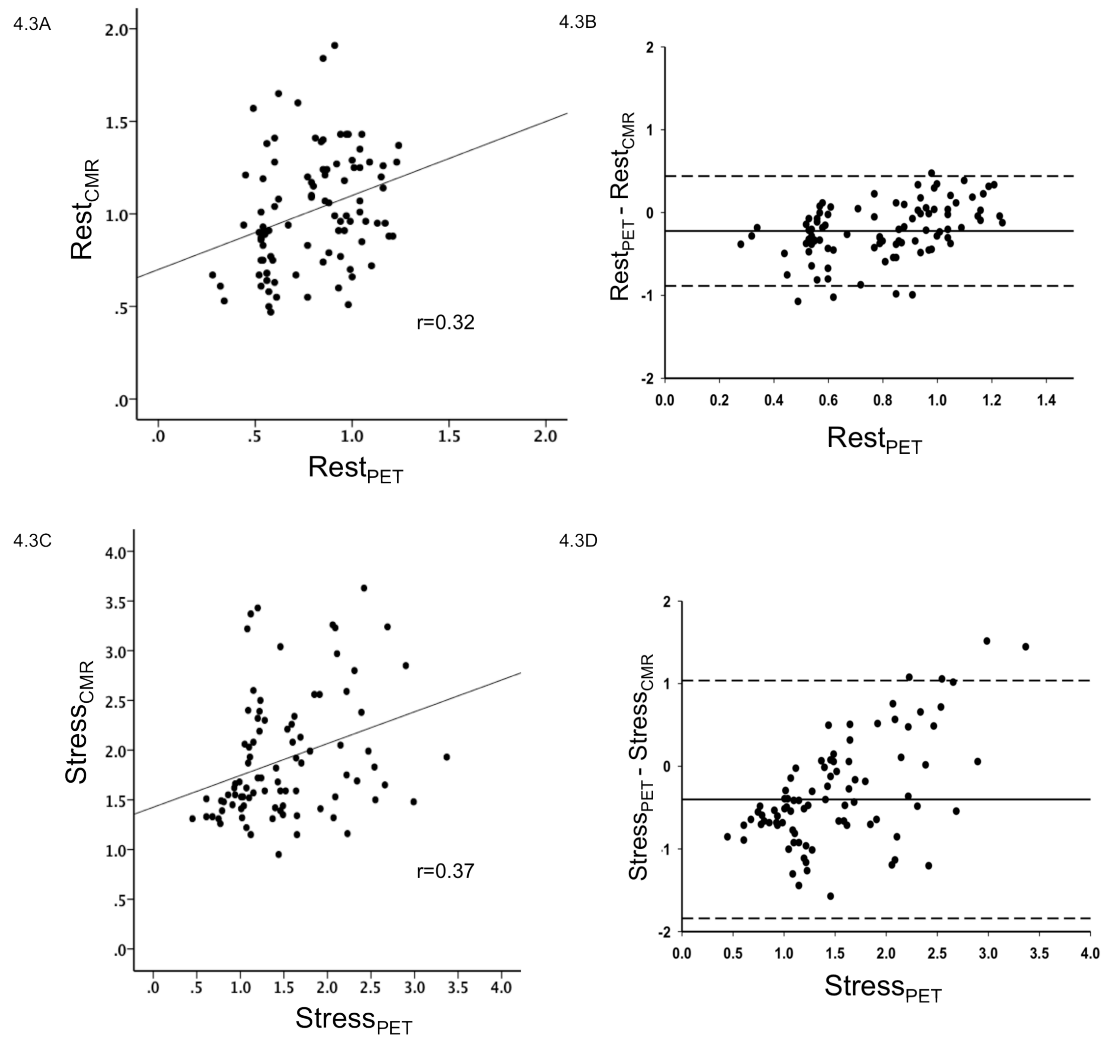


Figure 4.3: Correlation and agreement between CMR and PET derived absolute perfusion values.

Scatter plots illustrating the correlation between absolute measures of myocardial perfusion at rest (4.3A) and during peak stress (4.3C), along with the corresponding Bland Altman plots (4.3B and 4.3D respectively) with limits of agreement lines (2 standard deviations).

Reproducibility

Intra-observer CV for PET stress perfusion, rest perfusion and MPR were 9%, 12% and 15%. Corresponding CV for inter-observer reproducibility were 17%, 13% and 18%. CMR intra-observer CV were 9%, 14% and 20% and inter-observer CV 16%, 18% and 22%.

Diagnosis of CAD

Visual analysis: Sensitivity and specificity against QCA: PET 92% (95% confidence interval 72-99%) and 69% (41-88%); CMR 86% (64-96%) and 76% (50-92%). CMR and PET sensitivity and specificity were not significantly different ($p=0.65$ and 0.71 respectively). If only those patients with quantitative data suitable for analysis were considered sensitivity and specificity changed to 94% (71-99%) and 67% (39-87%) and 85% (61-96%) and 79% (49-94%) for PET and CMR respectively.

Quantitative analysis: AUC for $MPR2_{PET}$ to detect significant CAD was 0.83 (95% CI 0.73-0.94) and for $MPR2_{CMR}$ was 0.83 (0.74-0.92) ($p=0.96$). Sensitivity and specificity against QCA: $MPR2_{PET} \leq 1.44$, 82% and 87% and $MPR_{CMR} \leq 1.45$ 82% and 81% (figure 4.4). An example case is shown in figure 4.5.

AUC was 0.85 (0.75-0.95) for $MPR2_{PET}$ and $MPR2_{CMR}$ combined. There was no significant difference between AUC when $MPR2_{PET}$ and $MPR2_{CMR}$ were both included in the model and when $MPR2_{PET}$ ($p=0.406$) or $MPR2_{CMR}$ ($p=0.4749$) alone were used.

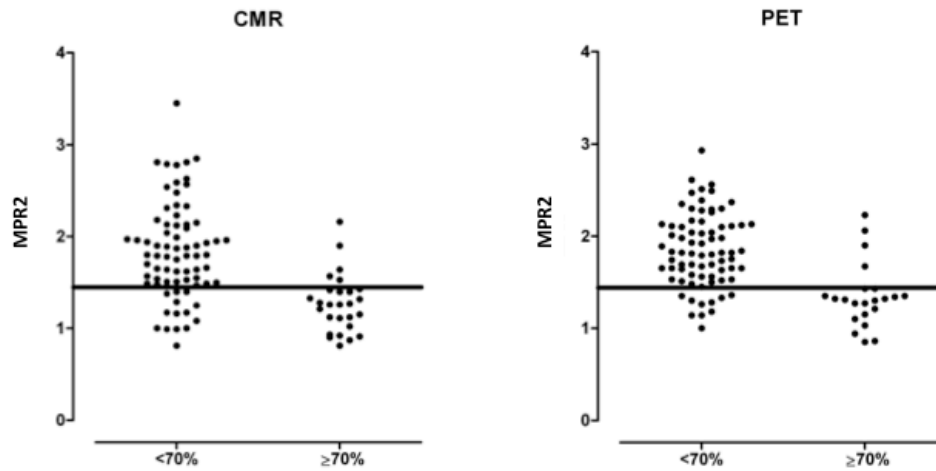
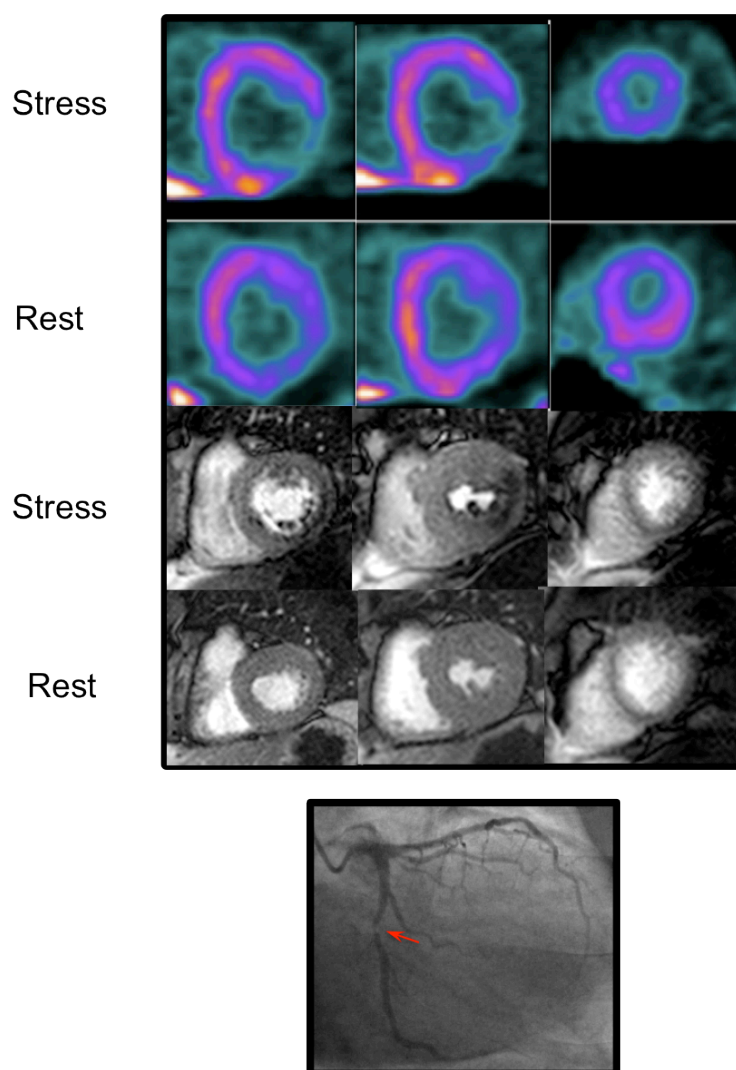


Figure 4.4: Diagnosis of significant CAD against QCA using quantitative CMR and PET derived MPR.

Mean myocardial perfusion reserve of the lowest 2 segments (MPR2) in remote (<70%) and stenotic (≥70%) territories. The best cut-off values for the detection of CAD (MPR_{CMR} 1.45 and MPR_{PET} 1.44) are shown.

MPR2_{PET} and MPR2_{CMR} were inversely related to the severity of CAD by QCA. For QCA subgroups <30%; 30-49%; 50-69%; 70-95% and >95% MPR2_{PET} and MPR2_{CMR} were 1.93±0.39 and 1.89±0.46; 1.73±0.33 and 1.86±0.67; 1.58±0.4 and 1.54±0.47; 1.49±0.33 and 1.28±0.42 and 1.18±0.20 and 1.26±0.22 respectively.

AUC for absolute perfusion values during stress to detect significant CAD: PET 0.69 (0.56-0.81) and CMR 0.72 (0.61-0.83). This was significantly lower than MPR2 AUC with PET ($p=0.049$) but not CMR ($p=0.12$). Optimal absolute stress perfusion cut-offs were PET $\leq 1.48\text{ml/min/g}$ (sensitivity 80%, specificity 53%) and CMR $\leq 1.50\text{ml/min/g}$ (sensitivity 63%, specificity 76%).



MPR2	LAD	CX	RCA
PET	1.7	1.3	1.97
CMR	1.9	1.42	1.87

Figure 4.5: Case example.

PET (top), CMR (middle) and the X-ray angiogram of the left coronary artery of a 54-year-old patient with diabetes and exertional angina. Basal, mid and apical slices have been taken from the PET study, which approximately correspond to the CMR slices. There is a stress-induced perfusion defect in the infero-lateral region from base to apex visible on both PET and CMR images. There is a corresponding severe (>95%) stenosis of the proximal circumflex artery. There was no other significant angiographic disease. MPR2 for each territory are shown in the table. MPR2 for the circumflex artery is below the cut-off of 1.44 and 1.45 for both PET and CMR respectively.

Diagnostic accuracy for each coronary artery

ROC curves for each individual coronary artery are shown in figure 4.6. Area under the ROC curve and sensitivity were highest for the RCA and lowest for the circumflex with both modalities (table 4.4). This difference was significant with CMR ($p=0.04$) but not with PET ($p=0.15$). The difference between the area under the LAD and circumflex and the LAD and RCA ROC curves were not significant with CMR ($p=0.1$ and 0.6 respectively) or PET ($p=0.2$ and 0.88 respectively). Sensitivity was highest for the RCA with both modalities. Specificity was also highest for the RCA and lowest for the circumflex with CMR.

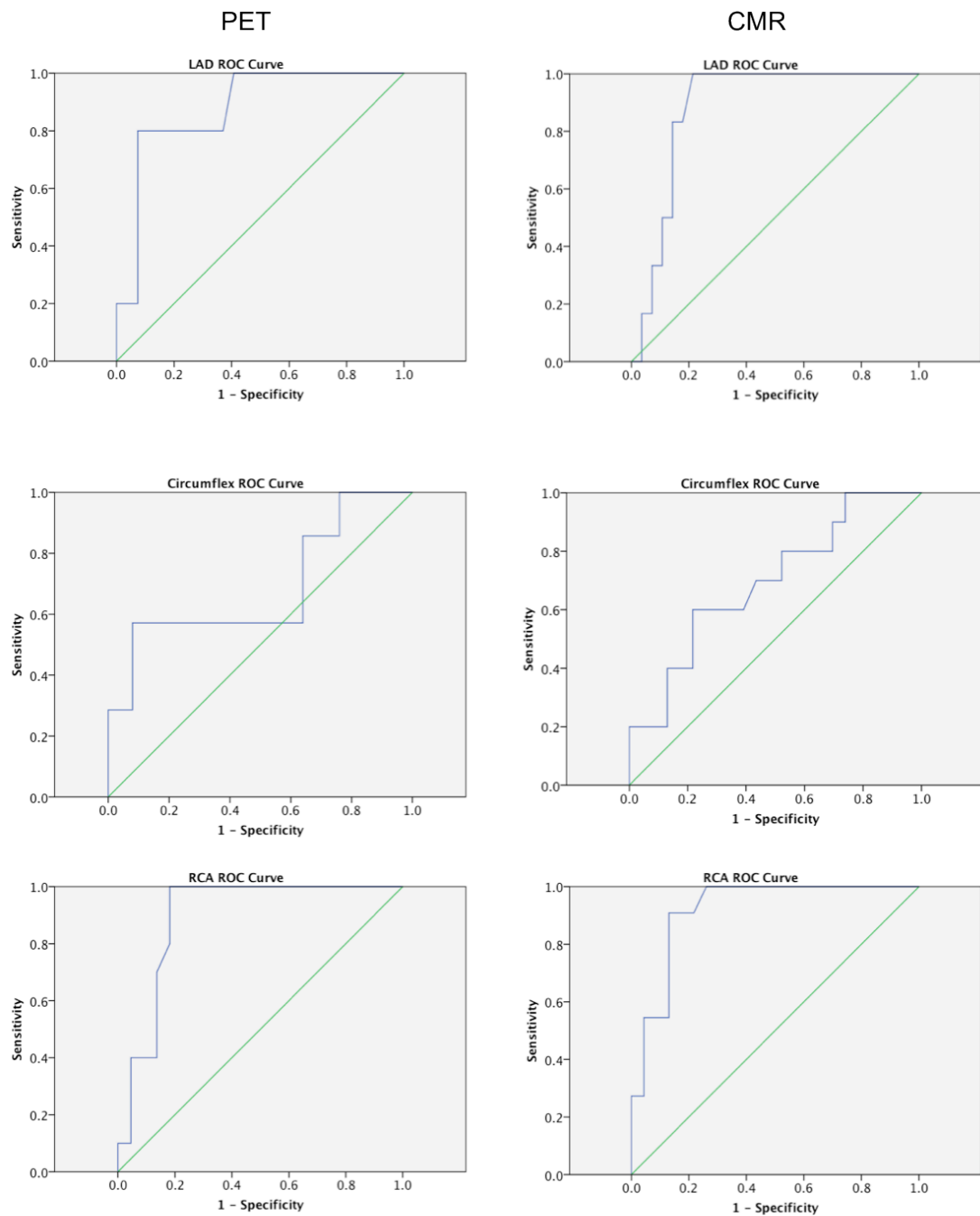


Figure 4.6: ROC curves for the identification of significant CAD in each individual coronary artery using MPR2_{PET} (left) and MPR2_{CMR} (right).

Table 4.4: Area under the ROC curves (ROC AUC), optimal MPR2 cut-off and sensitivity and specificity for detection of significant CAD in each coronary territory.

<i>PET</i>	<i>ROC AUC</i>	<i>95% CI</i>	<i>Optimal MPR2 cut-off</i>	<i>Sensitivity</i>	<i>Specificity</i>
PET					
Overall	0.83	0.73-0.94	≤1.44	82%	7%
LAD	0.88	0.73-1.0	≤1.33	80%	93%
Circumflex	0.69	0.43-0.94	≤1.42	57%	92%
RCA	0.89	0.78-1.0	≤1.44	100%	82%
CMR					
Overall	0.83	0.74-0.92	≤1.45	82%	81%
LAD	0.88	0.77-1.0	≤1.35	83%	86%
Circumflex	0.69	0.5-0.89	≤1.45	60%	78%
RCA	0.92	0.8-1.0	≤1.45	91%	87%

LAD n=7, circumflex n=12 and RCA n=13.

Discussion

We have demonstrated that in patients with known or suspected CAD there is good correlation between MPR_{PET} and MPR_{CMR} . $MPR2_{CMR}$ also appears to have a similar sensitivity and specificity to $MPR2_{PET}$ for the detection of significant coronary artery stenoses. However, the correlation between the absolute perfusion values from PET and CMR is relatively weak.

To our knowledge there are no previously published studies comparing quantitative CMR myocardial perfusion with PET in patients. Previous studies have been limited to semi-quantitative analysis methods^{100, 131} or have involved healthy volunteers¹²⁶⁻¹²⁸. Semi-quantitative analysis has been shown to be useful⁷² and to correlate well with MPR_{PET} in patients with CAD^{100, 131}. However, unlike fully quantitative analysis, these methods only provide an index of perfusion reserve not a true MPR, and might substantially underestimate perfusion, particularly at higher perfusion values¹³¹.

Studies using fully quantitative CMR methods are limited to small numbers of healthy volunteers. The results of these studies are inconsistent and difficult to compare as each study employed different PET and CMR methods. Parkka et al.¹²⁷ studied 18 healthy volunteers with ^{15}O -water PET and CMR. They used compartmental modeling and found that MPR and stress perfusion values were significantly correlated ($r=0.48$ and $r=0.7$ respectively). However, rest perfusion values were not significantly correlated. Fritz-Hansen et al.¹²⁶ studied 10 healthy volunteers with ^{13}N -ammonia PET using the same CMR quantification method. Similar to our findings they demonstrated a significant correlation between global MPR_{PET} and MPR_{CMR} ($r=0.7$). They found an even stronger correlation for the change in myocardial perfusion between rest and stress ($r=0.96$). Both of these studies found a tendency for CMR to underestimate MPR compared to PET. In a smaller study of five volunteers Pack et al.¹²⁸ found that 3T CMR and ^{13}N -ammonia PET perfusion and MPR values are well correlated but that MPR may be in better agreement.

Both PET and CMR perfusion and MPR values in our study are physiologically plausible and in the same range as in some previous studies^{126, 132-136} but lower than those reported by others¹³⁷. Patients are known to have lower stress and rest perfusion than normal volunteers do even in remote territories^{133, 134}. The mean difference between PET and CMR perfusion values is small however; the limits of agreement are broad, particularly at higher stress perfusion values. The findings that MPR, a ratio of stress and rest perfusion values, correlates well but that the absolute perfusion values correlate relatively poorly suggests that the errors in quantification had a similar influence on both rest and stress perfusion values and were subsequently cancelled by the calculation of MPR. These errors may be a result of either methodological or physiological factors.

Methodological considerations

Differences in voxel size and acquisition methods (3D segments were acquired with PET and 10mm slices through the 16 segments with CMR) and the use of different post-processing methods mean that despite calculating mean values in standard segments and territories there is likely to have been a small degree of misregistration between the modalities. Furthermore, whilst partial volume effects are corrected for using compartmental PET analysis¹²⁹ these were not taken into account with CMR.

PET and CMR have both been validated against gold-standard techniques however both still have limitations. PET studies have used different tracers (e.g.

^{13}N -ammonia versus ^{15}O water), acquisition protocols and analysis methods (e.g. Patlak, compartmental). In the present study the method may underestimate absolute perfusion¹³⁸-an effect which would also be cancelled by the calculation of MPR.

Quantitative CMR perfusion studies have used different magnetic field strengths, contrast agents, perfusion sequences and post processing algorithms. One of the main challenges faced by CMR quantification is that at higher concentrations of contrast agent there is a loss of linearity between contrast agent concentration and signal intensity. It is possible that these signal saturation effects influenced our CMR results. However, we used a dual bolus method to preserve signal linearity in the LV blood pool and allow calculation of the arterial input function. In addition, a previous study has demonstrated that myocardial signal intensity continues to increase at much higher doses of contrast agent (up to at least 0.15mmol/kg) than those used here¹¹⁹, although this study was in normal hearts imaged using a hybrid echo planar pulse sequence. Furthermore, a 14-minute interval between stress and rest imaging is insufficient for complete dissipation of the contrast agent. We used a published method¹³⁹ of baseline correction to account for this however this may also have introduced some error into rest perfusion measurements. In contrast to the previous volunteer studies, we did not find any evidence of systematic errors for low or high values, indicating that CMR is valid for a wide range of perfusion values.

It is also possible that systematic errors could relate to the fact that PET^{80, 140} and particularly CMR¹⁴¹ have only moderate inter-study reproducibility.

Regional measurements of perfusion in particular tend to be less reproducible than global measurements. Since the reproducibility of data analysis was relatively high this may be partly also explained by physiological variation of perfusion.

Physiological considerations

There are also likely to have been real changes in perfusion even though the interval between the PET and CMR scans was short. Little is known, for example, as to whether diurnal variation or changes in hydration affect myocardial perfusion. It is also possible that such differences are more pronounced in patients than in volunteers for example as a result of the use of medications which affect perfusion.

Clinical Implications

The novel finding that MPR_{CMR} correlates with MPR_{PET} is important given the proven utility of MPR_{PET} . MPR_{PET} correlates inversely with the degree of coronary artery stenosis at angiography⁴². Furthermore, recent studies have demonstrated that MPR_{PET} is an independent predictor of outcome and predicts major adverse cardiac events and cardiac death⁴⁴ in patients with suspected impaired perfusion and reduced survival in patients with left ventricular impairment⁴⁵.

In this study we identified $MPR2_{CMR}$ and $MPR2_{PET}$ cut-off values that detected CAD with a high sensitivity and specificity. MPR was superior to absolute stress

perfusion values for this purpose. MPR2_{PET} AUC was significantly higher than absolute stress perfusion values AUC and there was also a trend towards significance with MPR2_{CMR}. This was reflected by optimal cut-off values for absolute stress perfusion values that would be clinically less useful due to modest sensitivity (CMR) or specificity (PET). This is in contrast to some limited recent PET data suggesting that a single absolute stress perfusion cut-off value might be superior to MPR for the detection of CAD¹³². In addition, there does not appear to be any incremental value in combining MPR data from both PET and CMR for the diagnosis of CAD.

The optimal MPR cut-off was similar between both modalities in all 3 coronary arteries. It is noteworthy that the area under the ROC curve was lower for the detection of circumflex disease and this difference was significant with CMR (but not PET). Since this trend was seen with both PET and CMR it may be due to erroneous allocation of myocardial segments to coronary artery territories, as we used a standard method of allocation, even though there is known to be considerable inter-individual variability¹⁴². We attempted to adjust for this, to some extent, by allocating segment 15 variably to the dominant coronary artery. However variability in blood supply also affects other segments and there is no reliable method to correct for all segments, although this can be attempted by examining the CMR and angiogram together. Moreover, evaluation of individual coronary arteries reduces the sample size considerably, and increases the confidence intervals (table 4.1). It is therefore best to consider the overall results and study differences in diagnostic accuracy between the coronaries further in larger future studies.

Quantification of images in general results in more precise, reproducible and user-independent results. Although in this study there was no incremental benefit over visual analysis non-invasive quantification of perfusion may be particularly useful in cases where visual assessment is difficult such as multivessel disease, severe left ventricular impairment and after CABG. Moreover, it may eventually allow the definition of thresholds of perfusion associated with myocardial ischaemia⁴⁶ and viability both of which are known to be important for selecting patients for revascularization procedures. This study reinforces the evidence that quantitative CMR perfusion data can be useful for the assessment of patients with CAD and at present we can accurately differentiate normal from abnormal myocardial territories. However, further method refinement is required before the benefits can be fully realized.

Limitations

The sample size in this study is modest. However, this is the first study in patients and larger than previous volunteer studies. Furthermore, this limitation applies more to the secondary objective of exploring diagnostic accuracy than to the primary aim of comparing quantitative perfusion. Large sample sizes will be required to demonstrate any significant differences in diagnostic accuracy. We compared functional tests against an anatomic reference standard (QCA) despite the well-documented limitations of this approach. It may be better to use fractional flow reserve as a reference standard in future studies. However, X-ray coronary angiography is widely used as the

reference standard in both studies and in clinical practice, and does not affect the comparisons made between PET and CMR, which was the main goal of our study.

The patients included in this study had overall good left ventricular function and it is not clear how well these methods translate into patients with left ventricular systolic dysfunction. Finally, the relatively high prevalence CAD and the exclusion of segments where image quality precluded quantitative assessment means that these results are likely to represent best possible results using currently available quantitative techniques.

Conclusions

There is good correlation between MPR derived from quantitative CMR and PET data, which is important given the proven value of MPR_{PET} for detection of CAD, prognostication and assessment of the microcirculation. MPR_{PET} and MPR_{CMR} seem to predict significant CAD equally well and accurately. However, in patients, the absolute perfusion values from PET and CMR are only weakly correlated suggesting that further refinement of quantitative techniques is required.

5 PERFUSION IMAGING. Comparison of CMR Ischaemic Burden and the Angiographic Extent of Coronary Artery Disease.

Abstract

Objectives

Examine the relationship between the extent of angiographic CAD and myocardial ischaemic burden assessed with CMR.

Background

It is increasingly recognised that angiographic and functional data are both important for determining patient management and planning revascularisation. Despite this little is known about the correlation between angiographic and functional measures of the extent of CAD.

Methods

75 patients with angina and known or suspected CAD referred for coronary angiography prospectively underwent high-resolution CMR perfusion imaging. Correlation between the BCIS-1 Myocardial Jeopardy Score (BCIS-JS) and CMR ischaemic burden and the accuracy with which the BCIS-JS can predict a prognostic ischaemia threshold were evaluated.

Results

There was a strong correlation between the BCIS-JS and myocardial ischaemic burden: $r=0.75$, $p<0.0001$. Area under the ROC curve for BCIS-JS to detect $\geq 12\%$ myocardial ischaemic burden was 0.87 (95% CI 0.78-0.96). BCIS-JS ≥ 6 predicted $\geq 12\%$ myocardial ischaemic burden with a sensitivity of 68% and a specificity of 91%.

Conclusions

The BCIS-JS correlates well with myocardial ischaemic burden. A BCIS-JS ≥ 6 predicts the prognostically important ischaemic threshold of 12% with high specificity. These findings provide useful insight into the relationship between angiographic and functional measures of the extent of CAD. In addition they support the utility of the BCIS-JS for classification of CAD burden in clinical trials and suggest it may have a potential role in managing patients with CAD.

Background

The literature on coronary revascularization is dominated by anatomical classifications of CAD and as such there are very many reports on the relationship between the extent of CAD and patient management or prognosis. The extent of CAD frequently influences whether a patient is treated medically or is considered for revascularization. Patients with more extensive disease have a worse prognosis^{8, 143} and are thought to derive the most benefit from revascularization. Furthermore, the extent of disease also correlates with an increased risk of complications during revascularization procedures¹⁴⁴. Currently, the coronary angiogram remains the gold-standard investigation for the diagnosis and quantification of CAD.

However, more recently increasing recognition has been given to the limitations of anatomic investigations and the importance of assessing the functional consequences of CAD to guide revascularisation²¹. Myocardial ischaemia is also known to have an adverse affect on prognosis^{10, 12}. Furthermore, a myocardial ischaemic burden of approximately 12% has been identified as an important threshold. Revascularization may confer a prognostic benefit over medical therapy in patients above this threshold whilst medical therapy may be superior in patients with little or no ischaemia¹³.

Despite this recognition much less is known about the relationship between the extent of angiographic CAD and myocardial ischaemia. The primary aim of this study was therefore to examine this relationship in a contemporary cohort of

patients with CAD by assessing the correlation between the angiographic BCIS-1 Myocardial Jeopardy Score (BCIS-JS) and CMR myocardial ischaemic burden.

The recently described BCIS-JS¹⁴⁵ provides a semi-quantitative estimate of the extent of CAD and was used initially in a large multicentre study to define high-risk patients with a large amount of myocardium at risk¹⁴⁶. This angiographic score is a modification of the Duke Jeopardy Score¹⁴⁷, which allows classification of a broader range of anatomy, including left main coronary disease and coronary artery bypass grafts. Two points each are ascribed for disease in each of 6 major proximal coronary segments and the score adjusted to account for functioning bypass grafts; the overall score ranges from 0 (for no jeopardy) to 12 (reflecting maximum jeopardy). For the full BCIS-JS see Appendix B. This broader anatomical applicability is particularly relevant given the heterogeneity of patients seen in contemporary practice. There are increasing numbers of patients with previous CABG¹⁴⁸ and increasingly complex anatomy is being considered for revascularization. In contrast to other scores¹⁴⁹⁻¹⁵², the BCIS-JS can be simply calculated by visual analysis of the coronary angiogram.

Methods

Patient population and study design

Patients with a history of stable angina and known or suspected CAD referred for diagnostic X-ray coronary angiography were prospectively included.

Exclusion criteria were: an acute coronary syndrome within 6 weeks, and left

ventricular ejection fraction <30% in addition to the general criteria in chapter 2. Patients enrolled underwent CMR examination within 90 days of X-ray angiography either as part of their routine care or as an additional research investigation. Patients were randomly assigned to undergo CMR imaging at either 1.5T or 3T (2:1 ratio) to reflect the interchangeable use of both field strengths in clinical practice and in order to complete the study prior to a planned upgrade to the 3T system.

Data acquisition

X-ray coronary angiography was performed according to the standard techniques.

CMR imaging was performed using standard techniques All examinations included high-resolution *k-t* accelerated perfusion imaging, long and short axis cine and scar imaging. The *kt*-SSFP sequence was used at 1.5T. The following parameters were used for perfusion imaging at 3T: *k-t* Turbo Field Echo sequence with shortest echo time (range 0.9-0.95ms), shortest repetition time (range 2.54-2.67ms), flip angle 20°; 90° prepulse, 120ms prepulse delay and typical acquired resolution of 1.3 x 1.3 x 10mm. CA was administered as a dual bolus. The dose was optimized for visual assessment according to local protocols (0.1mmol/kg at 1.5T and 0.075mmol/kg at 3T). Scar imaging was commenced 10-15 minutes after a total dose of 0.2mmol/kg of gadolinium and was performed using an inversion recovery turbo gradient echo sequence with the prepulse delay optimized for maximum suppression of myocardial signal.

Data analysis

Expert observers blinded to all other clinical and imaging data performed the data analysis. X-ray coronary angiograms were assigned a BCIS-JS as previously described¹⁴⁵ (Appendix B).

CMR perfusion and scar images were segmented according to the standard AHA model⁹⁶ and 16 segments analysed (true apex excluded). Each segment was further subdivided into equal endocardial and epicardial sub-segments with each sub-segment considered to represent 3% of the myocardium. Sub-segments were analysed visually and classified as normal, ischaemic or scar. Scar was defined as LGE typical of myocardial infarction affecting >50% of the sub-segment thickness. Ischaemia was defined as >50% sub-segment thickness affected by a perfusion defect present only during stress and also <50% of the sub-segment affected by scar. All other sub-segments were classified as normal. This method permitted the calculation of the myocardial scar and ischaemic burden expressed as a percentage. In addition we also calculated the combined percentage of myocardium that was affected by either scar or ischaemia.

Statistical analysis

This was performed using IBM SPSS Statistics version 19. Correlation between the BCIS-JS and CMR ischaemic burden and also the combined burden of ischaemia and scar were determined using Pearson's test of correlation with a two-tailed test of significance. ROC analysis was performed to determine the accuracy of the BCIS-JS for predicting a myocardial ischaemic burden of $\geq 12\%$.

Haemodynamic data were compared using a paired t-test. Significance was determined at <0.05 . Data are presented as mean \pm standard deviation except where stated otherwise.

Results

75 patients were enrolled in the study. 7 patients were later excluded from the analysis, 5 from the 1.5T arm and 2 from the 3T arm. Reasons for exclusion included complete heart block during adenosine infusion (1 patient), LVEF $<30\%$ (1 patient), protocol violation (1 patient), claustrophobia (1 patient) and X-ray coronary angiography not performed within 90 days of CMR (3 patients). Patients included in the final analysis were 66 ± 10 years old. Table 5.1 summarizes patient characteristics and BCIS-JS.

Table 5.1: Characteristics of the patients included in the analysis.

<i>Characteristic (n=68)</i>	<i>Number (%) of patients</i>
Male	58 (85%)
Diabetes	19 (28%)
Previous CABG	13 (19%)
Previous PCI	24 (35%)
Previous MI	12 (18%)
Hypertension	46 (68%)
Recent/Current smoking	25 (37%)
Family history of premature CAD	24 (35%)
Hypercholesterolaemia	41 (60%)
BCIS-JS	
0	12 (18%)
2	8 (12%)
4	14 (21%)
6	13 (19%)
8	11 (16%)
10	5 (7%)
12	5 (7%)
LVEF	
>55%	49 (72%)
30-54%	19 (28%)

CMR

During adenosine stress there was a significant increase in heart rate and a reduction in diastolic blood pressure (table 5.2).

Table 5.2: Haemodynamics during CMR perfusion imaging.

	<i>Rest</i>	<i>Stress</i>	<i>p value</i>
Heart rate	66±11	87±12	<0.0001
Systolic blood pressure	136±20	131±20	0.06
Diastolic blood pressure	75±7	69±11	<0.0001

Left ventricular ejection fraction was 60±12% (range 30-78%). CMR ischaemic burden was 19±15%. Combined ischaemia/scar burden was 25±20%. Scar burden was 5±8% in the study population overall and 13±8% of the myocardium in those with scar. Mean ischaemia and scar burden across the range of BCIS-JS are shown in figure 5.1.

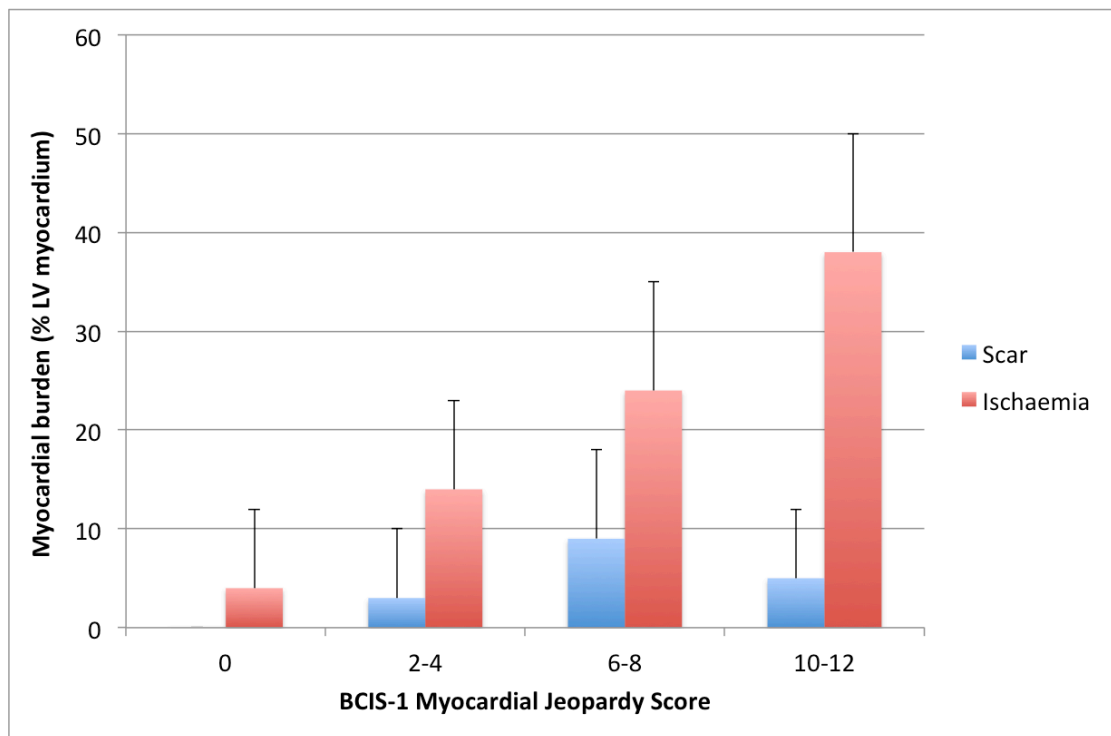


Figure 5.7: Mean LV myocardial ischaemia and scar burden according to BCIS-JS

Black bars are +1 standard deviation. Ischaemic burden increases with higher BCIS-JS in contrast to scar burden.

Scar was present on CMR imaging in every one of the 18% of patients who reported a previous myocardial infarction. In addition another 20% with no history of myocardial infarction also had scar, indicative of prior infarction, on CMR imaging. Scar was therefore present in 38% of patients overall.

Coronary angiography

The interval between CMR and coronary angiography was 23 ± 24 days. No patients reported unstable cardiac symptoms requiring hospital admission during this interval. 56 (82%) patients had significant CAD. The whole range of

CAD severity and BCIS-JS were covered as detailed in table 5.1. Figure 5.2 shows the coronary angiogram and CMR data with associated BCIS-JS and ischaemic burden from an example case.

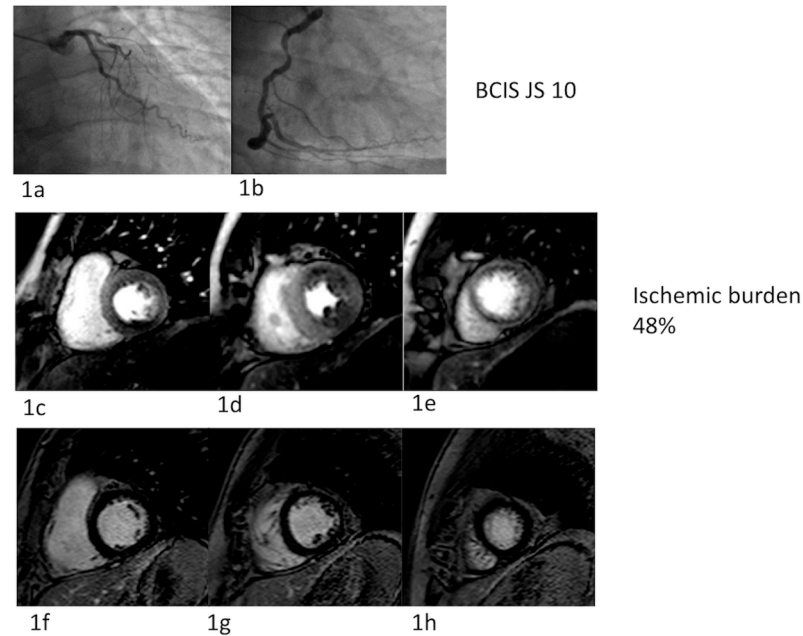


Figure 5.2: X-ray coronary angiogram and CMR stress perfusion and scar imaging from one patient.

The left anterior descending artery is proximally occluded and the circumflex is non-dominant and free from significant disease (1a). The right coronary artery is dominant and there is a severe proximal lesion. The BCIS-JS is therefore 10. High-resolution CMR stress perfusion short axis views of the basal (1c), mid (1d) and apical (1e) LV demonstrate anterior, anterolateral, inferior, inferolateral and apical perfusion defects. There is no scar in the corresponding slices (1f-1h). The myocardial ischaemic burden was calculated as 48%.

Correlation between BCIS-JS and myocardial ischaemic burden

There was a strong correlation between the BCIS-JS and myocardial ischaemic burden: Pearson's $r=0.75$, $p<0.0001$ (figure 5.3). The BCIS-JS also correlated well with the combined burden of scar and ischaemia: $r = 0.77$, $p<0.0001$.

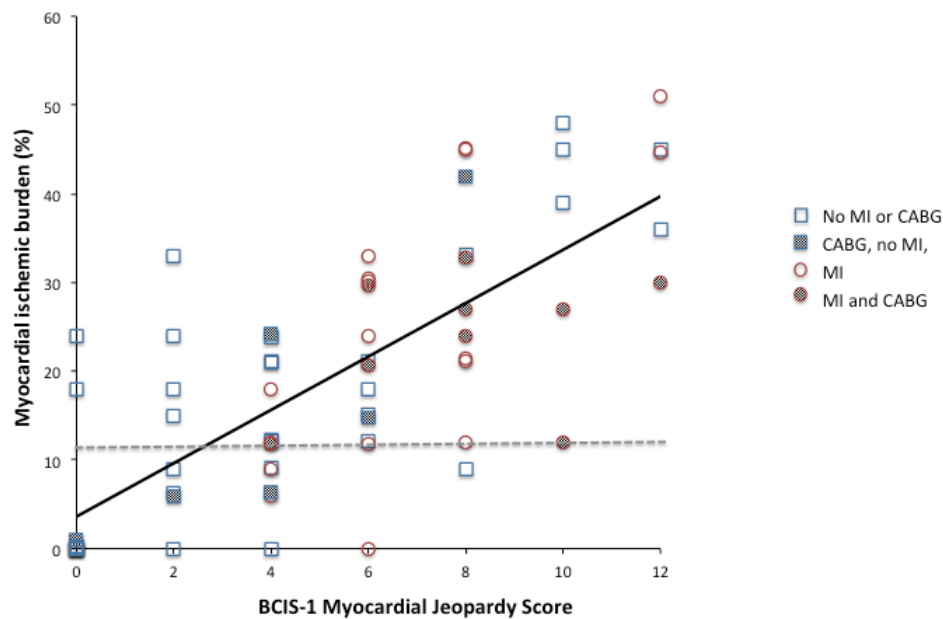


Figure 5.3: Correlation between the BCIS-JS and myocardial ischaemic burden

The graph shows the correlation between the angiographic BCIS-JS and ischaemic burden obtained using high-resolution CMR perfusion imaging. Patients without previous myocardial infarction (MI), defined as the presence of typical scar on CMR, are shown as open blue squares and those with previous MI as open red circles. Patients with previous CABG are denoted by the filled in points. Markers are offset slightly at points of overlap. The dashed line highlights the prognostically important threshold of 12% ischaemic burden.

Area under the ROC curve for BCIS-JS to detect $\geq 12\%$ myocardial ischemic burden was 0.87, 95% confidence interval 0.78-0.96. A BCIS-JS of ≥ 6 predicted $\geq 12\%$ myocardial ischaemic burden with 68% sensitivity and 91% specificity (figure 5.4).

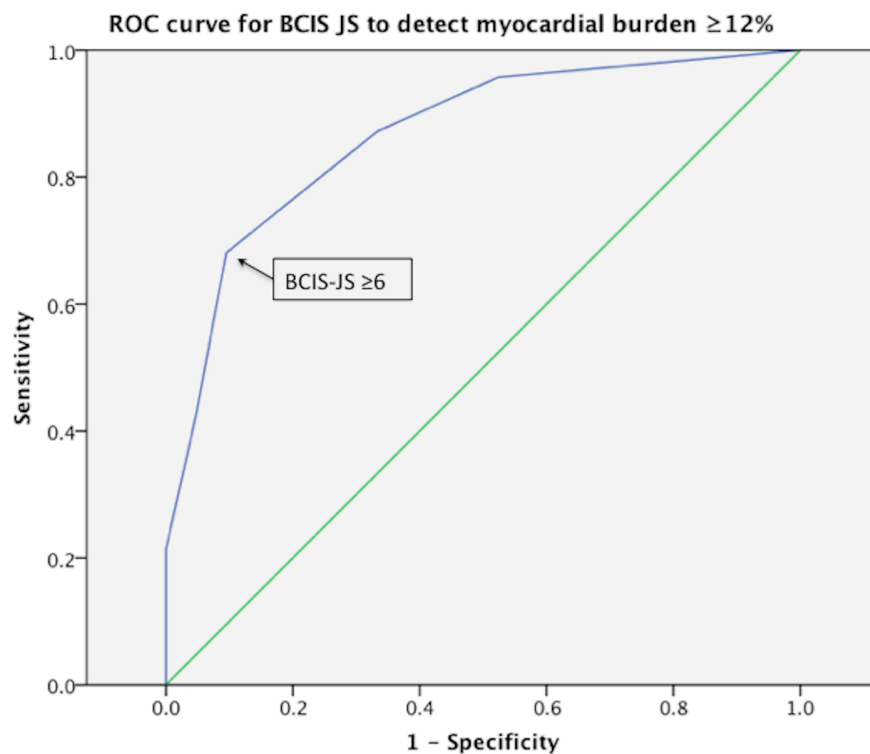


Figure 5.4: ROC curve for BCIS-JS to detect myocardial ischaemic burden $\geq 12\%$.

BCIS-JS ≥ 6 detected this threshold with sensitivity 68% and specificity 91%.

Discussion

This study demonstrates that the BCIS-JS correlates well with myocardial ischaemic burden in patients with stable angina. Furthermore, a BCIS-JS ≥ 6 predicts the prognostically important threshold of $\geq 12\%$ myocardial ischaemia with high specificity. This ischaemic threshold is important as it differentiates patients who are likely to gain a survival benefit from revascularization from those who are not¹³.

Treatment of CAD has historically been based on anatomic criteria, but more recently increasing recognition is being given to the importance of also assessing the associated myocardial pathophysiology. Despite this little is known about the functional relevance of angiographic scores. Some recent studies have examined the correlation between angiographic scores and CMR findings. However, these studies have focused on CMR methods for the determination of myocardial area at risk in patients with acute myocardial infarction. These studies also found significant correlations between CMR measures of myocardial oedema and scar burden and the Duke Jeopardy¹⁵³, the myocardial jeopardy index from the Bypass Angioplasty Revascularization Investigation (BARI)¹⁴² and the Alberta Provincial Project for Outcome Assessment in Coronary Heart Disease (APPROACH)^{142, 153, 154} scores. In contrast, the goal of this study was to combine functional and anatomic data in stable patients, and examine the ability of an angiographic score to predict ischaemic burden. To our knowledge, this has not been described previously.

BCIS-JS

Extensive CAD is known to be a marker of poor prognosis and a number of angiographic scores have been developed to quantify the extent of CAD.

We used the BCIS-JS in preference to other scores as it has a number of advantages which made it the most suitable for this study. Firstly, the purpose of the BCIS-JS is to quantify the anatomic extent of CAD. Secondly, it is universally applicable and can be used in patients with left main stem disease and CABG. Consequently it was not necessary to exclude patients on the basis of their coronary anatomy, which is a better reflection of clinical practice. Thirdly, the BCIS-JS can be quickly and easily calculated from the coronary angiogram and may therefore be more applicable in clinical practice. Finally, we have also recently validated the score as an independent predictor of outcome¹⁵⁵.

Many other angiographic scoring systems have been shown to be useful and to provide prognostic information over and above simple descriptions of anatomy. The Duke Jeopardy Score, BARI, APPROACH¹⁵¹ and other scoring systems¹⁵⁰ have all been found to be independent predictors of mortality. Similarly high SYNTAX scores have been associated with an increased risk of major adverse cardiovascular or cerebrovascular adverse events in patients treated with PCI, although the same is not true for patients undergoing CABG. However, these scoring systems vary in their primary purpose, ease of use and applicability across different groups of patients and were less suited to this study. The Duke Jeopardy score, for example, cannot be used in patients with left main stem disease or CABG. Similarly the SYNTAX score¹⁴⁹ cannot be used in patients with CABG, is complex and was designed to reflect the technical complexity of CAD

from a revascularization perspective rather than simply quantify the extent of CAD. In addition, the complexity of some scores limits their use in routine practice¹⁴⁹⁻¹⁵².

Clinical Implications

This study has implications for coronary disease classification in clinical trials and also suggests that the BCIS-JS could inform management in routine clinical practice. The BCIS-JS correlates with the amount of myocardium at risk, and as such is a potentially valuable tool for use in clinical trials of patients with CAD, undergoing any form of revascularization, medical or device therapy.

Furthermore, the finding that the BCIS-JS score can be used as a marker of myocardial ischaemia in patients with angina, confirms that the BCIS-JS can be a useful tool in the catheter laboratory. A BCIS-JS ≥ 6 is likely to be associated with a high ischaemic burden and thus may support a decision to perform revascularization. However, whilst the BCIS-JS might be used to influence management, revascularization is unlikely to be guided by the BCIS-JS alone. Moreover the prognostic significance of the 12% ischaemic burden threshold is derived from SPECT data and it remains unproven whether this threshold can be applied in CMR imaging.

It is important to note that the sensitivity of a BCIS-JS ≥ 6 for predicting $\geq 12\%$ ischaemia was modest at 68% and therefore around a third of patients with an ischaemic burden above this threshold have a BCIS-JS < 6 . This is also reflected in figure 1, as the mean ischaemic burden in patients with BCIS-JS 2-4 was

14±9% and figure 3 where similar numbers of patients with a BCIS-JS 2 or 4 lie either side of the 12% threshold.

This modest sensitivity is likely to be the result of a number of factors. Firstly, predicting the haemodynamic significance of CAD from the coronary angiogram can be difficult, and is likely to have been incorrect in some cases. In patients with fewer lesions, and thus lower BCIS-JS, the relative importance of each lesion increases. Consequently incorrect assessment of a lesions' haemodynamic significance will have a greater effect in patients with lower BCIS-JS. Secondly, the BCIS-JS simply involves scoring the proximal coronary tree segments and does not directly measure the size of the myocardial territory supplied by each vessel. For example, a patient with single vessel disease involving a dominant right coronary artery has a BCIS-JS of 4 whether this lesion is at the ostium of the vessel or just proximal to the origin of the posterior descending artery, even though the ostial lesion will result in a larger ischaemic burden. However, whilst more precise scoring systems exist, they do not have the same attributes of simplicity and universal applicability. Finally, subgroups of patients with angina, detectable myocardial ischaemia and normal epicardial arteries have been well described¹⁵⁶. Whilst this is less common than epicardial CAD there were patients with significant myocardial ischaemia and a low BCIS-JS. Such patients may be identified more frequently by high-resolution imaging techniques. As high-resolution CMR becomes more widespread it is likely these patients will be better characterized in future.

It is also noteworthy that a small number of patients with higher BCIS-JS also had an ischaemic burden close to the 12% threshold although these patients were predominantly from the group with previous myocardial infarction as discussed in more detail below. All of the above considerations are also likely to account for the fact that the correlation between the BCIS-JS and ischaemic burden, despite being good, is imperfect. These limitations underscore the fact that functional investigations continue to be important for appropriate management of many of these patients.

Myocardial scar is also relevant in many patients with established CAD and also influences both management⁸⁶ and prognosis⁹¹. It is interesting that whilst only 18% of patients in this cohort had a history of known myocardial infarction 38% of patients had CMR evidence of infarction. This finding is in keeping with a previous study⁹¹, which found that there is a high prevalence of scar in patients with known or suspected CAD but without a known prior myocardial infarction. Given the importance of scar we also examined the correlation between BCIS-JS and combined ischaemia and scar burden. Addition of scar data however had little effect on the correlation with the BCIS-JS. This is likely to be partly due to the relatively low scar burden ($5\pm 8\%$) and preserved LV function (mean ejection fraction $60\pm 12\%$) in this study cohort. This is also likely partly due to the fact that, in contrast to ischaemia, scar has a variable relationship with severe coronary stenoses. An infarct related artery, subtending a region of scar, may or may not be severely diseased; revascularization or spontaneous recanalization may alter the culprit lesion, while infarcts are also known to occur at the site of non flow-limiting stenoses.

Therefore, in patients with lower ejection fraction, a high BCIS-JS may not reflect a high ischaemic burden, as some of these patients will have extensive scar and little or no ischaemia. In this study patients with LVEF<30% were excluded in order to limit these potentially confounding effects of scar. A cut-off of 30% was chosen, rather than including only patients with normal LVEF, as patients with more severe ischaemia may have impaired LV function in the absence of scar. Functional investigation also remains particularly important in patients with extensive CAD and significant LV impairment. These patients probably need an assessment of hibernation and ischaemia to complement the anatomic information before a decision on revascularization can be made²⁶.

It may have been preferable to perform the CMR and the angiogram on the same day and use FFR to determine the significance of all lesions. However, the study was designed to represent a real world scenario where there is usually an interval between non-invasive and invasive investigations and FFR is not routinely used. The mean interval between the CMR and the X-ray coronary angiogram was 23 days, which is a short duration in the natural history of CAD. Given that there were no adverse cardiac events reported by participants during this interval it is unlikely to have had a significant impact on our findings. Nevertheless it would be of interest to incorporate routine FFR assessment as part of future studies exploring the relationship between invasive and non-invasive assessment of CAD.

Limitations

The main limitation of this study is the modest number of patients included. However, despite this limitation, enough patients were included to demonstrate a highly significant correlation. All participants had a history of angina and as a result the prevalence of CAD was high. It is not clear whether these findings can be applied in populations with a lower incidence of CAD and to patients without angina.

There are small differences between perfusion imaging at 1.5T and 3T. Higher resolution imaging at 3T may mean that ischaemic or scar burden estimation may vary according to field strength. This may be particularly relevant in the presence of scar where higher resolution perfusion imaging may allow identification of peri-infarct ischaemia. However, to date, in contrast to SPECT imaging, little is known about ischaemic burden measured by CMR. In this study we classified each sub-segment (50% of every myocardial segment) as normal, ischaemic or scar. In order to be classified as ischaemic or scar these sub-segments had to be at least 50% abnormal themselves (i.e at least 25% transmural scar or ischaemia). Since abnormalities of this magnitude were well within the resolution of imaging at both field strengths we anticipated that any differences would therefore be small and will not have influenced the overall findings. However we did not systematically assess for differences between the field strengths as part of this study.

Conclusions

The anatomic BCIS-JS correlates well with myocardial ischaemic burden measured using CMR perfusion imaging. A BCIS-JS ≥ 6 also predicts the prognostically important ischaemic threshold of 12% with high specificity.

These findings provide insight into the relationship between anatomic and functional measures of CAD severity. Furthermore, they support the use of the BCIS-JS for classification of CAD burden in clinical trials and for assisting in the clinical management of patients.

6 PERFUSION IMAGING. Inter-Study Reproducibility of Quantitative CMR Myocardial Perfusion Imaging.

Abstract

Objectives

Evaluate the inter-study reproducibility of hyperaemic and rest myocardial perfusion and MPR and whether these parameters vary during the day.

Background

Absolute quantification of myocardial perfusion with CMR is increasingly available and can potentially improve current qualitative and semi-quantitative analysis. The absence of ionising radiation makes CMR ideal for serial examinations for patient management or in clinical trials. Inter-study reproducibility is crucial for serial examinations but data for quantitative CMR perfusion are very limited.

Methods

Sixteen healthy volunteers underwent high-resolution 3T perfusion imaging three times during a single day to evaluate inter-study reproducibility and for effects of daytime variation.

Absolute perfusion was determined in each coronary artery territory and globally by Fermi constrained deconvolution of myocardial signal intensity curves. LV volumes and function were also calculated.

Results

Eleven full datasets were suitable for quantitative perfusion analysis. Inter-study reproducibility was reasonable with rest perfusion more reproducible than stress and global better than territorial. The coefficient of variation (CV) for global stress and rest perfusion and MPR was 26.8%, 16.0% and 23.9% respectively. Corresponding territorial CV were 35.2%, 27.5% and 33.5%. The reproducibility of left ventricular volumes and function was excellent (CV 4%, 7.7% and 4.6% for end diastolic volume, end-systolic volume and ejection fraction respectively). There were no significant detectable changes in perfusion or LV volumes and function during the day.

Conclusions

The inter-study reproducibility of quantitative myocardial perfusion is reasonable and best for global rest perfusion. No significant daytime variation in perfusion was observed.

Introduction

Evaluation of myocardial perfusion is a key function of CMR imaging¹⁵⁷. As previously discussed quantification of myocardial perfusion may be superior to visual analysis as it eliminates the requirement for the presence of a normally perfused region of myocardium. Moreover it should allow more robust calculation of ischaemic burden and more precise characterisation of changes in perfusion due to physiological variation, disease and therapeutic interventions. One of the main advantages of CMR over other imaging modalities is that the absence of ionising radiation makes it ideal for serial examinations. Serial examinations have an important place both in clinical practice and in studies. However, in order for quantitative CMR perfusion imaging to be a useful tool for repeated studies, inter-study reproducibility must be acceptable.

Data on the reproducibility of myocardial perfusion imaging are limited. PET studies have reported reasonably good inter-study reproducibility in volunteers¹⁵⁸. However the inter-study reproducibility of fully quantitative CMR has only previously been reported in terms of MPR¹⁵⁹ or with long intervals between studies¹⁴¹. Furthermore, cardiovascular function is affected by diurnal variation and changes in heart rate, blood pressure and ischaemic threshold during the course of the day are well recognised¹⁶⁰. Previous studies have not assessed whether myocardial perfusion varies during the course of the day despite the fact that this is important in determining whether serial measurements need to be performed under the same conditions

The objectives of this study were therefore to evaluate the inter-study reproducibility of hyperaemic and rest myocardial perfusion and MPR and also whether these changed during the course of the day.

Methods

Population

Sixteen healthy volunteers were recruited by University email. Volunteers underwent 3 stress and 3 rest perfusion scans on the same day. Exclusion criteria were: known cardiac, respiratory or renal disease or a contraindication to MRI.

Data acquisition

CMR imaging was performed on the 3 Tesla clinical MRI scanner. Participants were asked to abstain from caffeine and smoking for 24 hours prior to any imaging and to fast from midnight on the day of the scans. Those who did not were excluded. Participants then underwent 3 CMR examinations as close as possible to 09:00 (Scan A), 09:30 (Scan B) and 14:00 (Scan C). Between scan 2 and 3 participants left the department and were allowed to eat and drink freely apart from the restrictions on adenosine antagonists described above. Scan A and B were used to evaluate perfusion inter-study reproducibility under the same conditions. Scan C was used to evaluate whether variations in perfusion could be detected, due to circadian rhythms, changes in subject hydration or any other cause.

Each CMR scan lasted approximately 30-minutes and followed the same protocol as follows:

- survey, coil reference scan and planning to define imaging planes
- 4-chamber cine
- 2-chamber cine
- test perfusion
- stress perfusion
- short axis stack to cover entire LV
- 3-chamber cine
- rest perfusion

Cine images were acquired using a standard balanced steady state free precession (SSFP) sequence. Perfusion imaging was performed using the same high-resolution *k-t* accelerated gradient echo sequence described in chapter 5 (shortest echo time {range 0.85-0.99ms}, shortest repetition time {range 2.45-2.75ms}, 20° flip angle; 90° prepulse, 120ms prepulse delay and acquired resolution of 1.3 x 1.3 x 10mm). Perfusion imaging was planned according to standard methods and images acquired every heartbeat. The imaging geometry and field of view were kept constant for each perfusion sequence. In order to account for higher heart rates at stress, if required, the voxel size was increased stepwise, to maintain imaging at every heartbeat. (This was required in 3 subjects; 2 were imaged at 1.6 x 1.6 x 10mm and 1 at 1.9 x 1.9 x 10mm). Hyperaemia was induced with the standard adenosine regimen. For this study the dual bolus consisted of equal volumes of 0.0045mmol/kg followed by 0.045mmol/kg of CA separated by a 25-second pause. This allowed six

perfusion scans to be performed and limited the total dose of CA to $<0.3\text{mmol/kg}$. During perfusion image acquisition participants held their breath at end-expiration during both contrast agent boluses and breathed gently during the pause. Participants were removed from the scanner between each exam.

Data analysis

Myocardial Perfusion

Quantitative analysis was performed by a blinded observer using dedicated prototype software (ViewForum, Philips Healthcare, Best, The Netherlands). The mid myocardial slice was used for further analysis. The data were analysed visually initially and any studies affected by severe artefact during the first pass of the main bolus of contrast agent, such that reliable signal intensity curves would not be produced, were excluded. Myocardial border detection was automated and manually corrected where required. Global myocardial perfusion and perfusion in each of the 3 myocardial territories according to a standard definition⁹⁶ were determined using Fermi deconvolution⁷⁵. Cases where deconvolution was not possible were also excluded. MPR was defined as the ratio of stress to rest perfusion.

Left ventricular volumes and function

Images were analysed in a random order by a blinded experienced observer using CMR42 (Circle, Calgary, Canada). The mitral valve plane and apex were identified from the 4-chamber view in end-diastole and end-systole. The LV

endocardial border was automatically defined in the corresponding end-systolic and end-diastolic SA slices and was manually corrected where required.

Papillary muscles were excluded.

Statistical analysis

Statistical analysis was performed using Microsoft Excel and IBM SPSS Statistics version 19. For inter-study reproducibility evaluation a coefficient of variation (CV), and Bland Altman plots were calculated in keeping with previous reproducibility studies¹⁶¹. Mean segmental and global perfusion and MPR values and the intra-subject differences between exam A and B were calculated. The CV was defined as the standard deviation of these differences divided by the mean. Analyses were all performed on a per observation basis. The Shapiro-Wilk test determined that the data were normally distributed. Mean values from Scans A, B and C were compared with ANOVA with repeated measures. Post hoc tests using the Bonferroni correction were used for pairwise comparisons. Continuous data are presented as mean \pm standard deviation. Significance was determined as $p < 0.05$.

Results

Sixteen volunteers were included. Five were later excluded and 11 full datasets included in the final analysis. Reasons for exclusion were: 1 subject withdrawal, 1 failure of scanner gradients prior to test completion and in 3 subjects 1 or more perfusion scans were unsuitable for quantitative analysis due to artefact. Of those excluded due to artefact one volunteer failed to hear the breath-hold

commands during two perfusion sequences due to intermittent headphone failure and one volunteer failed to breath hold adequately during the rest perfusion sequence of Scan B. The third volunteer was excluded as during the rest perfusion scan from Scan B there was no increase in myocardial signal intensity and deconvolution was not possible.

Participants included in the final analysis were 27 ± 5 years old and five were male. Body mass index was 28.0 ± 7.4 (median 26.2; range 20-48). They were all non-smokers with no significant medical problems and were not taking any medications.

Perfusion imaging

There were ≥ 10 minutes between all perfusion scans. During Scans A and B the interval between CA injections was 13.9 ± 2.8 minutes and during Scan C it was 16 ± 3.7 minutes. The interval between Scans B and C was 236.9 ± 29.3 minutes.

A representative stress perfusion study with territorial segmentation is shown in figure 6.1. Myocardial perfusion and haemodynamics for all three studies, and the significance of associated differences, are shown in table 6.1. Stress heart rate and rate pressure product (RPP) were significantly higher in scan A. There was a trend for rest and stress perfusion to be lower in Scan B than in Scan A although this did not meet statistical significance. No significant daytime variation in perfusion could be detected.

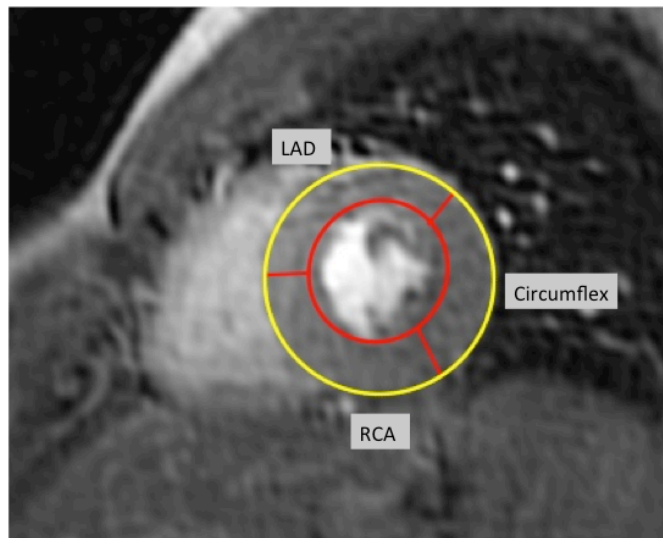


Figure 6.1: Stress perfusion image with territorial segmentation.

Still image, from a representative study, showing a single frame from the first pass of the main bolus of contrast agent. The standard coronary artery territories used for the study are demonstrated. LAD-left anterior descending artery; RCA-right coronary artery.

Table 6.1: Myocardial perfusion and haemodynamics for the 11 subjects during each of the three scans.

	<i>Scan A</i>	<i>Scan B</i>	<i>Scan C</i>	<i>p value</i>
Perfusion-Territorial (ml/min/g)				
Stress				
Mean	2.5±0.8	2.1±0.6	2.2±0.8	0.05
LAD	2.5±0.9	2.2±0.6	2.2±0.8	
Circumflex	2.2±0.7	2.0±0.7	2.0±0.6	
RCA	2.7±0.8	2.1±0.7	2.4±0.9	
Rest				
Mean	0.6±0.2	0.5±0.1	0.5±0.2	0.05
LAD	0.6±0.1	0.5±0.1	0.6±0.1	
Circumflex	0.5±0.1	0.5±0.1	0.5±0.1	
RCA	0.7±0.2	0.6±0.2	0.6±0.2	
Perfusion-global (ml/min/g)				
Stress	2.5±0.5	2.1±0.5	2.2±0.7	0.19
Rest	0.6±0.1	0.5±0.2	0.5±0.2	0.1
MPR				
Territorial	4.3±1.3	4.3±1.4	4.1±1.1	0.34
Global	4.3±0.9	4.2±1.2	4.0±0.6	0.37
Heart rate (bpm)				
Stress	111±14	105±16	106±17	0.03
Rest	74±10	73±9	73±14	0.92
SBP (mmHg)				
Stress	121±16	120±14	122±16	0.54
Rest	119±21	119±16	120±23	0.92
RPP (HR.SBP)				
Stress	13550±2747	12696±2592	13009±2758	0.046
Rest	8919±2639	8764±1698	8789±2377	0.90
DBP (mmHg)				
Stress	73±7	70±11	70±8	0.24
Rest	69±9	66±6	64±9	0.06

Data are mean ± standard deviation. Small differences in the average values are due to rounding.

SBP=systolic blood pressure; RPP=rate pressure product; DBP=diastolic blood pressure.

The mean differences between perfusion in Scan A and B with associated CV are shown in table 6.2 and between Scan A and C in table 6.3. These demonstrate reasonable inter-study reproducibility. Global perfusion is more reproducible than territorial perfusion and rest perfusion more reproducible than stress perfusion. Bland Altman plots for territorial rest and stress perfusion and MPR are shown in figure 6.2.

Table 6.2: Inter-study reproducibility of perfusion imaging (Scan A vs B).

		<i>Territorial</i> <i>(n=33)</i>	<i>Global</i> <i>(n=11)</i>
Stress perfusion (ml/min/g)	Mean Difference±SD	0.35±0.81	0.36±0.62
	Coefficient of Variation	35.2%	26.8%
Rest perfusion (ml/min/g)	Mean Difference±SD	0.07±0.16	0.07±0.09
	Coefficient of Variation	27.5%	16.0%
MPR	Mean Difference±SD	0.07±1.43	0.07±1.03
	Coefficient of Variation	33.5%	23.9%

Table 6.3: Inter-study reproducibility between Scans A and C.

		<i>Territorial</i>	<i>Global</i>
		<i>(n=33)</i>	<i>(n=11)</i>
Stress perfusion (ml/min/g)	Mean Difference±SD	0.28±0.82	0.28±0.69
	Coefficient of Variation	34.9%	29.0%
Rest perfusion (ml/min/g)	Mean Difference±SD	0.04±0.17	0.04±0.11
	Coefficient of Variation	29.6%	19.0%
MPR	Mean Difference±SD	0.19±1.54	0.23±1.04
	Coefficient of Variation	36.3%	25.2%

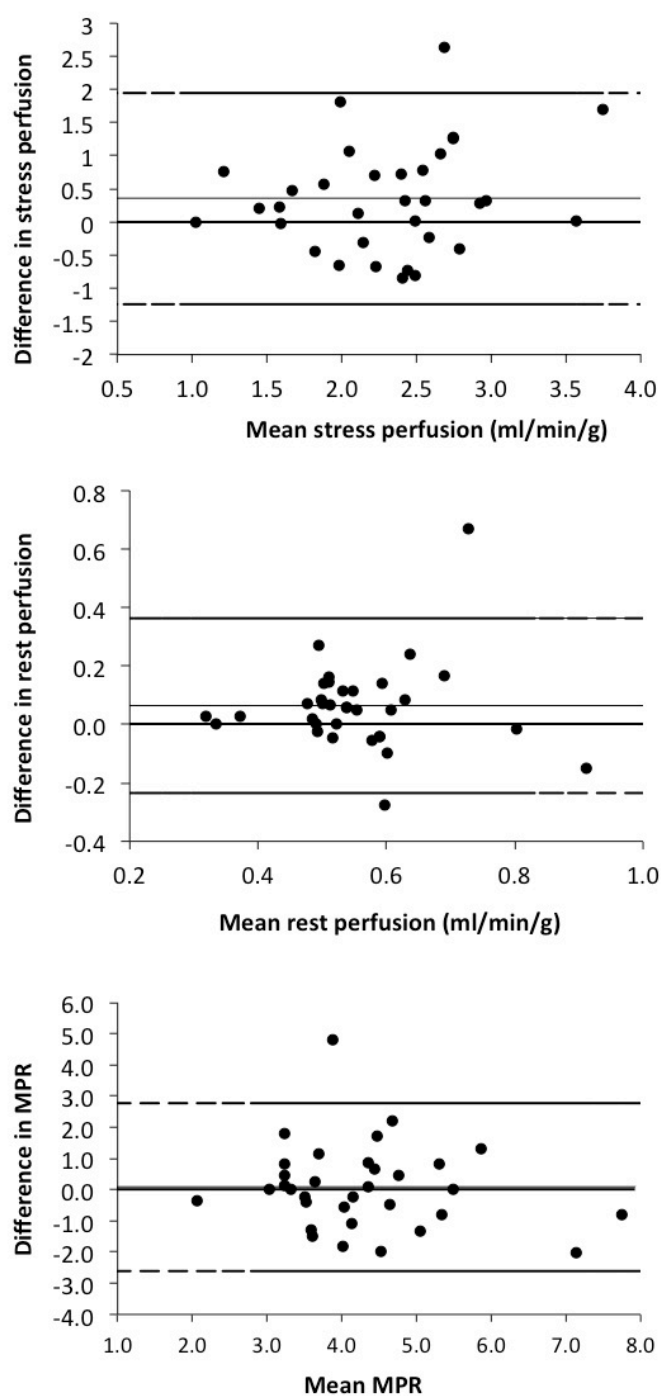


Figure 6.2: Perfusion imaging inter-study agreement

Bland Altman plots showing the inter-study agreement between stress and rest perfusion and MPR between Scans A and B. The mean difference and limits of agreement (1.96 standard deviations) are shown.

Left ventricular volumes and function

LV mean volumes and ejection fractions, mean differences between Scan A and B and associated CV are shown in table 6.4. There were no significant changes in LV volumes or function between scans. Inter-study reproducibility was excellent with low CV for all parameters.

Table 6.4: Mean values, intra-subject differences and inter-study reproducibility for LV volumes and function.

	<i>Scan</i>			<i>p</i>	<i>Mean</i>	<i>CV*</i>
	<i>A</i>	<i>B</i>	<i>C</i>		<i>difference</i> <i>± SD</i>	
LVEDV	161.7±33.3ml	162.5±37.0ml	161.2±39.7ml	0.76	-2.1±6.7	4.0%
LVESV	67.5±17.3ml	68.9±20.0ml	64.9±18.3ml	0.28	-1.9±5.5	7.7%
LVEF	58.5±3.2%	58.0±4.3%	59.6±4.5%	0.86	0.55±2.7	4.6%

*CV=coefficient of variation based on scans A and B.

LVEDV=left ventricular end-diastolic volume; LVESV= left ventricular end-systolic volume; LVEF=left ventricular ejection fraction.

Discussion

This study demonstrates that fully quantitative CMR perfusion analysis has moderate inter-study reproducibility in normal hearts. Global perfusion is more reproducible than territorial and rest more reproducible than stress.

Furthermore, with current techniques, daytime variations in perfusion are not detectable.

The value of inter-study reproducibility

CMR does not use ionising radiation and there are no known long-term adverse sequelae as a result of repeated examinations. Consequently CMR is an ideal modality for serial examinations. Many diseases affecting myocardial perfusion are chronic and patients require serial examinations. This may be in order to monitor disease progression or to determine the timing or efficacy of therapeutic interventions. This is applicable to patients with CAD but also to other patient groups, for example, PET studies have demonstrated that quantitative perfusion can provide additional information about the coronary microcirculation³⁶. Quantitative perfusion therefore also has a potential role in the characterisation and management of patients with microvascular disease, such as those with hypertension, diabetes and angina with normal epicardial coronary arteries. In addition to routine clinical practice serial examinations and surrogate end-points are required for clinical trials. Quantitative perfusion could potentially detect changes in perfusion, which cannot be detected by non-quantitative analysis. Furthermore inter-study reproducibility is related to the number of subjects required for studies to detect significant results. Improved

reproducibility means fewer subjects and studies that are easier and less expensive to complete. It is, therefore, crucially important to know the inter-study reproducibility to understand the potential role for CMR imaging in these clinical and research settings.

Inter-study reproducibility of quantitative perfusion imaging

The degree of variability between measurements, and hence the magnitude of the CV, which is acceptable will vary depending on what is clinically relevant. It is therefore important to interpret these findings in the context of the magnitude of changes that need to be detected. For example, studies in patients with coronary artery disease^{42, 43} have shown that stress perfusion differs by approximately 100% or more between coronary territories subtended by normal arteries and severely diseased arteries. In keeping with this stress perfusion values in the normal volunteers in this study were also approximately 100% greater than those in stenotic territories of patients included in the PET comparison study in chapter 4. MPR was also approximately 200% greater in these volunteers. Therefore, based on the reproducibility findings reported here, it would be expected that stress perfusion imaging could reliably detect changes of this magnitude. Conversely, large studies would be required to detect smaller changes in perfusion, such as those that may be expected as a result of drug therapy. Of note in the previous PET comparison study differences of approximately 26% in stress perfusion between stenotic and remote territories were described with CMR. However in this study remote territories were not normal and were subtended by arteries with diameter stenosis of 0-69%.

To date there are very limited data on the inter-study reproducibility of quantitative CMR perfusion. A previous study by Elkington et al. analysed the inter-study reproducibility of quantitative CMR perfusion¹⁵⁹ in a combined cohort of volunteers and patients with coronary artery disease. They performed two perfusion studies at a mean interval of 13 ± 18 days, and also quantified perfusion from a single a midventricular slice, acquired at high-resolution, using Fermi deconvolution. However, in contrast to our study, they did not report absolute perfusion values. They reported a CV for global MPR of 21% and CVs for regional perfusion of 26-35%. These values are very similar to the corresponding global and territorial values in our study (23.9% and 27.5-35.2% respectively). They also found absolute quantification to be more reproducible than semi-quantitative analysis. Important differences between the previous study and ours include the fact that our study was performed at 3T using a *k-t* accelerated perfusion technique whereas the former was performed at 1.5T using a spoiled gradient echo (FLASH) sequence. It is therefore noteworthy that these differences do not appear to result in superior reproducibility.

A sub-study of the Multi-Ethnic Study of Atherosclerosis¹⁴¹ evaluated inter-study reproducibility of quantitative CMR perfusion. This study also demonstrated reasonable reproducibility and, in agreement with our study, they also found global and rest perfusion to be the most reproducible. However the interval between the two examinations was very long (mean 334 days) as reproducibility assessment was not the primary aim of the main study.

Semi-quantitative analysis of CMR perfusion has also been found to have moderate to good reproducibility in another study of a mixed cohort of normal volunteers and patients with coronary artery disease¹⁶². The reproducibility of a semi-quantitative index of MPR derived from normalised upslope analysis was also comparable to ours. However although of a similar magnitude, they reported consistently lower CV than we found for fully quantitative MPR. Furthermore there was also less of a difference between global (17.6%) and territorial (17.6-20.7%) CV.

Data on the inter-study reproducibility of quantitative PET myocardial perfusion are also limited. One recent study performed serial 82-Rubidium PET perfusion imaging in volunteers without cardiac disease at a median interval of 22 days¹⁵⁸. This study reported repeatability coefficients (1.96 x standard deviation of differences divided by mean) in 56 true normal subjects of 35%, 34% and 38% for global rest and stress perfusion and MPR respectively. The equivalent repeatability coefficients for this study are 32%, 53% and 47% suggesting that CMR may be less reproducible than PET at present. However, it is noteworthy that in this PET study reproducibility was significantly worse in subjects who were retrospectively classified as not normal on the basis extensive clinical, biochemical and ECG screening. This is by far the largest PET study of inter-study reproducibility. Previous studies have been similar to ours involving relatively small cohorts of normal subjects^{51, 80, 140, 163, 164}. Follow-up perfusion studies were performed either immediately, as in our study, or after a short interval. These studies reported similar reproducibility to the 82-Rb study

described above and some also found that reproducibility was best for global and rest perfusion⁸⁰.

In this study we found that there was a significant reduction in stress RPP between Scans A and B despite using the same adenosine protocol.

Furthermore there was a trend towards reduced territorial stress and rest perfusion although this did not reach significance ($p=0.05$ for both). Inter-individual variation in the response to adenosine is well reported¹⁶⁵ and significant reductions in heart rate response are seen when adenosine infusion is repeated after caffeine intake¹⁶⁶. However, in this study it may be that familiarisation with the protocol meant that subjects were less anxious during the second administration of adenosine. This change in RPP could explain the trend towards reduced stress perfusion between Scans A and B but does not account for the trend towards reduced rest perfusion. Quantitative CMR perfusion relies on myocardial signal intensity analysis. The half-life of the contrast agent used in this study is approximately 90-minutes whereas the interval between perfusion imaging between Scans A and B was much shorter. Consequently the baseline myocardial signal continues to increase after each dose of contrast agent. The signal intensity in a region of interest at the start of each perfusion scan was subtracted for baseline correction of each signal curve. However, this correction may result in an under-estimation of perfusion in subsequent studies. This finding has implications for quantitative analysis of serial perfusion studies repeated at a short interval. For example, both in clinical practice and in studies it is common to perform both stress and rest perfusion during the same examination. Moreover both stress and rest

perfusion are clearly required for calculation of MPR. It is therefore important that this observation is evaluated further in future studies.

A number of different CMR techniques and perfusion sequences are used for clinical and research perfusion imaging. For this study we used our standard 3 Tesla clinical perfusion sequence, which includes three slices at basal, mid and apical left ventricular levels, in order to establish reproducibility of a sequence and methods in routine clinical use. Since this study only included normal volunteers we do not expect that there are important differences in the reproducibility of perfusion estimates between slices and therefore selected segments to represent all three coronary territories from the mid-slice for analysis. However it would be interesting to assess whether there are any systematic differences in perfusion and perfusion reproducibility between slices in an appropriately powered prospective study.

Myocardial perfusion values reported here are lower than some studies have previously reported¹⁶⁷ and may therefore represent an underestimate. However, they are very similar to values previously reported for healthy volunteers in previous ¹³N-ammonia PET studies^{140, 168}. Discrepancies in normal perfusion ranges seen in studies may arise due to small sample sizes. Alternatively they may arise as a result of differences in study populations, scanners, tracers or contrast agents, methods of sampling arterial input function or myocardial regions of interest, or mathematical perfusion models^{169, 170}. Since MPR is a ratio of stress to rest perfusion this corrects for many of

these differences and the MPR values found in this study are in keeping with previous literature.

Diurnal variation

Many biological processes exhibit circadian rhythms and heart rate and blood pressure changes are well known¹⁷¹. Consequently studies are often designed to minimise the effects of physiological variation either as a result of circadian rhythms or changes in participants' volume status and therefore ventricular volumes¹⁶¹. However, data on whether detectable diurnal changes in left ventricular volumes and function actually occur are limited^{172, 173}. Previous echocardiographic studies have suggested that there are no diurnal variations in LV volumes and systolic function. Nonetheless variations in some parameters reflecting diastolic function have been demonstrated in healthy volunteers^{172, 174}. In keeping with these studies, and despite designing the study to try and maximise variation between Scan A and C, we could not detect any significant changes in LV volumes or function or myocardial perfusion during the course of the day. This suggests that daytime variations in perfusion are not important for study design or clinical practice at present. However it is also important to note that small differences in perfusion are unlikely to have been detectable using current methods. It is also noteworthy that we only measured perfusion at two different times of day and if we had examined participants at more time points, particularly during the night, it may have been possible to detect diurnal variation. However most perfusion CMR imaging takes place during working hours, in keeping with the times used here, and therefore the findings are of

practical relevance. Finally this study confirms the excellent inter-study reproducibility of CMR LV volumes and function described in previous studies¹⁷⁵.

Limitations

The main limitations of the study are the small sample size and inclusion of healthy volunteers rather than patients. However there are no previously reported quantitative CMR perfusion studies reporting absolute perfusion values from multiple examinations performed within a short space of time. Furthermore, the equivalent PET literature consists of a modest number of studies, most which have small sample sizes and involve normal volunteers.

The *k-t* accelerated sequence is susceptible to respiratory artefacts, which can be problematic for quantification. Three subjects were excluded as a result of the unsuitability of one or more of the perfusion scans for quantitative analysis. However this relatively high exclusion rate also reflects the fact that three stress and three rest scans were required for each subject whereas usually fewer scans would be required for clinical care or studies.

Conclusions

Quantitative CMR myocardial perfusion analysis has reasonable inter-study reproducibility using current methods. Global perfusion is more reproducible than territorial perfusion and rest perfusion more reproducible than stress. No significant daytime variation in myocardial perfusion could be detected. On-

going refinement of quantitative post-processing methods should result in further improvements in inter-study reproducibility in the future.

7 MYOCARDIAL VIABILITY AND ISCHAEMIA. Evaluation of the Inter-Study Reproducibility of CMR Feature Tracking

Abstract

Objectives

Determine the inter-study reproducibility of CMR feature tracking and whether strain analysis using feature tracking changes during the course of the day .

Background

Cardiovascular magnetic resonance myocardial feature tracking (CMR-FT) is a recently described method of post processing routine cine acquisitions which aims to provide quantitative measurements of circumferentially and radially directed ventricular wall strain. Inter-study reproducibility is important for serial assessment however has not been defined for CMR-FT.

Methods

Sixteen healthy volunteers were imaged three times within a single day. The first examination was performed at 0900 after fasting and was immediately followed by the second. The third, non-fasting scan, was performed at 1400.

CMR-FT measures of segmental and global strain parameters were calculated. LV circumferential and radial strain were determined in the short axis orientation (Ecc_{SAX} and Err_{SAX} respectively). LV and right ventricular

longitudinal strain and LV radial strain were determined from the 4-chamber orientation (Ell_{LV} , Ell_{RV} , and Err_{LAX} respectively). LV volumes and function were also analysed.

Inter-study reproducibility and study sample sizes required to demonstrate 5% changes in absolute strain were determined by comparison of the first and second exams. The third exam was used to determine whether daytime variation in CMR-FT derived strain affected reproducibility.

Results

CMR-FT strain analysis inter-study reproducibility was variable. Global strain assessment was more reproducible than segmental analysis. Overall Ecc_{SAX} was the most reproducible measure of strain: coefficient of variation (CV) 38% and 20.3% and intraclass correlation coefficient (ICC) 0.68 (0.55-0.78) and 0.7 (0.32-0.89) for segmental and global analysis respectively. The least reproducible segmental measure was Ell_{RV} : CV 60% and ICC 0.56 (0.41-0.69) whilst the least reproducible global measure was Err_{LAX} : CV 33.3% and ICC 0.44 (0-0.77). Variable reproducibility was also reflected in the calculated sample sizes, which ranged from 11 (global Ecc_{SAX}) to 156 subjects (segmental Ell_{RV}). The reproducibility of LV volumes and function was excellent. There was no variation in global strain or LV volumetric measurements during the day.

Conclusions

Inter-study reproducibility of CMR-FT varied between different parameters, as

summarized above and was better for global rather than segmental analysis. It was not measurably affected by daytime variation. CMR-FT may have potential for quantitative wall motion analysis with applications in patient management and clinical trials. However, inter-study reproducibility was relatively poor for segmental and long axis analyses of strain, which have yet to be validated, and may benefit from further development.

Background

Myocardial wall motion analysis is key for assessment of LV and right ventricular (RV) function. It is important for the evaluation of viability and ischaemia during dobutamine stress in patients with CAD¹⁷⁶ and for identification of cardiomyopathies¹⁷⁷. CMR is an established method for wall motion assessment as it provides excellent endocardial border definition and can be combined with other techniques for a comprehensive, radiation-free, cardiac assessment in a single session¹⁵⁷. Currently visual assessment of wall motion is standard however this is limited by inter-observer variability¹⁷⁸. To date quantitative techniques for assessment of wall motion, such as myocardial tagging, have not been widely adopted due to the requirement to perform additional scans and the associated complex and time-consuming post-processing^{179, 180}. Novel methods, which allow more robust and user-independent quantitative wall motion assessment, are therefore desirable.

CMR myocardial feature tracking (CMR-FT) has been recently described^{181, 182} and is a method of quantitative wall motion assessment, which is analogous to echocardiographic speckle-tracking. Standard CMR cine images are analysed off-line and acquisition of additional sequences is therefore not required. CMR-FT aims to provide measurements of circumferentially, radially and longitudinally directed ventricular wall strain. However, in order to be robust and useful, analytical techniques must be sufficiently reproducible. Reasonable inter and intra-observer reproducibility of feature tracking has already been demonstrated^{183, 184}. The aim of this study therefore was to evaluate the inter-

study reproducibility of CMR-FT and ascertain whether this is affected by detectable physiological variation.

Methods

Population

The same 16 healthy volunteers recruited for the previous study (chapter 6) formed this study cohort.

Data acquisition

CMR protocols were as described in the previous chapter (page 166). Cine images were acquired using a standard balanced steady state free precession (SSFP) sequence. Planning and acquisition were as follows: A pseudo 2-chamber cine was planned from the axial survey images and this was subsequently used to plan a pseudo 4-chamber cine. Systolic frames from the pseudo 2 and 4-chamber cines were then used to plan 3 short axis cine slices of the basal, mid and apical LV. Diastolic frames from preceding cines were then used to plan definitive views. The pseudo 2-chamber and short axis views were used to plan the 4-chamber cine. This 4-chamber view and the pseudo short axis slices were used to plan the 2-chamber cine. The 2 and 4-chamber views were used to plan, contiguous short axis (SA) cine slices covering the entire LV, and the 4-chamber and short axis views to plan a 3-chamber cine. SSFP cine in-plane resolution was 1.8 x 2mm and slice thickness 8mm. The protocol was the same for all three scans and for all participants.

Data analysis

Feature tracking

Images were analysed in a random order by a blinded experienced observer. CMR-FT strain analysis was performed using dedicated prototype software (Diogenes MRI, Tomtec, Unterschleissheim, Germany). Endocardial contours were manually drawn in all views included in the analysis. The 4-chamber view was used to determine RV and LV longitudinal strain and LV radial strain (Ell_{RV} and Ell_{LV} and Err_{LAX}). LV short axis circumferential (Ecc_{SAX}) and radial strains (Err_{SAX}) were calculated from a mid-ventricular short-axis view containing both papillary muscles. The RV upper septal insertion point was manually defined to allow accurate segmentation according to a recognized standard model⁹⁶. All parameters were analysed for all three exams. Strain values (% change from baseline) were obtained for each segment and global values defined as the mean of all segmental values.

Left ventricular volumes and function

Images were analysed in a random order by a blinded experienced observer using CMR42 (Circle, Calgary, Canada) as described in the previous chapter.

Statistical analysis

Statistical analysis was performed using Microsoft Excel and IBM SPSS Statistics version 19. For inter-study reproducibility evaluation a CV, intraclass correlation coefficient (ICC) and Bland Altman plots were calculated. The CV

was defined as the standard deviation of the differences divided by the mean as previously. Analyses were all performed on a per observation basis.

The significance of differences in reproducibility between exam A and B (reproducibility AB) and exam A and C (reproducibility AC) was evaluated by comparing the squared differences between the observations. These were compared directly with a paired t test if normally distributed (LV volumes and function) or after natural log transformation if not normally distributed (strain)¹⁶¹. The Shapiro-Wilk test determined normality. The mean values for each strain parameter from Scan A, B and C were not normally distributed and therefore were compared using the Friedman test. Left ventricular volumes and function were compared using ANOVA with repeated measures as described in the previous chapter.

Study sample sizes required to show a 5% absolute change in strain with a power of 90% and an α error of 0.05 were calculated as follows¹⁶¹:

$$n = f(\alpha, P) \cdot \sigma^2 \cdot 2 / \delta^2$$

where n is the sample size, $f = 10.5$ for α 0.05 and P 0.9, σ the inter-study standard deviation and δ the magnitude of the difference to be detected.

Continuous data are presented as mean \pm standard deviation. Significance was determined as $p < 0.05$.

Results

Participant details

Participant age was 27.9 ± 5.7 and body mass index 26.2 ± 6.8 . Eight were male and eight female. One participant chose not to re-attend for Scan C after Scans A and B. All other participants completed the protocol. The CMR data of one other participant was found to be incompatible with the CMR-FT software (transient high signal in the pulmonary arteries affected the grey scaling obscuring endocardial border tracking). This participant was therefore only included in the volumetric assessments. Image quality was otherwise good or excellent in all subjects.

Feature tracking

Mean segmental and global strain parameters for all three exams are summarised in table 7.1. Mean segmental Err_{SAX} was significantly different ($p=0.04$) between the scans although the largest difference was between Scans A and B. There were no significant differences in any of the other strain parameters.

Table 7.1: Strain values for the combined study population.

	<i>Scan</i>			<i>p value</i>
	A	B	C	
Segmental (n=90)				
Err _{SAX}	22.4±9.6	19.2±8.0	20.9±9.0	0.04*
Ecc _{SAX}	-17.6±8.1	-16.6±8.4	-18.2±8.9	0.06
Err _{LAX}	16.2±10.2	17.7±10.3	17.9±10.5	0.25
Ell _{LV}	-21.0±11.0	-20.0±11.0	-19.2±12.8	0.23
Ell _{RV}	-23.7±16.4	-21.7±13.5	-20.6±14.7	0.25
Global (n=15)				
Err _{SAX}	22.6±7.9	19.4±6.7	20.5±5.2	0.40
Ecc _{SAX}	-17.6±5.0	-16.6±4.4	-18.1±4.3	0.81
Err _{LAX}	16.2±5.6	17.7±5.6	17.9±3.8	0.29
Ell _{LV}	-21.0±5.1	-20.0±5.3	-19.2±5.3	0.06
Ell _{RV}	-23.8±9.9	-21.8±5.7	-19.1±8.7	0.26

Values are in %. p values refer to the significance of differences between the mean values from Scans A, B and C.

Inter-study reproducibility

CV, ICCs and sample size calculations for each strain parameter are summarised in table 7.2. Reproducibility was highly variable. Global strain assessment was more reproducible than segmental analysis. Overall Ecc_{SAX} was the most

reproducible measure of strain; CV 38% and 20.3% and ICC 0.68 (0.55-0.78) and 0.7 (0.32-0.89) for segmental and global analysis respectively. The least reproducible segmental measure was Ell_{RV} : CV 60% and ICC 0.56 (0.41-0.69) whilst the least reproducible global measure was Err_{LAX} : CV 33.3% and ICC 0.44 (0-0.77). Bland-Altman plots demonstrate the reproducibility of segmental Ecc_{SAX} and Ell_{RV} (figure 1).

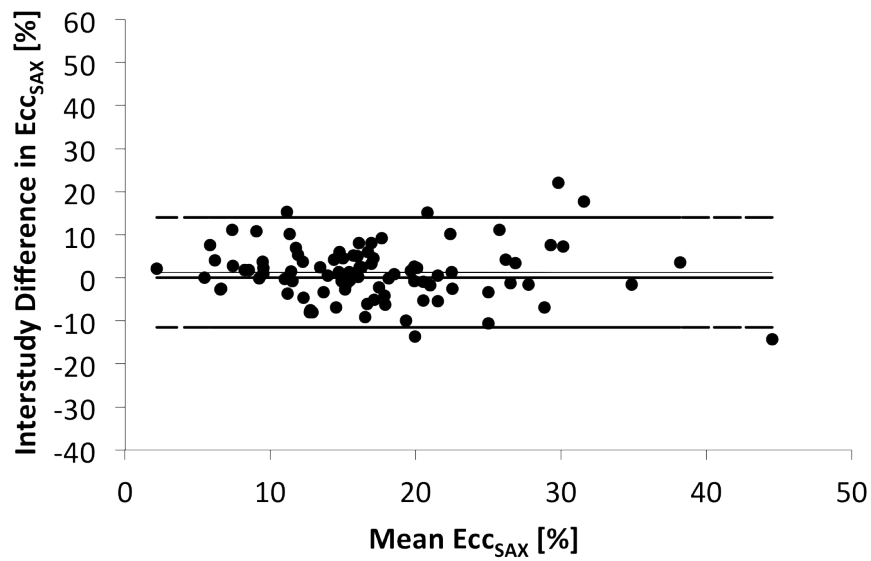
Table 7.2: The inter-study reproducibility of CMR-FT strain.

	<i>Mean difference±SD</i>	<i>Coefficient of Variation</i>	<i>ICC (95%CI)</i>	<i>Sample size</i>
Segmental (n=90)				
Err _{SAX}	-3.5±7.5%	35.9%	0.57 (0.35-0.71)	48
ECC _{SAX}	1.2±6.5%	38.0%	0.68 (0.55-0.78)	36
Err _{LAX}	1.5±9.2%	53.2%	0.62 (0.47-0.73)	72
Ell _{LV}	-1.0±11.3	55.4%	0.59 (0.44-0.71)	108
Ell _{RV}	-1.9±13.6	60.0%	0.56 (0.41-0.69)	156
Global (n=15)				
Err _{SAX}	-3.2±5.7%	27.2%	0.61 (0.15-0.85)	28
ECC _{SAX}	1.0±3.5%	20.3%	0.70 (0.32-0.89)	11
Err _{LAX}	1.5±5.8%	33.3%	0.44 (0-0.77)	29
Ell _{LV}	-1.08±5.4%	26.4%	0.44 (0-0.77)	25
Ell _{RV}	-1.9±6.8%	29.9%	0.62 (0.20-0.85)	39

ICC=Intraclass correlation coefficient; CI=Confidence Interval.

Sample size required to detect an absolute change of 5% with 90% power and an α error of 0.05. Sample size numbers must be doubled for studies comparing active treatment vs. placebo.

Left Ventricular Circumferential Strain (Ecc_{SAX})



Right Ventricular Longitudinal Strain (Ell_{RV})

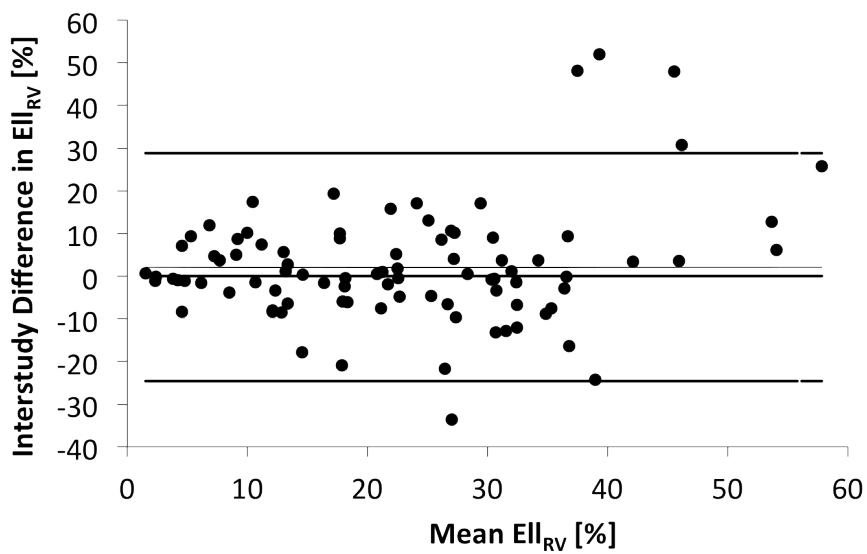


Figure 78.1: Inter-study agreement of CMR-FT segmental strain analysis

Bland Altman plots with limits of agreement (95% confidence intervals) demonstrating the inter-study reproducibility of CMR-FT segmental LV circumferential and RV longitudinal strain.

This variable reproducibility is reflected in the sample size calculations. 5% changes in absolute global strain can be detected in follow-up studies with relatively few patients whilst many more are required for some segmental strain parameters. Sample sizes for global strain parameters ranged from 11 (ECC_{SAX}) to 39 (Ell_{RV}) and for segmental strain from 36 (ECC_{SAX}) to 156 (Ell_{RV}).

Comparison of inter-study reproducibility AB with AC

Inter-study reproducibility AC was not significantly different from reproducibility AB for any segmental or global parameters ($p > 0.05$ for all).

LV volumes and function

Inter-study reproducibility

Mean LV volumes and function are shown in table 7.3. There were no significant differences in LV volumes or function between the three scans. Inter-study reproducibility was excellent overall. CV and ICC for LV end-diastolic volume, end-systolic volume and ejection fraction were 4.2% and 0.98; 8.3% and 0.95; and 4.6% and 0.75 respectively (table 7.4).

Table 7.3: Mean LV volumes and function for the entire study population.

n=16	<i>Scan</i>			<i>p</i>
	A	B	C	
LVEDV	161.7±33.3ml	162.5±37.0ml	161.2±39.7ml	0.76
LVESV	67.5±17.3ml	68.9±20.0ml	64.9±18.3ml	0.28
LVEF	58.5±3.2%	58.0±4.3%	59.6±4.5%	0.86

p values refer to the significance of differences between Scans A, B and C.

LVEDV=left ventricular end-diastolic volume; LVESV=left ventricular end-systolic volume; LVEF=left ventricular ejection fraction

Table 7.4: Inter-study reproducibility of LV volumes and function.

<i>n=16</i>	<i>Mean difference±SD</i>	<i>Coefficient of</i>	<i>Intraclass correlation</i>
		<i>Variation</i>	<i>coefficient (95%CI)</i>
LVEDV	-2.1±6.7	4.0%	0.98 (0.97-1.0)
LVESV	-1.9±5.5	7.7%	0.95 (0.88-0.98)
LVEF	0.55±2.7	4.6%	0.75 (0.43-0.91)

Comparison of inter-study reproducibility AB with AC

There were no significant differences between reproducibility AB and AC for LV volumes or function (p>0.05 for all).

Discussion

This study demonstrates that the inter-study reproducibility of CMR-FT parameters is highly variable and is better for global rather than segmental measures. Ecc_{SAX} is the most reproducible whilst others such as Ell_{RV} and Err_{LAX} are less reproducible. Furthermore there was no measurable variation during the day.

CMR Feature Tracking

Abnormalities or inter-study changes in myocardial strain can occur without any detectable changes in LV volumes or function. This has been demonstrated, for example, in studies examining the treatment effect of stem cells in myocardial infarction^{185, 186}. Myocardial strain imaging may therefore allow early detection of abnormalities and subsequently allow early diagnosis and intervention. However, despite this imaging techniques for strain analysis have not been widely adopted. CMR-FT has been described in detail previously¹⁸² and appears to be a promising new tool for quantitative assessment of wall motion analysis. Borders within the image, such as the border between the LV endocardium and LV blood, are identified and then tracked from frame to frame. This relies on quantification of changes in signal intensity within voxels from one frame to the next. Frame-to-frame displacement of these signal changes is used to calculate local myocardial velocity and deformation or strain.

The accuracy of CMR-FT is likely to depend on the orientations and dimensions of the relevant border or features relative to voxels of the slice. Furthermore,

CMR- FT software derives strain measurements from the apparent in-plane movements. However, the apparent movements of features in 2D cine images may be caused by through-plane displacements of oblique or tapering structures, and not only by in-plane movements. This potential limitation of the technique may explain some of the variability seen in reproducibility in this study.

Global Ecc_{SAX} from the mid LV slice has been shown to correlate strongly with myocardial tagging using Harmonic Phase Imaging (HARP) in patients with Duchene Muscular Dystrophy and varying LV dysfunction and also in normal volunteers¹⁸⁷. Ecc_{SAX} has also been compared with a complementary spatial modulation of magnetization (CSPAMM) myocardial tagging reference method in a subsequent study¹⁸⁸; agreement was modest and notably segmental strain measurements were less good than global Ecc_{SAX} measurements. However, to date, other CMR-FT parameters have not been validated against a reference standard for the evaluation of myocardial strain. Further validation of CMR-FT strain measurements, particularly segmental measurements, is therefore desirable.

Inter-study reproducibility

To our knowledge this is the first assessment of CMR-FT inter-study reproducibility. However, previous studies by our group have suggested that inter and intra observer reproducibility is higher for Ecc_{SAX} than for Err_{SAX} both in volunteers and in patients with ischaemic cardiomyopathy^{183, 184}. Inter-study

variability was of a similar magnitude to the intra-observer and inter-observer variability reported previously although intra and inter-observer reproducibility may be superior to inter-study reproducibility.

Inter-study reproducibility of a technique is key where repeated examinations are required as discussed in detail in the previous chapter. Wall motion assessment with CMR-FT could therefore potentially be useful for serial examinations of ventricular function to assess disease progression, treatment efficacy or determine the timing of therapy. Serial examinations are important in a multitude of clinical conditions and also form a key component of many studies. Higher reproducibility means that smaller changes can be detected with increased reliability. This also results in cost-efficiencies, as fewer subjects are required in clinical trials¹⁷⁵.

Our sample size calculations demonstrate that relatively small sample sizes are required to detect 5% changes in global strain parameters, particularly ECC_{SAX} . However, a 5% change might be a relatively large effect, and larger sample sizes would be required if subtle changes in strain were likely to be clinically relevant. Furthermore, lower reproducibility of some segmental strain parameters means that large sample sizes would be required to detect differences in these. This is likely to be particularly relevant for assessing patients with CAD when regional analysis is crucial. Therefore whilst this new technique is promising for quantitative wall motion assessment its utility would be greater if further method developments improved reproducibility.

This study included normal volunteers and image quality was good to excellent in all cases. Reproducibility and sample sizes may therefore be different in patient studies or when image quality is reduced. However, in previous studies of volunteers¹⁸³ and patients with ischaemic cardiomyopathy¹⁸⁴, CMR-FT intra- and inter-observer reproducibility were no worse during low-dose dobutamine infusion than at rest, even though dobutamine is often associated with a deterioration in image quality. Furthermore, CMR-FT reproducibility in patients with ischaemic cardiomyopathy appeared to be comparable to that of healthy volunteers despite reduced LV function in the patients. These observations suggest that the findings of this study can be applied to patients. However, it is important to note that in the patient study 13% of segments were excluded, mainly due to breathing artefacts.

This study also confirms the excellent inter-study reproducibility of CMR for evaluating LV volumes and function demonstrated in previous studies^{161, 175}. In keeping with these studies, using CV as a measure of inter-study reproducibility, we also found LV end-systolic volume to be slightly less reproducible than both LV end-diastolic volume and LV ejection fraction. However, ICC was lower for ejection fraction than for LV volumes, emphasizing the fact that multiple measures of inter-study reproducibility exist, and the potential difficulties in comparing results from studies using different statistical methods. We have reported multiple measures of reproducibility in order to be comprehensive.

Physiological variation

In keeping with the previous study we did not detect any changes in LV volumes and function or in LV or RV myocardial strain during the day. Furthermore, the inter-study reproducibility of LV volume and function and strain measurements was not measurably affected by daytime variation. These findings suggest that daytime variations are not currently important considerations when repeated studies are performed for CMR-FT and/or volumetric analysis. However, it is important to note that the higher variability of the strain measurements means that small changes are unlikely to have been detected. The sample size calculations suggest that our sample was large enough to detect a 5% change in ECC_{SAX} .

Comparison with speckle tracking

Speckle tracking with echocardiography is a more established technique than CMR-FT¹⁸⁹. Previous echocardiography based studies have shown the clinical utility of speckle tracking for LV viability assessment and planning of revascularisation. Speckle tracking also has a role in the assessment of patients with acute myocardial infarction and heart failure with normal ejection fraction and as an early marker of LV dysfunction in patients with Tetralogy of Fallot¹⁹⁰⁻¹⁹⁴. Data on the inter-study reproducibility of strain analysis speckle tracking is limited and it is therefore difficult to draw comparisons with the CMR findings of this study. Reasonable inter-study reproducibility of left ventricular rotation parameters (as opposed to strain) has been demonstrated¹⁹⁵ using different measures of reproducibility.

Echocardiographic global longitudinal speckle strain was recently shown to be an independent predictor of mortality in a population of 546 consecutive patients undergoing echocardiography for left ventricular assessment¹⁹⁶. Global longitudinal strain was a stronger predictor than both ejection fraction and wall motion scoring. This raises the possibility that the analogous global longitudinal LV feature tracking strain measured in this study, and possibly other strain parameters, may also be useful prognostic markers and our data show reasonably good reproducibility of global parameters. Larger scale long-term CMR studies are required to test this hypothesis.

Comparative studies between CMR-FT and speckle tracking have not yet been performed. Both techniques have potential advantages. Reliable endocardial border detection is key for strain imaging and superior image quality and endocardial border definition with CMR may be an advantage.

Echocardiography has different axial and lateral resolutions and can also be affected by limited acoustic windows. Border tracking may therefore be more reliable with better image quality. Conversely although CMR provides relatively good contrast to noise at most epi and endocardial boundaries it may not be able to detect similar intra-myocardial features, and therefore intra-myocardial strain, as well as speckle tracking. CMR myocardial tagging imaging techniques may also be superior to CMR-FT in this respect. Moreover, echocardiography has superior temporal resolution, which may translate into an advantage for speckle tracking over CMR-FT.

Limitations

The main limitations of this study are its small size and the inclusion of normal volunteers rather than patients. However it is common to evaluate emerging techniques in volunteers initially and these studies are important platforms for further method improvement and subsequent patient studies. Moreover limited previously published data suggest that volunteer and patient reproducibility may well be similar as discussed above.

Conclusions

The inter-study reproducibility of CMR-FT is highly variable. At present reproducibility is best for global measurements and LV circumferential strain is the most reproducible strain parameter. CMR-FT strain analysis is not measurably influenced by variation during the day. CMR myocardial strain analysis with feature tracking may have potential clinical and research applications. However the technique, particularly segmental and long axis analyses of strain, would benefit from improved inter-study reproducibility and also further validation studies.

8 MYOCARDIAL VIABILITY. Evaluation of a Novel Dual Inversion Recovery Sequence for Improved Visualization of Myocardial Infarction

Abstract

Objectives

Evaluate whether a dual inversion recovery (dual-IR) pre-pulse improves scar-to-blood contrast and observer confidence and consistency in the detection and evaluation of scar in late gadolinium enhancement (LGE) images.

Introduction

Accurate assessment of the extent and transmural extent of scar is key for guiding revascularisation in patients with CAD and previous myocardial infarction. The standard inversion recovery (IR) technique for scar imaging can be limited by poor scar-to-blood contrast, which can compromise accurate assessment of scar size and identification of small sub-endocardial scars. A dual-IR pre-pulse may overcome this limitation by reducing signal from the blood pool.

Methods

Twelve patients with known scar secondary to myocardial infarction were imaged at 10, 20 and 30 minutes post contrast administration with both the IR sequence and the dual-IR sequence with delays optimized for T1min of 50, 100, 200 and 300ms and T1max of 1400ms.

Results

Scar-to-blood CNR was significantly improved with the dual-IR technique compared to the standard IR method for all time points ($p<0.05$). Experienced readers gave higher confidence scores for infarct detection and transmural assessment to dual-IR images. The dual-IR sequence also resulted in more consistent assessment of scar size and transmural assessment between readers compared to the IR technique.

Conclusion

In this preliminary patient study, the novel dual-IR pre-pulse improved scar-to-blood-contrast compared to the IR technique. Dual-IR imaging also resulted in improved expert confidence and reduced differences between readers in scar transmural assessment and size assessment.

Introduction

LGE imaging permits visualization of areas of cellular necrosis and extracellular fibrosis (scar) and is the basis of CMR imaging of acute and chronic myocardial infarction. LGE imaging is key for viability assessment prior to revascularization, and is also a valuable diagnostic^{177, 197} and prognostic tool^{91, 177}. It is a strength of CMR imaging that is unequalled by other modalities.

Current imaging sequences exploit the kinetics of extracellular gadolinium based contrast agents. Following intravenous administration the contrast agent rapidly reaches all cardiac tissue with a normal blood supply but is delayed in reaching areas with a reduced supply. This forms the basis of perfusion imaging. There is an intermediate stage 1-2 minutes after injection when contrast agent has started to wash out of normal myocardium but still has not reached areas of microvascular obstruction. This is used to detect areas of microvascular obstruction. Finally approximately 5-60 minutes after injection a late stage is reached where most of the contrast has washed out of normal myocardium but has accumulated in areas of cellular necrosis and interstitial fibrosis due to the higher volume of distribution and delayed wash out in these regions. During this late phase contrast agent has therefore accumulated in areas of both acute and chronic myocardial infarction.

In order to image these areas of myocardial injury inversion recovery (IR) gradient echo sequences are used as standard. T1 reduces with increasing tissue contrast agent concentration and this allows differentiation of scar from normal myocardium following a non-selective 180-degree (inversion) RF

prepulse. Imaging is performed at a pre-selected time point after the prepulse (TI) when there is no signal from normal myocardium (nulled myocardium) but there is signal from areas of necrosis and scar (figure 8.1).

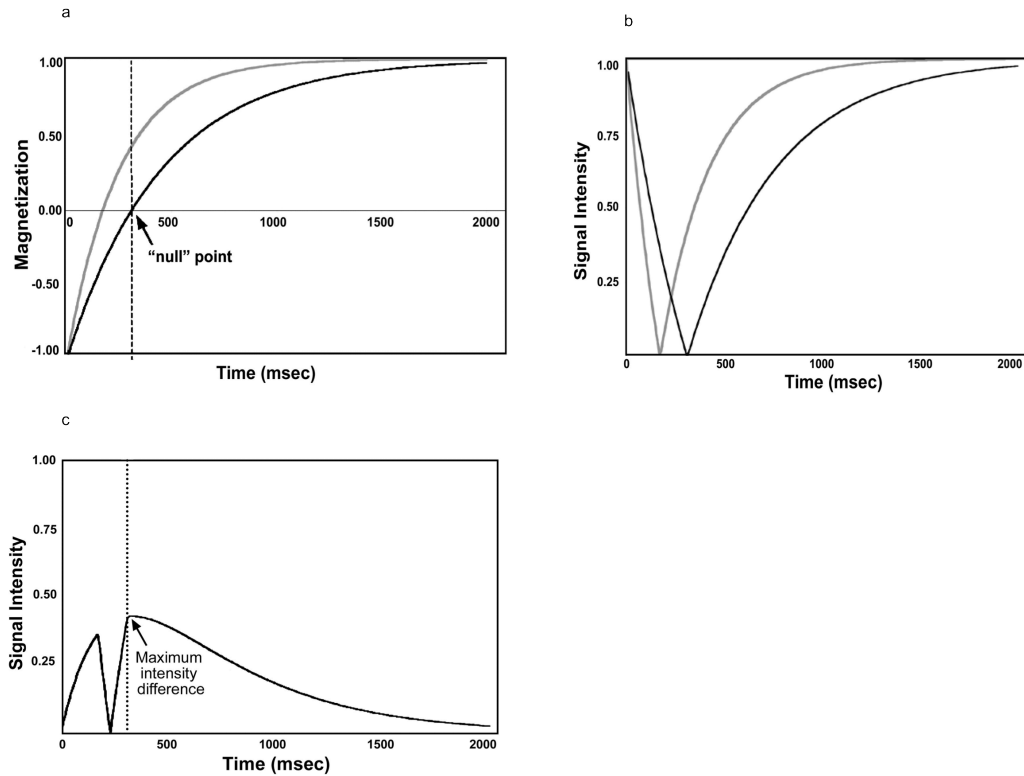


Figure 8.1: The inversion recovery technique

a) Inversion recovery curves of normal and infarcted myocardium. The time at which the magnetization of normal myocardium reaches zero is defined as the inversion time to "null" normal myocardium (312 msec in this example). b) Image intensities resulting from an inversion prepulse with various inversion delay times. c) Difference in image intensities between infarcted and normal myocardium as a function of inversion time. The optimal inversion time is when the maximum intensity difference occurs. From¹⁹⁸.

LGE scar imaging has been validated against histology in dogs and areas of LGE correspond very closely to area of scar⁸⁴. Furthermore areas of scar are 1080%

times brighter than areas of normal myocardium¹⁹⁹. However, the IR sequence only nulls normal myocardium, therefore although differentiating scar from normal myocardium is rarely a problem in CAD, high signal from blood can make differentiation of blood pool and scar difficult. In some cases, this can make accurate delineation of the endocardial border difficult, which in turn can compromise accurate assessment of scar size and identification of small sub-endocardial scars.

A modified IR sequence was developed by other researchers within our department to address this problem. This novel sequence included the addition of a second inversion prepulse prior to imaging (dual-IR). The second prepulse results in the nulling of all tissues except those with very short T1 values (figure 8.2). Provided blood has lower signal than scarred myocardium it should be possible to null blood as well as myocardium but preserve the signal from infarct.

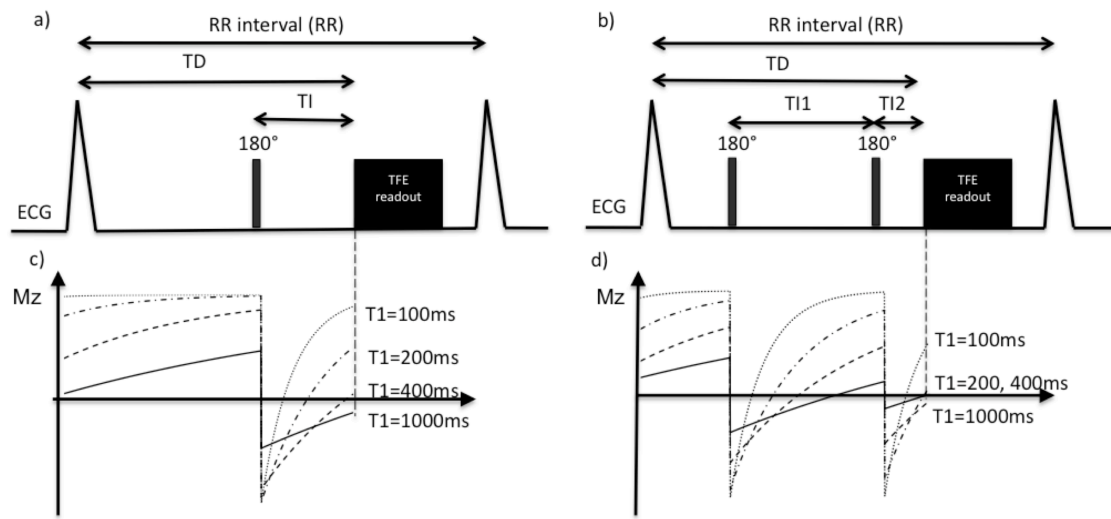


Figure: 8.2: Schematic representation of the inversion recovery (IR) (a) and dual inversion recovery (dual-IR) (b) sequences.

TD=trigger delay. TI=inversion time. The dual-IR sequence contains two inversion prepulses and two inversion times TI1 and TI2. The plots below show the evolution of the steady state longitudinal magnetization (Mz) for T1=100, 200, 400 and 1000ms for the IR (c) and dual-IR (d) sequence. The second inversion prepulse results in nulling of all except very short T1 values.

The aim of this study was to compare the dual-IR to the standard IR sequence for scar imaging in patients with CAD and prior myocardial infarction. We sought to investigate the effect on the contrast between scar and blood and whether confidence and consistency in the detection and evaluation of scar could be improved.

Methods

Data acquisition

Sixteen patients with a history of myocardial infarction, at least 3 months prior, and who were known to have scar from previous clinical IR images were recruited and imaged at 3T. Three patients were used to optimize the MR protocol. The remaining patients were then imaged as follows:

- Survey, coil reference scan and planning to define imaging planes
- 0.2mmol/kg of Gadobutrol/Gadovist administered
- 5 minutes post contrast:
 - look locker
 - short axis (SA) breath-hold IR gradient-echo (TFE) scans in expected scar location until suitable slice identified.
- **All further imaging performed using the slice identified above.**
- Starting 10, 20 and 30 minutes post contrast:
 - look locker
 - IR TFE
 - dual-IR x4 with T1min 50, 100, 200 and 300ms (see below).

Imaging parameters included:

IR-TFE: spatial resolution=1.5x1.5x10mm, repetition time 3.8ms, echo time 2ms, flip angle 25°, imaging every other heartbeat. TFE factor adjusted to achieve a 12 second breath-hold for each patient. The TI was set to null the myocardium according to the preceding Look Locker scan.

Dual-IR: spatial resolution, repetition time, echo time, flip angle, the same as IR-TFE, imaging every heartbeat with the TFE factor adjusted to achieve a 12 second breath-hold for each patient. The T1 and T2 delays were optimised (depending on the heart rate) to suppress the signal within a user defined T1 range: T1min-T1max. T1min was varied between 50, 100, 200 and 300ms with T1max always set at 1400ms. There were therefore 4 dual-IR scans at each time point. The order of the dual-IR scans was randomized for each patient prior to the start of the imaging session.

In five of the patients, additional 2 or 4 chamber views were also acquired at 25 or 35 minutes post-contrast.

Data analysis

Data analysis was performed with Osirix Imaging Software.

Blinded expert analysis:

All IR and dual-IR scar images were presented one at a time in a random order to two blinded experts. They were asked to i) identify whether myocardial scar was present; ii) grade transmural as 0-25, 26-50, 51-75 and 76-100%; iii) outline scar border and iv) assign a confidence score from 1) negative low confidence, 2) negative medium confidence, 3) negative high confidence, 4) positive low confidence, 5) positive medium confidence to 6) positive high confidence for both the presence and transmural of scar.

Signal and Contrast to noise analysis

Mean signal values were taken from regions of interest in scar, remote myocardium and left ventricular blood pool. The signal standard deviation from a region of interest in the lung was taken to be noise. SNR of blood pool, myocardium and scar and CNR of scar-to-blood, scar-to-myocardium and blood-to-myocardium CNR were calculated for all short-axis images at all time points.

Statistical analysis:

Prism software (GraphPad Software, California, USA) was used to compare SNR and CNR measurements at each time point with a one-way Analysis of Variance between groups (ANOVA) comparison followed by a post-hoc Newman-Keuls paired t-test. The differences between the confidence scores were compared using a Wilcoxon matched-pairs signed ranks test. The percentage of infarcts where the experts gave a different transmural assessment was compared using a student t-test. Inter-observer variability for the scar size was assessed using the Bland Altman test.

Results

15 patients completed the protocol successfully. One patient was excluded as he did not fit in the scanner with the 32 channel-coil (previous clinical imaging performed with 6-channel coil). Patient characteristics are shown in table 8.1.

Table 8.1: Characteristics of the 12 patients included in the analysis

<i>Characteristic (mean \pm SD)</i>	
Age	63 \pm 8 years
Weight	84 \pm 12 kg
Heart rate	60 \pm 8 bpm
Time since infarct	60 \pm 74 months
LVEF*	44 \pm 9 %.
Male	100%
Diabetes	17%
Hypertension	83%
Smokers	42%
Hypercholesterolemia	58%
Previous PCI	83%
Previous CABG	42%
Scar location*	
Anterior/Septal	4 (33%)
Inferior	7 (58%)
Lateral	2 (17%)

*Determined from clinical scan. One patient had 2 discrete infarcts.

The dual-IR technique achieved blood signal reduction in all patients.

Representative images from a patient are shown in figure 8.3. The dual-IR sequence results in reduced blood signal compared to the IR sequence at all 3

time points post contrast administration. The degree to which the signal from blood is reduced depends on the T1min value.

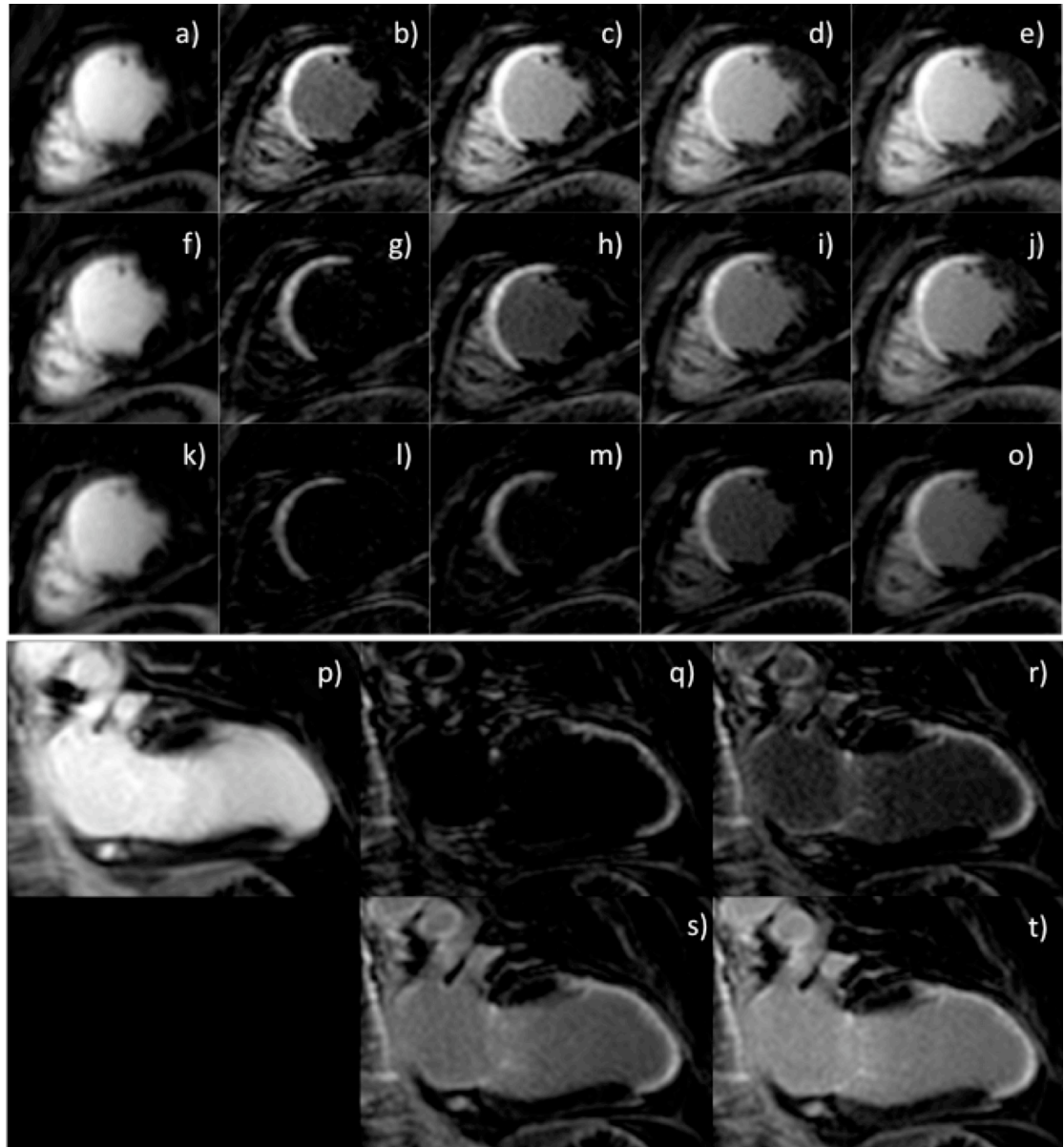


Figure 8.3: Dual IR and standard IR scar images from a patient with transmural scar in the LAD territory.

Top panel: Images in a short axis view acquired at 10 minutes (top row), 20 minutes (middle row) and 30 minutes (bottom row) after CA administration. From left to right: IR, dual IR with T1min=50ms, dual IR with T1min=100ms,

dual-IR with T1min=200ms, and dual-IR with T1min=300ms. Bottom panel: 2-chamber view using p) IR, q) dual-IR T1min=50ms, r), dual-IR T1min=100ms, s) dual-IR T1min=200ms and t) dual-IR T1min=300ms.

Dual-IR images show reduced blood signal compared to the IR images at all 3 time points post CA administration. As the time from CA increases there is less signal from the blood at a given T1min value as the T1 of blood increases.

IR images and dual-IR images taken at 20 minutes post-contrast with a T1min of 200ms in two patients with different scar location and transmuralities are shown in figure 8.4.

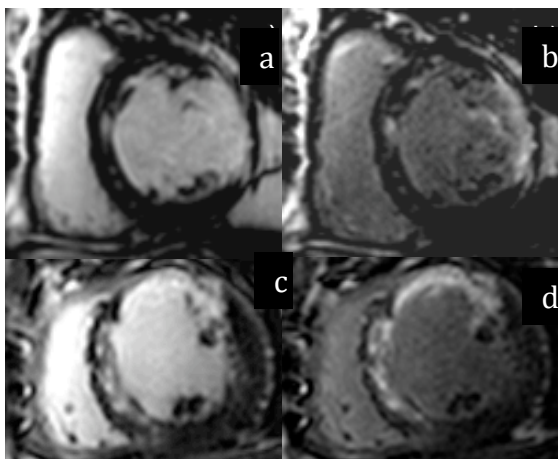


Figure 8.4: Standard versus dual-IR scar images.

Short axis IR (left) and dual-IR (right) images from a patient with partial thickness lateral wall scar (a, b) and a second patient with a full-thickness anterior and partial thickness septal scar (c, d). Images were acquired 20 minutes post contrast administration. A T1min of 200ms was used for the dual-IR images. The blood pool is darker in the dual-IR images, which improves the appreciation of the presence of scar and also transmuralities assessment.

Four-chamber views taken at 25 minutes post-contrast and a two-chamber view taken at 35 minutes post-contrast administration (figure 8.5) also show reduced blood signal with dual-IR technique and areas of contrast uptake are shown more clearly.

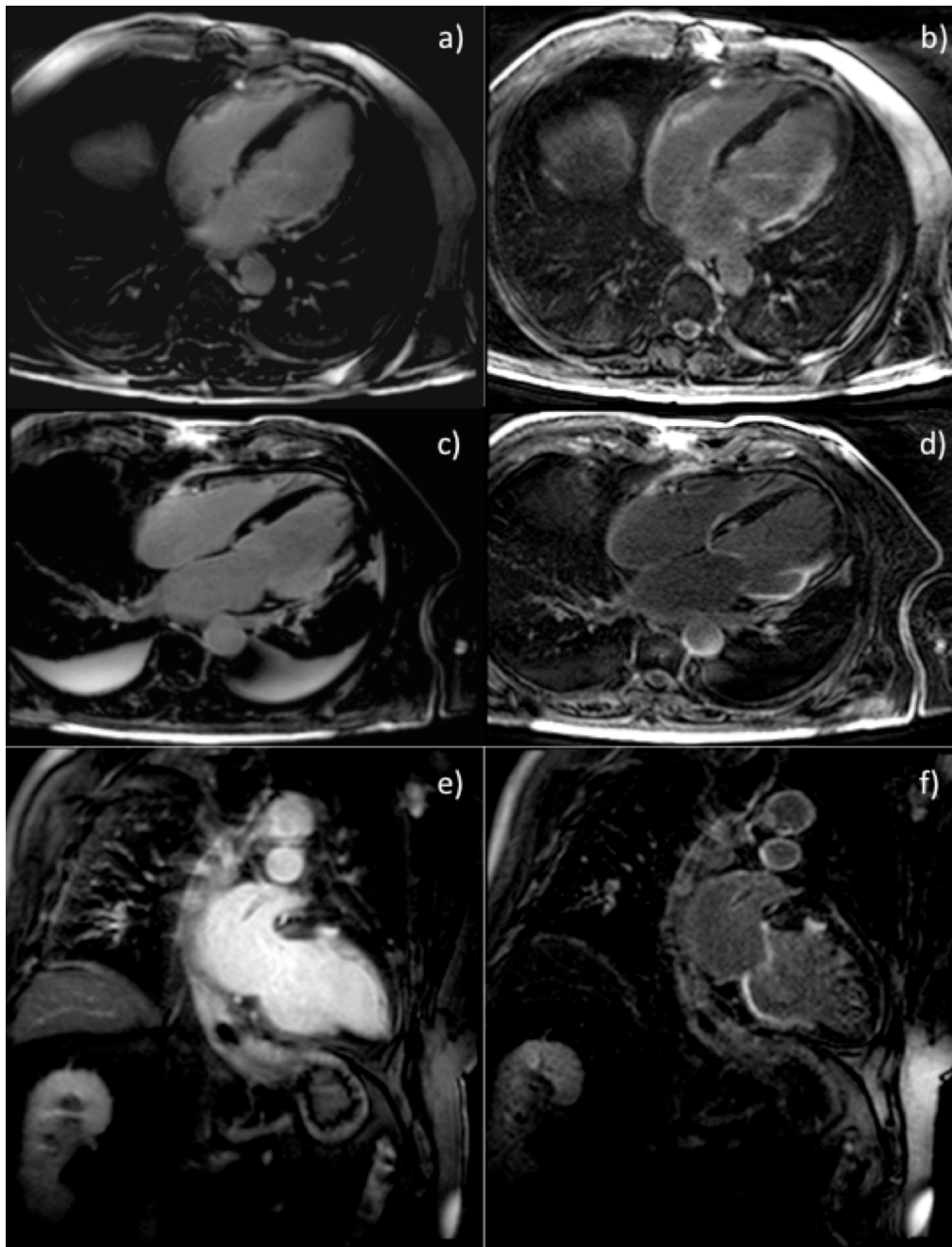


Figure 8.5: Long axis scar imaging using the IR and dual IR techniques.

Four-chamber views of a patient with a subendocardial basal to mid lateral wall scar using a) the IR and b) the dual-IR sequence with a T1min of 200ms at 25 minutes. Four-chamber view of a different patient with a transmural basal to mid lateral wall scar using c) the IR and d) the dual-IR sequence with a T1min of 200ms at 25 minutes. Two-chamber view of a patient with a transmural basal to mid inferior wall scar and a small basal anterior wall scar using e) the IR and f) the dual-IR sequence with a T1min of 200ms taken at 35 minutes post-contrast administration.

Expert observer quantitative and qualitative analysis

Scar presence (figure 8.6a) and transmural assessment (figure 8.6b) confidence scores were higher with the dual-IR sequence (with T1min of 100, 200 and 300ms) compared to the IR sequence for both experts. The differences in transmural confidence scores were significant for expert 1 when the IR sequence was compared to the dual-IR sequence with T1min of 100, 200 and 300ms ($p < 0.05$). Differences for expert 2 were not significant. With the dual-IR sequence, there were fewer differences in transmural assessment between the two experts compared to the IR sequence (figure 8.6c). This was significant for the dual-IR technique with a T1min of 100ms and 300ms ($p < 0.05$). There was also a trend towards better agreement in scar size assessment with the dual-IR sequence with T1min values of 100ms, 200s and 300ms as shown in the Bland Altman plots (figure 8.7).

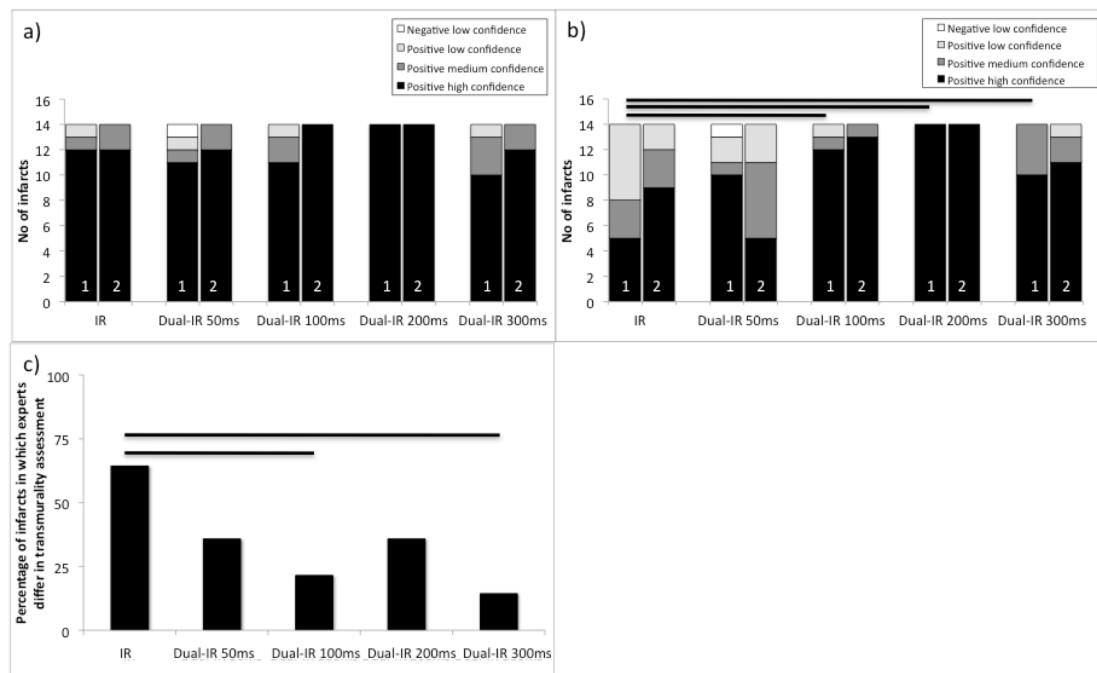


Figure: 8.6: Expert observer confidence scores.

a) Scar presence and b) transmural assessment confidence scores from the two independent experts (1 and 2). c) Percentage of scars in which there was a difference of 25% in the transmural between the two experts. The bars show the statistically significant differences ($p < 0.05$).

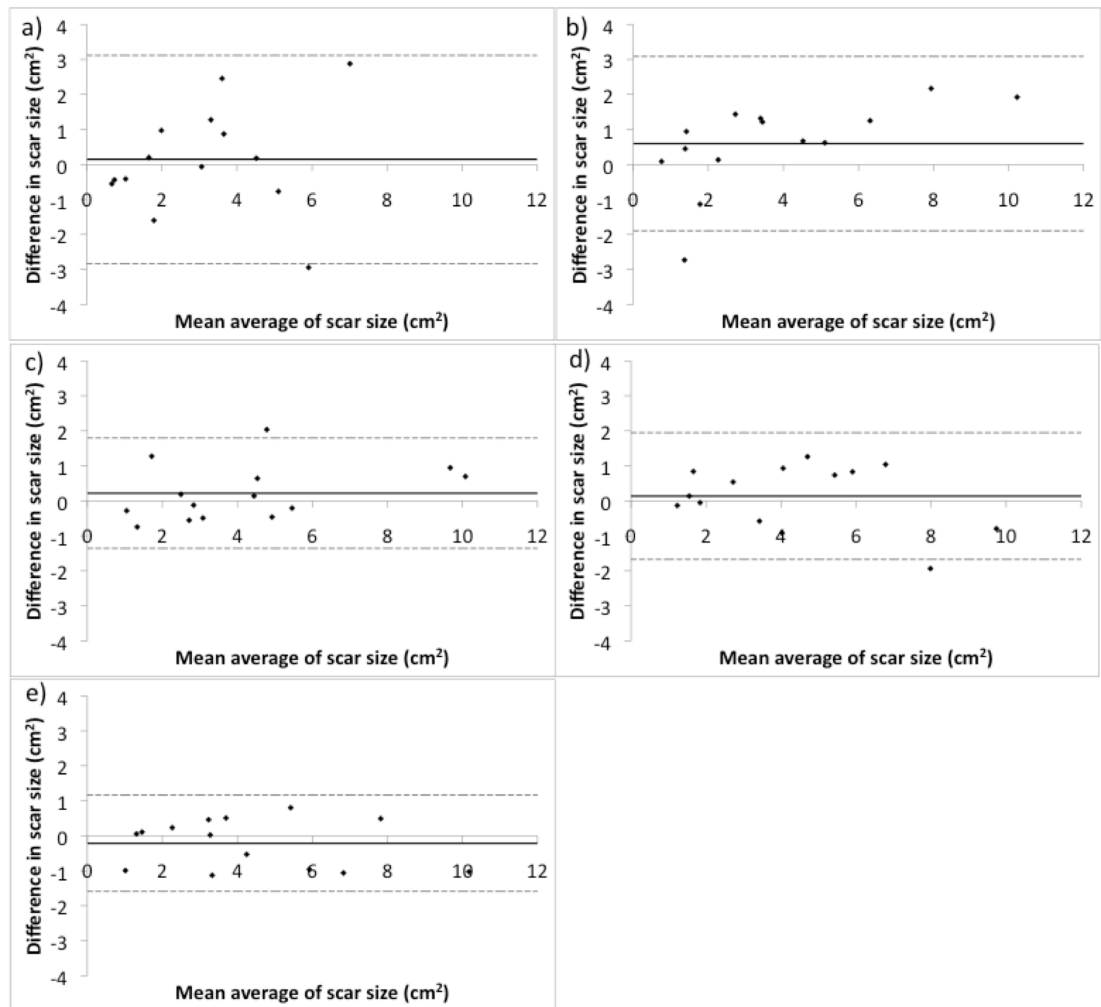


Figure 8.7: Agreement between observers for scar size assessment with IR and dual-IR scar imaging.

Bland Altman plots demonstrating the agreement between scar size assessment by the two experts for a) IR images, b) dual IR images with T1min=50ms, c) dual IR images with T1min=100ms, d) dual IR images with T1min=200ms and e) dual IR images with T1min=300ms. Solid line indicates the mean of the differences and the dashed lines indicate 1.96 standard deviations above and below the mean of the differences.

In order to make a direct comparison between the sequences, data presented in figures 8.6 and 8.7 are based on the analysis of the 14 scars, which were identified by both experts in all the images. There were discrepant results in 4 patients with either one expert reporting a scar whilst the other did not or the identification of scar in some images but not in others from the same patient by one or both observers. In one patient expert 1 defined an anterior infarct in all dual-IR images, which he had not identified on IR images. In two patients expert 2 identified antero-lateral infarcts on the IR image, which he excluded as blood pool in all dual-IR images. Finally in one patient expert 1 identified enhancement as an infero-lateral infarct whereas expert 2 excluded it as papillary muscle enhancement.

SNR and CNR

Mean SNR of blood was significantly higher for the IR sequence compared to the dual-IR sequence for all T1min values and at all time points ($p < 0.05$). Scar SNR was significantly higher with IR than with dual-IR at 20 minutes post CA with a T1min of 50ms and at 30 minutes with a T1min of 50ms and 100ms. There were no significant differences for all other T1min and imaging time point combinations.

Scar-to-blood CNR was found to be significantly higher in the dual-IR sequence with all T1min values compared to the IR sequence at all time points ($p < 0.05$) except for a T1min of 50ms at 30 minutes. There was no significant difference in scar-to-myocardium CNR between the sequences for all time points except

for a T1min of 50ms at 20 and 30 minutes IR CNR significantly higher). The blood-to-myocardium CNR was found to be significantly higher in the IR sequence compared to the dual-IR sequence with all T1min values at all time points ($p<0.05$).

Discussion

These pilot data demonstrate that, compared to the standard IR sequence, a novel dual-IR sequence improves scar-to-blood contrast and also improves confidence in the assessment of the presence and transmural extent of myocardial infarct scar. Furthermore consistency between observers for scar size and transmural extent assessment was also improved with the dual-IR sequence.

The ability to differentiate irreversibly damaged from normal myocardium is a key advantage of MR over other imaging modalities. LGE IR scar imaging is the CMR gold standard for viability assessment and assessment of scar transmural extent is crucial for guiding revascularisation as discussed previously. Scar imaging also allows differentiation of ischaemic from non-ischaemic cardiomyopathy.

Assessment of scar transmural extent and detection of small sub-endocardial scar can be hindered by the poor scar-to-blood contrast in IR images. Potential solutions to this limitation have been proposed. It is possible to delineate the endocardial border on SSFP cine images¹⁹⁸ or T2 weighted images²⁰⁰ which can then be used as a visual aid to interpret the IR image. However, this can be time-

consuming and inaccurate, as the two images should ideally be overlaid.

Alternatively, a new LGE sequence was recently described which employs an additional slice selective pulse to prepare the blood and myocardium magnetization differently in order to achieve black blood properties²⁰¹.

However, this relies on sufficient blood flow between the slice-selective and non-selective inversion pulses and it was found to work less reliably in patients with an ejection fraction of less than 40%. Furthermore, this approach still relies on the exact timing of inversion pulses to suppress the two individual T1 values of blood and of tissue.

The dual-IR sequence is a modification of the quadruple inversion recovery (QIR) sequence which was developed to achieve T1-independent blood suppression in carotid plaque imaging²⁰². Whereas with the QIR sequence, the aim was to null only the blood signal, we have shown that the dual-IR sequence achieves blood and tissue signal suppression within the defined T1-range. It is not dependent on out-flow of blood from the imaging slice and should therefore be applicable to patients with impaired LV function which is clearly crucial for imaging patients with myocardial scar. In this study the highest confidence scores were given to the dual-IR sequence with a T1min of 200ms, which may be due to a combination of sufficient left ventricular blood reduction combined with good visualization of the myocardium. Shorter T1min values resulted in lower blood signal whereas longer T1min values provided higher blood-to-myocardium CNR, which improved myocardium visualization and border definition.

In addition to viability assessment in patients with CAD the dual-IR technique may also have other clinical applications such as imaging diffuse fibrosis, for example as seen in amyloidosis or severe aortic stenosis where diffuse contrast uptake can make the correct choice of TI difficult. These exciting possibilities remain to be tested.

Limitations

This study successfully demonstrates proof-of-concept but it has the usual limitations associated with pilot studies. We only investigated 12 patients with a wide range of scar chronicity. Instead of covering the entire left ventricle, we only tested the sequence in a single slice with confirmed scar on the IR sequence. However this approach minimized the time between the IR and dual-IR sequence in order to allow comparison of both sequences at different times points post contrast injection. We also used identical read-out parameters for the IR and dual-IR sequences to minimize the impact of the imaging sequence on image contrast. In order to achieve an identical 12-second breath-hold for the IR and dual-IR images, the TFE factor and the acquisition time were approximately double for the IR images, which may have increased image blurring. SENSE acceleration is frequently used with IR sequences, to reduce the acquisition time, but was not employed in order to allow an accurate calculation of the SNR and CNR values. However, shorter acquisition times may have improved IR image quality and confidence scores. Apart from these specific adjustments the parameters of the standard IR sequence were not adjusted in this study.

We tested the dual-IR sequence using Gadovist with a dose of 0.2mmol/kg. This is consistent with both our clinical practice and with accepted international guidelines for LGE imaging⁸¹. However, with the IR sequence, little reduction in blood pool signal was observed in the 30 minutes post CA injection in most patients (figure 8.1). This was unexpected as, although we have limited experience of imaging late after gadovist administration, the half-life of all gadolinium based CA is reported to be similar¹¹⁸. A lower dose of CA may have produced less marked differences in blood signal between the two sequences, and increased confidence scores in the IR sequences, especially at later time points after administration. Future work should include an investigation of different contrast agents, doses, and field strengths and include a range of infarct ages. Finally, further studies should possibly include animal studies so that the new dual-IR sequence can be validated against a histological gold standard.

Conclusion

In conclusion, we have tested a novel dual-IR sequence, which achieves adjustable tissue suppression over a wide T1 range. Preliminary patient data show an improvement in scar-to-blood CNR, higher expert confidence with regard to the presence of scar and the assessment of transmuralities and more consistent assessment of scar size and transmuralities between experts compared to the IR technique.

9 MYOCARDIAL PERFUSION AND VIABILITY. Feasibility of Combined CMR Imaging and PCI in a Hybrid Laboratory

Abstract

Objectives

Determine the feasibility of performing CMR studies combined with coronary angiography, pressure wire studies and PCI in a hybrid X-ray and MRI (XMR) laboratory.

Background

The relationship between anatomy and associated pathophysiology in CAD is complex and incompletely understood, yet is important for patient management. This information cannot be comprehensively provided by a single investigative modality. A hybrid XMR laboratory will potentially overcome this limitation. However, the feasibility of combined invasive and non-invasive studies and PCI in an XMR laboratory is unknown.

Methods

10 patients with angina scheduled for coronary angiography or PCI underwent combined procedures in a 3 Tesla XMR laboratory. These procedures included serial non-invasive high-resolution perfusion, functional and scar imaging and invasive angiography, FFR measurements and PCI.

Results

All studies were well tolerated without complication. Eight patients underwent both CMR and invasive studies. Six patients had single vessel PCI. FFR and stress perfusion imaging were both performed in 14 coronary territories (4 post PCI). Management was guided by functional information in 8 patients.

Conclusions

Combined CMR and interventional coronary procedures are feasible and well tolerated in an XMR laboratory. This set-up has many exciting potential research and clinical applications, which should improve the understanding and management of CAD.

Background

Optimal management and revascularisation of patients with CAD requires accurate anatomic and functional information. The relationship between these is clinically very important but is difficult to predict^{203, 204} and frequently poorly understood. To date, no single investigation can comprehensively assess coronary artery anatomy and coronary and myocardial physiology. Moreover, since direct assessment of important functional parameters, such as myocardial ischaemia, is not possible the available investigations target a number of different surrogate markers. Our understanding of the exact relationship between these different methods for assessing ischaemia is also incomplete. Improving understanding of the underlying disease pathophysiology and of how results from different investigative modalities relate to each other should, in turn, improve patient assessment and management.

X-ray coronary angiography is the reference standard for the assessment of CAD and allows precise evaluation of coronary anatomy, invasive assessment of coronary physiology and is a precursor to PCI. However, it is invasive, uses ionising radiation and does not permit adequate evaluation of the myocardium. CMR imaging allows comprehensive evaluation of myocardial function, perfusion and scar without using ionising radiation. However, CMR cannot adequately assess coronary blood flow or pressures, nor can it be used for coronary intervention.

Ideally acquisition of all anatomic and functional data should be simultaneous. This eliminates any temporal changes related to disease progression, intrinsic

diurnal variation or treatment effects. However simultaneous acquisition of data from different modalities is usually not practical. Hybrid XMR laboratories have been described²⁰⁵ and are ideal for the acquisition of high-quality anatomic and functional data during a single examination. An XMR laboratory will also allow assessment of changes in myocardial perfusion, both in the target and remote territories, immediately after PCI. This may be clinically important but data are very limited. To date, combined invasive and non-invasive studies of patients with CAD and PCI in an XMR laboratory have not been described. We therefore sought to determine the feasibility of patient assessment and treatment in an XMR set-up.

Methods

XMR laboratory

The XMR laboratory consists of a Philips Healthcare 3 Tesla Achieva MRI scanner and an Allura Xper single plane X-ray catheter system (figure 9.1). Both components can operate independently as well as in combination. The floating tabletop allows direct transfer of patients between the X-ray and MRI components of the laboratory without the need for patient movement.



Figure 9.1: The XMR laboratory.

In the foreground there is a fully equipped single-plane interventional cardiac catheter laboratory. The red line on the floor is the 5-Gauss line and behind this there is a clinical 3T MRI scanner. The catheter and MRI tables can be moved together allowing the floating table top, and the patient, to slide directly from one modality to another. Doors between the catheterisation and MRI sections can be closed and shield radiofrequency.

Safety

Patient, staff and equipment safety are, of course, extremely important within the XMR environment as particular hazards are posed by the use of ferromagnetic materials in close proximity to the MRI scanner. Prior to the commencement of studies comprehensive safety protocols were implemented involving staff training, safety checks, restricted access to the laboratory,

labelling equipment according to MR-compatibility and tethering of ferromagnetic objects to the floor.

Patient recruitment

10 patients with angina and known or suspected CAD and a clinical indication for PCI or a coronary angiogram with ad hoc PCI were recruited to participate in the first pilot study.

Data acquisition

The first 3 patients were used to test the XMR set-up and procedures. Subsequent patients underwent an initial CMR examination followed, as indicated, by: an invasive angiogram, coronary artery pressure wire interrogation and FFR measurement, PCI, repeat pressure wire assessment and repeat CMR examination. Patients were moved directly on the floating tabletop between modalities. The arterial sheath was left in situ throughout but all other equipment was removed from the sheath prior to transfer to the CMR. The cardiac coils were removed from under the patient prior to X-ray examinations to prevent artefacts from interfering with X-ray screening; this was achieved by rolling the patient to one side.

CMR examination

The CMR examination was performed with either a 6-channel (4 patients) or a 32-channel (4 patients) cardiac phased-array receiver coil. A survey, coil reference scan and planning were performed at the start of each separate

examination. The first examination included SSFP long axis cines and a short axis stack to cover the entire LV and high-resolution *k-t* accelerated stress perfusion imaging. Rest perfusion and LGE imaging were performed as indicated. Subsequent examinations included stress perfusion and also functional, rest perfusion and/or scar imaging as indicated.

Perfusion imaging was performed as previously described using the same *k-t* accelerated ultrafast gradient echo sequence described previously (acquired resolution of 1.3 x 1.3 x 10mm), a dual bolus of 0.0075 then 0.075mmol/kg of CA and adenosine stress.

Scar imaging was performed using an inversion recovery turbo gradient echo sequence with the prepulse delay optimized for maximum suppression of myocardial signal and an acquired spatial resolution of 1.75 x 1.75 x 8mm.

Invasive examinations

X-ray coronary angiography was performed from the right femoral artery according to the standard techniques. For calculation of FFR adenosine was infused using the same protocol as above. FFR was defined as $(P_d - P_v) / P_v$ during hyperaemia where P_d , P_a , P_v are mean distal coronary, and aortic pressures respectively. FFR <0.75 was considered to be positive.

Percutaneous coronary intervention

PCI was guided by functional data and performed when clinically indicated, using standard techniques, at the discretion of the operator.

Results

Four females and six males with mean age 73 (range 51-86) were included. All procedures were completed and well tolerated with no complications or patient withdrawals. Seven patients had both CMR imaging and invasive studies. Two of the first three patients who were used to test XMR procedures underwent invasive procedures only and angiography was no longer indicated after CMR in one patient (see below). Mean study duration in patients who underwent both invasive and non-invasive studies was 117 minutes (range 36-208). Four patients had single vessel CAD; three had 2-vessel disease; two 3-vessel disease and one minor disease. Details of all of the procedures and outcomes are shown in table 9.1. Six patients had single vessel PCI and four patients were treated medically. Four patients had a CMR both pre and post PCI. Fourteen coronary territories in six patients had FFR with corresponding stress perfusion imaging; four of these territories were post PCI.

Table 9.1: Patient characteristics and summary of XMR cases.

<i>Patient number</i>	<i>Age</i>	<i>Sex</i>	<i>Coronary disease</i>	<i>Perfusion imaging</i>	<i>FFR</i>		<i>Outcome</i>
					Pre PCI	Post PCI	
1	65	F	Minor	N/A	N/A		Medical
2	77	M	LAD	Negative	N/A		Medical
			Cx	Negative			
3	71	M	RCA	N/A	N/A		PCI RCA
4	76	F	LAD	Positive	0.68		PCI LAD
5	79	M	LAD	Positive	0.38	0.92	PCI LAD
6	79	F	LAD	Negative	0.73	0.83	PCI LAD
			Cx	Negative	0.90		
7	86	F	LAD	Scar	N/A		Medical
8	61	M	Cx	Positive	0.55	0.95	PCI Cx
			RCA	Negative	0.29		
9	75	M	LAD	Negative	0.83		Medical
			Cx	Negative			
			RCA	Negative	0.91		
10	51	M	LAD	+	0.45	0.98	PCI LAD
			Cx	-	0.96		
			RCA	+			

M=male; F=female; LAD=left anterior descending artery; Cx=circumflex artery; RCA=right coronary artery; Med=medical therapy, +/- =presence/absence of a stress induced perfusion defect in the corresponding territory.

Results from 3 patients are shown in figures 9.2-9.5.

Figure 9.2

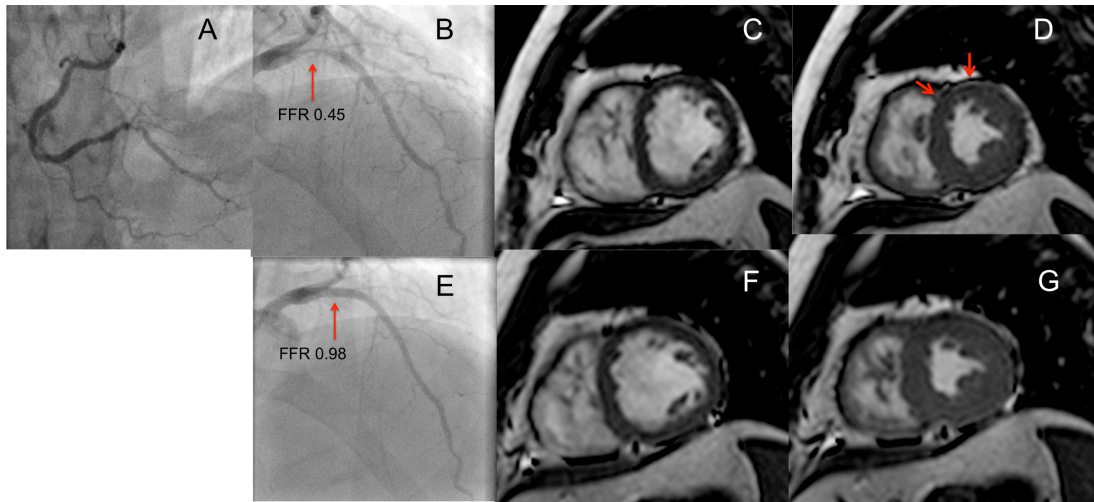


Figure 9.3

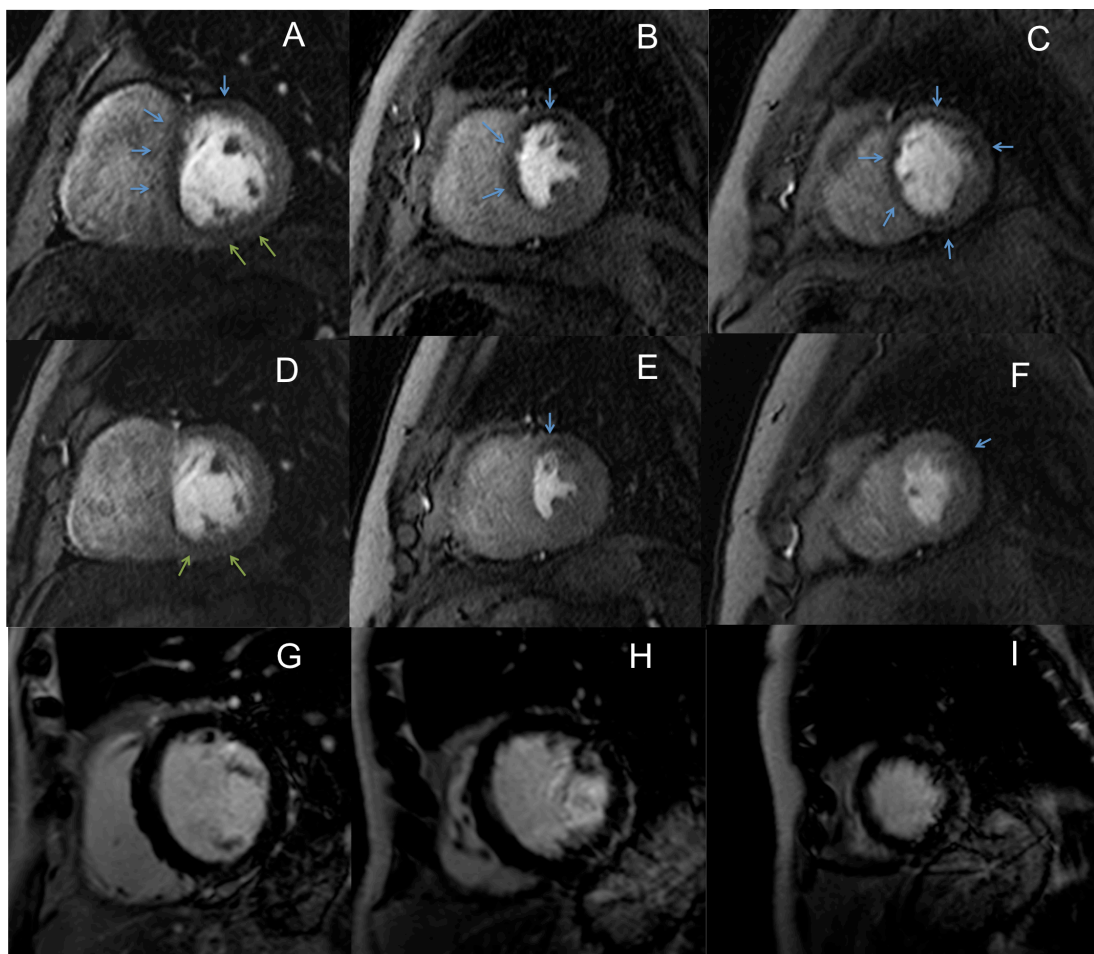


Figure 9.2 and 9.9: CMR and X-ray coronary angiogram from patient 10.

Coronary angiography demonstrated severe disease at the origin of the posterior descending artery (2A) and in the proximal LAD (2B). FFR of the LAD lesion was 0.45.

Prior to PCI the CMR demonstrated an anterior/anteroseptal wall motion abnormality visible from the end-diastolic (2C) and end-systolic (2D; red arrows) frames from the short axis cine. Stress perfusion imaging demonstrated a severe perfusion defect in the LAD territory from base to apex (3A-C; blue arrows) and a defect in the RCA territory (3D; green arrows).

Following PCI to the LAD FFR increased to 0.98, there was an immediate improvement in wall motion (2F-G) and stress perfusion was significantly improved (3D-F). The RCA territory defect remained (3D; green arrows) but there was also persistent hypoperfusion in the mid anterior slice (3E; blue arrow) and apical lateral wall (3F; blue arrow) despite the absence of scar on LGE imaging (3G-I). No clear angiographic reason for this was identified although it may have been due to disease in smaller diagonal or obtuse marginal vessels.

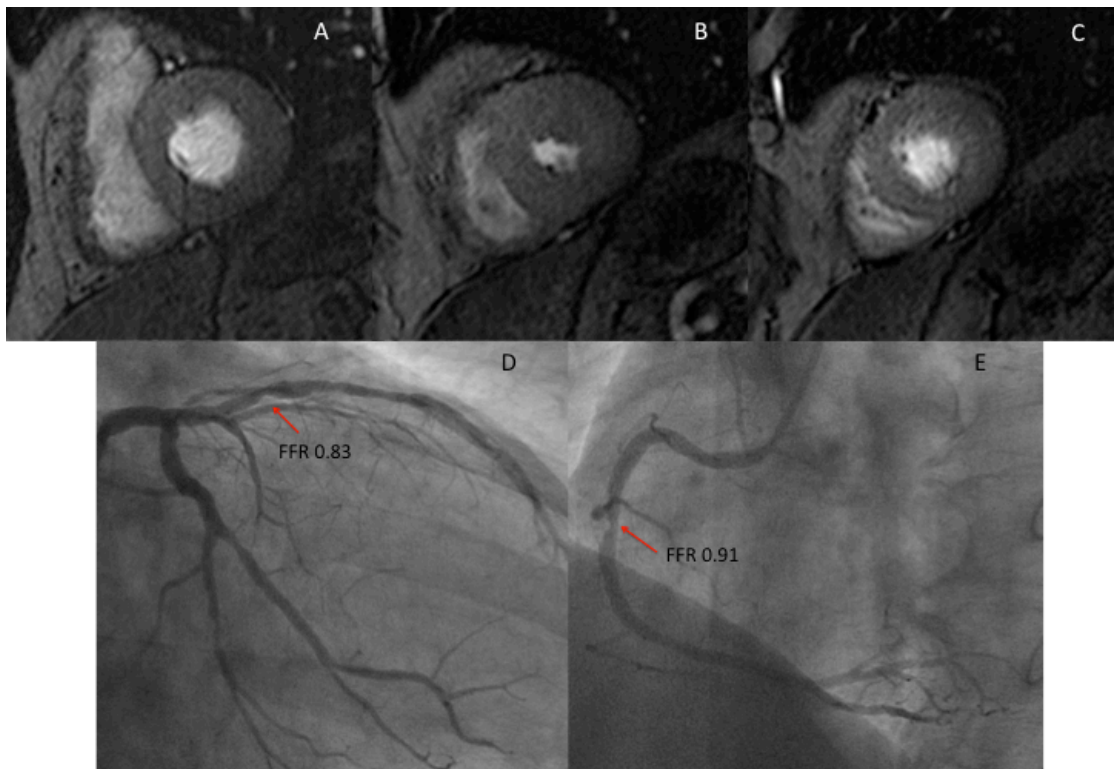


Figure: 9.4: Coronary angiogram and stress perfusion images from patient 9.

Stress perfusion did not reveal any significant defects (A-C). The X-ray coronary angiogram demonstrated moderate disease in the proximal LAD (D), with a corresponding FFR of 0.83, in the proximal dominant right coronary artery (E) with an FFR of 0.91 and also in the obtuse marginal and a small circumflex artery. The patient was treated medically.

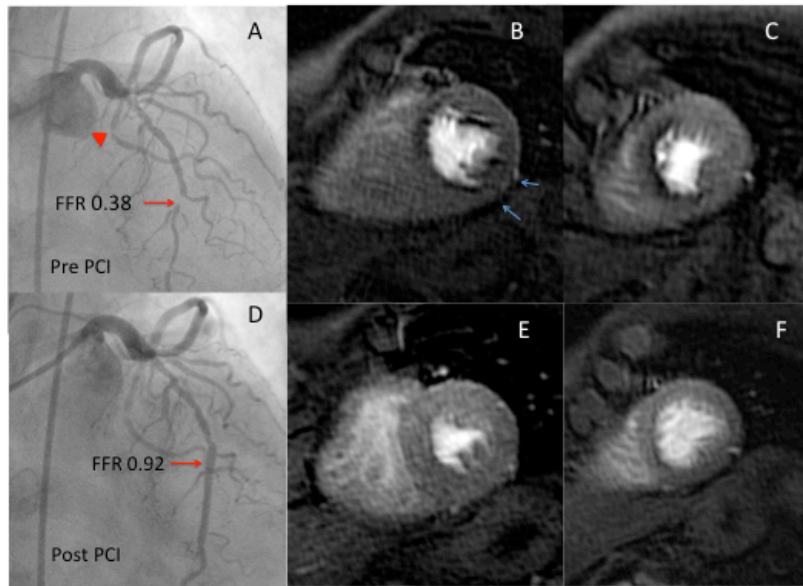


Figure 9.5: Coronary angiogram and stress perfusion images pre and post PCI.

Mid and apical LV stress perfusion images from patient 5 demonstrated an obvious perfusion defect in the mid to apical anterior wall and anteroseptum (B, C.). There is also a more subtle defect in the inferolateral wall (blue arrows B). Coronary angiography revealed diffuse coronary artery disease with focal severe lesions in the mid-distal LAD (A arrow) and proximal circumflex artery (A arrowhead). FFR was 0.38 in the LAD lesion and increased to 0.92 post PCI. Post PCI perfusion during stress improved in the anterior wall/anteroseptum but it also improved in the inferolateral wall (E, F) despite no other coronary intervention.

FFR and stress perfusion results were concordant in 10 of 12 vessels pre PCI. Of the 2 patients with discordant results one (patient 6) had mid LAD disease with an FFR of 0.73 and no perfusion defect. One had severe disease in the LV branch of the RCA, an FFR of 0.29 and no perfusion defect.

One subject (patient 7) had predominantly breathlessness on exertion with some chest tightness. A previous coronary angiogram had demonstrated severe disease of the proximal LAD and she attended for PCI. The initial CMR demonstrated that the LAD territory was predominantly transmural scar with no significant ischaemia. On the basis of these findings PCI was not felt to be in her best interests and she was treated medically.

Discussion

This pilot-study demonstrates the feasibility of acquiring near-simultaneous invasive coronary anatomic and physiological data and non-invasive myocardial structural and functional data in an XMR laboratory. It was also possible to deliver targeted coronary revascularisation in this setting. The procedures were well tolerated by all subjects and all the required data collection and treatments were completed successfully.

Interventional Cardiovascular Magnetic Resonance

X-ray guided percutaneous interventional cardiology has gained huge momentum over recent years. PCI is now by far the dominant method for coronary revascularisation. However, X-ray guidance is limited by poor

visualisation of soft-tissues and an inability to adequately assess the myocardium. MR-guided interventions were initially proposed more than 15 years ago²⁰⁶ as a possible method to overcome some of these limitations. Since then MR-guided diagnostic cardiac catheterisation²⁰⁵, pulmonary valve dilatation²⁰⁷, and peripheral arterial stent placement²⁰⁸ have been described in humans using dedicated MR-compatible catheters and equipment. These preliminary studies are encouraging, and highlight areas where MR-guided procedures are likely to have an increasing clinical role.

Importantly, although MR-guided coronary intervention has been described in an animal model²⁰⁹, it has not been performed in humans. Furthermore MR-guided PCI is unlikely to be feasible in the near future for two main reasons. Firstly, there is no commercially available MR-compatible equipment for PCI. Secondly, PCI requires very precise manipulation of equipment in small vessels and, unlike X-ray technology, at present MRI does not have sufficient spatial or temporal resolution to permit this. Consequently, for patients with CAD, the main advantage of the XMR laboratory is the availability of sequential, complimentary multimodal data rather than using MRI to perform the PCI. CMR data is rapidly available before, after, and at any point during the procedure.

XMR laboratory applications

The set-up we describe here has both clinical and research applications. Sequential CMR and invasive assessment will improve our understanding of the relationship between coronary pressure and flow and myocardial perfusion.

The advent of specialised Doppler and pressure sensor-tipped coronary guidewires in recent years has allowed calculation of hyperaemic microvascular resistance, CFR and FFR. High-resolution CMR imaging allows perfusion imaging with unprecedented spatial resolution permitting differentiation of endocardial and epicardial perfusion and scar from peri-infarct ischaemia. Quantitative perfusion assessment allows calculation of absolute perfusion and true MPR. These tools are available and can be used to analyse data from the XMR laboratory to assist our understanding of the relationship between MPR, CFR and FFR, how revascularisation affects perfusion and whether this changes over time. In patients with multivessel CAD it is likely that revascularisation of one territory affects perfusion in other territories, as suggested by the data in figure 5 in this study. Furthermore, although perfusion is known to improve post PCI¹³⁶ full improvement may not be immediate as suggested by figure 9.3 above.

In this study there were two territories in two patients with discordant FFR and CMR perfusion results. In the first patient the FFR was just below the threshold of positivity (0.73) and it is likely to have been a false negative perfusion scan. Quantification of perfusion or detailed analysis of the epi-endocardial perfusion gradients may allow us to understand such discordant results better. The second patient had disease in a distal branch of the right coronary artery. The FFR was strongly positive (0.29) however the distal nature of the disease probably explains the lack of a perfusion defect. MPR would have been informative in these patients but we did not have rest perfusion data in either case. In this study since data was not collected according to a systematic

protocol retrospective ad hoc data analysis was avoided as it could be **misleading**. On the basis of the CMR scan the patient had a PCI to a proximal circumflex lesion, which was associated with a perfusion defect, but not to the right coronary artery and was free of angina at a 6-week follow-up.

The immediate availability of CMR data after PCI means that the XMR is an ideal set-up to investigate the relationship between anatomy and physiology and between the different physiological parameters. In addition to patients with epicardial CAD the XMR laboratory has potential applications in other patient groups. For example the combination of high-resolution perfusion imaging and estimation of microvascular resistance from Doppler pressure wire data will allow improved characterisation of patients with microvascular disease.

The catheter laboratory component is fully equipped and allows the whole PCI procedure to be performed, therefore routine clinical cases can also be performed in the XMR set-up with the added advantage of the immediate availability of state-of-the-art CMR imaging. Furthermore, since the system registers the position of the patient this allows image fusion²¹⁰ whereby CMR images can be superimposed on the X-ray images in real time. The soft tissues can therefore also be visualised during interventions and this approach has been utilised for cardiac resynchronisation therapy device implantation²¹¹. The disadvantage of using the XMR set-up for clinical cases is that each patient treated requires the presence of both catheter and MRI staff throughout the procedure and only one modality can operate at a time which is less efficient than operating both modalities in parallel in separate laboratories. Therefore

even though routine clinical work can be performed in the XMR laboratory realistically its predominant use will be for research applications or as a single modality laboratory for routine work.

Limitations

This was a pilot study to allow us to test the feasibility of the XMR set-up and as such the equipment used and data collected deliberately varied and were tailored to individual patients. Further studies are underway using systematic methods and materials.

Conclusion

We have demonstrated that advanced CMR imaging can be combined with invasive X-ray-guided coronary angiography, pressure wire interrogation and intervention in a hybrid XMR laboratory. The procedures were well tolerated by patients. This set-up allows acquisition of high-quality, sequential data on coronary anatomy and coronary and myocardial physiology and has many exciting research and clinical applications.

10 DISCUSSION AND CONCLUSIONS

Discussion

CMR imaging is already established as a valuable tool for assessment of patients with CAD and for guiding revascularisation. However on-going research and development in both image acquisition and post-processing methods means that its role is continues to evolve. As new techniques become available it is important that they are evaluated carefully in clinical studies. The objective of this work was to perform some of this evaluation and to identify strengths and limitations with some emerging CMR methods with potential utility in guiding revascularisation.

Quantification of perfusion with CMR

Absolute quantification of myocardial perfusion with CMR is an exciting emerging technique. There are a number of clinical situations where it is anticipated that quantification will be advantageous although to date data to support this are very limited. Currently quantitative analysis is not widely available, prone to errors and the effects of artefacts, time-consuming and lacks standardization. The techniques used here, and previously published data suggest that, at present, inter-study reproducibility is modest. Furthermore the comparison with PET, the non-invasive reference standard, had mixed results as reported in chapter 4. Much of this is in contrast to visual analysis of perfusion, which is now a routine clinical tool.

A number of different factors are likely to contribute to the current problems associated with quantitative CMR perfusion imaging all of which will need to be addressed in order to overcome the current limitations.

Data acquisition

Image quality and artefacts

Quantitative analysis is reliant on the generation of high quality myocardial SI curves. Despite the early work (chapter 3) to identify and use the best possible perfusion sequence and CA dose myocardial SI curves were not always sufficiently robust for quantitative analysis. This is reflected in the fact that the data from 11% of coronary territories in the comparison with PET (chapter 4) and 3 of the 16 volunteers included in the inter-study reproducibility analysis (chapter 6) were not suitable for quantitative analysis. In contrast all studies and territories were suitable for visual analysis. Inadequate SI curves were a result of respiratory artefacts or insufficient myocardial CNR. Further improvements in perfusion sequences to achieve even higher SNR and CNR and reduce respiratory artefacts (and also DRA) are therefore desirable.

Temporal resolution

Currently images, and therefore the myocardial SI curve, are acquired for only part of the cardiac cycle thus the first-pass of CA is sampled rather than acquired in its entirety. This is likely to be a source of error for absolute quantification, as curves generated by this method will vary depending on the

exact time points sampled. Image acquisition during the entire cardiac cycle will eliminate this error. However this will necessitate the acquisition of multiple slices simultaneously rather than in series as is currently standard.

Contrast agent

The properties of the CA currently in use for perfusion imaging are not ideal for quantitative analysis. Firstly, as previously discussed, the relationship between CA concentration and SI is non-linear at higher doses of CA. Secondly, the CA are extravascular and therefore the SI is influenced by both the arrival of new CA and the effects of extravascular CA already in the myocardial tissue. Thirdly, the myocardial extraction fraction is typically 0.3-0.6 and varies at different myocardial perfusion rates²¹².

CA with a linear relationship between SI and myocardial concentration would be preferable to avoid errors due to signal saturation effects. Intravascular CA may be preferable and are available but experience of their use in myocardial perfusion imaging is lacking. Alternatively, an extravascular CA with high and consistent first pass uptake will at least overcome the limitations related to the variable and relatively low extraction of CA.

Post-processing software

A number of factors related to the post processing software currently limit the reliability of quantitative perfusion analysis. Many of these are generally applicable to all software programmes however the heterogeneous nature of

the tools available means that some are more specific to the methods used for this work.

One of the main sources of variability and error is user interaction with post-processing software. At present automated post-processing is not sufficiently robust to remove the requirement for input from users. SI curves are affected by myocardial border placement. It is important therefore to define these borders carefully to prevent contamination from the ventricular blood pool and consistently include equivalent segments of myocardium in the regions of interest. However automated border detection is sub-optimal and manual correction of myocardial borders is frequently required.

Quantitative analysis is also extremely dependent on obtaining an accurate arterial input function (AIF) and subsequently accurate definition of the onset and offset of the AIF and the onset of the myocardial response. LV signal, and thus AIF, is likely to vary depending on whether it is taken from the basal, mid or apical LV. In this work the AIF was automatically defined, using a defined area within the endocardial border of the basal slice. However, manual correction was required, for example in the presence of significant respiratory motion or the presence of papillary muscle in the region of interest. AIF onset and offset and the onset of the myocardial signal were also manually defined. Although this was done by blinded observers in a consistent manner automated algorithms to define these time points would be preferable. It is unlikely that user-interaction with post processing methods can be completely abolished in

the near future but improving automated algorithms and minimising this interaction will improve consistency.

Quantification of perfusion with the post-processing software used for these studies is based on deconvolution of SI curves derived from pixel-wise analysis of the myocardium. Whilst this method is extremely sensitive for perfusion abnormalities it is also susceptible to the effects of noise and artefact. Averaging SI within a given region or segment and excluding extreme outliers as artefact prior to deconvolution may therefore improve reliability.

Finally as discussed in chapters 4 and 6 difficulties in accurately correcting for baseline SI may reduce the accuracy of quantitative analysis, particularly after repeated administration of CA.

Lack of a true gold-standard for validation

Another problem currently limiting the development of quantitative methods is the absence of an obvious gold standard as it is not possible to measure true myocardial perfusion in human subjects. Simulations, phantoms, animal studies and human studies can all be used as reference standards. Simulated data have been used previously^{213, 214} and allow precise control over the conditions of perfusion. However simulations are not standardised and non-physiological.

Animal models are physiological and allow the use of microspheres for histological evaluation of perfusion. However these are limited by availability,

cost and ethical considerations. Furthermore microspheres are only a surrogate marker of perfusion. An isolated, perfused, pig-heart model has been described by our research group to allow exact control of perfusion²¹⁵ however it remains limited by cost and availability. The perfusion phantom described above allows precise control over perfusion and overcomes the cost and ethical restraints associated with animal models, however, it is non-physiological.

Human studies are the most relevant for validation and PET or invasive measurement of coronary flow using Doppler probe tipped guidewires can be used as the perfusion reference standard. However quantitative PET methods are also affected by many of the same problems that affect CMR. These methods are not standardised and use a number of mathematical models, each with potential limitations. It is recognised that different tracers provide different normal and abnormal perfusion ranges¹²². This is reflected in the paucity of published data using quantitative PET and the lack of consensus regarding normal ranges for perfusion¹⁵⁸. Finally, invasive methods can be used to measure coronary flow and the XMR set-up is ideal for comparison of CMR and invasive measurements. However these methods are an indirect measure, estimate coronary flow rather than perfusion and are not routinely available.

Further developments should allow many of these limitations to be overcome eventually. However, calculation of a quantitative MPR will correct many of these differences, which occur as a result of the lack of method standardisation. MPR may therefore be more robust than absolute values as suggested in the comparison with PET reported here.

Novel CMR methods for guiding revascularisation

Although the focus of this work was perfusion and quantitative CMR perfusion two other novel CMR methods with potential applications for guiding revascularisation were evaluated. CMR endocardial border definition and image quality are unrivalled by other imaging modalities and as a result CMR has become accepted as the gold standard for wall motion analysis. The potential to accurately quantify wall motion in a user-independent fashion with CMR feature tracking is therefore extremely promising as it may then allow improved selection of territories and patients for revascularisation procedures. In addition to this feature tracking has potential applications for early detection and monitoring of cardiomyopathies and monitoring disease progression, for example in patients taking cardiotoxic chemotherapeutic agents or prior to or after therapeutic interventions. Moreover CMR-FT derived parameters could be used as surrogate end-points in research studies, particularly if reproducibility can be improved.

The early work with the dual-IR sequence was also extremely promising. LGE imaging is one of the main strengths of CMR imaging both for guiding revascularisation and for other applications such as identifying the aetiology of cardiomyopathies. Despite the obvious successes of this method it is sometimes limited by inadequate contrast between LGE and blood and this novel sequence appears useful in these situations. Further studies using both of these techniques are supported by the results of this work and are now warranted.

Future perspectives

In addition to further development of the techniques discussed above the role of CMR in guiding revascularisation in future is likely to be influenced by improved hardware and software, new clinical studies and multimodal cardiac imaging.

Technical advances

Technical advances will result in many future developments. As an example, Blood Oxygen Level-Dependent (BOLD) magnetic resonance allows CMR perfusion imaging to be performed without CA administration as SI changes are detected as the ratio of oxygenated and deoxygenated haemoglobin in the myocardium changes. This method appears to allow visualisation of true ischaemia rather than a surrogate²¹⁶. However, at present, BOLD techniques are not available for routine clinical use.

Clinical studies

A number of important clinical questions remain unanswered and are the focus of current clinical trials. With respect to ischaemia it remains unclear whether reducing myocardial ischaemic burden per se is of prognostic benefit. It is also of interest whether a non-invasive test, and specifically CMR, can guide revascularisation in the same way that FFR can. An international, multi-centre study is currently recruiting to address this question (MR-INFORM; clinical trials number NCT01236807).

Despite publication of the much-anticipated STICH study prospective imaging-guided revascularisation outcome studies are still lacking. Much of the CMR viability work published previously has focused on patients with moderate LV systolic dysfunction. The accuracy of CMR for predicting viability in more severe LV dysfunction is less well established. In addition the mechanism of how prognosis is improved by revascularisation in the absence of an improvement in LV function remains unanswered. It is likely that the application of novel techniques and high spatial resolution imaging will be used to better understand these issues.

Multimodality Imaging

Each imaging modality has its own advantages and limitations and no single modality can adequately provide all the information required to guide revascularisation. There is increasing interest in combining modalities to achieve even better results²¹⁷. This can involve simultaneous dual modality imaging in hybrid scanners or sequential multimodality imaging with or without retrospective image fusion as described in chapter 9. This approach has been successfully applied in the field of oncology where images from different modalities are fused for the diagnosis and staging of cancers. There has been some early limited success in the application of this approach to cardiac imaging. For example PET perfusion imaging and CT angiography have been successfully combined in a hybrid scanner to improve detection of flow-limiting CAD²¹⁸. The possibility of combining CMR with CT, for example, is also an appealing prospect and an area of current research.

Conclusions

In patients with CAD decisions regarding revascularization are central to patient management as revascularisation can improve both symptoms and prognosis in certain sub-groups of patients. From the available evidence, it is clear that information on coronary anatomy alone is often insufficient to make this decision, and it is crucial to know also about myocardial ischaemia and viability. CMR can already provide much of the relevant functional information to guide revascularisation. However CMR techniques and clinical practice continue to evolve and some of these changes will ultimately result in improved patient and lesion selection. Quantitative analysis of perfusion is an exciting prospect with great potential and has demonstrated clinical utility, however its application remains challenging. Novel scar and strain imaging techniques with the potential to guide revascularisation have also shown promising results. Further method refinement and subsequent clinical studies will allow the full potential of these tools to be realised and consolidate the role of CMR at the forefront of guiding coronary revascularisation.

References

1. WorldHealthOrganization.
<http://www.Who.Int/mediacentre/factsheets/fs310/en/index.Html>.
2008
2. BritishHeartFoundation. <Http://www.Bhf.Org.Uk/heart-health/statistics/mortality.Asp>x. 2011
3. Gould KL, Lipscomb K, Hamilton GW. Physiologic basis for assessing critical coronary stenosis. Instantaneous flow response and regional distribution during coronary hyperemia as measures of coronary flow reserve. *The American Journal of Cardiology*. 1974;33:87-94
4. White CW, Wright CB, Doty DB, Hiratzka LF, Eastham CL, Harrison DG, Marcus ML. Does visual interpretation of the coronary arteriogram predict the physiologic importance of a coronary stenosis? *N Engl J Med*. 1984;310:819-824
5. Meijboom WB, Van Mieghem CAG, van Pelt N, Weustink A, Pugliese F, Mollet NR, Boersma E, Regar E, van Geuns RJ, de Jaegere PJ, Serruys PW, Krestin GP, de Feyter PJ. Comprehensive assessment of coronary artery stenoses: Computed tomography coronary angiography versus conventional coronary angiography and correlation with fractional flow reserve in patients with stable angina. *Journal of the American College of Cardiology*. 2008;52:636-643
6. Silber S, Albertsson P, Avilés FF, Camici PG, Colombo A, Hamm C, Jørgensen E, Marco J, Nordrehaug JE, Ruzyllo W, Urban P, Stone GW, Wijns W. Guidelines for percutaneous coronary interventions. The task force for

percutaneous coronary interventions of the european society of cardiology.

Eur Heart J. 2005;26:804-847

7. *Serruys PW, Morice MC, Kappetein AP, Colombo A, Holmes DR, Mack MJ, Ståhle E, Feldman TE, van den Brand M, Bass EJ, Van Dyck N, Leadley K, Dawkins KD, Mohr FW. Percutaneous coronary intervention versus coronary-artery bypass grafting for severe coronary artery disease. N Engl J Med. 2009*
8. *Yusuf S, Zucker D, Peduzzi P, Fisher LD, Takaro T, Kennedy JW, Davis K, Killip T, Passamani E, Norris R. Effect of coronary artery bypass graft surgery on survival: Overview of 10-year results from randomised trials by the coronary artery bypass graft surgery trialists collaboration. Lancet. 1994;344:563-570*
9. *Mark DB, Shaw L, Harrell FE, Jr., Hlatky MA, Lee KL, Bengtson JR, McCants CB, Califf RM, Pryor DB. Prognostic value of a treadmill exercise score in outpatients with suspected coronary artery disease. N Engl J Med. 1991;325:849-853*
10. *Shaw L. Prognostic value of gated myocardial perfusion spect. Journal of Nuclear Cardiology. 2004;11:171-185*
11. *Sicari R, Pasanisi E, Venneri L, Landi P, Cortigiani L, Picano E. Stress echo results predict mortality: A large-scale multicenter prospective international study. Journal of the American College of Cardiology. 2003;41:589-595*
12. *Jahnke C, Nagel E, Gebker R, Kokocinski T, Kelle S, Manka R, Fleck E, Paetsch I. Prognostic value of cardiac magnetic resonance stress tests:*

Adenosine stress perfusion and dobutamine stress wall motion imaging.
Circulation. 2007;115:1769-1776

13. *Hachamovitch R, Kang X, Amanullah A, Abidov A, Hayes S, Friedman J, Cohen, Thomson L, Germano G, Berman D. Comparison of the short-term survival benefit associated with revascularization compared with medical therapy in patients with no prior coronary artery disease undergoing stress myocardial perfusion single photon emission computed tomography. Circulation.* 2003;107:2900-2907
14. *Davies RF, Goldberg AD, Forman S, Pepine CJ, Knatterud GL, Geller N, Sopko G, Pratt C, Deanfield J, Conti CR. Asymptomatic cardiac ischemia pilot (ACIP) study two-year follow-up: Outcomes of patients randomized to initial strategies of medical therapy versus revascularization. Circulation.* 1997;95:2037-2043
15. *Erne P, Schoenenberger A, Burckhardt D, Zuber M, Kiowski W, Buser P, Dubach P, Resink T, Pfisterer M. Effects of percutaneous coronary interventions in silent ischemia after myocardial infarction: The SWISSI II randomized controlled trial. JAMA: The Journal of the American Medical Association.* 2007;297:1985-1991
16. *Boden WE, O'Rourke RA, Teo KK, Hartigan PM, Maron DJ, Kostuk WJ, Knudtson M, Dada M, Casperson P, Harris CL, Chaitman BR, Shaw L, Gosselin G, Nawaz S, Title LM, Gau G, Blaustein AS, Booth DC, Bates ER, Spertus JA, Berman DS, Mancini GB, Weintraub WS, Group CTR. Optimal medical therapy with or without PCI for stable coronary disease. N Engl J Med.* 2007;356:1503-1516

17. Shaw L, Berman D, Maron D, Mancini G, Hayes S, Hartigan P, Weintraub W, O'rourke R, Dada M, Spertus J, Chaitman B, Friedman J, Slomka P, Heller G, Germano G, Gosselin G, Berger P, Kostuk W, Schwartz R, Knudtson M, Veledar E, Bates E, Mccallister B, Teo K, Boden W. *Optimal medical therapy with or without percutaneous coronary intervention to reduce ischemic burden: Results from the clinical outcomes utilizing revascularization and aggressive drug evaluation (COURAGE) trial nuclear substudy. Circulation. 2008;117:1283-1291*
18. van den Brand MJ, Rensing BJ, Morel MA, Foley DP, de Valk V, Breeman A, Suryapranata H, Haalebos MM, Wijns W, Wellens F, Balcon R, Magee P, Ribeiro E, Buffolo E, Unger F, Serruys PW. *The effect of completeness of revascularization on event-free survival at one year in the arts trial. Journal of the American College of Cardiology. 2002;39:559-564*
19. Hannan E, Racz M, Holmes DR, King, III SB, Walford G, Ambrose JA, Sharma S, Katz S, Clark LT, Jones RH. *Impact of completeness of percutaneous coronary intervention revascularization on long-term outcomes in the stent era. Circulation. 2006;113:2406-2412*
20. Pijls NH, van Schaardenburgh P, Manoharan G, Boersma E, Bech JW, van't Veer M, Bär F, Hoorntje J, Koolen J, Wijns W, De Bruyne B. *Percutaneous coronary intervention of functionally nonsignificant stenosis: 5-year follow-up of the DEFER study. Journal of the American College of Cardiology. 2007;49:2105-2111*
21. Tonino PA, De Bruyne B, Pijls NH, Siebert U, Ikeno F, van' t Veer M, Klauss V, Manoharan G, Engstrøm T, Oldroyd KG, Ver Lee PN, MacCarthy PA,

- Fearon WF, Investigators FS. Fractional flow reserve versus angiography for guiding percutaneous coronary intervention. N Engl J Med. 2009;360:213-224*
22. *De Bruyne B, Pijls NH, Kalesan B, Barbato E, Tonino PA, Piroth Z, Jagic N, Mobius-Winckler S, Rioufol G, Witt N, Kala P, Maccarthy P, Engström T, Oldroyd KG, Mavromatis K, Manoharan G, Verlee P, Frobert O, Curzen N, Johnson JB, Jüni P, Fearon WF. Fractional Flow Reserve-Guided PCI versus Medical Therapy in Stable Coronary Disease.. N Engl J Med 2012;367:991-1001.*
 23. *Barner H. Operative treatment of coronary atherosclerosis. The Annals of Thoracic Surgery. 2008;85:1473-1482*
 24. *Sharir T, Germano G, Kang X, Lewin HC, Miranda R, Cohen I, Agafitei RD, Friedman JD, Berman DS. Prediction of myocardial infarction versus cardiac death by gated myocardial perfusion spect: Risk stratification by the amount of stress-induced ischemia and the poststress ejection fraction. Journal of Nuclear Medicine. 2001;42:831-837*
 25. *Bax JJ, van der Wall EE, Harbinson M. Radionuclide techniques for the assessment of myocardial viability and hibernation. Heart. 2004;90 Suppl 5:v26-33*
 26. *Allman KC, Shaw LJ, Hachamovitch R, Udelson JE. Myocardial viability testing and impact of revascularization on prognosis in patients with coronary artery disease and left ventricular dysfunction: A meta-analysis. Journal of the American College of Cardiology. 2002;39:1151-1158*
 27. *Bonow RO, Maurer G, Lee KL, Holly TA, Binkley PF, Desvigne-Nickens P, Drozd J, Farsky PS, Feldman AM, Doenst T, Michler RE, Berman DS,*

- Nicolau JC, Pellikka PA, Wrobel K, Alotti N, Asch FM, Favaloro LE, She L, Velazquez EJ, Jones RH, Panza JA, Investigators ST. Myocardial viability and survival in ischemic left ventricular dysfunction. *N Engl J Med*. 2011;364:1617-1625
28. Nesto RW, Kowalchuk GJ. The ischemic cascade: Temporal sequence of hemodynamic, electrocardiographic and symptomatic expressions of ischemia. *The American Journal of Cardiology*. 1987;59:23C-30C
 29. Leong-Poi H, Rim S, Le DE, Fisher NG, Wei K, Kaul S. Perfusion versus function: The ischemic cascade in demand ischemia: Implications of single-vessel versus multivessel stenosis. *Circulation*. 2002;105:987-992
 30. Nagel E, Lehmkuhl HB, Bocksch W, Klein C, Vogel U, Frantz E, Ellmer A, Dreyse S, Fleck E. Noninvasive diagnosis of ischemia-induced wall motion abnormalities with the use of high-dose dobutamine stress mri: Comparison with dobutamine stress echocardiography. *Circulation*. 1999;99:763-770
 31. Nandalur KR, Dwamena BA, Choudhri AF, Nandalur MR, Carlos RC. Diagnostic performance of stress cardiac magnetic resonance imaging in the detection of coronary artery disease: A meta-analysis. *Journal of the American College of Cardiology*. 2007;50:1343-1353
 32. Wahl A, Paetsch I, Gollesch A, Roethemeyer S, Foell D, Gebker R, Langreck H, Klein C, Fleck E, Nagel E. Safety and feasibility of high-dose dobutamine-atropine stress cardiovascular magnetic resonance for diagnosis of myocardial ischaemia: Experience in 1000 consecutive cases. *Eur Heart J*. 2004;25:1230-1236

33. Lurz P, Muthurangu V, Schievano S, Nordmeyer J, Bonhoeffer P, Taylor AM, Hansen MS. Feasibility and reproducibility of biventricular volumetric assessment of cardiac function during exercise using real-time radial k-t sense magnetic resonance imaging. *J. Magn. Reson. Imaging*. 2009;29:1062-1070
34. Schalla S, Nagel E, Lehmkuhl H, Klein C, Bornstedt A, Schnackenburg B, Schneider U, Fleck E. Comparison of magnetic resonance real-time imaging of left ventricular function with conventional magnetic resonance imaging and echocardiography. *The American Journal of Cardiology*. 2001;87:95-99
35. Camici PG, Rimoldi OE. The clinical value of myocardial blood flow measurement. *Journal of Nuclear Medicine*. 2009;50:1076-1087
36. Camici PG, Crea F. Coronary microvascular dysfunction. *N Engl J Med*. 2007;356:830-840
37. Algranati D, Kassab GS, Lanir Y. Why is the subendocardium more vulnerable to ischemia? A new paradigm. *Am J Physiol Heart Circ Physiol*. 2011;300:H1090-1100
38. Toyota E, Ogasawara Y, Hiramatsu O, Tachibana H, Kajiya F, Yamamori S, Chilian WM. Dynamics of flow velocities in endocardial and epicardial coronary arterioles. *AJP: Heart and Circulatory Physiology*. 2004;288:H1598-H1603
39. Cerqueira MD, Nguyen P, Staehr P, Underwood SR, Iskandrian AE, Investigators A-MT. Effects of age, gender, obesity, and diabetes on the efficacy and safety of the selective A2A agonist regadenoson versus

- adenosine in myocardial perfusion imaging integrated advance-MPI trial results. JACC Cardiovasc Imaging. 2008;1:307-316*
40. Robinson PJ. Radiology's achilles' heel: Error and variation in the interpretation of the röntgen image. *Br J Radiol. 1997;70:1085-1098*
 41. Ghosh N, Rimoldi OE, Beanlands RSB, Camici PG. Assessment of myocardial ischaemia and viability: Role of positron emission tomography. *Eur Heart J. 2010;31:2984-2995*
 42. Uren NG, Melin JA, De Bruyne B, Wijns W, Baudhuin T, Camici PG. Relation between myocardial blood flow and the severity of coronary-artery stenosis. *N Engl J Med. 1994;330:1782-1788*
 43. Di Carli M, Czernin J, Hoh CK, Gerbaudo VH, Brunken RC, Huang SC, Phelps ME, Schelbert HR. Relation among stenosis severity, myocardial blood flow, and flow reserve in patients with coronary artery disease. *Circulation. 1995;91:1944-1951*
 44. Herzog BA, Husmann L, Valenta I, Gaemperli O, Siegrist PT, Tay FM, Burkhard N, Wyss CA, Kaufmann PA. Long-term prognostic value of ¹³N-ammonia myocardial perfusion positron emission tomography added value of coronary flow reserve. *Journal of the American College of Cardiology. 2009;54:150-156*
 45. Tio RA, Dabeshlim A, Siebelink H-MJ, de Sutter J, Hillege HL, Zeebregts CJ, Dierckx RAJO, van Veldhuisen DJ, Zijlstra F, Slart RHJA. Comparison between the prognostic value of left ventricular function and myocardial perfusion reserve in patients with ischemic heart disease. *J Nucl Med. 2009;50:214-219*

46. Vogel R, Indermuhle A, Seiler C. Determination of the absolute perfusion threshold preventing myocardial ischaemia in humans. *Heart*. 2007;93:115-116
47. Fox K, Garcia MAA, Ardissino D, Buszman P, Camici PG, Crea F, Daly C, De Backer G, Hjelm Dahl P, Lopez-Sendon J, Marco J, Morais J, Pepper J, Sechtem U, Simoons M, Thygesen K, Priori SG, Blanc J-J, Budaj A, Camm J, Dean V, Deckers J, Dickstein K, Lekakis J, McGregor K, Metra M, Morais J, Osterspey A, Tamargo J, Zamorano JL. Guidelines on the management of stable angina pectoris: Executive summary: The task force on the management of stable angina pectoris of the european society of cardiology. *Eur Heart J*. 2006;27:1341-1381
48. Wagner A, Mahrholdt H, Holly TA, Elliott MD, Regenfus M, Parker M, Klocke FJ, Bonow RO, Kim RJ, Judd RM. Contrast-enhanced MRI and routine single photon emission computed tomography (SPECT) perfusion imaging for detection of subendocardial myocardial infarcts: An imaging study. *Lancet*. 2003;361:374-379
49. Lee DC, Simonetti OP, Harris KR, Holly TA, Judd RM, Wu E, Klocke FJ. Magnetic resonance versus radionuclide pharmacological stress perfusion imaging for flow-limiting stenoses of varying severity. *Circulation*. 2004;110:58-65
50. Nandalur KR, Dwamena BA, Choudhri AF, Nandalur SR, Reddy P, Carlos RC. Diagnostic performance of positron emission tomography in the detection of coronary artery disease: A meta-analysis. *Acad Radiol*. 2008;15:444-451

51. Manabe O, Yoshinaga K, Katoh C, Naya M, deKemp RA, Tamaki N. *Repeatability of rest and hyperemic myocardial blood flow measurements with ⁸²Rb dynamic pet. Journal of Nuclear Medicine. 2009;50:68-71*
52. Marwick TH, Shan K, Patel S, Go RT, Lauer MS. *Incremental value of rubidium-82 positron emission tomography for prognostic assessment of known or suspected coronary artery disease. The American Journal of Cardiology. 1997;80:865-870*
53. Dorbala S, Hachamovitch R, Curillova Z, Thomas D, Vangala D, Kwong RY, Di Carli MF. *Incremental prognostic value of gated Rb-82 positron emission tomography myocardial perfusion imaging over clinical variables and rest LVEF. JACC Cardiovascular Imaging. 2009;2:846-854*
54. Bhatia VK, Senior R. *Contrast echocardiography: Evidence for clinical use. J Am Soc Echocardiogr. 2008;21:409-416*
55. Tsutsui JM, Elhendy A, Anderson J, Xie F, McGrain AC, TR Porter. *Prognostic value of dobutamine stress myocardial contrast perfusion echocardiography. Circulation. 2005;112:1444-1450*
56. Raman SV, Shah M, McCarthy B, Garcia A, Ferketich AK. *Multi-detector row cardiac computed tomography accurately quantifies right and left ventricular size and function compared with cardiac magnetic resonance. American Heart Journal. 2006;151:736-744*
57. Blankstein R, Shturman LD, Rogers IS, Rocha-Filho JA, Okada DR, Sarwar A, Soni AV, Bezerra H, Ghoshhajra BB, Petranovic M, Loureiro R, Feuchtner G, Gewirtz H, Hoffmann U, Mamuya WS, Brady TJ, Cury RC. *Adenosine-induced stress myocardial perfusion imaging using dual-source cardiac*

- computed tomography. Journal of the American College of Cardiology.*
2009;54:1072-1084
58. Kido T, Kurata A, Higashino H, Inoue Y, Kanza RE, Okayama H, Higaki J, Murase K, Mochizuki T. Quantification of regional myocardial blood flow using first-pass multidetector-row computed tomography and adenosine triphosphate in coronary artery disease. *Circ J.* 2008;72:1086-1091
 59. George RT, Silva C, Cordeiro MAS, Dipaula A, Thompson DR, Mccarthy WF, Ichihara T, Lima JAC, Lardo AC. Multidetector computed tomography myocardial perfusion imaging during adenosine stress. *Journal of the American College of Cardiology.* 2006;48:153-160
 60. Cury RC, Magalhães TA, Borges AC, Shiozaki AA, Lemos PA, Júnior JS, Meneghetti JC, Cury RC, Rochitte CE. Dipyridamole stress and rest myocardial perfusion by 64-detector row computed tomography in patients with suspected coronary artery disease. *The American Journal of Cardiology.* 2010;106:310-315
 61. Ko SM, Choi JW, Song MG, Shin JK, Chee HK, Chung HW, Kim DH. Myocardial perfusion imaging using adenosine-induced stress dual-energy computed tomography of the heart: Comparison with cardiac magnetic resonance imaging and conventional coronary angiography. *Eur Radiol.* 2011;21:26-35
 62. Einstein AJ, Moser KW, Thompson RC, Cerqueira MD, Henzlova MJ. Radiation dose to patients from cardiac diagnostic imaging. *Circulation.* 2007;116:1290-1305
 63. Salerno M, Beller GA. Noninvasive assessment of myocardial perfusion. *Circulation: Cardiovascular Imaging.* 2009;2:412-424

64. Wyrick JJ, Kalvaitis S, Mcconnell KJ, Rinkevich D, Kaul S, Wei K. Cost-efficiency of myocardial contrast echocardiography in patients presenting to the emergency department with chest pain of suspected cardiac origin and a nondiagnostic electrocardiogram. *The American Journal of Cardiology*. 2008;102:649-652
65. Schwitter J, Wacker CM, van Rossum AC, Lombardi M, Al-Saadi N, Ahlstrom H, Dill T, Larsson HB, Flamm SD, Marquardt M, Johansson L. MR-IMPACT: Comparison of perfusion-cardiac magnetic resonance with single-photon emission computed tomography for the detection of coronary artery disease in a multicentre, multivendor, randomized trial. *Eur Heart J*. 2008;29:480-489
66. Greenwood JP, Maredia N, Younger JF, Brown JM, Nixon J, Everett CC, Bijsterveld P, Ridgway JP, Radjenovic A, Dickinson CJ, Ball SG, Plein S. Cardiovascular magnetic resonance and single-photon emission computed tomography for diagnosis of coronary heart disease (CE-MARC): A prospective trial. *Lancet*. 2012;379:453-460
67. Rieber J, Huber A, Erhard I, Mueller S, Schweyer M, Koenig A, Schiele TM, Theisen K, Siebert U, Schoenberg SO, Reiser M, Klauss V. Cardiac magnetic resonance perfusion imaging for the functional assessment of coronary artery disease: A comparison with coronary angiography and fractional flow reserve. *Eur Heart J*. 2006;27:1465-1471
68. Costa MA, Shoemaker S, Futamatsu H, Klassen C, Angiolillo DJ, Nguyen M, Siuciak A, Gilmore P, Zenni MM, Guzman L, Bass TA, Wilke N. Quantitative magnetic resonance perfusion imaging detects anatomic and physiologic coronary artery disease as measured by coronary angiography and

- fractional flow reserve. Journal of the American College of Cardiology.*
2007;50:514-522
69. Watkins S, Mcgeoch R, Lyne J, Steedman T, Good R, Mclaughlin M-J, Cunningham T, Bezlyak V, Ford I, Dargie HJ, Oldroyd KG. Validation of magnetic resonance myocardial perfusion imaging with fractional flow reserve for the detection of significant coronary heart disease. *Circulation.* 2009;120:2207-2213
 70. Kraitchman DL, Wilke N, Hexeberg E, Jerosch-Herold M, Wang Y, Parrish TB, Chang CN, Zhang Y, Bache RJ, Axel L. Myocardial perfusion and function in dogs with moderate coronary stenosis. *Magn Reson Med.* 1996;35:771-780
 71. Klocke FJ, Simonetti OP, Judd RM, Kim RJ, Harris KR, Hedjbeli S, Fieno DS, Miller S, Chen V, Parker MA. Limits of detection of regional differences in vasodilated flow in viable myocardium by first-pass magnetic resonance perfusion imaging. *Circulation.* 2001;104:2412-2416
 72. Nagel E, Klein C, Paetsch I, Hettwer S, Schnackenburg B, Wegscheider K, Fleck E. Magnetic resonance perfusion measurements for the noninvasive detection of coronary artery disease. *Circulation.* 2003;108:432-437
 73. Ishida M, Sakuma H, Murashima S, Nishida J, Senga M, Kobayasi S, Takeda K, Kato N. Absolute blood contrast concentration and blood signal saturation on myocardial perfusion MRI: Estimation from CT data. *J. Magn. Reson. Imaging.* 2009;29:205-210
 74. Jerosch-Herold M, Wilke N, Stillman AE. Magnetic resonance quantification of the myocardial perfusion reserve with a fermi function model for constrained deconvolution. *Med Phys.* 1998;25:73-84

75. Christian TF, Rettmann DW, Aletras AH, Liao SL, Taylor JL, Balaban RS, Arai AE. Absolute myocardial perfusion in canines measured by using dual-bolus first-pass mr imaging. *Radiology*. 2004;232:677-684
76. Christian TF, Aletras AH, Arai AE. Estimation of absolute myocardial blood flow during first-pass mr perfusion imaging using a dual-bolus injection technique: Comparison to single-bolus injection method. *J. Magn. Reson. Imaging*. 2008;27:1271-1277
77. Utz W, Greiser A, Niendorf T, Dietz R, Schulz-Menger J. Single- or dual-bolus approach for the assessment of myocardial perfusion reserve in quantitative mr perfusion imaging. *Magn Reson Med*. 2008;59:1373-1377
78. Gatehouse PD, Elkington AG, Ablitt NA, Yang G-Z, Pennell DJ, Firmin DN. Accurate assessment of the arterial input function during high-dose myocardial perfusion cardiovascular magnetic resonance. *J. Magn. Reson. Imaging*. 2004;20:39-45
79. Kurita T, Sakuma H, Onishi K, Ishida M, Kitagawa K, Yamanaka T, Tanigawa T, Kitamura T, Takeda K, Ito M. Regional myocardial perfusion reserve determined using myocardial perfusion magnetic resonance imaging showed a direct correlation with coronary flow velocity reserve by doppler flow wire. *Eur Heart J*. 2009;30:444-452
80. Kaufmann PA, Gneccchi-Ruscione T, Yap JT, Rimoldi O, Camici PG. Assessment of the reproducibility of baseline and hyperemic myocardial blood flow measurements with 15O-labeled water and PET. *J Nucl Med*. 1999;40:1848-1856
81. Kramer CM, Barkhausen J, Flamm SD, Kim RJ, Nagel E. Standardized cardiovascular magnetic resonance imaging (CMR) protocols, society for

cardiovascular magnetic resonance: Board of trustees task force on standardized protocols. J. Cardiovasc Magnetic Resonance 2008;10:35

82. Baer FM, Voth E, Schneider CA, Theissen P, Schicha H, Sechtem U. Comparison of low-dose dobutamine-gradient-echo magnetic resonance imaging and positron emission tomography with [18f]fluorodeoxyglucose in patients with chronic coronary artery disease. A functional and morphological approach to the detection of residual myocardial viability. *Circulation. 1995;91:1006-1015*
83. Gunning MG, Anagnostopoulos C, Knight CJ, Pepper J, Burman ED, Davies G, Fox KM, Pennell DJ, Ell PJ, Underwood SR. Comparison of 201tl, 99mtc-tetrofosmin, and dobutamine magnetic resonance imaging for identifying hibernating myocardium. *Circulation. 1998;98:1869-1874*
84. Kim RJ, Fieno DS, Parrish TB, Harris K, Chen EL, Simonetti O, Bundy J, Finn JP, Klocke FJ, Judd RM. Relationship of mri delayed contrast enhancement to irreversible injury, infarct age, and contractile function. *Circulation. 1999;100:1992-2002*
85. Klein C, Nekolla SG, Bengel FM, Momose M, Sammer A, Haas F, Schnackenburg B, Delius W, Mudra H, Wolfram D, Schwaiger M. Assessment of myocardial viability with contrast-enhanced magnetic resonance imaging: Comparison with positron emission tomography. *Circulation. 2002;105:162-167*
86. Kim RJ, Wu E, Rafael A, Chen EL, Parker MA, Simonetti O, Klocke FJ, Bonow RO, Judd RM. The use of contrast-enhanced magnetic resonance imaging to identify reversible myocardial dysfunction. *N Engl J Med. 2000;343:1445-1453*

87. Wellnhofer E, Olariu A, Klein C, Gräfe M, Wahl A, Fleck E, Nagel E. *Magnetic resonance low-dose dobutamine test is superior to scar quantification for the prediction of functional recovery. Circulation. 2004;109:2172-2174*
88. Kaandorp T. *Cardiovascular mr to assess myocardial viability in chronic ischaemic LV dysfunction. Heart. 2005;91:1359-1365*
89. McCrohon JA, Moon JCC, Prasad SK, McKenna WJ, Lorenz CH, Coats AJS, Pennell DJ. *Differentiation of heart failure related to dilated cardiomyopathy and coronary artery disease using gadolinium-enhanced cardiovascular magnetic resonance. Circulation. 2003;108:54-59*
90. Bruder O, Schneider S, Nothnagel D, Dill T, Hombach V, Schulz-Menger J, Nagel E, Lombardi M, van Rossum AC, Wagner A, Schwitter J, Senges J, Sabin GV, Sechtem U, Mahrholdt H. *Eurocmr (European cardiovascular magnetic resonance) registry: Results of the german pilot phase. Journal of the American College of Cardiology. 2009;54:1457-1466*
91. Kwong RY, Chan AK, Brown KA, Chan CW, Reynolds HG, Tsang S, Davis RB. *Impact of unrecognized myocardial scar detected by cardiac magnetic resonance imaging on event-free survival in patients presenting with signs or symptoms of coronary artery disease. Circulation. 2006;113:2733-2743*
92. Roes SD, Kelle S, Kaandorp TAM, Kokocinski T, Poldermans D, Lamb HJ, Boersma E, van der Wall EE, Fleck E, de Roos A, Nagel E, Bax JJ. *Comparison of myocardial infarct size assessed with contrast-enhanced magnetic resonance imaging and left ventricular function and volumes to predict mortality in patients with healed myocardial infarction. The American Journal of Cardiology. 2007;100:930-936*

93. Kim WY, Danias PG, Stuber M, Flamm SD, Plein S, Nagel E, Langerak SE, Weber OM, Pedersen EM, Schmidt M, Botnar RM, Manning WJ. Coronary magnetic resonance angiography for the detection of coronary stenoses. *N Engl J Med.* 2001;345:1863-1869
94. Sakuma H, Ichikawa Y, Chino S, Hirano T, Makino K, Takeda K. Detection of coronary artery stenosis with whole-heart coronary magnetic resonance angiography. *Journal of the American College of Cardiology.* 2006;48:1946-1950
95. Messroghli DR, Bainbridge GJ, Alfakih K, Jones TR, Plein S, Ridgway JP, Sivananthan MU. Assessment of regional left ventricular function: Accuracy and reproducibility of positioning standard short-axis sections in cardiac mr imaging. *Radiology.* 2005;235:229-236
96. Cerqueira MD, Weissman NJ, Dilsizian V, Jacobs AK, Kaul S, Laskey WK, Pennell DJ, Rumberger JA, Ryan T, Verani MS. Standardized myocardial segmentation and nomenclature for tomographic imaging of the heart: A statement for healthcare professionals from the cardiac imaging committee of the council on clinical cardiology of the american heart association. *Circulation.* 2002;105:539-542
97. Ishida M, Schuster A, Morton G, Chiribiri A, Hussain S, Paul M, Merkle N, Steen H, Lossnitzer D, Schnackenburg B, Alfakih K, Plein S, Nagel E. Development of a universal dual-bolus injection scheme for the quantitative assessment of myocardial perfusion cardiovascular magnetic resonance. *J. Cardiovasc Magnetic Resonance.* 2011;13:28

98. Hsu LY, Rhoads KL, Holly JE, Kellman P, Aletras AH, Arai AE. Quantitative myocardial perfusion analysis with a dual-bolus contrast-enhanced first-pass mri technique in humans. *J. Magn. Reson. Imaging.* 2006;23:315-322
99. Greenwood JP, Maredia N, Radjenovic A, Brown JM, Nixon J, Farrin AJ, Dickinson C, Younger JF, Ridgway JP, Sculpher M, Ball SG, Plein S. Clinical evaluation of magnetic resonance imaging in coronary heart disease: The CE-MARC study. *Trials.* 2009;10:62
100. Schwitter J, Nanz D, Kneifel S, Bertschinger K, Buchi M, Knusel PR, Marincek B, Luscher TF, von Schulthess GK. Assessment of myocardial perfusion in coronary artery disease by magnetic resonance: A comparison with positron emission tomography and coronary angiography. *Circulation.* 2001;103:2230-2235
101. Elkindon AG, Gatehouse PD, Cannell TM, Moon JC, Prasad SK, Firmin DN, Pennell DJ. Comparison of hybrid echo-planar imaging and flash myocardial perfusion cardiovascular MR imaging. *Radiology.* 2005;235:237-243
102. Lyne JC, Gatehouse PD, Assomull RG, Smith GC, Kellman P, Firmin DN, Pennell DJ. Direct comparison of myocardial perfusion cardiovascular magnetic resonance sequences with parallel acquisition. *J. Magn. Reson. Imaging.* 2007;26:1444-1451
103. Weber S, Kronfeld A, Kunz RP, Fiebich M, Horstick G, Kreitner K-F, Schreiber WG. Comparison of three accelerated pulse sequences for semiquantitative myocardial perfusion imaging using sensitivity encoding incorporating temporal filtering (tsense). *J. Magn. Reson. Imaging.* 2007;26:569-579

104. Fenchel M, Helber U, Simonetti OP, Stauder NI, Kramer U, Nguyen C-N, Finn JP, Claussen CD, Miller S. Multislice first-pass myocardial perfusion imaging: Comparison of saturation recovery (sr)-truefisp-two-dimensional (2d) and sr-turboflash-2d pulse sequences. *J. Magn. Reson. Imaging.* 2004;19:555-563
105. Wang Y, Moin K, Akinboboye O, Reichek N. Myocardial first pass perfusion: Steady-state free precession versus spoiled gradient echo and segmented echo planar imaging. *Magn. Reson. Med.* 2005;54:1123-1129
106. Pruessmann KP, Weiger M, Scheidegger MB, Boesiger P. Sense: Sensitivity encoding for fast MRI. *Magn Reson Med.* 1999;42:952-962
107. Kozerke S, Plein S. Accelerated CMR using zonal, parallel and prior knowledge driven imaging methods. *J. Cardiovasc Magnetic Resonance.* 2008;10:29
108. Chiribiri A, Schuster A, Ishida M, Hautvast G, Nooralipour N, Paul M, Hussain S, Batchelor P, Breeuwer M, Schaeffter T, Nagel E. Dynamic simulation of first pass myocardial perfusion MR with a novel perfusion phantom. *J. Cardiovasc Magnetic Resonance.* 2011;13(Suppl 1):O43
109. Plein S, Ryf S, Schwitter J, Radjenovic A, Boesiger P, Kozerke S. Dynamic contrast-enhanced myocardial perfusion MRI accelerated with k-t sense. *Magn Reson Med.* 2007;58:777-785
110. Maredia N, Radjenovic A, Kozerke S, Larghat A, Greenwood JP, Plein S. Effect of improving spatial or temporal resolution on image quality and quantitative perfusion assessment with k-t sense acceleration in first-pass cmr myocardial perfusion imaging. *Magn Reson Med.* 2010;64:1616-1624

111. Plein S, Schwitter J, Suerder D, Greenwood JP, Boesiger P, Kozerke S. *K-space and time sensitivity encoding-accelerated myocardial perfusion MR imaging at 3.0T: Comparison with 1.5T. Radiology. 2008;249:493-500*
112. Manka R, Vitanis V, Boesiger P, Flammer AJ, Plein S, Kozerke S. *Clinical feasibility of accelerated, high spatial resolution myocardial perfusion imaging. JACC Cardiovasc Imaging. 2010;3:710-717*
113. Thiele H, Plein S, Ridgway JP, Breeuwer M, Higgins D, Schuler G, Sivananthan M. *Effects of missing dynamic images on myocardial perfusion reserve index calculation: Comparison between an every heartbeat and an alternate heartbeat acquisition. J. Cardiovasc Magnetic Resonance. 2003;5:343-352*
114. Muhling OM, Dickson ME, Zenovich A, Huang Y, Wilson BV, Wilson RF, Anand IS, Seethamraju RT, Jerosch-Herold M, Wilke NM. *Quantitative magnetic resonance first-pass perfusion analysis: Inter- and intraobserver agreement. J. Cardiovasc Magnetic Resonance. 2001;3:247-256*
115. Schreiber WGN, Schmitt M, Kalden P, Mohrs OK, Kreitner K-F, Thelen M. *Dynamic contrast-enhanced myocardial perfusion imaging using saturation-prepared truefisp. J. Magn. Reson. Imaging. 2002;16:641-652*
116. Kellman P, Mcveigh ER. *Image reconstruction in SNR units: A general method for SNR measurement. Magn Reson Med. 2005;54:1439-1447*
117. Di Bella EVR, Parker DL, Sinusas AJ. *On the dark rim artifact in dynamic contrast-enhanced mri myocardial perfusion studies. Magn Reson Med. 2005;54:1295-1299*
118. Idée J-M, Port M, Raynal I, Schaefer M, Le Greneur S, Corot C. *Clinical and biological consequences of transmetallation induced by contrast agents for*

magnetic resonance imaging: A review. Fundam Clin Pharmacol.

2006;20:563-576

119. *Giang TH, Nanz D, Coulden R, Friedrich M, Graves M, Al-Saadi N, Lüscher TF, von Schulthess GK, Schwitter J. Detection of coronary artery disease by magnetic resonance myocardial perfusion imaging with various contrast medium doses: First european multi-centre experience. Eur Heart J. 2004;25:1657-1665*
120. *Wolff SD, Schwitter J, Coulden R, Friedrich MG, Bluemke DA, Biederman RW, Martin ET, Lansky AJ, Kashanian F, Foo TKF, Licato PE, Comeau CR. Myocardial first-pass perfusion magnetic resonance imaging: A multicenter dose-ranging study. Circulation. 2004;110:732-737*
121. *Klem I, Heitner J, Shah D, Jr S, Michael H, Behar V, Weinsaft J, Cawley P, Parker M, Elliott M, Judd R, Kim R. Improved detection of coronary artery disease by stress perfusion cardiovascular magnetic resonance with the use of delayed enhancement infarction imaging. Journal of the American College of Cardiology. 2006;47:1630*
122. *Knuuti J, Kajander S, Mäki M, Ukkonen H. Quantification of myocardial blood flow will reform the detection of cad. J Nucl Cardiol. 2009;16:497-506*
123. *Kajander SA, Joutsiniemi E, Saraste M, Pietila M, Ukkonen H, Saraste A, Sipila HT, Teras M, Maki M, Airaksinen J, Hartiala J, Knuuti J. Clinical value of absolute quantification of myocardial perfusion with 15O-water in coronary artery disease. Circulation: Cardiovascular Imaging. 2011;1-31*
124. *Patel AR, Antkowiak PF, Nandalur KR, West AM, Salerno M, Arora V, Christopher J, Epstein FH, Kramer CM. Assessment of advanced coronary*

artery disease: Advantages of quantitative cardiac magnetic resonance perfusion analysis. Journal of the American College of Cardiology. 2010;56:561-569

125. *Ichihara T, Ishida M, Kitagawa K, Ichikawa Y, Natsume T, Yamaki N, Maeda H, Takeda K, Sakuma H. Quantitative analysis of first-pass contrast-enhanced myocardial perfusion MRI using a patlak plot method and blood saturation correction. Magn. Reson. Med. 2009;62:373-383*
126. *Fritz-Hansen T, Hove JD, Kofoed KF, Kelbaek H, Larsson HBW. Quantification of mri measured myocardial perfusion reserve in healthy humans: A comparison with positron emission tomography. J Magn Reson Imaging. 2008;27:818-824*
127. *Pärkkä JP, Niemi P, Saraste A, Koskenvuo JW, Komu M, Oikonen V, Toikka JO, Kiviniemi TO, Knuuti J, Sakuma H, Hartiala JJ. Comparison of MRI and positron emission tomography for measuring myocardial perfusion reserve in healthy humans. Magn Reson Med. 2006;55:772-779*
128. *Pack NA, DiBella EVR, Rust TC, Kadrmas DJ, McGann CJ, Butterfield R, Christian PE, Hoffman JM. Estimating myocardial perfusion from dynamic contrast-enhanced CMR with a model-independent deconvolution method. J. Cardiovasc Magnetic Resonance. 2008;10:52*
129. *Choi Y, Huang SC, Hawkins RA, Kuhle WG, Dahlbom M, Hoh CK, Czernin J, Phelps ME, Schelbert HR. A simplified method for quantification of myocardial blood flow using nitrogen-13-ammonia and dynamic pet. Journal of Nuclear Medicine. 1993;34:488-497*
130. *Lockie T, Ishida M, Perera D, Chiribiri A, De Silva K, Kozerke S, Marber M, Nagel E, Rezavi R, Redwood S, Plein S. High-resolution magnetic resonance*

- myocardial perfusion imaging at 3.0-tesla to detect hemodynamically significant coronary stenoses as determined by fractional flow reserve. Journal of the American College of Cardiology. 2010;57:70-75*
131. Ibrahim T, Nekolla SG, Schreiber K, Odaka K, Volz S, Mehilli J, Güthlin M, Delius W, Schwaiger M. Assessment of coronary flow reserve: Comparison between contrast-enhanced magnetic resonance imaging and positron emission tomography. *Journal of the American College of Cardiology. 2002;39:864-870*
 132. Hajjiri MM, Leavitt MB, Zheng H, Spooner AE, Fischman AJ, Gewirtz H. Comparison of positron emission tomography measurement of adenosine-stimulated absolute myocardial blood flow versus relative myocardial tracer content for physiological assessment of coronary artery stenosis severity and location. *JACC Cardiovasc Imaging. 2009;2:751-758*
 133. Iida H, Kanno I, Takahashi A, Miura S, Murakami M, Takahashi K, Ono Y, Shishido F, Inugami A, Tomura N. Measurement of absolute myocardial blood flow with ¹⁵O and dynamic positron-emission tomography. Strategy for quantification in relation to the partial-volume effect. *Circulation. 1988;78:104-115*
 134. Karamitsos T, Leccisotti L, Arnold J, Recio-Mayoral A, Bhamra-Ariza P, Howells R, Searle N, Robson M, Rimoldi O, Camici P, Neubauer S, Selvanayagam J. Relationship between regional myocardial oxygenation and perfusion in patients with coronary artery disease: Insights from cardiovascular magnetic resonance and positron emission tomography. *Circulation: Cardiovascular Imaging. 2009*

135. Czernin J, Müller P, Chan S, Brunken RC, Porenta G, Krivokapich J, Chen K, Chan A, Phelps ME, Schelbert HR. Influence of age and hemodynamics on myocardial blood flow and flow reserve. *Circulation*. 1993;88:62-69
136. Selvanayagam J, Cheng A, Jerosch-Herold M, Rahimi K, Porto I, Van Gaal W, Channon K, Neubauer S, Banning A. Effect of distal embolization on myocardial perfusion reserve after percutaneous coronary intervention: A quantitative magnetic resonance perfusion study. *Circulation*. 2007;116:1458-1464
137. Nesterov SV, Han C, Mäki M, Kajander S, Naum AG, Helenius H, Lisinen I, Ukkonen H, Pietilä M, Joutsiniemi E, Knuuti J. Myocardial perfusion quantitation with 15O-labelled water pet: High reproducibility of the new cardiac analysis software (CARISMAS). *Eur J Nucl Med Mol Imaging*. 2009;36:1594-1602
138. Mullani NA. Is the patlak graphical analysis method applicable to measurement of myocardial blood flow with nitrogen-13-ammonia? *J Nucl Med*. 1993;34:1831-1834
139. Jerosch-Herold M, Seethamraju RT, Swingen CM, Wilke NM, Stillman AE. Analysis of myocardial perfusion MRI. *J. Magn. Reson. Imaging*. 2004;19:758-770
140. Nagamachi S, Czernin J, Kim AS, Sun KT, Böttcher M, Phelps ME, Schelbert HR. Reproducibility of measurements of regional resting and hyperemic myocardial blood flow assessed with PET. *Journal of Nuclear Medicine*. 1996;37:1626-1631
141. Jerosch-Herold M, Vazquez G, Wang L, Jacobs DR, Folsom AR. Variability of myocardial blood flow measurements by magnetic resonance imaging in

the multi-ethnic study of atherosclerosis. Investigative radiology.

2008;43:155-161

142. *Ortiz-Perez JT, Meyers SN, Lee DC, Kansal P, Klocke FJ, Holly TA, Davidson CJ, Bonow RO, Wu E. Angiographic estimates of myocardium at risk during acute myocardial infarction: Validation study using cardiac magnetic resonance imaging. Eur Heart J. 2007;28:1750-1758*
143. *Moise A, Clement B, Saltiel J. Clinical and angiographic correlates and prognostic significance of the coronary extent score. The American Journal of Cardiology. 1988;61:1255-1259*
144. *Kimmel SE, Berlin JA, Strom BL, Laskey WK. Development and validation of simplified predictive index for major complications in contemporary percutaneous transluminal coronary angioplasty practice. The registry committee of the society for cardiac angiography and interventions. Journal of the American College of Cardiology. 1995;26:931-938*
145. *Perera D, Stables R, Booth J, Thomas M, Redwood S. The balloon pump-assisted coronary intervention study (bcis-1): Rationale and design. American Heart Journal. 2009;158:910-916.e912*
146. *Perera D, Stables R, Thomas M, Booth J, Pitt M, Blackman D, de Belder A, Redwood S, Investigators B-. Elective intra-aortic balloon counterpulsation during high-risk percutaneous coronary intervention: A randomized controlled trial. The Journal of the American Medical Association. 2010;304:867-874*
147. *Califf RM, Phillips HR, Hindman MC, Mark DB, Lee KL, Behar VS, Johnson RA, Pryor DB, Rosati RA, Wagner GS. Prognostic value of a coronary artery*

jeopardy score. Journal of the American College of Cardiology.

1985;5:1055-1063

148. Kappetein AP, Dawkins KD, Mohr FW, Morice MC, Mack MJ, Russell ME, Pomar J, Serruys PWJC. Current percutaneous coronary intervention and coronary artery bypass grafting practices for three-vessel and left main coronary artery disease. Insights from the syntax run-in phase. *Eur J Cardiothorac Surg.* 2006;29:486-491
149. Sianos G, Morel M-A, Kappetein AP, Morice M-C, Colombo A, Dawkins K, van den Brand M, Van Dyck N, Russell ME, Mohr FW, Serruys PW. The syntax score: An angiographic tool grading the complexity of coronary artery disease. *EuroIntervention.* 2005;1:219-227
150. Liao L, Kong DF, Shaw LK, Sketch MH, Milano CA, Lee KL, Mark DB. A new anatomic score for prognosis after cardiac catheterization in patients with previous bypass surgery. *Journal of the American College of Cardiology.* 2005;46:1684-1692
151. Graham MM, Faris PD, Ghali WA, Galbraith PD, Norris CM, Badry JT, Mitchell LB, Curtis MJ, Knudtson ML. Validation of three myocardial jeopardy scores in a population-based cardiac catheterization cohort. *American Heart Journal.* 2001;142:254-261
152. Alderman E, Stadius M. The angiographic definitions of the bypass angioplasty revascularization investigation. *Coronary Artery Disease.* 1992;3:1189-1207
153. Berry C, Kellman P, Mancini C, Chen MY, Bandettini WP, Lowrey T, Hsu L-Y, Aletras AH, Arai AE. Magnetic resonance imaging delineates the ischemic

- area at risk and myocardial salvage in patients with acute myocardial infarction. Circulation: Cardiovascular Imaging. 2010;3:527-535*
154. *Fuernau G, Eitel I, Franke V, Hildebrandt L, Meissner J, de Waha S, Lurz P, Gutberlet M, Desch S, Schuler G, Thiele H. Myocardium at risk in st-segment elevation myocardial infarction comparison of t2-weighted edema imaging with the MR-assessed endocardial surface area and validation against angiographic scoring. JACC. Cardiovascular imaging. 2011;4:967-976*
 155. *Morton G, De Silva K, Sicard P, Chong E, Rashid R, Indermuhle A, Clapp B, Redwood S, Perera D. The BCIS-1 myocardial jeopardy score predicts mortality after percutaneous coronary intervention. Journal of the American College of Cardiology. 2010;56:B40*
 156. *Lanza GA, Buffon A, Sestito A, Natale L, Sgueglia GA, Galiuto L, Infusino F, Mariani L, Centola A, Crea F. Relation between stress-induced myocardial perfusion defects on cardiovascular magnetic resonance and coronary microvascular dysfunction in patients with cardiac syndrome X. Journal of the American College of Cardiology. 2008;51:466-472*
 157. *Morton G, Schuster A, Perera D, Nagel E. Cardiac magnetic resonance imaging to guide complex revascularization in stable coronary artery disease. Eur Heart J. 2010;2209-2216*
 158. *Sdringola S, Johnson NP, Kirkeeide RL, Cid E, Gould KL. Impact of unexpected factors on quantitative myocardial perfusion and coronary flow reserve in young, asymptomatic volunteers. JACC Cardiovasc Imaging. 2011;4:402-412*

159. Elkington A, Gatehouse P, Ablitt N, Yang G-Z, Firmin D, Pennell D.
Interstudy reproducibility of quantitative perfusion cardiovascular magnetic resonance. J. Cardiovasc Magnetic Resonance. 2005;7:815-822
160. Fox KM, Mulcahy DA. Circadian rhythms in cardiovascular function.
Postgrad Med J. 1991;67 Suppl 3:S33-36
161. Grothues F, Smith GC, Moon JCC, Bellenger NG, Collins P, Klein HU, Pennell DJ. Comparison of interstudy reproducibility of cardiovascular magnetic resonance with two-dimensional echocardiography in normal subjects and in patients with heart failure or left ventricular hypertrophy. *The American Journal of Cardiology. 2002;90:29-34*
162. Chih S, Macdonald PS, Feneley MP, Law M, Graham RM, McCrohon JA.
Reproducibility of adenosine stress cardiovascular magnetic resonance in multi-vessel symptomatic coronary artery disease. J. Cardiovasc Magnetic Resonance. 2010;12:42
163. Wyss CA, Koepfli P, Mikolajczyk K, Burger C, von Schulthess GK, Kaufmann PA. Bicycle exercise stress in pet for assessment of coronary flow reserve: Repeatability and comparison with adenosine stress. *Journal of Nuclear Medicine. 2003;44:146-154*
164. El Fakhri G, Kardan A, Sitek A, Dorbala S, Abi-Hatem N, Lahoud Y, Fischman A, Coughlan M, Yasuda T, Di Carli MF. Reproducibility and accuracy of quantitative myocardial blood flow assessment with ^{82}Rb pet: Comparison with ^{13}N -ammonia PET. *Journal of Nuclear Medicine. 2009;50:1062-1071*

165. Wilson RF, Wyche K, Christensen BV, Zimmer S, Laxson DD. Effects of adenosine on human coronary arterial circulation. *Circulation*. 1990;82:1595-1606
166. Reyes E, Loong CY, Harbinson M, Donovan J, Anagnostopoulos C, Underwood SR. High-dose adenosine overcomes the attenuation of myocardial perfusion reserve caused by caffeine. *Journal of the American College of Cardiology*. 2008;52:2008-2016
167. Muehling O, Jerosch-Herold M, Panse P, Zenovich A, Wilson B, Wilson R, Wilke N. Regional heterogeneity of myocardial perfusion in healthy human myocardium: Assessment with magnetic resonance perfusion imaging. *J. Cardiovasc Magnetic Resonance*. 2004;6:499-507
168. Muzik O, Duvernoy C, Beanlands RS, Sawada S, Dayanikli F, Wolfe ER, Schwaiger M. Assessment of diagnostic performance of quantitative flow measurements in normal subjects and patients with angiographically documented coronary artery disease by means of nitrogen-13 ammonia and positron emission tomography. *Journal of the American College of Cardiology*. 1998;31:534-540
169. Ishida M, Morton G, Schuster A, Nagel E, Chiribiri A. Quantitative assessment of myocardial perfusion MRI. *Curr Cardiovasc Imaging Rep*. 2010;3:65-73
170. Schwaiger M, Muzik O. Assessment of myocardial perfusion by positron emission tomography. *The American Journal of Cardiology*. 1991;67:35D-43D
171. Pickering TG, Harshfield GA, Kleinert HD, Blank S, Laragh JH. Blood pressure during normal daily activities, sleep, and exercise. Comparison of

- values in normal and hypertensive subjects. *The Journal of the American Medical Association*. 1982;247:992-996
172. Karabag T, Aydin M, Dogan SM, Sayin MR, Cetiner MA. The influence of circadian variations on echocardiographic parameters in healthy people. *Echocardiography*. 2011;28:612-618
 173. Bull SC, Main ML, Stevens GR, Goldman JH, Constable SA, Becher H. Cardiac toxicity screening by echocardiography in healthy volunteers: A study of the effects of diurnal variation and use of a core laboratory on the reproducibility of left ventricular function measurement. *Echocardiography*. 2011;28:502-507
 174. Voutilainen S, Kupari M, Hippelainen M, Karppinen K, Ventila M. Circadian variation of left ventricular diastolic function in healthy people. *Heart*. 1996;75:35-39
 175. Bellenger N, Davies L, Francis J, Coats A, Pennell D. Reduction in sample size for studies of remodeling in heart failure by the use of cardiovascular magnetic resonance. *J. Cardiovasc Magnetic Resonance*. 2000;2:271-278
 176. Schuster A, Morton G, Chiribiri A, Perera D, Vanoverschelde J, Nagel E. Imaging in the management of ischemic cardiomyopathy: Special focus on magnetic resonance. *Journal of the American College of Cardiology*. 2012;59(4): 359-70.
 177. Karamitsos TD, Francis JM, Myerson S, Selvanayagam JB, Neubauer S. The role of cardiovascular magnetic resonance imaging in heart failure. *Journal of the American College of Cardiology*. 2009;54:1407-1424
 178. Paetsch I, Jahnke C, Ferrari VA, Rademakers FE, Pellikka PA, Hundley WG, Poldermans D, Bax JJ, Wegscheider K, Fleck E, Nagel E. Determination of

- interobserver variability for identifying inducible left ventricular wall motion abnormalities during dobutamine stress magnetic resonance imaging. Eur Heart J. 2006;27:1459-1464*
179. Ibrahim E-SH. Myocardial tagging by cardiovascular magnetic resonance: Evolution of techniques--pulse sequences, analysis algorithms, and applications. *J. Cardiovasc Magnetic Resonance. 2032;13:36*
 180. Schuster A, Nagel E. Toward full quantification of wall motion with mri. *Curr Cardiovasc Imaging Reports. 2011:85-86*
 181. Maret E, Todt T, Brudin L, Nylander E, Swahn E, Ohlsson JL, Engvall JE. Functional measurements based on feature tracking of cine magnetic resonance images identify left ventricular segments with myocardial scar. *Cardiovasc Ultrasound. 2009;7:53*
 182. Hor KN, Baumann R, Pedrizzetti G, Tonti G, Gottliebson WM, Taylor M, Benson W, Mazur W. Magnetic resonance derived myocardial strain assessment using feature tracking. *Journal of Visaulized Experiments. 2011*
 183. Schuster A, Kutty S, Padiyath A, Parish V, Gribben P, Danford DA, Makowski MR, Bigalke B, Beerbaum P, Nagel E. Cardiovascular magnetic resonance myocardial feature tracking detects quantitative wall motion during dobutamine stress. *J. Cardiovasc Magnetic Resonance. 2011;13:58*
 184. Schuster A, Paul M, Bettencourt N, Morton G, Chiribiri A, Ishida M, Hussain S, Jogiya R, Kutty S, Bigalke B, Perera D, Nagel E. Cardiovascular magnetic resonance myocardial feature tracking for quantitative viability assessment in ischemic cardiomyopathy. *International Journal of Cardiology. 2011;[E-pub ahead of print], doi:10.1016/j.ijcard.2011.10.137*

185. Hopp E, Lunde K, Solheim S, Aakhus S, Arnesen H, Forfang K, Edvardsen T, Smith H-J. Regional myocardial function after intracoronary bone marrow cell injection in reperfused anterior wall infarction - a cardiovascular magnetic resonance tagging study. *J. Cardiovasc Magnetic Resonance*. 2011;13:22
186. Herbots L, D'hooge J, Eroglu E, Thijs D, Ganame J, Claus P, Dubois C, Theunissen K, Bogaert J, Dens J, Kalantzi M, Dymarkowski S, Bijnens B, Belmans A, Boogaerts M, Sutherland G, Van De Werf F, Rademakers F, Janssens S. Improved regional function after autologous bone marrow-derived stem cell transfer in patients with acute myocardial infarction: A randomized, double-blind strain rate imaging study. *Eur Heart J*. 2008;30:662-670
187. Hor KN, Gottliebson WM, Carson C, Wash E, Cnota J, Fleck R, Wansapura J, Klimeczek P, Al-Khalidi HR, Chung ES, Benson DW, Mazur W. Comparison of magnetic resonance feature tracking for strain calculation with harmonic phase imaging analysis. *JACC Cardiovasc Imaging*. 2010;3:144-151
188. Harrild DM, Han Y, Geva T, Zhou J, Marcus E, Powell AJ. Comparison of cardiac MRI tissue tracking and myocardial tagging for assessment of regional ventricular strain. *The international journal of cardiovascular imaging*. 2012; doi: 10.1007/s10554-012-0035-3
189. Pavlopoulos H, Nihoyannopoulos P. Strain and strain rate deformation parameters: From tissue doppler to 2d speckle tracking. *The international journal of cardiovascular imaging*. 2008;24:479-491

190. Bansal M, Jeffriess L, Leano R, Mundy J, Marwick TH. Assessment of myocardial viability at dobutamine echocardiography by deformation analysis using tissue velocity and speckle-tracking. *JACC Cardiovasc Imaging*. 2010;3:121-131
191. Roes SD, Mollema SA, Lamb HJ, van der Wall EE, de Roos A, Bax JJ. Validation of echocardiographic two-dimensional speckle tracking longitudinal strain imaging for viability assessment in patients with chronic ischemic left ventricular dysfunction and comparison with contrast-enhanced magnetic resonance imaging. *The American Journal of Cardiology*. 2009;104:312-317
192. Phan TT, Shivu GN, Abozguia K, Gnanadevan M, Ahmed I, Frenneaux M. Left ventricular torsion and strain patterns in heart failure with normal ejection fraction are similar to age-related changes. *Eur J Echocardiogr*. 2009;10:793-800
193. Sjoli B, Orn S, Grenne B, Ihlen H, Edvardsen T, Brunvand H. Diagnostic capability and reproducibility of strain by doppler and by speckle tracking in patients with acute myocardial infarction. *JACC. Cardiovascular imaging*. 2009;2:24-33
194. Kempny A, Diller GP, Orwat S, Kaleschke G, Kerckhoff G, Bunck AC, Maintz D, Baumgartner H. Right ventricular-left ventricular interaction in adults with tetralogy of fallot: A combined cardiac magnetic resonance and echocardiographic speckle tracking study. *International Journal of Cardiology*. 2010
195. Van Dalen BM, Soliman OII, Vletter WB, Kauer F, Van Der Zwaan HB, Ten Cate FJ, Geleijnse ML. Feasibility and reproducibility of left ventricular

- rotation parameters measured by speckle tracking echocardiography. European Journal of Echocardiography. 2009;10:669-676*
196. *Stanton T, Leano R, Marwick TH. Prediction of all-cause mortality from global longitudinal speckle strain: Comparison with ejection fraction and wall motion scoring. Circulation: Cardiovascular Imaging. 2009;2:356-364*
 197. *Assomull R, Pennell D, Prasad S. Cardiovascular magnetic resonance in the evaluation of heart failure. Heart. 2007;93:985-992*
 198. *Kim RJ, Shah DJ, Judd RM. How we perform delayed enhancement imaging. J. Cardiovasc Magnetic Resonance. 2003;5:505-514*
 199. *Simonetti OP, Kim RJ, Fieno DS, Hillenbrand HB, Wu E, Bundy JM, Finn JP, Judd RM. An improved MR imaging technique for the visualization of myocardial infarction. Radiology. 2001;218:215-223*
 200. *Kellman P, Chung Y-C, Simonetti OP, McVeigh ER, Arai AE. Multi-contrast delayed enhancement provides improved contrast between myocardial infarction and blood pool. J Magn Reson Imaging. 2005;22:605-613*
 201. *Farrelly C, Rehwald W, Salerno M, Davarpanah A, Keeling AN, Jacobson JT, Carr JC. Improved detection of subendocardial hyperenhancement in myocardial infarction using dark blood-pool delayed enhancement mri. AJR Am J Roentgenol. 2011;196:339-348*
 202. *Yarnykh VL, Yuan C. T1-insensitive flow suppression using quadruple inversion-recovery. Magn Reson Med. 2002;48:899-905*
 203. *Tonino PAL, Fearon WF, de Bruyne B, Oldroyd KG, Leesar MA, Ver Lee PN, MacCarthy PA, Van't Veer M, Pijls NHJ. Angiographic versus functional severity of coronary artery stenoses in the fame study fractional flow*

- reserve versus angiography in multivessel evaluation. Journal of the American College of Cardiology. 2010;55:2816-2821*
204. *Falk E, Shah PK, Fuster V. Coronary plaque disruption. Circulation. 1995;92:657-671*
 205. *Razavi R, Hill DLG, Keevil SF, Miquel ME, Muthurangu V, Hegde S, Rhode K, Barnett M, van Vaals J, Hawkes DJ, Baker E. Cardiac catheterisation guided by mri in children and adults with congenital heart disease. Lancet. 2003;362:1877-1882*
 206. *Schenck JF, Jolesz FA, Roemer PB, Cline HE, Lorensen WE, Kikinis R, Silverman SG, Hardy CJ, Barber WD, Laskaris ET, et al. Superconducting open-configuration MR imaging system for image-guided therapy. Radiology. 1995;195:805-814*
 207. *Tzifa A, Krombach GA, Kramer N, Kruger S, Schutte A, Von Walter M, Schaeffter T, Qureshi S, Krasemann T, Rosenthal E, Schwartz CA, Varma G, Buhl A, Kohlmeier A, Bucker A, Gunther RW, Razavi R. Magnetic resonance-guided cardiac interventions using magnetic resonance-compatible devices: A preclinical study and first-in-man congenital interventions. Circulation: Cardiovascular Interventions. 2010;3:585-592*
 208. *Dick AJ, Raman VK, Raval AN, Guttman MA, Thompson RB, Ozturk C, Peters DC, Stine AM, Wright VJ, Schenke WH, Lederman RJ. Invasive human magnetic resonance imaging: Feasibility during revascularization in a combined XMR suite. Catheterization and cardiovascular interventions. 2005;64:265-274*

209. Spuentrup E, Ruebben A, Schaeffter T, Manning WJ, Günther RW, Buecker A. *Magnetic resonance--guided coronary artery stent placement in a swine model. Circulation. 2002;105:874-879*
210. Rhode KS, Hill DLG, Edwards PJ, Hipwell J, Rueckert D, Sanchez-Ortiz G, Hegde S, Rahunathan V, Razavi R. *Registration and tracking to integrate x-ray and mr images in an xmr facility. IEEE Trans Med Imaging. 2003;22:1369-1378*
211. Duckett SG, Ginks MR, Knowles BR, Ma Y, Shetty A, Bostock J, Cooklin M, Gill JS, Carr-White GS, Razavi R, Schaeffter T, Rhode KS, Rinaldi CA. *Advanced image fusion to overlay coronary sinus anatomy with real-time fluoroscopy to facilitate left ventricular lead implantation in CRT. Pacing and Clinical Electrophysiology. 2010;34:226-234*
212. Ishida M, Ichihara T, Nagata M, Ishida N, Takase S, Kurita T, Ito M, Takeda K, Sakuma H. *Quantification of myocardial blood flow using model based analysis of first-pass perfusion mri: Extraction fraction of gd-dtpa varies with myocardial blood flow in human myocardium. Magn Reson Med. 2011;66:1391-1399*
213. Ferreira P, Gatehouse P, Bucciarelli-Ducci C, Wage R, Firmin D. *Measurement of myocardial frequency offsets during first pass of a gadolinium-based contrast agent in perfusion studies. Mag Reson Med. 2008;60:860-870*
214. Schmitt M, Viallon M, Thelen M, Schreiber WG. *Quantification of myocardial blood flow and blood flow reserve in the presence of arterial dispersion: A simulation study. Magn Reson Med. 2002;47:787-793*

215. Schuster A, Grünwald I, Chiribiri A, Southworth R, Ishida M, Hay G, Neumann N, Morton G, Perera D, Schaeffter T, Nagel E. An isolated perfused pig heart model for the development, validation and translation of novel cardiovascular magnetic resonance techniques. *J. Cardiovasc Magnetic Resonance*. 2010;12:53
216. Jahnke C, Gebker R, Manka R, Schnackenburg B, Fleck E, Paetsch I. Navigator-gated 3d blood oxygen level-dependent cmr at 3.0-t for detection of stress-induced myocardial ischemic reactions. *JACC. Cardiovascular imaging*. 2010;3:375-384
217. Blankstein R, Carli MFD. Integration of coronary anatomy and myocardial perfusion imaging. *Nat Rev Cardiol*. 2010;7:226-236
218. Kajander S, Joutsiniemi E, Saraste M, Pietila M, Ukkonen H, Saraste A, Sipila HT, Teras M, Maki M, Airaksinen J, Hartiala J, Knuuti J. Cardiac positron emission tomography/computed tomography imaging accurately detects anatomically and functionally significant coronary artery disease. *Circulation*. 2010;122:603-613

Appendix A Study Protocols, Patient Information Sheets and Consent Forms

**Validation of new quantitative MR perfusion algorithms in
comparison to SPECT, PET-CT and fractional flow reserve in a
prospective group of patients with suspected or known
coronary artery disease**

**Study protocol Version 4
28 October 2010**

Introduction

Background: Myocardial perfusion and functional assessment of the haemodynamic significance of coronary stenoses, as well as the extent and distribution of ischaemia are determining factors in the management of coronary artery disease (CAD) in clinical practice.

Non-invasive assessment of perfusion is usually performed with single photon emission computed tomography (SPECT) or positron emission tomography (PET-CT). Both PET and SPECT involve exposure of patients to ionising radiation. In addition PET-CT has limited availability and higher expense when compared to SPECT, whereas the latter has a higher rate of attenuation artefacts. A recent multicenter study showed that perfusion Cardiac Magnetic Resonance (CMR) can be used as an alternative method of detecting and assessing CAD (1). Normal perfusion CMR predicts approximately a 0.7% 2 -year cumulative event rate whereas the detection of ischaemia 12.2% (2).

CMR combines the advantage of higher spatial resolution (3x3mm versus 10x10mm for SPECT) with no exposure to ionising radiation and shorter acquisition times in comparison to nuclear imaging. MR perfusion imaging can be further improved using higher field strengths and advanced acceleration methods such as k-t sensitivity encoding (k-t SENSE) (3, 4, 5). k-t SENSE allows acceleration of data acquisition in dynamic MR studies through sparse data sampling along the spatial (k) and temporal (t) encoding axes and spatio- temporal data correlation. Data undersampling leads to faster acquisition times and has been validated in previous studies mainly at 1.5 Tesla. Preliminary data have demonstrated the superiority of 3 Tesla accelerated with k-t SENSE in perfusion imaging.

Aim: In this prospective study we aim to evaluate the diagnostic accuracy of perfusion CMR at 1.5 and 3 Tesla with SPECT and PET-CT in a population with suspected or known CAD planned to have diagnostic coronary angiography. We will also compare CMR perfusion findings with invasive measurements such as Fractional Flow Reserve (FFR), Coronary Flow Reserve (CFR) and Hyperaemia Stenosis Resistance (HSR).

Primary end points

1. To validate new CMR methods of assessing myocardial perfusion and ischaemia burden in patients with suspected or known CAD against other non-invasive methods such as SPECT and PET-CT and invasive coronary angiography with FFR, CFR and HSR measurement.
2. Identify the optimal cut off point for the detection of significant coronary artery stenoses requiring further intervention.

Secondary end points

1. To evaluate image quality by using the new methods of assessing perfusion and ischaemia burden at a 1.5 Tesla and a 3 Tesla (stronger magnet) MR scanner.
2. To assess the type, frequency, and severity of the artefacts.

3. To assess the reproducibility of perfusion CMR at 1.5 and 3 Tesla
4. To quantify the CMR examination time
5. To assess the feasibility of full quantification of CMR perfusion
6. To validate perfusion CMR algorithms at 1.5 and 3 Tesla
7. To assess the prognostic value of perfusion CMR at 1.5 and 3 Tesla
8. To assess image quality of CMR, PET and SPECT with ECG and respiratory monitoring

Study Design

Methods: In a randomly selected population (77 patients) with suspected or known CAD prior to their planned diagnostic coronary angiography we will perform perfusion CMR and either SPECT (17 patients) or PET-CT (60 patients). Patients will be identified from the chest pain clinic, the diagnostic coronary angiography list or the waiting lists for clinical SPECT or PET-CT studies. This is a validation study, which will provide data for future larger trials. The following study steps are planned:

Step 1: Patient identification from the chest pain clinic, the diagnostic coronary angiography list or the waiting lists for SPECT or PET-CT. Inform patients about the study and obtain informed consent.

Step 2: Perform perfusion CMR at 1.5 or 3 Tesla.

Step 3: Perform either PET-CT or SPECT. Quantitative and qualitative CMR measurements will be compared with PET-CT and SPECT measurements to explore agreement among different methods of non-invasive assessment of CAD.

Step 4: Coronary Angiography providing with a qualitative assessment of CAD initially for all patients. A number of patients with 40-90-% luminal reduction will undergo a second coronary angiography with invasive measurements including FFR, HSR, CFR. These measurements will be compared with MRI findings.

Step 5: A small number of patients will be asked to have a second CMR to assess reproducibility.

Step 6: Patients from the PET arm who are subsequently revascularised will be invited back for one final CMR during the first 6 months post operatively.

Step 7: Follow up at 2, 5 and 10 years for adverse cardiac events to assess the prognostic value of CMR at 1.5 and 3 Tesla.

The flow chart of the study is as shown in Figure 1.

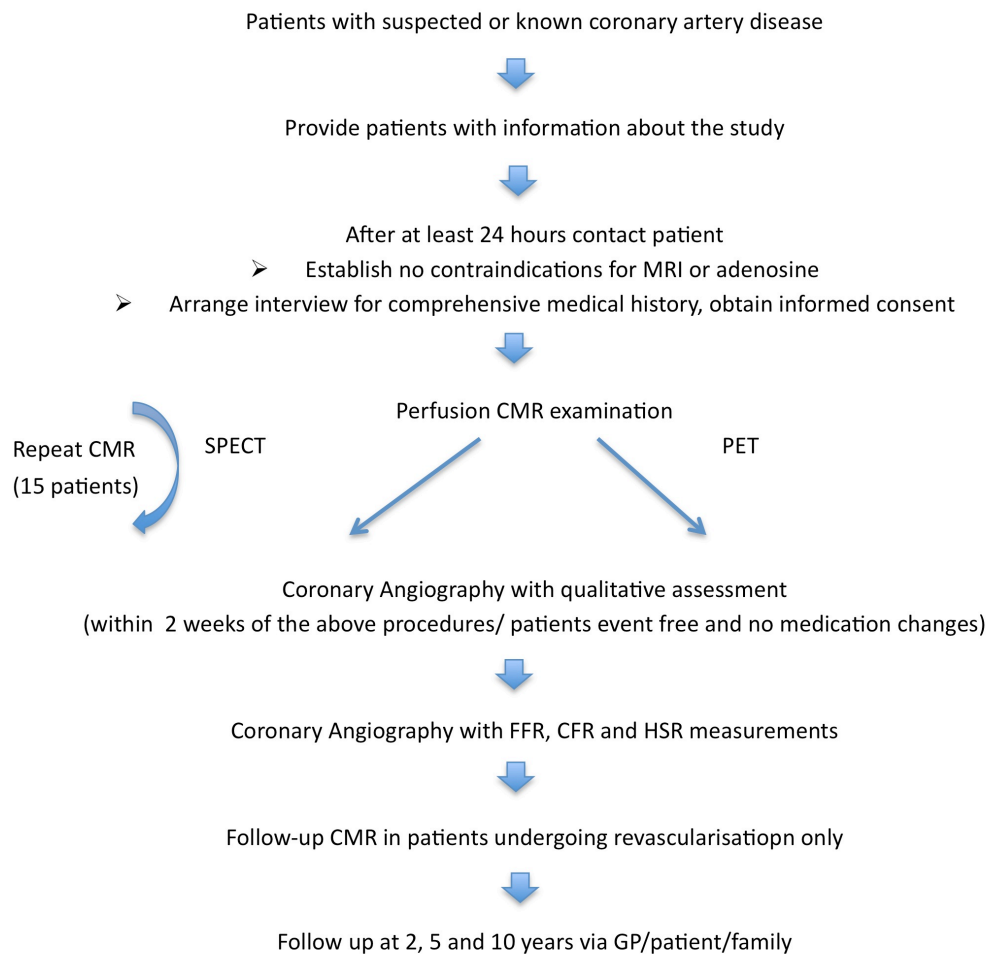


Figure 1. Study Flow chart

Eligibility

Inclusion Criteria

1. Patients with suspected or known CAD undergoing invasive coronary angiography
2. Patients with a history of angina Canadian Cardiovascular Society Class I, II and III
3. Patients who have given informed written consent

Exclusion Criteria

1. Contraindications to MR (implanted electronic devices, metallic foreign bodies, and others according to manufacturer's recommendations and generally accepted guidelines)(6, 7)
2. Pregnancy/breastfeeding/females of child-bearing age
3. Claustrophobia
4. Mental disability/ Inability to consent
5. Allergy to contrast media
6. Poor renal function eGFR<30ml/min
7. Heart Failure New York Heart Association Class III/IV
8. Inability to lie flat (i.e MSK disease/ COPD with cor pulmonale)
9. Body weight > 140kg and waist perimeter > 95cm
10. Unstable medically
11. Atrio-ventricular block II/III, sick sinus syndrome, symptomatic bradycardia, asthma or Chronic Obstructive Pulmonary Disease as contraindications to adenosine
12. Previous ST Elevation Myocardial Infarction or Coronary Artery Bypass Graft.

Investigation protocols

CMR study

1. Consent

Written informed consent will be obtained for participation to the study.

2. Patient preparation

Prior to the examination, the patient will be provided with detailed information about the course of the examination, the breathhold procedure, the use of contrast agents and the use of medication. Generally breathholding should be performed during end-expiration to ensure reproducible slice geometry. A venous line will be inserted into the cubital vein of one arm and connected to the contrast pump. A second venous line will be inserted into the other arm and connected to the adenosine infusion. An MR compatible blood pressure monitor will be connected. Patients will be instructed not to take caffeine, tea or smoke if smokers for 24 hours prior to the scan. They will be also told not to take medications such as b-blockers, nitrates and calcium channel blockers for 24 hours prior to the scan.

3. CMR protocol

The CMR studies will be carried out on a 1.5 or 3Tesla cardiac research scanner (Philips) at Guy's and St Thomas' NHS Foundation Trust or at Bart's and The London NHS Trust. The study will include localisers, cine images and rest and Adenosine-stress perfusion imaging. Rest and adenosine stress myocardial perfusion flow studies will be performed. Adenosine will be administered as a continuous peripheral intravenous infusion at 140 mcg/kg/min for 3-6 minutes. First-pass contrast-enhanced perfusion imaging will use a bolus intravenous injection of non-ionic gadolinium (up to 0.2mmol/kg bodyweight). Late enhancement will take place 15mins after the gadolinium injection.

4. Stress agent adenosine

Adenosine, an endogenous nucleotide, is a potent vasodilator of most vascular beds, except for hepatic and renal arterioles. With adenosine a maximal coronary vasodilatation can be achieved safely with an intravenous infusion at a rate of 140 µg/kg/min.

The short biological half-life (approximately 20 seconds) of this agent allows for repeated administration of this agent.

Side Effects

The vasodilatory effect of adenosine may result in a mild-to-moderate reduction in systolic, diastolic and mean arterial blood pressure (< 10 mmHg) with a reflex increase in heart rate. Most patients complain about chest discomfort. These effects, however, are transient and usually do not require medical intervention.

Since adenosine exerts a direct depressant effect on the SA and AV nodes transient first-, second- and third-degree AV block and sinus bradycardia have been reported in 2.9%, 2.6% and 0.8% of patients. Also, adenosine can cause hypotension. Patients with intact baroreceptor reflex are able to maintain blood pressure in response to adenosine by increasing cardiac output and heart rate.

Adenosine can also cause a paradoxical increase in systolic and diastolic blood pressure, which mostly develops in individuals with significant left ventricular hypertrophy. These increases are transient and resolve spontaneously. Because adenosine is a respiratory stimulant primarily through activation of carotid body chemoreceptors, intravenous administration showed increases in minute ventilation, reduction in arterial PCO₂ and respiratory alkalosis. Approximately 14% of patients complain of dyspnea and an urge to breathe deeply during adenosine infusion.

Contraindications

Adenosine should be used with caution in patients with pre-existing AV block or bundle branch block and should be avoided in patients with high-grade AV block or sinus node dysfunction. Adenosine should be used with caution if a patient is receiving any medications that already depress the sinus node and/or AV node (e.g. beta-blockers, calcium channel blockers, cardiac glycosides). Adenosine should be discontinued in patients who develop persistent or symptomatic high-grade block or significant drop in systolic blood pressure (>20 mmHg). The drug should be discontinued in case of persistent or symptomatic hypotension.

Also, adenosine should be used with caution in patients with autonomic dysfunction, stenotic valvular heart disease, pericarditis and pericardial effusion, stenotic carotid artery disease, cerebrovascular insufficiency and uncorrected hypovolemia.

Adenosine infusion should be exercised with caution in patients with obstructive lung disease not associated with broncho-constriction (emphysema, bronchitis, etc), and should be avoided in patients with bronchoconstriction or bronchospasm (e.g. asthma). If a patient develops severe respiratory difficulties, adenosine should be immediately discontinued.

5. Monitoring and Safety

During the entire CMR examination, volunteers and patients are being monitored closely. In general, monitoring during a MR examination requires the same precautions and emergency equipment as any other stress examination.

Monitoring requirements for adenosine stress MR imaging:

Heart rate and rhythm	Continuously
Blood pressure	During Adenosine infusion every 2 min
Vector-ECG	Continuously
Symptoms	Continuously

6. Termination criteria

- Clinical symptoms (significant chest pain, severe respiratory difficulty)
- Blood pressure increase > 240/120 mmHg
- Persistent or symptomatic hypotension
- Complex cardiac arrhythmias

SPECT protocol

This study will be conducted as in routine clinical practice. Patient preparation and instructions regarding medications and caffeinated drinks prior to the scan are very similar to the CMR study. SPECT rest and stress studies though are conducted in two separate sessions.

- A) Rest study: An intravenous line will be inserted and the radioactive tracer Technecium 99m Tetrafosmin (maximum dose 10mSv) will be injected. 45 minutes later imaging will be initiated.
- B) Stress study: This study involves in comparison to the rest study the additional injection of adenosine, the pharmacological stressor used in CMR. Similar patient monitoring and safety regulations to the CMR study will apply.

PET-CT protocol

This study is conducted as in routine clinical practice. ^{13}N Ammonia will be used as a radioactive tracer and stress will be induced with adenosine both of which will be injected intravenously. Patient instructions prior to the scan, monitoring and safety are as per the MR study.

Coronary angiography

Angiography will be performed by clinical indication using a standard technique. Multiple projections will be acquired of the left and right coronary artery systems. Invasive measurements of FFR, CFR and HSR will be obtained only if patients have a 40-90% luminal reduction and require a second procedure. FFR will be measured in all first order coronary arteries using an intracoronary flow wire and intracoronary or peripheral administration of Adenosine.

Data analysis

Perfusion CMR, SPECT and PET-CT results will be read by 2 readers with over two years of experience blinded to patients' clinical information or results of any other studies. In case of a significant inter-reader variation a third reader will review the scan in question.

Myocardial perfusion with CMR will be analysed in a quantitative manner using model-independent deconvolution analysis and various "semi"-quantitative methods (such as upslopes derived from signal-time intensity profiles). Data will be therefore transferred to a Philips "Viewforum" workstation.

SPECT and PET-CT data will be also analysed in a quantitative manner. Data from the three non- invasive tests will be compared to explore agreement.

CMR perfusion data will be also compared to angiography qualitative data from all patients. In patients undergoing invasive measurements during angiography CMR perfusion analysis methods will be compared against invasive pressure-wire derived FFR using a cut-off for normal FFR of 0.75.

The correlation of CMR and X-ray measurements will be determined.

The diagnostic accuracy of CMR to detect the presence of flow-limiting coronary stenosis on x-ray angiography defined as >70% luminal stenosis of a first order coronary artery segment will be determined.

Statistical Analysis

All analyses will be conducted using appropriate quantitative methods for each test. 1) ROC curves will be used to determine a cut off value for MR measurements predicting ischaemia. Sensitivity and specificity will be equally weighted and thus the Youden index will be used to determine the best possible cut off value. 2) To compare the prediction of ischaemia by different parameters MRI, SPECT and PET ROC curves will be used. Additionally the measurements of MRI and SPECT or MRI and PET will be compared using correlation analysis and weighted K values.

References

1. Schwitter, J., et al., *MR-IMPACT: comparison of perfusion-cardiac magnetic resonance with single-photon emission computed tomography for the detection of coronary artery disease in a multicentre, multivendor, randomized trial*. Eur Heart J, 2008. **29**(4): p. 480-9.
2. Jahnke, C., et al., *Prognostic value of cardiac magnetic resonance stress tests: adenosine stress perfusion and dobutamine stress wall motion imaging*. Circulation, 2007. **115**(13): p. 1769-76.
3. Gebker, R., et al., *Diagnostic performance of myocardial perfusion MR at 3 T in patients with coronary artery disease*. Radiology, 2008. **247**(1): p. 57-63.
4. Gebker, R., et al., *MR myocardial perfusion imaging with k-space and time broad-use linear acquisition speed-up technique: feasibility study*. Radiology, 2007. **245**(3): p. 863-71.
5. Plein, S., et al., *Dynamic contrast-enhanced myocardial perfusion MRI accelerated with k-t sense*. Magn Reson Med, 2007. **58**(4): p. 777-85.
6. Pennell DJ et al Clinical indications for cardiovascular magnetic resonance (CMR): Consensus Panel report. JCMR 2004;6:727-65.
7. Hendel RC et al, Appropriateness criteria for CMR imaging, JACC 2006;48:1475-97

St Thomas' Hospital Research Ethics Committee

PATIENT INFORMATION SHEET

Title of Project: Validation of quantitative CMR perfusion in patients with suspected or known coronary artery disease

CMR compared to PET-CT and angiography

Principal Investigator: Prof. Eike Nagel

Code No: 08/H0802/137

Version No: 4 Date: 30/04/2010

You are being invited to take part in a research study. Before you decide it is important for you to understand why the research is being done and what it will involve. Please take time to read the following information carefully. Talk to others about the study if you wish.

- *Part 1 tells you the purpose of this study and what will happen to you if you take part.*
- *Part 2 gives you more detailed information about the conduct of the study.*

Ask us if there is anything that is not clear or if you would like more information. Take time to decide whether or not you wish to take part.

PART 1

What is the purpose of the study?

Magnetic Resonance Imaging (MRI) is an effective method of taking images of the internal organs of the body. It can also provide information of the blood supply to the heart muscle. This information is particularly important in patients who have chest pain because of blocked or narrowed heart arteries. This is usually the disease called coronary artery disease (CAD).

MRI has several advantages over other tests as it is simple, does not involve radiation and can lead to images of very high detail. We have recently developed a new method that allows us to further improve the clarity of the MRI images of the heart's blood supply.

In this study, we want to test this new method and find out how it compares to other tests called Positron Emission Tomography (PET-CT), single photon emission tomography (SPECT) and coronary angiography. This may allow us in future to assess patients with suspected without needing invasive tests or scans using radiation.

Our study has different parts and each participant will be involved only in some, therefore we will provide you only with the relevant information. Participant selection to the different parts is done in randomised fashion.

Why have I been chosen?

We are interested in patients that have or may have CAD and you have been referred for a coronary angiography to investigate your heart's blood supply.

Do I have to take part?

No. It is up to you to decide whether or not to take part. If you do, you will be given this information sheet to keep and be asked to sign a consent form. You

are still free to withdraw at any time and without giving a reason. A decision to withdraw at any time, or a decision not to take part, will not affect your medical management.

What will happen to me if I take part?

1) We will contact you by phone to discuss the study and if you wish to participate we will arrange an appointment to sign a consent form and perform an MRI scan.

2) MRI scan (research scan)

This involves placing you in a tunnel shaped scanner, so it is important you feel comfortable in closed spaces. While the images are taken, you will be asked to lie quietly on your back and follow breathing instructions. Inside the scanner, you will hear loud machine-like noises, as part of the imaging process – this is normal.

The purpose of this exam is to identify the areas of your heart where blood supply is reduced. During the test we will make the heart stress that aims to maximise blood flow to the heart. For this reason two intravenous lines will be inserted in arm veins and will be used to inject the contrast agent (a substance allowing to take images of the heart) for the blood flow measurements and the medicine causing the heart to stress. Throughout the scan we will be monitoring your heart tracing, pulse and breathing. If you feel uncomfortable at any point you can let us know by squeezing a small ball that will be placed in your hand. The scan will take approximately 60mins.

3) PET-CT (research scan)

The procedure is very similar to MRI and takes approximately 1 hour and 20 minutes. It requires the injection of a radioactive dye that is taken up by the heart and is imaged by the PET scanner.

4) We would like with your permission to compare the results of your coronary angiography with our scans.

5) You may be asked to perform another MRI scan on another day if you agree. This is to help us demonstrate that this technique can provide us with reproducible results.

6) If you go on to have an operation to improve the blood supply to the heart we may invite you back for one final MRI scan in the 6 months after the operation.

7) We would like to follow you up at 2, 5 and 10 years. Follow up will involve initially contacting your GP and then you and obtaining information about your health. In the case you are unable to provide us with information for the follow up we would like to obtain it with your permission from your next of kin or GP.

What do I have to do?

1) Sign a consent form

2) Attend the MRI and PET scans, scheduled according to yours and the hospital's convenience, that involves two visits.

What is the procedure that is being tested?

The procedure tested is perfusion MRI at 3 Tesla. Perfusion MRI at 1.5 Tesla has been so far used in clinical practice however in this study we aim to improve standard MRI using a stronger magnet (3 Tesla).

What are the alternatives for diagnosis?

PET, SPECT, MRI at 1.5 Tesla and coronary angiography are also used in clinical practice as methods of evaluating CAD.

What are the side effects of taking part?

The MRI scan cannot be done under certain circumstances such as if you suffer from claustrophobia or have previously had any metal implants inserted in your body. It is noisy, so ear protection is provided. Overall, it is very low risk.

The medication which increases the blood flow to the heart and will be used in both MRI and PET-CT can cause shortness of breath, chest pain, dizziness, flushing and changes to the heart rhythm. All these effects, if they occur, last for a few minutes only and settle completely thereafter.

All scans are painless and you should be able to return home on the same day without any side effects or restriction to your normal daily activities.

What are the possible disadvantages and risks of taking part?

A) The PET-CT scan and the radioactive dye gives you a radiation dose. The radiation in this study is the same amount that is used for this type of scan in routine clinical practice. The risk from the radiation is equivalent to 4 years of background radiation in the UK i.e. the radiation anyone receives by living in the UK 4 years.

B) A small number of participants undergoing MRI develop feelings of claustrophobia. If you feel claustrophobic then you can ask for the study to be terminated.

C) During MRI and PET-CT there is the potential for an allergic reaction to the contrast agent. If you have had an allergic reaction to a contrast agent we will not perform the tests. Should an allergic reaction develop you are in the hospital environment and will be treated immediately

D) The medication which increases the blood flow to the heart can cause changes to the heart rhythm that usually settles completely thereafter.

What happens when the research study stops?

Your further management depends on the findings in angiography.

What if there is a problem?

Any complaint about the way you have been dealt with during the study or any possible harm you might suffer will be addressed. The detailed information on this is given in Part 2

Will my taking part in the study be kept confidential?

Yes. All the information about your participation in this study will be kept confidential. The details are included in Part 2.

This completes Part 1 of the Information Sheet.

If the information in Part 1 has interested you and you are considering participation, please continue to read the additional information in Part 2 before making any decision.

PART 2**What if relevant new information becomes available?**

Sometimes during the course of a research project, new information becomes available about the procedure that is being studied. If this happens, your research doctor will tell you about it and discuss whether you want to or should continue in the study. If you decide not to carry on, your research doctor will make arrangements for your care to continue. If you decide to continue in the study you will be asked to sign an updated consent form. Also, on receiving new information your research doctor might consider it to be in your best interests to withdraw you from the study. He/she will explain the reasons and arrange for your care to continue. If the study is stopped for any other reason, you will be told why and your continuing care will be arranged.

What will happen if I don't want to carry on with the study?

You can withdraw at any point and this will not affect your medical treatment. If you withdraw from the study, we will need to use the data collected up to your withdrawal.

What if there is a problem?

Complaints: If you have a concern about any aspect of this study, you should ask to speak with the researchers who will do their best to answer your questions (Prof. Eike Nagel; Office number +44 20 7188 8363. If you remain unhappy and wish to complain formally, you can do this through the NHS Complaints Procedure. Details can be obtained from the hospital.

Harm: In the event that something does go wrong and you are harmed during the research study there are no special compensation arrangements. If you are harmed and this is due to someone's negligence then you may have grounds for a legal action for compensation against Guy' & St. Thomas' NHS Trust but you may have to pay your legal costs. The normal National Health Service complaints mechanisms will still be available to you.

Will my taking part in this study be kept confidential?

Procedures for handling, processing, storage and destruction of your data are compliant with the Data Protection Act 1998.

All information which is collected about you during the course of the research will be kept strictly confidential. Any information about you which leaves the hospital will have your name and address removed so that you cannot be recognised from it.

Your data will be collected from the referral letter and hospital notes, as well from discussing with you during the interview; Data will be stored securely, in an encrypted format; Authorised persons such as researchers, regulatory authorities and Research and Development (for monitoring of the quality of the research) will have access to these data; Data will be retained for 15 years.

Your own GP may be notified of your participation in the trial, after your consent.

What will happen to the results of the research study?

These will be published in a research paper with the aim of advancing the knowledge of MRI and ischemic heart disease. All patient identities are treated as strictly confidential and anonymous in any publication.

Who is organising and funding the research?

The research is organised by Professor Eike Nagel and will be partially funded by Kings College London and Guy's and St Thomas' Hospital NHS Foundation Trust.

Who has reviewed the study?

The study has been independently reviewed by the St Thomas' Hospital Ethics Committee.

Contact Details:

Professor Eike Nagel, St Thomas' Hospital, 4th Floor Lambeth Wing.
Telephone: 02071887242. Mobile phone: 07949680239.

Dr Geraint Morton, St Thomas' Hospital, 4th Floor Lambeth Wing.
Telephone: 020 7188 7188 ext 52022. Mobile phone: 07859 857357.
Email: geraint.morton@kcl.ac.uk

A copy of the information sheet and a signed consent form to keep will be given to you.

Thank you for considering taking part or taking time to read this sheet.

PATIENT INFORMATION SHEET

Study title: MRI sequence development in a clinical setting.

REC Study No: 09-H0802-78.

Chief Investigator: Prof Eike Nagel.

You are being invited to take part in some research during your Magnetic Resonance Imaging (MRI) scan. Before you decide whether to take part it is important that you understand why the research is being done and what it will involve. Please take your time to read the following information carefully.

Your doctor has requested that you undergo an MRI scan as part of your clinical care. Unlike most medical imaging methods, MRI **does not use ionising radiation** but instead uses magnetic fields and radio-frequency (RF) waves to produce images of the internal structure of the human body. A clinical examination will consist of a number of sequences of magnetic and RF pulses with each sequence producing an image or set of images. Whilst MRI is an established and safe technique we are continually looking for ways of improving the information that we get from the scan. Improved information from the scan means better quality images and better care for patients. With MRI small adjustments in the way we take the images (sequences) can lead to very different results. In order to work out whether an adjustment we make is useful we need to try it out in patients.

In addition to the imaging you need for clinical reasons we would also like to test new imaging sequences during your scan. From your point of view this simply involves spending a few extra minutes in the MRI scanner. Your normal MRI scan will last approximately 60 minutes. The extra time required for this research would add a maximum further 15 minutes. We will not administer any extra dye or medication to you over and above what is required for clinical purposes. The extra scanning is not painful or dangerous. There are no known extra risks to you should you agree to this extra scanning.

It is entirely voluntary whether you allow us to perform this extra scanning for research purposes. If you refuse your clinical care will not be affected and you do not have to give a reason for your refusal. You are free to change your mind at any point during the scan. Should you do so we will not take any further research images.

Information collected during this research will be kept strictly confidential. The procedures for handling, processing, storage and destruction of your data are compliant with the Data Protection Act 1998. Any information about you, which

leaves the NHS, will be entirely anonymous, as your name and address will be removed.

If you have any questions please ask a member of the MRI department staff. If you are happy to take part we will ask you to sign a consent form.

CONSENT FORM

Study title: MRI Sequence Development in a Clinical Setting

REC Study No: 09-H0802-78

Chief Investigator: Prof Eike Nagel

May we take some extra images for research?

This will require no extra injections and will take a maximum of an extra 15 minutes in the scanner. Participation is entirely voluntary and choosing not to participate will not affect your medical care.

Please initial box

1. I confirm that I have read and understand the information sheet dated 17/07/2009 (version 2) for the above study. I have had the opportunity to consider the information, ask questions and have had these answered satisfactorily.

☐

2. I understand I may choose at any point not to have any further research scans without giving any reason, without my medical care or legal rights being affected.

☐

3. I give my consent to have some additional scans for research.

☐

Name of Patient

Signature

Date

Name of Person taking consent
(if different from researcher)

Signature

Date

Researcher

Signature

Date

When completed, 1 for patient; 1 for researcher site file; 1 (original) to be kept in medical notes

Appendix B: BCIS-1 Jeopardy Score

The Duke Jeopardy Score ¹⁴⁵ ascribes 2 points each for 6 myocardial territories, those subtended by the Left Anterior Descending (LAD), Diagonal Branch (DG), Circumflex (Cx), Obtuse Marginal branch (OM), Right Coronary (RCA) and Posterior Descending Branch (PDA) arteries. 2 points are allocated to each coronary lesion plus 2 further points if the lesion affects 2 of the 6 downstream myocardial territories. The BCIS-1 Jeopardy Score is a modification of this scoring system which allows classification of left main coronary artery disease as well as coronary bypass graft disease.

- Coronary or graft lesions $\geq 70\%$ diameter stenosis on visual estimation should be considered significant. Left main coronary lesions $\geq 50\%$ should be considered significant.
- Where a main vessel gives rise to multiple branches (DG, OM or PDA), only lesions in the branch supplying the largest territory (called the Major Branch below) should be scored.
- For anatomical variations, equivalent myocardial territories should be assessed (Example 1: the Ramus Intermedius Branch could be scored as Major DG or Major OM, if considered to supply a similar territory; Example 2: when RCA dominant, the Proximal Cx should be scored as Major OM)
- For true anatomic co-dominance assign the right coronary artery as dominant
- When using the scoring table below, it is important to complete each numbered row sequentially.

	Coronary Artery/Graft	Instructions	Score
1	LMS	if $\geq 50\%$ lesion, score 8 and go to row 11 if $< 50\%$ lesion, score 0 and go to row 2	
2	Proximal LAD (Before DG)	if $\geq 70\%$ lesion, score 6 and go to row 5 if $< 70\%$ lesion, score 0 and go to row 3	
3	Mid LAD (After DG)	if $\geq 70\%$ lesion, score 2 and go to row 4 if $< 70\%$ lesion, score 0 and go to row 4	
4	Major DG	if $\geq 70\%$ lesion, score 2 and go to row 5 if $< 70\%$ lesion, score 0 and go to row 5	
5		If Cx dominant, go to row 8 If RCA dominant, go to row 6	
6	Proximal RCA (Before PDA)	if $\geq 70\%$ lesion, score 4 and go to row 10 if $< 70\%$ lesion, score 0, go to row 7	
7	PDA	if $\geq 70\%$ lesion, score 2 and go to row 10 if $< 70\%$ lesion, score 0, go to row 10	
8	Proximal Cx (Before OM)	if $\geq 70\%$ lesion, score 6 and go to row 14 if $< 70\%$ lesion, score 0, go to row 9	
9	Mid Cx (After OM)	if $\geq 70\%$ lesion, score 2 and go to row 10 if $< 70\%$ lesion, score 0, go to row 10	
10	Major OM	if $\geq 70\%$ lesion, score 2 and go to row 14 if $< 70\%$ lesion –score 0 and go to row 14	
11		If Cx dominant, score 4 and go to row 14 If RCA dominant, score 0 and go to row 12	
12	Proximal RCA (Before PDA)	if $\geq 70\%$ lesion, score 4 and go to row 14 if $< 70\%$ lesion, score 0 and go to row 13	
13	PDA	if $\geq 70\%$ lesion, score 2 and go to row 14 if $< 70\%$ lesion, score 0, go to row 14	
14		Previous CABG? If yes, go to row 15 If no, go to row 21	
15	LAD graft beyond DG	if $< 70\%$ graft lesion, score -4, go to row 16 if $> 70\%$, poor run-off or n/a, score 0, go to row 16	
16	Major DG graft	if $< 70\%$ graft lesion, score -2, go to row 17 if $\geq 70\%$, poor run-off or n/a, score 0, go to row 17	
17	Major OM graft	if $< 70\%$ graft lesion, score -2, go to row 18 if $\geq 70\%$, poor run-off or n/a, score 0, go to row 18	
18	Cx graft beyond OM (Cx dominant system)	if $< 70\%$ graft lesion, score -4, go to row 19 if $\geq 70\%$, poor run-off or n/a, score 0, go to row 19	
19	RCA graft (before PDA)	if $< 70\%$ graft lesion, score -4, go to row 21 if $\geq 70\%$ poor run-off or n/a, score 0, go to row 20	
20	PDA graft	if $< 70\%$ graft lesion, score -2, go to row 21 if $\geq 70\%$ poor run-off or n/a, score 0, go to row 21	
21	TOTAL SCORE	add filled in scores and enter (range: 0 to 12)	